ARCH STABILITY AND FAILURE BEHAVIOR IN UNCONSOLIDATED NATURAL SANDS

by

Gbolahan Oladele Lasaki

A thesis submitted to the Faculty and the Board of Trustees of the Colorado School of Mines in partial fulfillment of the requirements for the degree of Doctor of Philosophy, Petroleum Engineering.

Signed: Gbolahan O. Lasaki

Gbolahan O. Lasaki

Golden, Colorado

Date: May 2nd, 1980

Approved: C. A. Kohlhaas

Dr. C. A. Kohlhaas
Thesis Advisor

Craig W. Van Kirk

Dr. C. W. Van Kirk
Head of Department

Golden, Colorado

Date: May 2nd, 1980

To

Abiose

Abimbola and Tolulope

ABSTRACT

The flow of sand into the wellbore of a producing oil well may cause the failure of surface and downhole equipment through abrasive wear. This may lead to the total loss of the well or serious environmental problems requiring a huge expense in addition to loss of production. The growing world need for petroleum and the increasing cost of developing new fields make the search for effective and permanent sand-control methods quite opportune. Hall, et al. (1970) drew attention to the arching phenomenon of unconsolidated sand and its relevance to sand control. This was the subject of the investigations by Tippie(1973), Cleary (1978), Melvan (1978),and Wood (1979). The scope of these studies has been further extended.

This thesis reports a study of the arching behavior of unconsolidated natural sands under loading stresses simulating a producing oil formation. Three natural sand samples with different physical and mechanical properties, but almost identical sand grain distributions, were used. The stability and failure behavior of arch structures in these sands was investigated at overburden stresses of 500, 750, 1000, 1500, and 1800/2250 psi.

X-ray diffraction analysis showed that about 1% by weight of each sand was composed of traces of various clay minerals including illites, montmorillonite, and kaolite. A fourth sand sample used was a mixture of equal parts of 20-40 and 80-100 mesh Gopher State frac sand.

In all cases, sandfree production was achieved as a result of stable sand arches. The arches were more stable in the natural sands than in the Gopher State sand. The arch structures were weaker at low overburden stresses (500, 750 psi) and stronger at high stresses (1500 and 2250 psi) than the sand. The following failure criterion was also established: $\frac{\Delta P}{847.2Q\mu} k_{cor} R \geq 0.002807\left(\frac{\sigma_1 - P_{in}}{\sigma_1}\right)^{-6.601}$.

Suggestions for practical applications are based on the findings of this study. These are expected to assist operators in dealing with sand problems.

TABLE OF CONTENTS

LIST OF TABLES

LIST OF FIGURES

ACKNOWLEDGEMENT

The author wishes to express his gratitude to the Petroleum Engineering Department for the use of its facilities; to the sponsors of this project: Amoco Oil Company, Atlantic Richfield Company, Chevron Oil Company, Compagnie Francaise des Petroles, Continental Oil Company, Exxon, Koninklijke/Shell, Marathon Oil Company, and Tenneco Oil Company; and to the Government of Ogun State of Nigeria for its scholarship. The author also wishes to thank the numerous people that have assisted in various ways during this study. In particular the author wishes to thank Mr. Larry Mower of Amoco Production Company, Mr. Jim Baker of the USGS, Mr. Dave Cox, of Energy Consulting Associates, Mr. Jim Boze of the Mining Department, and Messrs. Russell J. Miller and Ray Owen of the Earth Mechanics Institute.

Finally the author would like to express his gratitude to Dr. C.A. Kohlhaas, thesis advisor, and to Dr. D.M. Bass (Kerr McGee Professor), Dr. D.W. Hilchie, Dr. D.I. Dickinson and Dr. F.J. Stermole for serving on this thesis committee.

Chapter 1

INTRODUCTION

Sand production is a major problem in oil wells producing from unconsolidated or loosely consolidated formations all over the world. This is common in younger Tertiary sediments as found in the Gulf Coast, the Los Angeles Basin of California, the North Sea, Libya, Venezuela, Trinidad, Indonesia, and Nigeria. Sand production in oil wells has serious and adverse effects on both reservoir performance and the operating cost of wells. The flow of sand into the wellbore reduces productivity and fills up the borehole with sand. It may also cause the failure of surface and downhole equipment through abrasive wear. These may lead to the total loss of the well and serious environmental problems. At best, expensive workover operations are required.

Sand problems were first recognized in the field of groundwater hydrology. Experience in this area has been of tremendous value to the petroleum industry. However, the growing world need for petroleum and the increasing cost of developing new fields make the search for more effective and permanent sand control methods quite opportune at this time. Sand control refers to the general practice and technology of excluding sand influx into the wellbore, and thereby eliminating the inconveniences of production losses and costly damages to producing wells. Widespread control methods are basically employed by mechanical or chemical means. These include:

(i) Bridging flow of sand into the wellbore by either wire screens or gravels

(ii) Consolidating (or glueing) sand grains in place by plastics or resins

(iii) A combination of (i) and (ii).

Field experience shows that sand production in some formations is rate sensitive. In this case, successful control can be achieved by rate and rate-variation control. Sand-free production can be achieved if the rate is kept below a critical value. Sudden rate increases can cause sand flow for a short while. However, control by holding down production rate is quite inadequate for many practical cases as the critical rate may be uneconomical. Other formations are stress sensitive as regards sand production. Kohlhaas (1976) noted that sand failure depends partly on well history: rate effects dominate short-term behavior while stress effects dominate long-term behavior. In effect, most unconsolidated formations are stress sensitive in the long run. He suggested that stress alteration was the mechanism which would control sand on a long-term basis. Suman (1975) suggested installing inflatable packers in the borehole to alter the stress field. This packer can be inflated with a cement slurry which, when hardened, maintains the stress field around the wellbore at a new level.

Analyses are made by calculating stresses and comparing them with the failure conditions of the sand. Elastic rock behavior is usually assumed. However, while hard rocks or consolidated sand may behave as elastic media, this assumption can hardly be justified for loose or unconsolidated sand, especially under a high confining pressure as experienced in a producing reservoir. Other theoretical developments involving stresses around a wellbore have been approached with the assumption of a partial yield. The region close to the borehole is assumed to be in a plastic state. This is surrounded by a region stressed below the limit of plasticity.

Actual behavior of unconsolidated producing sand formation is influenced by the ability of the sand to form an arch around a perforation. The behavior of such arches was studied by Tippie (1973), Melvan (1978), Cleary (1978), and Wood (1979) at the Colorado School of Mines. Tippie conducted experiments with 20/40 US mesh Gopher State frac sand, simulating reservoir conditions at low overburden stresses. Melvan and Cleary continued this work at high stresses, while Wood extended it to include various mixtures of 20/40 and 80/100 US mesh sands. The scope of these studies has been further extended by using natural sands. This thesis reports therefore, a study of the behavior of unconsolidated natural sands under loading stresses simulating a producing formation, in a triaxial pressure cell. Three natural sand samples were used. Tests were also conducted with equal mixtures of 20/40 and 80/100 US mesh Gopher State frac sand to answer questions raised from the previous works of Melvan, Cleary, and Wood. Stability and failure conditions of sand arch structure were studied. Criteria for predicting sand production are presented, and suggestions are made for field practice that can minimize sand problems in producing wells.

Chapter 2

DEFINITIONS AND THEORETICAL BACKGROUND

The following theoretical background is reviewed from textbooks and literature on rock and soil mechanics:

2.1 Applied Stress: The applied stress acting on a formation at any depth is the weight of the overburden load that the formation supports at that depth. This weight is jointly supported by both the formation grains and the reservoir fluids:

$$P_{ob} = \sigma + P_p \qquad 2.1$$

where P_{ob} = Overburden pressure

σ = Intergranular stress

P_p = Pore pressure.

The overburden pressure is also equal to the total weight of the overlying rocks and fluids. Thus:

$$P_{ob} = [(1-\phi)\rho_g g + \phi\rho_f g]D \qquad 2.2$$

where ρ_g = average grain density

ρ_f = average fluid density

D = Depth of formation

g = acceleration due to gravity

ϕ = porosity.

Average overburden pressure gradient is commonly assumed to be 1 psi/ft. The value can be less in young sediments. In the Gulf Coast area an average gradient of 0.85 psi/ft has been established (Eaton, 1968).

2.2 Formation Elastic Constants

2.2.1 Modulus of Elasticity (Young's Modulus), E, is defined similarly for rocks as for metals. It is the ratio of longitudinal stress to longitudinal strain in an elastic deformation. It can be determined in the laboratory by the triaxial testing machine or by acoustic velocity measurements. Young's modulus of rock is discussed in detail in section 3.3.1.

2.2.2 Bulk Modulus, K. Formation bulk modulus is the ratio of effective hydrostatic pressure acting on the formation to the resulting volumetric strain $\frac{\Delta V}{V}$ on the formation. It is also the inverse of total compressibility, $\frac{1}{c_b}$. Volumetric strain is the sum of strains in the three principal directions:

$$\frac{\Delta V}{V} = e_1 + e_2 + e_3 \qquad 2.3$$

2.2.3 Modulus of Rigidity (Shear Modulus), G, is defined as the ratio of shear stress to shear strain.

$$G = \tau/\gamma \qquad 2.4$$

where τ = shear stress

γ = shear strain.

2.2.4 Poisson's Ratio, ν, of a formation is the ratio of the lateral extension to longitudinal contraction under a longitudinal compressive stress. It ranges in value between 0 and 0.5 for rocks. For example, typical values of Poisson's ratio for shale are between 0.01 and 0.15; for consolidated sand, sandstone, and limestone, between 0.15 and 0.27; and for unconsolidated sand, between 0.28 and 0.45.

The different elastic constants are related as expressed below:

(i) $G = \frac{E}{2(1 + \nu)}$

(ii) $K = \lambda + \frac{2}{3} G$

where $\lambda = \frac{\nu E}{(1 + \nu)(1 - 2\nu)}$ 2.5

(iii) $\nu = \frac{\lambda}{2(\lambda + G)}$

(iv) $E = \frac{G(3\lambda + 2G)}{\lambda + G}$.

Poisson's ratio for a rock material can be obtained in the laboratory, either directly from triaxial tests or from acoustic velocity measurements. From Hooke's law, the stress-strain relationship in a triaxial cell is

$$e_{ij} = \frac{1 + \nu}{E} \tau_{ij} - \frac{\nu}{E} \delta_{ij} e_{kk} \quad 2.6$$

where ν = Poisson's ratio

δ_{ij} = Kronecker delta

$$\left(\delta_{ij}\begin{cases} = 1 \text{ if } i = j \\ = 0 \text{ if } i \neq j \end{cases}\right)$$

τ_{ij} = stress tenor

e_{ij} = strain tensor

and $e_{kk} = e_{11} + e_{22} + e_{33}$.

In the triaxial test,

$$\tau_{ij} = \begin{bmatrix} \sigma_x & 0 & 0 \\ 0 & \sigma_y & 0 \\ 0 & 0 & \sigma_z \end{bmatrix} \qquad 2.7$$

and the above equation when expanded becomes:

$$\begin{aligned} e_x &= \frac{1}{E}\left[\sigma_x - \nu(\sigma_y + \sigma_z)\right] \\ e_y &= \frac{1}{E}\left[\sigma_y - \nu(\sigma_x + \sigma_z)\right] \\ e_z &= \frac{1}{E}\left[\sigma_z - \nu(\sigma_x + \sigma_y)\right] . \end{aligned} \qquad 2.8$$

Both compressional and longitudinal acoustic-wave velocities are related to the formation elastic constants by

$$V_p = \sqrt{\frac{\lambda + 2G}{\rho}} \qquad 2.9$$

$$V_s = \sqrt{\frac{G}{\rho}} \qquad 2.10$$

where V_p = Velocity of compression wave

V_s = Velocity of longitudinal shear wave

ρ = formation density .

Combining these equations:

$$\left(\frac{V_s}{V_p}\right)^2 = \frac{(\Delta t_p)^2}{(\Delta t_s)^2} = \frac{G}{\lambda + 2G} \qquad 2.11$$

where Δt_p, Δt_s, are the travel times between two points for the compressional and longitudinal waves, respectively. Since

$$\nu = \frac{\lambda}{2(\lambda + 2G)} = \frac{\frac{1}{2} - (\frac{G}{\lambda + 2G})}{1 - (\frac{G}{\lambda + 2G})} \qquad 2.12$$

$$\nu = \frac{\frac{1}{2} - (\frac{\Delta t_p}{\Delta t_s})^2}{1 - (\frac{\Delta t_p}{\Delta t_s})^2} \qquad 2.13$$

Δt_p, Δt_s, and the time ratio $\frac{\Delta t_p}{\Delta t_s}$ can be obtained from laboratory measurements under simulated reservoir conditions. Acoustic measurements give dynamic moduli which are generally higher than static moduli. A correlation between dynamic and static bulk modulus was suggested by Towle (1976).

2.3 Rock Compaction: Petroleum accumulation in a reservoir always has a fluid pressure in the pore space. When this pressure is reduced by the withdrawal of fluid from the reservoir, a slight reservoir compaction may follow. Maximum compaction is related to change in porosity:

$$\Delta H = \left[\frac{\phi_1 - \phi_2}{1 - \phi_2}\right] H \qquad 2.14$$

where H = thickness of zone

ΔH = vertical compaction

ϕ_1 and ϕ_2 are initial and final porosities, respectively.

2.4 Mohr's Circle: A convenient graphical method for representing stresses within an element of material is a plot of shear stress on a plane as a function of normal stress. A two-dimensional construction of a Mohr's circle for a triaxial test is shown in Figure 1. Compressive stresses are assumed positive and tensile stresses are assumed negative. In Figure 1, OB and OA represent the magnitude of the major and minor principal stresses, σ_1 and σ_2 respectively. The circle is drawn on AB as diameter. The diameter also shows the magnitude of maximum stress inequality in the material. Stress at any point contained in a plane making angle θ to the direction of the major principal stress can be obtained from the Mohr's circle:

(i) $\sigma = OF = (\frac{\sigma_1 + \sigma_3}{2}) + (\frac{\sigma_1 - \sigma_3}{2})\cos 2\theta$ 2.15

(ii) $\tau = FD = \frac{1}{2}(\sigma_1 - \sigma_3) \sin 2\theta$

2.5 Mohr Failure Envelope. When enough data are available several Mohr's Circles may be constructed for different stress conditions. At failure of a rock material a Mohr failure envelope can be drawn to these Circles as shown in Figure 2. This envelope is symmetrical about the x-axis and characterizes the material.

When the normal and shear stresses give a circle that plots within the envelope, no failure can be expected. However, if the circle extends outside the envelope, failure occurs. Mohr failure envelope for a perfectly elastic cohesionless material is represented by two straight lines that intersect at the origin. The envelope follows a curved path in the case of a granular sedimentary formation.

2.6 Fundamental Stress Equations: Biot (1941) described soil consolidation as a process of adaptation of formation to load variation. Load variation can be experienced in the life of an oil reservoir either as a result of varying borehole pressure in drilling and completion operations or due to fluid withdrawal from the reservoir. The stresses acting at any point are obtained by considering a diminishing microscopic boundary condition in a macroscopic framework of the formation. These can be represented by a second rank tensor. There is generally a symmetry of stresses at any point in the formation.

2.6.1 Equations of Equilibrium: the stress field in a given system at any point satisfies the equation of equilibrium:

$$\tau_{ij,j} = - F_i \quad . \qquad 2.16$$

Where expanded, this becomes:

$$\text{(i)} \quad \frac{\partial \tau_{xx}}{\partial x} + \frac{\partial \tau_{yx}}{\partial y} + \frac{\partial \tau_{zx}}{\partial z} = - F_x$$

$$\text{(ii)} \quad \frac{\partial \tau_{xy}}{\partial x} + \frac{\partial \tau_{yy}}{\partial y} + \frac{\partial \tau_{zy}}{\partial z} = - F_y \qquad 2.17$$

$$\text{(iii)} \quad \frac{\partial \tau_{xz}}{\partial x} + \frac{\partial \tau_{yz}}{\partial y} + \frac{\partial \tau_{zz}}{\partial z} = - F_z$$

F_x, F_y and F_z are the component of the body force.

2.6.2 Equations of Compatibility: Continuity of displacement is maintained throughout the material under a stress system. The following equations are therefore satisfied:

$$e_{ij,kl} + e_{kl,ij} - e_{ik,jl} - e_{il,jk} = 0 \quad . \qquad 2.18$$

This can be written out as:

$$\text{(i)} \quad \frac{\partial^2 e_{yx}}{\partial y\ \partial z} = \frac{\partial}{\partial x}\left[-\frac{\partial e_{yz}}{\partial x} + \frac{\partial e_{zx}}{\partial y} + \frac{\partial e_{xy}}{\partial z}\right]$$

$$\text{(ii)} \quad \frac{\partial^2 e_{yy}}{\partial x\ \partial z} = \frac{\partial}{\partial y}\left[-\frac{\partial e_{zx}}{\partial y} + \frac{\partial e_{xy}}{\partial z} + \frac{\partial e_{yz}}{\partial x}\right]$$

$$\text{(iii)} \quad \frac{\partial^2 e_{zz}}{\partial x\ \partial y} = \frac{\partial}{\partial z}\left[-\frac{\partial e_{xy}}{\partial z} + \frac{\partial e_{yz}}{\partial x} + \frac{\partial e_{zx}}{\partial y}\right] \qquad 2.19$$

$$\text{(iv)} \quad 2\frac{\partial^2 e_{xy}}{\partial x\ \partial y} = \frac{\partial^2 e_{xx}}{\partial y^2} + \frac{\partial^2 e_{yy}}{\partial x^2}$$

$$\text{(v)} \quad 2\frac{\partial^2 e_{yz}}{\partial y\ \partial z} = \frac{\partial^2 e_{yy}}{\partial z^2} + \frac{\partial^2 e_{zz}}{\partial y^2}$$

$$\text{(vi)} \quad 2\frac{\partial^2 e_{zx}}{\partial z\ \partial x} = \frac{\partial^2 e_{zz}}{\partial x^2} + \frac{\partial^2 e_{xx}}{\partial z^2} \quad .$$

The rest of the expansions are either taken care of by symmetry or some repetition of the above. With adequate boundary conditions,both the equations of equilibrium and compatibility can be combined to give solution to stresses in a given system. A stress function Φ satisfies the biharmonic equation:

$$\frac{\partial^4 \Phi}{\partial x^4} + \frac{\partial^4 \Phi}{\partial x^2 \partial y^2} + \frac{\partial^4 \Phi}{\partial y^4} = 0 \qquad 2.20$$

Φ is known as the Airy's stress function.

Chapter 3

LITERATURE SURVEY

3.1 Introduction: Most of the unconsolidated sediments of the earth's crust are composed mainly of solid mineral particles derived from the physical and chemical weathering of rock and varying amounts of moisture, organic matters, air, and other gases. Terzaghi (1943) defined soil as "those sediments and unconsolidated accumulation of solid particles produced by the mechanical or chemical disintegration of rocks." Like inorganic and non-plastic silt, sand falls into the category of unconsolidated sediments which is composed only of those particles derived from primary minerals.

The behavior of soil is largely influenced by its structure and composition. A small percentage of extremely fine-grained soil can dominate and effectively control the behavior of mixed soil. Unconsolidated sands are generally referred to as single-grain structured. Individual grains or particles have definite sizes and shapes which collectively form a continuous, relatively incompressible solid framework, as compared with fine-grained or colloidal soil. Fluid saturation plays an important part in the behavior of a sand body. Overburden load is jointly supported by both the formation grains and the reservoir fluids, as discussed in Section 2.1.

Rock compressibility is greatly affected by fluid saturation. Three types of compressibility commonly defined in the petroleum industry were described by Geerstma (1957). Formation strength is derived from inherent tensile strength, cohesive strength, and the shear resistance due to internal friction between grains. The formation and stability of arches in loose sand depends on the level of confining stresses and the existence of cohesive forces within the sand body.

Analysis of stresses in soil is usually based on the theory of elasticity. However, there have been suggestions as to the inaccuracies of this assumption as applied to unconsolidated sediments. Harrison, et al. (1954) observed that failure in much of the earth's crust is governed by "non elastic properties, the shear strength, cohesiveness, and the frictional resistance to deformation." These authors suggested that weaker formations that lie below relatively shallow depths exist in the plastic state. Gassmann (1951) stated that the behavior of "polyphase systems," such as porous solids or loose aggregate of grains whose pores are filled with liquids or gases, deviates considerably from perfect elasticity. The deformations caused by small variations in stress, as experienced under elastic-wave propagation, are, however, reversible and can be considered elastic. Dealing with deformation around a wellbore in an oil well, Scot, et al. (1953) suggested that a material in a thick-walled cylinder may only yield partially so that a plastic region is surrounded by a region stressed below the limit of plasticity. Gnirk (1972) also based his analysis of stresses around the borehole on this assumption.

Other factors that affect the behavior of unconsolidated sands include creep and relaxation effects which are due to the viscoelastic properties of the formation. Creep effect shows an increase in strain with time for a constant load or stress, while stress relaxation is the phenomenon in which the stress decreases with time for a constant strain. Cyclic effects have also been reported for a number of experiments with formation sand (Carpenter, et al., 1940; Hughes, et al., 1953; and Fatt, 1958).

Various factors affecting the behavior of unconsolidated sand and their effects on sand control are considered in the following section:

3.2 Compressibilities of Porous Media: The three types of formation compressibilities described by Geertsma (1957) are:

(i) Rock Matrix Compressibility, c_r. This is the fractional change in volume of the solid material per unit change in uniform pressure

$$c_r = -\frac{1}{V_r}\left(\frac{\partial V_r}{\partial p}\right)_{\bar{\sigma}} \qquad 3.1$$

where V_r = rock grain volume

and $\bar{\sigma}$ = composite or external hydrostatic stress

For all practical purposes the rock matrix compressibility may be considered constant.

(ii) Rock Bulk Compressibility, c_b, is the fractional change in the total or bulk volume of the porous rocks per unit change in stress

$$c_b = \frac{1}{V_b}\left(\frac{\partial V_p}{\partial \bar{\sigma}}\right)_p \qquad 3.2$$

where V_b = Bulk volume.

(iii) Pore Compressibility, c_p. This is the fractional change in pore volume per unit change in stress

$$c_p = \frac{1}{V_p}\left(\frac{\partial V_p}{\partial \bar{\sigma}}\right)_p \qquad 3.3$$

where $V_p = \phi V_b$

and $\phi = \frac{V_b - V_r}{V_b}$, porosity .

Two types of stress variations can be distinguished. These are: (i) the internal or pore pressure, p, variation, all external stresses being constant; and (ii) external or bulk stress variation while internal or fluid and pressure in the pores is kept constant. While internal pressure is usually hydrostatic, external stress can result from both hydrostatic fluid pressure and external stresses on rocks. External stress may therefore vary in both magnitude and direction. The three types of compressibilities are related by the following relationships:

$$\text{(i)} \quad \frac{1}{V_b}\left(\frac{\partial V_b}{\partial p}\right)_{\bar{\sigma}} = -(c_b - c_r) \qquad 3.4$$

$$\text{(ii)} \quad c_p = \frac{1}{V_p}\left(\frac{\partial V_p}{\partial \bar{\sigma}}\right)_p = \frac{1}{\phi}(c_b - c_r)$$

where $\bar{\sigma} = \frac{1}{3}(\sigma_1 + \sigma_2 + \sigma_3)$,

and σ_1, σ_2 and σ_3 are the principal stresses.

The net effective stress is $(\sigma - p)$ and the change in Net Effective Stress is $(d\sigma - dp)$.

Carpenter, et al. (1940) and Fatt (1958) measured rock compressibilities in the laboratory. Fatt determined $\frac{1}{V}\left(\frac{\partial V_p}{\partial p}\right)_{\bar{\sigma}}$ on a number of cores and obtained a correlation with "net overburden pressure". He defines net overburden pressure as $(\bar{\sigma} - 0.85p)$. This author introduced the factor of 0.85 to take account of the fact that the internal pressure does not wholly react against the external pressure. He found that pore compressibility was a function of pressure, but did not obtain any correlation with porosity. Hall (1953) designated the compressibility term $\frac{1}{V_p}\left(\frac{\partial V_p}{\partial \bar{\sigma}}\right)_p$ as the formation compaction component of the total rock compressibility. He obtained a correlation of "formation compaction component with porosity."

Rock compressibility has also been described by a number of investigators in the area of Civil and Construction Engineering as pore pressure coefficient. Bishop (1952) and Skempton, et al. (1955) used the pore pressure coefficient in estimating the stability of an earth dam. Pore pressure ratio defined by Skempton (1954) is given by the expression

$$\frac{\Delta P_p}{\Delta \sigma_1} = \bar{B} = B\left[1 - (1-A)(1 - \frac{\Delta \sigma_3}{\Delta \sigma_1})\right] \quad 3.5$$

where $\bar{B}$ is the overall pore pressure coefficient and A and B are constants defined by the equation:

$$\Delta P_p = B\left[\Delta \sigma_3 + A(\Delta \sigma_1 - \Delta \sigma_3)\right]. \quad 3.6$$

ΔP_p denotes an increase in pore pressure and $\Delta \sigma_1$ and $\Delta \sigma_3$ denote changes in the major and minor principal stresses, respectively. Bishop (1973) expressed pore pressure coefficient as:

$$\frac{\Delta P_p}{\Delta \sigma} = \frac{1}{1 + \phi(c_p - c_s)/(c - c_s)} \qquad 3.7$$

where c denotes the compressibility of the soil skeleton, c_p denotes compressibility of the pore fluid, and c_s is the compressibility of the solid grains.

The pore pressure coefficient as defined in the manner above is clearly a function of the compressibilities of the porous soil, the pore fluid, and the solid material. It is, however, not usual to present rock compressibilities in this manner in the petroleum industry.

Biot (1940) described rock compressibilities by two physical constants, H and R, related by the equation:

$$\theta = \frac{1}{3H} (\sigma_x + \sigma_y + \sigma_z) + \frac{\sigma}{R} \qquad 3.8$$

where θ is the water content in the porous material,

$$\theta = \frac{dV_p}{V_b} = \phi \frac{dV_p}{V_p} \quad . \qquad 3.9$$

σ_x, σ_y, and σ_z are the stresses in three orthorgonal directions, x, y, and z.

σ is the fluid pressure.

1/H is a measure of the compressibility of the soil for a change in fluid pressure, and 1/R is a measure of the change in fluid content for a given change in fluid pressure. A coefficient α which measures the ratio of the fluid volume squeezed out, to the volume change in rock under compaction is defined by

$$\alpha = \frac{2(1 + \nu)G}{3(1 - 2\nu)H} \qquad 3.10$$

Geertsma (1957) expressed these constants in terms of the three compressibilities earlier discussed as:

$$\text{(i)} \quad \frac{1}{H} = c_b - c_r$$

$$\text{(ii)} \quad \frac{1}{R} = c_b - (1 + \phi)c_r \qquad 3.11$$

$$\text{(iii)} \quad \alpha = 1 - c_r/c_b .$$

3.3 Behavior of Porous Media

3.3.1 Application of the Theory of Elasticity: Both the macroscopic and microscopic behavior of rock differ significantly from that of metal. As a result, concepts of Theory of Elasticity as known from experience with metals cannot be applied to rocks indiscriminately if reliable results are to be expected. Rock Mechanics is therefore based on the actual behavior of rocks, rather than adapted from the Theory of Elasticity. Fairhurst (1963) described Rock

Mechanics as the field of study devoted to the understanding of "the basic processes of rock deformation and their technological significance."

The terms "ductility" and "brittleness" are commonly used to describe yield or failure of metals. These terms are similarly applicable for rocks. Jaeger, et al. (1969) defined "ductility" as a condition under which a material under a stress load sustains a permanent deformation without losing its ability to resist the load. These authors described "brittleness" as a condition in which the ability of a material to resist a load decreases with increasing deformation. These definitions will be adhered to in the following discussion.

Stress-Strain Relationship: The mechanical properties of different types of rock have been experimentally studied in the laboratory. Axial compression of a cyclindrical sample in a triaxial cell is the most common method of testing. The elastic modulus and compressive strengths of rock are determined for design purposes. The brittle-ductile transition and the plastic behavior of rocks, especially at high confining pressure and temperature, are of much importance in geophysical activities. In all cases stress-strain relationships of the material depict the rock behavior and properties.

Three types of elastic behavior will be distinguished:

(i) Linear Elasticity

(ii) Perfect Elasticity

(iii) Simple Elastic Behavior

Linear Elastic behavior is one in which the stress and strain are linearly related:

$$\sigma = E\varepsilon \qquad 3.12$$

where σ = stress

ε = strain

and E = Young's Modulus or Modulus of Elasticity.

Most consolidated rocks fall into this category at low stresses.

Perfect Elasticity implies that stress is a certain function of strain, not necessarily linear:

$$\sigma = f\,(\varepsilon). \qquad 3.13$$

The same path of stress-strain curve is traversed during stress loading and unloading; no permanent strain is established. There is no unique Young's Modulus in this case. Two types of Young's Modulus can be defined at any particular point: Tangent Modulus at any point is the slope of stress-strain curve at that point:

$$E_t = \frac{d\sigma}{d\varepsilon}. \qquad 3.14$$

Secant Modulus at any point is simply the ratio of stress to strain at that point:

$$E_s = \frac{\sigma}{\varepsilon} \; . \qquad 3.15$$

Simple Elastic Behavior refers to the situation when no permanent strain is left in a material when the applied stress is removed. The unloading condition may not necessarily follow the same path as the loading condition. When this happens an effect known as "hysteresis" occurs. More work is done on a material which exhibits hysteresis effects during loading than is recovered during unloading. Behavior of most rocks can be approximately described by Figure 3. The figure can be divided into four regions:

(i) Region OA (slightly convex upwards)

(ii) Region AB (very nearly linear)

(iii) Region BC (concave downwards reaching a maximum at C)

(iv) A following region, CD.

The strength of a rock is determined by the value of the stress at point C_o. There is usually no permanent strain if the rock is stressed within the regions OA and AB. However, permanent strains may be established if the rock is stressed beyond point B. If a rock is restressed after it had a permanent strain, a stress-strain curve similar to OABCD is repeated along the path QRCD. This is known as "cyclic effect." Most investigators working with rock samples have observed either hysteresis or cyclic effects on stress-strain curves. Carpenter, et al. (1940) observed "cyclic hysteresis" on their experiment with Woodbine sands. Hughes and Cook (1953) reported that Berea and Stevens sandstones showed hysteresis effects. Fatt (1958) also observed hysteresis effects in those samples whose porosities were greater than 20%.

In a linear elastic material with constant Young's modulus and Poisson's ratio, volumetric strain during compression varies linearly, as a function of stress, with a positive slope. However, for most rocks a deviation from a straight line is observed. Brace, et al. (1966) state that the volumetric strain starts to deviate from a straight line when the stress reaches one-half of the strength of the rock. Relative negative volumetric strain (expansion) with increased stress is a phenomenon known as "dilatancy." Dilatancy is very important in unconsolidated sand. Hall and Harrisberger (1970) established from their experiment that dilatancy is a critical factor in the ability of a sand body to form a stable arch. Experimenting with 20-40 mesh Ottawa sand, they obtained volumetric increases of the sand during a compression test. Their result is shown in Figure 4. At low stress level, sand failure is accompanied by dilatancy. At high pressure, failure is due to crushing of individual grains. A re-arrangement of grains may result in a negative volumetric change. A transition zone exists between these two conditions. Hall and Harrisberger were able to conclude from their experiment that arch stability was only possible if the stress conditions were such that sand failure was accompanied by dilatancy. Failure criteria are discussed in more detail in Section 3.3.3.

All rocks show time-dependent effects which are known as an-elasticity or time-dependent elasticity. The stress strain curve may therefore vary with time of application of stress. The strength of a rock increases with confining pressure. This conclusion was reached by von Karman (1911) and Boker (1915). Von Karman noted a transition from a brittle behavior to a ductile behavior exists with increasing confining pressures for Carrara marble. In most rocks this transition is ill-defined. Work-hardening results at high confining stress. This is a phenomenon in which the axial stress increases steadily with stress after the yield point has been exceeded. Brittle-ductile transition occurs at lower stresses, in an elevated temperature environment. The brittle-ductile transition is therefore crucial in determining the behavior of rock in the lower earth crust which exists at elevated temperatures.

3.3.2 Application of the Theory of Plasticity. The theory of plasticity is often applied to the analysis of yield in sedimentary rocks. Actual behavior of real soil, however, differs considerably from an ideal plastic material. Nevertheless, like the theory of elasticity, this can form a theoretical basis against which actual rock and soil behavior can be measured. The onset of plasticity is that point of irreversibility in the stress-strain path. Non-linearity of the stress-strain curve does not necessarily indicate plasticity. Plasticity is generally characterized by a point beyond which permanent strains appear.

If stress remains constant from the onset of plasticity, and the strain increases, the material is described as perfect plastic. As mentioned earlier, most rocks show work hardening effects. When this happens, the stress is a certain function of strain: $\sigma = f(\varepsilon)$. Besides the deformation of the individual grains, plastic or irreversible deformation may result from friction losses due to relative motion of grains that may occur during compression. It may also result from crushing and rearrangement of grains at high stresses.

Failure condition is independent of the path of loading. The material fails under only a given set of stresses irrespective of the loading sequence that leads to this stress condition. The major application of the theory of plasticity to rock is in the failure criteria. No distinction is hereby made between "yield" and "failure" in sedimentary rocks.

3.3.3 Failure Criteria

(i) Mohr-Coulomb Criterion: Following his investigation, Coulomb (1773) suggested that the shear stress tending to cause shear failure of rock across any plane is resisted by the force of cohesion of the rock and by a constant multiplied by the normal stress across the plane:

$$\tau = \tau_o + \mu_o \sigma \qquad 3.16$$

where τ = shear stress acting along any plane

σ = normal stress acting on the plane

τ_o = cohesion

μ_o = tan ϕ.

μ_o is known as the coefficient of internal friction and ϕ is the angle of friction.

In another hypothesis, Mohr (1900) proposed that when shear failure takes place along a plane, the normal stress and the shear stress along the plane are related in a manner characteristic of the material:

$$\tau = f(\sigma). \tag{3.17}$$

It can be noted from the foregoing that Coulomb's failure criterion is a particular form of Mohr's failure theory. While Coulomb's failure criterion assumes a linear function, the generalized Mohr's hypothesis shows that the relationship between shear stress and normal stress need not be linear. This criterion is sometimes referred to as the Mohr-Coulomb failure criterion. The characteristic of the rock described by Mohr can be obtained by drawing an envelope tangential to Mohr's Circles corresponding to failure condition of the rock at different stresses. The intermediate stress is not of any consequence in constructing a Mohr's Circle. However, it is assumed that the fracture plane contains the direction of the intermediate stress.

(ii) Von Mise's Criterion: Von Mise's criterion of failure is most commonly used, and is adequate for most problems on metals. It is also known as the Maximum Distortional Strain Energy Failure Criterion; and it applies mainly to failure in the plastic region. Von Mise's criterion is applied to rock at high confining pressure and temperature. As mentioned earlier, for this condition, most rocks exhibit ductile behavior similar to metals.

This criterion maximizes the function:

$$\text{Max}\ (V) = (\sigma_2 - \sigma_3)^2 + (\sigma_3 - \sigma_1)^2 + (\sigma_1 - \sigma_2)^2$$

$$\text{and}\ V = 2\sigma_0^{\,2} \qquad 3.18$$

where σ_0 = yield point

and σ_1, σ_2, and σ_3 are the principal stresses.

The strain Energy of Distortion = $\frac{\sigma_0^{\,2}}{6G}$

where G is the Bulk Modulus.

Various modifications of the Von Mise's failure criterion have been used by different investigators. Stassi-D'Alia (1959) used the following modified form:

$$(\sigma_1 - \sigma_2)^2 + (\sigma_2 - \sigma_3)^2 + (\sigma_3 - \sigma_2)^2$$

$$= 2(C_0 - T_0)\ (\sigma_1 + \sigma_2 + \sigma_3) + 2C_0T_0 \qquad 3.19$$

where C_0 and T_0 are the yield strength in compression and tension, respectively.

Bishop (1966) described his criterion for failure as:

$$(\sigma_1 - \sigma_3) = \frac{\alpha}{3}\ (\sigma_1 + \sigma_2 + \sigma_3)$$

$$\text{and}\quad (\sigma_1 - \sigma_3)^2 + (\sigma_2 - \sigma_3)^2 + (\sigma_3 - \sigma_1)^2 \qquad 3.20$$

$$= \frac{\alpha^2}{9}\ (\sigma_1 + \sigma_2 + \sigma_3)^2$$

α is a constant.

3.4 Literature Related to the Petroleum Industry

A great number of the oil and gas fields around the world are producing from unconsolidated formations, with the enormous problem of sand production. The sand problem was long recognized by groundwater hydrologists from whom the petroleum industry learned the early techniques of sand control. Most of the techniques centered around mechanical processes of gravel packing. Hall and Harrisberger (1970) drew the attention of the industry to the arching behavior of a sand structure and its relevance to sand control. Arching phenomena of loose sand were by no means a new subject. Terzaghi (1943) reported that Engesser (1882), Bierbaumer (1913), Caquot (1934) and Vollmy (1937) had studied the equilibrium behavior of sand arches. Terzaghi (1936) also reported arching of stressed sandpack in his trap-door experiments. He described arching as "the ability of a material to transfer load from one location to another in response to relative displacement between the locations by the mechanism of shear stress."

Hall and Harrisberger (1970) tested samples of unconsolidated sand in a cylindrical chamber of 3-3/4 inches I.D. fitted with a hydraulically operated piston. The samples were loaded vertically in a pre-determined way over a 7/16-inch diameter trapdoor located at the bottom center of the chamber. They observed arching of the sand when the trapdoor was removed. Hall and Harrisberger also investigated the stability of the arch to fluid flow and changing load. They conducted a series of tests with well-rounded 20-40 mesh Ottawa sand, angular 20-40 mesh Arkola sand, and Miocene sands. They varied the initial saturation, fluid flow and loading conditions. They observed that the stability of the arches required some restraints on the grains forming the inner free surface of the arch. These restraints were provided by the cohesive force resulting from the interfacial tension between pore fluids. They reported that the wetting phase should be in the pendular flow regime for the interfacial tension to develop. They also observed that the arch formed by the more angular sands failed with grain crushing under loads at lower stresses. They concluded that dilatancy and cohesiveness are necessary conditions for the stability of a sand arch.

Stein and Hilchie (1972) assumed that the stability of a friable sand required the formation of a stable sand arch around each perforation. They considered that the pressure drop of the flowing fluid was the major factor affecting the stability of any sand arch. They conducted a production test on one well, and used this as a standard against which other wells in the area were measured. The test consisted of a series of increasing production rates, and "equivalent reservoir pressure drawdown," to a critical point where "sand production became excessive, and would not stop or slow down significantly with continued production." They assumed that the critical pressure drawdown, ΔP_c, would be proportional to the shear modulus of the sand. Thus the allowable pressure drawdown in any zone is related to the critical pressure drawdown in the test:

$$\Delta P_{well} \leq [\Delta P_c]_{Test\ well} \cdot \frac{G_{well}}{G_{test\ well}} . \qquad 3.21$$

Stein and Hilchie estimated the formation shear modulus by assuming that $(\lambda + 2G)$, which they referred to as the dynamic combined modulus, correlated with the rock strength. $(\lambda + 2G)$ values can be estimated from density and acoustic velocity logs:

$$\lambda + 2G = 1.34 \times 10^{10} \frac{\rho}{(\Delta t)^2} . \qquad 3.22$$

Neglecting changes in density, Stein and Hilchie plotted Δt against ΔP_c for various sands indicating 'safe', 'risky', and possible 'failure' regions. By neglecting changes in density, Stein and Hilchie did not consider the effect of pore fluid on rock bulk density and acoustic travel time. Oil and gas affect these properties differently. Density is less and travel time is greater if the pore fluid is gas rather than oil. These authors also plotted variation of $(\lambda + 2G)$ with formation depth. They assumed that at zero depth the curve must be asymptotic to the bulk modulus.

From the relationship: $\lambda + 2G = K + 4/3\ G$, they equated the difference between $(\lambda + 2G)$ values at any depth and the asymptotic value at the surface to $4/3\ G$.

In a follow-up, Stein, et al. (1973) estimated the shear modulus differently by assuming that the maximum pressure gradient at each arch face for sandfree production was proportional to the strength of the sand:

$$\frac{dp}{dr} = \frac{qB\mu}{1.123E\text{-}3kAN} \propto G \qquad 3.23$$

where N is the number of perforations. They therefore related the allowable pressure gradient of a well to that of a test well assuming:

$$\frac{\left[\frac{dp}{dr}\right]_{well}}{\left[\frac{dp}{dr}\right]_{Test\ well}} = \frac{[qB\mu]_{well}}{[qB\mu]_{Test\ well}} \cdot \frac{[kAN]_{Test\ well}}{[kAN]_{well}} \qquad 3.24$$

The sand control research of the Colorado School of Mines started with the work of Tippie in 1973. Tippie used a semi-cylindrical cell with simulated 4-inch casing made of plexiglass. The casing simulator was removable so that arch structures could be physically examined at the end of each test. Tippie conducted his tests at 260 psi overburden load on a 20-40 mesh Gopher State frac sand, flowing mineral spirits. He found that the initial arch size was a function of the initial producing rate. Based on this work Tippie and Kohlhaas (1973) reported that arch growth is a function of flow rate and initial arch size, and that a critical flow rate and arch size exist below which a stable arch can form. They also noted that terminal arch velocity decreases as stable arch size increases. Tippie and Kohlhaas (1974) concluded that fines migration contributes to arch instability.

Based on his interpretation of sand arch experiments of Hall, et al. (1970), the concepts of stress equilibrium around a wellbore, and field observations, Suman, Jr. (1975) presented methods of stabilizing unconsolidated sand in an oil field. He described arch behavior as a function of increasing loads categorized into four ranges. Range I is at low arch loads. Range II is at somewhat greater loads, while Range III is at greater loads than Range II. Range IV is greater loads than Range III. In Range I dilatant action of the sand body dominates, and only 'very tenuous' arches form. Dilatant action also occurs in Range II. Arches formed in this range are rate sensitive and fail with the expansion of the inner row of sand grains, followed by rolling and sliding motion between grains. Suman, Jr.,suggested that some of the experiments of Hall, et al. (1970) and those of Tippie (1973) were conducted with arch loads in this range. Arches formed in Range III are stable, with interlocked sand grains. According to Suman, Jr., arch failures in this region are accompanied by grain shearing rather than dilatancy. He suggested that loads in Range IV are large enough to cause the failure of the arch by crushing the inner row of sand grains, and no arch can possibly exist in this range. The behavior of a producing well will depend on the effective load due to a combination of the effects of pressure draw-down and the initial loading condition. Suman, Jr. proposed a relationship for mud pressure during drilling or workover operations such that the mud pressure P_m is high enough to prevent dilatant action of the sand or shear crushing without causing a formation breakdown:

$$P_m \geq \frac{F_p - P_p}{k + \frac{1-k}{2}} + P_p \quad , \quad k = \frac{1 + \sin\phi}{1 - \sin\phi} \qquad 3.25$$

where k is the ratio of the maximum to minimum principal stresses in a dry and cohesionless sand. F_p is the formation breakdown pressure and P_p is the formation pore pressure. Suman, Jr. also suggested that dilatation disturbs tenuous cementation of clay material and other particles causing fine mobility and the resulting productivity impairment. He proposed the installation of inflatable packers to adjust the stresses around the wellbore in a manner that will ensure an arch load in the stable region, as a long term stability control.

Cleary (1978), Melvan (1978), and Wood (1979) used the equipment described in Chapter 4 in their experiments. Cleary and Melvan continued the work of Tippie at higher stresses while Wood investigated the effects of sand sizes and sorting on arch stability. Cleary and Melvan used the 20-40 mesh Gopher State frac sand that Tippie used. They conducted their experiments concurrently flowing mineral spirits and kerosene in a stressed sandpack. They were the first to monitor stresses within the sandpack during a test. They observed that the behavior of sand arches around the perforation was reflected by stress variation within the sandpack. Cleary, Melvan, and Kohlhaas (1979) confirmed the formation of an arch by unconsolidated sand. They observed that the stability of the arch increased while cavity size decreased with increasing stress. They also noted two modes of arch instability which include an initial restructuring and a total arch failure.

Wood used various mixtures of 20-40 and 80-100 mesh Gopher State frac sand and flowed kerosene through a stressed sandpack. He observed that grain sizes have no influence on the ability of unconsolidated sand to form a stable arch. In his experiments the arches formed at flow rates of ½ to 2 barrels per day and failed at flow rates of 5 to 10 barrels per day.

Recently, Bratli and Risnes (1979) also reported a study of the arching behavior of 20-40 and 80-100 mesh Ottawa sand under stresses due to flowing fluid. They flowed air and oil vertically through a stressed sandpack in a steel cylinder with a central hole at the bottom. Their observations were quite similar to those of Cleary and Melvan. They also distinguished between two modes of arch failures. They found that thin inner shells of arch collapsed several times before a total arch failure occurred. They developed a theoretical stability criterion for spherical arches in their model:

$$\frac{\mu Q}{4\pi k_c R} \leq \left(\frac{T+1}{T}\right) 4 S_o \tan\alpha \qquad 3.26$$

where $T = 2(\tan^2\alpha - 1)$

and $\alpha = \pi/4 + \phi/2$

ϕ is the internal friction angle of the sand,

So is the shear strength of the sand,

k_c is the permeability of the sand arch, and

R is the radius of the inner arch structure.

They proposed that both modes of failure occurred in their model when:

$$\left(\frac{T + 1}{T}\right) 4So \tan\alpha > \frac{\mu Q}{4\pi k_c R_1} > \frac{k_e}{k_c}\left(\frac{T + 1}{T}\right) 4So \tan\alpha \qquad 3.27$$

where k_e/k_c is the ratio of the effective permeability of sandpack to the reduced permeability in the arch.

It is clear from the foregoing that most of the experimental works that are reported in the literature were conducted with well-rounded 20-40 and 80-100 mesh sands. Hall and Harrisberger (1970) did most of their studies with the 20-40 mesh Ottawa sand and only very limited studies were conducted with the angular sands. This thesis has extended the study of arch stability and failure behavior to unconsolidated natural sands. Rate effects as well as pressure drop effects have been studied and reported. Tests have also been conducted with a mixture of equal parts of 20-40 and 80-100 mesh Gopher State frac sand which answer questions raised from previous works, and show the effect of water production on arch stability.

Chapter 4

DISCUSSION OF EQUIPMENT

4.1 The equipment used in this study was designed to simulate a reservoir formation and the environment of a cased perforated wellbore. A simple transformation of the cell geometry will duplicate actual field conditions. The main body of the equipment shown in figure 5 is a cylindrical pressure cell made of solid steel and mounted on a structural steel frame that enables it to rotate around a horizontal axis. Any position of the cell can be maintained by two winches holding it. A vertical position was maintained during all tests. The cell has an external diameter of 30 inches, an internal diameter of 16 inches and a length of 87 inches. About 52-3/4 inches of the length is available during tests for the sandpack. Two plexiglass view ports, 8 inches in diameter, are symmetrically located on the flow outlet side of the cell. They are located 24 inches apart and include ½-inch bores simulating perforations. The view ports have the same thickness as the cell, with 2-inch arc sections machined into their inside ends. The section adjoins a similar plexiglass section inside the cell, spanning a total length of 32 inches. The section simulates casing in the well. Five inlet ports are lined up symmetrically on the opposite sides of the cell such that the inlet and outlet ports are along a diameter of the cell. Only the middle three ports were used during the tests. A 2-inch diameter steel screen was glued over each inlet port, inside the cell. This functioned as a flow diffuser. Four ports are also symmetrically located on the top and bottom of the cell for desaturating the cell. Six other ports symmetrically located on either side of the flow ports are designed for instrument probing of the cell. One of these was used for the leads of the strain gauges.

A complete assembly of the cell includes two hydraulic jacks or rams, held by two buttress-threaded end caps on either end of the cell. These and other features of the equipment are further discussed below.

4.2 Hydraulic Rams

The hydraulic rams were designed to apply stress load on the sandpack. The hydraulic system is complete with a Sprague pneumatic/hydraulic pump. This air operated device pumps hydraulic fluid into the inner chamber of the rams at increasingly higher pressures. The amount of fluid being pumped into each ram can be checked by a set of control valves along the hydraulic fluid flow line. The fluid pressure displaces an 11-inch-diameter piston which transmits the pressure onto the sandpack. Attached externally to the piston of each ram is a 1½-inch-thick steel plate, 16 inches in diameter, held by a single flat-head allen bolt. This ensures that the pressure or stress is applied over the whole area of the sandpack. The inner chamber of the ram is complete and sealed with a cover plate held to its body by nineteen allen-head ½-inch bolts. The ram is basically designed to operate at a maximum fluid pressure of 10,000 psi. (However it was found that owing to the limitations imposed by the inadequate strength of the bolts, the maximum operating pressure should not exceed 7,500 psi.) A system of relief valves ensures that the fluid pressure does not exceed 10,000 psi. The pressure is also relieved from a small hole on the side of the rams, if the piston tries to extend beyond 3½ inches. This offers a protection against shear failure of the bottom part of the rams. Two O-rings are placed around the rams to ensure adequate pressure seal between the cell and the rams.

4.3 Stress Transducers

Five new diaphragm stress transducers were constructed using Micro-Measurement's 'JB' pattern strain gauges. The gauges were mounted in aluminum housings in a manner similar to that used by Melvan. New aluminum housings were manufactured in order to ensure adequately clean mounting surfaces. They are cylindrical in shape, 2½ inches diameter by 1¼ inches high. A hollow concentric circular section is drilled on one end to a depth of 1 inch leaving a diaphragm thickness of ¼-inch. The gauges were glued and protected according to the manufacturer's specifications. Each housing is complete with an O-ring-sealed stainless steel cap screwed onto it. The center of the cap is threaded for easy attachment to an adaptor. Three transducers are arranged orthogonally on ½-inch adaptors. An ½-inch diameter stainless steel feeder tube runs on the side of the cell and bends midway to position the transducers in the middle of the cell, one pointing in the vertical direction and the two others in perpendicular horizontal directions.

The transducers were calibrated while imbedded in a wet sand in a small calibration cell designed by Melvan. The cell was loaded during the calibration by a soil testing machine located at the Earth Mechanics Institute.

4.4 Flow System

The flow system includes two pumps that can be alternately used, and may also be simultaneously used with little modification to the flow network. One of them is a double-plunger type positive displacement, Penwatt Corporation's Wallace and Tiernan Series 150A Metering Pump, with a Reeves variable-speed drive, 3/4 horsepower motor, equipped with 1-inch-diameter plungers. Manufacturer's manual shows that it is capable of delivering 43.4 barrels per day of water at a maximum discharge pressure of 190 psig. The other pump is a positive displacement Moyno type pump equipped with a 7½ horsepower Reeves variable-speed motor, capable of delivering water at high rates at a maximum discharge pressure less than 400 psig. Both pumps were used at different times during the experiments.

The flow line includes a bypass to regulate how much flow goes through the cell. The flow rate was monitored by a differential pressure transducer connected to pressure points tapped along two horizontal 49-inch tubings through either of which the liquid can flow downstream. The tubings are 1/8-inch and ¼-inch in diameters and are used for low and high flow rates, respectively. The smaller tubing was calibrated for flow rates below 8.5 barrels per day and the bigger tubing was calibrated for flow rates up to 55 barrels per day. The transducer was connected through a pressure demodulator to a Honeywell strip chart recorder. The flow rate was calibrated by timing measured volumes with the corresponding pen position on the recorder. The demodulator adjustments were kept at fixed positions during the calibration and throughout the tests.

4.5 Pressure Monitor

Two Data Instrument pressure transducers were located at the inlet and outlet of the cell to monitor the inlet and outlet pressures, respectively. The inlet transducer had a 500-psi range and the outlet transducer had a 100-psi range. Both transducers were connected to Honeywell strip chart recorders with which they were previously calibrated. The pressure calibrations were established with a deadweight tester. All the calibrations are shown in figures 6 through 12.

4.6 Fluid Injection

A second Wallace and Tiernan plunger metering pump was available to inject water into the cell in order to establish some water saturation in the area around the perforation and thereby ensure a pendular water saturation during the test. This procedure was established by Cleary and Melvan. However, the injection of water was not found necessary to establish an arch or a cavity in tests with natural sands. The use of the pump was limited to the tests with Gopher State frac sand.

4.7 Separator

The 'separator' is a 2½-inch-diameter 18-inch-long plexiglass tube connected to the outlet of the cell.

Connection is made to the side of the tube. The axis of the tube, while connected, is positioned in the vertical direction. The 'separator' catches any produced sand and water and facilitates a free flow of fluid. The produced sand during any test was emptied from the separator before the next test to prevent mixing up the sands. The sand in each case was examined, dried and analyzed for grain size distribution. Tests were terminated when the produced sand was so excessive as to fill the separator completely and plug the flow line.

Chapter 5

DESCRIPTION OF THE SAND SAMPLES

5.1 The experiments are divided into four groups: A, B, C, and D; each using different types of sand. In the Group A tests a mixture of equal parts of 20-40 and 80-100 mesh Gopher State frac sand was used. Three different natural sand samples containing clay materials were used in test Groups B, C, and D. The different sands will henceforth be referred to as sands A, B, C, and D, respectively. At the start of this work, a large number of natural sand samples were collected from various gravel pits at outcrops around the Golden area. Preliminary permeability tests were conducted on all the samples. Sands B, C, and D were selected because they demonstrated sufficient and highest permeabilities among the samples tested. Coarser grains than 20-mesh size were removed from the natural sand samples subsequently used. This improved the sand homogeneity and permeability.

Comparative sieve analyses of the samples are shown in table 1 and figure 13. Although sand A included grain sizes between 20-mesh and 170 mesh, the distribution was not normal. The sand contained only 10% of 60-mesh size, 11% of 80-mesh size, 54% of 40-mesh size and less than 8%

greater than 100-mesh. In contrast, the grain sizes of each of the natural sand samples varied between 20-mesh and smaller than 400-mesh and closely approximated a normal distribution. The figure shows that sample B was better sorted than either samples C or D. Statistical parameters of the samples are shown in table 2.

Clay analysis was obtained on all natural samples by x-ray diffraction at the Amoco Production Company Laboratory in Tulsa, Oklahoma. The estimated mineral percentages of the samples are shown in table 3. The table shows that the samples were predominantly quartz and feldspar. Various traces of clay minerals including illites, montmorillonite, and kaolite, were present which totalled about 1% by weight of the samples. This was consistent with the sieve analysis which showed about 1% by weight finer than 200 mesh in all the samples. A small quantity of mica was optically detected in all the samples. Opaque magnetic minerals were also present in quantities too small to measure. About 3% actinolite was detected in sample B. A chemical analysis of the fines (170-mesh and smaller) was also obtained independently. The results are shown in table 4. The table shows elemental constituents obtained by x-ray fluorescence. Silicate clay minerals like illites and kaolite are grouped under SiO_2. The results also agreed with the x-ray diffraction analysis.

Triaxial tests were conducted on dry and wet specimens of all the natural sand samples at different confining pressures between 50 psi and 2000 psi. The Material Testing System equipment located at the Earth Mechanics Institute was used. The essential features of the set-up are shown in figure 14. The equipment is complete with an automatic recorder. (Reduced copies of the test printouts for tests with wet sands are included in the last two pages of this thesis). Stress-strain relations obtained from the tests are shown in figures 15 through 17. The levels of yield stresses increased with increasing confining pressures; and plastic yield was evident in all cases. Points of sudden sand failures are indicated on the figures. Mohr failure envelopes of the samples have been constructed, and are shown in figures 18 through 20, showing a pronounced plasticity in sand C. In all cases the dry samples showed evidence of grain crushing at the failure points indicated. The levels of cohesion in all the natural sands were about equal.

Chapter 6

EXPERIMENTAL PROCEDURE

6.1 Sand A was packed in fresh water. Sands B, C, and D were packed in brine solution of 250 grams of NaCl per liter of water because of the clay minerals they contained. This provided adequate salinity to minimize clay expansion in water without much problem of salt precipitation. The aqueous phase in all the tests will henceforth be referred to as simply water. The following procedures apply to all cases.

6.2 Loading of Cell

There is no major difference between the loading procedure used here and that previously used by Cleary, Melvan, and Wood. The step-by-step procedure is contained in Cleary's (1978) and Melvan's (1978) theses. Essentially, the cell was loaded in the upright position with the lower ram and end cap in place. Large quantities of sand and water were measured out in excess of what were required. The amounts left at the end of the loading process were also measured, so that the amounts used could be accurately estimated. During loading, the sand saturated with water was carried in buckets, and loaded as a slurry into the cell. The sandpack was continually tapped as loading progressed to eliminate trapped air and ensure a homogeneous packing. Precautions were taken to ensure adequate compaction around the strain gauges without damaging them. The cell was packed to about 5 inches below the ram seat. The cell thread was cleaned and excess water removed from it. This was measured along with the unused water. The upper ram and end cap were then positioned to complete the process.

6.3 Desaturation

During this process the water saturation of the sandpack was reduced from 100% to "irreducible" by displacement with kerosene. The kerosene was injected at low rate through a saturation valve located in the top part of the cell. The displacement fluid was produced from a similar valve in the lower part of the cell. A hydrostatic pressure head was maintained through a standpipe to prevent any gravity drainage in the cell. This desaturation process continued until the water cut in the produced fluid was less than 1%. This usually took 15 to 24 hours. The total amount of water produced in this process was also measured.

At this stage, all flow lines and the hydraulic fluid lines were connected. The strain gauges, the transducers and the differential transducer calibrated to measure the flow rate were connected to the various Honeywell strip chart recorders. The procedure up to this point was followed at the beginning of each group of tests after a new sand had been loaded into the cell. The following are test procedures for each group of tests.

6.4 Stress-Loading

The application of stress load on the sandpack was achieved by pumping hydraulic fluid Super-21 into the hydraulic-jack rams using the pneumatic pump. This applied pressure on the sandpack equivalent to the hydraulic line pressure, reduced by the ratio of the piston to ram bottom plate areas. In order to achieve a mid-cell grain-to-grain vertical stress of 2250 psi, the hydraulic line pressure reached about 9000 psi. All attempts to load the sandpack to 3000 psi vertical stress failed. The nineteen bolts holding each of the rams failed on two occasions. On two other occasions the single flat-head allen bolt holding the ram lower plates failed. As a result, the maximum vertical midpoint grain-to-grain stress attainable was 2250 psi. Even this level was unattainable in sand C; the maximum in sand C was 1960 psi. Sand A was tested only at an initial vertical mid-cell stress of 1500 psi, while other sands were tested at 500, 750, 1000, 1500, and 1800 or 2500 psi.

The bypass flow line valve was kept opened and kerosene was flowed at low rate, as stress load was being applied on the sandpack. This prevented both excessive pressure build-up inside the cell and backflow of the sand. Damage to the flow diffuser screen, glued over the inlet ports, was also prevented. During the stress-loading process the hydraulic fluid was continuously pumped into the rams until the required stress level was reached. At very high stresses it was sometimes necessary to stress continually over a 24-hour period or more to reach the desired stress level.

6.5 Test Runs

During the various tests, the inlet and outlet pressures, the flow rate, and the three orthogonal stresses midway in the sandpack were continuously recorded on strip charts. The two types of pumps were used at different times during the experiments. The tests were started with the positive displacement, double piston pump, and continued with the Moyno pump, after a breakdown during the Group B tests. The pump was operated at maximum capacity. Inlet pressure to the cell was varied by adjusting the bypass valve. In most cases, tests were started at low inlet pressure - achieved by fully opening the bypass valve. A particular inlet pressure was maintained until a constant flow rate was reached. In some cases, rate decline followed a brief period of constant rate. This was believed to result from increasing skin effect owing to the migration of fine sand and clay. The inlet pressure was increased after flow became stable or as soon as a flow decline was observed. The sand behavior around the perforation was continually observed through the lucite port. Arch failures were monitored on the recorders by pressure changes. All the parameters being recorded were affected by a major arch failure. Minor arch failures and restabilization were monitored by the strain gauges.

Tests were conducted beyond points of arch failures, unless excessive sand was produced that could not be handled without terminating the test. Tests would normally continue until the bypass valve had been completely shut off and the maximum pump pressure was imposed on the cell. When the sand arch had been essentially stable in a test, a follow-up test was started at the maximum pressure. Also when skin effects were evident in a test, a back-flow was found necessary to clean up areas around the perforation before the next test.

Chapter 7

DISCUSSION OF RESULTS

7.1 Cleary (1978), Melvan (1978), and Wood (1979) reported that during their experiments, cavities developed at the perforation and extended upwards. The exact cause of this was not specified but may be due to asymmetry of stress application on the sandpack, flow of injected water in that direction, or gravity effect. Test AI conducted with a mixture of equal parts of 20-40 and 80-100 mesh Gopher State frac sand, was carried out to clarify this point. Fluid was flowed through the lower perforation instead of the upper perforation as in the previous experiments. It was expected that if the cavities had grown upward in the previous tests as a result of asymmetry of stress application, this arrangement would shift the stress asymmetry toward the bottom of the cell, and thereby cause the cavity to extend downward. About 200 cc of water, which was injected before the test to create a pendular saturation around the perforation, was bled downwards. Thus, if the direction of cavity growth had reflected the direction of pendular saturation, this procedure should ensure that the cavity extended downwards. If despite all these procedures, the cavity still grew upwards, it would become clear that the growth was due to gravity effects. Data recorded during the tests are digitized and presented in tables 5 through 41. A summary of the observations made during the tests is included in these tables under the comment column. The following are reviews of some of the observations made during the tests:

Cavities formed and extended above the perforation in all the tests. In test AI, no major failure of the initial arch structure was observed. The recorders indicated an essentially constant sandpack stress. Test A II was a repeat of A I. It was conducted to determine how long the arch structure could remain stable. Maximum flow rate in test A I was 10.2 bbls/day but the maximum flow rate attainable in test A II was 5.23 bbls/day. The arch remained stable for 14 hours of continuous test, during which no sand was produced.

Test A III was a displacement of kerosene by water. Field experience shows that sand production becomes intense when a well starts producing water. This test was conducted to determine if the establishment of a stable arch before starting to produce water could hold back the sand. The flow was started at 0.9 bbls/day and stabilized at 0.825 bbls/day. Conditions remained stable for about 36 minutes of flow, before the first drop of water appeared in the separator. Almost immediately, sand fell into and partly filled the cavity, leaving the cavity outline still observable. Subsequently, lumps of sand were dropping out, and within a few minutes the separator was completely full of sand slurry. The flow of sand was so intense that the test had to be terminated. About 3.13 liters of water had been pumped into the cell before the test was terminated. Total arch failure was monitored on the stress recorders from the onset of water production.

The procedure in test A IV was similar to that of test A I. The test was conducted after reducing the water saturation in the sandpack to "irreducible" level, following test A III. The aim was to determine if a well that was producing water could re-establish a stable arch if the water ceases and a pendular water saturation is once more established around the perforation. The flow was started at a rate of about 0.45 bbls/day, increased gradually and stabilized at about 2.28 bbls/day. An initial cavity developed as flow started. Flow rate was increased to 2.58 bbls/day after a stable condition had been established. Sand was produced at this rate and a partial arch failure was observed on the recorders. The cavity grew as the arch restabilized. After a period of stable flow, the pump was stopped and restarted at the previous rate. The arch failed almost immediately resulting in a heavy sand production.

The flow rate increased to about 5.66 bbls/day under the same pump condition and more sand was produced. Unexpectedly, a stable arch finally re-established, and a larger cavity developed. The stable condition was maintained through an increasing flow rate reaching 8.28 bbls/day. The arch failed again at this rate and more sand was produced. Sandfree production was able to continue after the arch restabilized.

In test B I, conducted with natural sample B, arch and cavity were formed as the sandpack was being stressed. It was therefore not necessary to inject water into the cell before starting this test, as was the case in the earlier tests. Following this experience, no water was injected in the rest of the tests conducted with the natural sand samples. The test started at a flow rate of 1.3 bbls/day and a pressure drop of 15.6 psi. Cavity size increased with increasing flow rate and pressure. Sand was produced in the process, but there were no major failures during the test.

In test B II excess fluid was allowed to build up in the cell. The aim of this was to build up energy in the sandpack, similar to oil field reservoir energy, which could produce the fluid. The test was conducted to establish the feasibility of such test procedure. The outlet valve was closed when the sandpack was being stressed to 750 psi.

Although there was an indication that an arch was formed, no cavity was observed during stress loading. One horizontal stress became greater than the vertical stress as a result of a re-distribution of stress load by the arch.

With the pump shut down, the test was conducted as a bleed-off or drawdown. Although the valve was opened slowly, the sand production was heavy. This stopped after a brief period, leaving a cavity about 1 inch high and ½ inch wide. The flow rate during this test reached a maximum of 2.24 bbls/day before it started to decay gradually to 0.18 bbls/day.

Test B III was conducted to determine the stability of the arch formed during test B II. In this test cavity size enlarged to about 3 inches by 1 inch; and the arch remained essentially stable. A partial arch failure occurred as test B IV started at high pressure. The test was a continuation of test B III at higher pressures. The pop-off and check valves in the flow line that had limited pressure in the previous tests were removed before the test. However, flow impairment was severe, and flow rate only got to 9 bbls/day with 1642 psi pressure drop. Before the next test, the flowline was examined and cleaned up, and a backflow was initiated to clean any skin around the perforation. The initial arch formed in the following test failed with stresses dropping and increasing. Subsequent arch failure during the test occurred while flow rate was declining, as shown in table 13. The failure resulted from a lack of complete stability after the previous failure rather than rate or pressure effect. A major arch failure occurred in test B X at a flow rate of 3.1 bbls/day and 190 psi pressure drop. The test that preceded this, which was conducted at the same stress level of 2250 psi, was essentially stable although the flow rate reached 7 bbls/day. The major arch failure in test B X could therefore only be attributed to increasing skin effect. The failure was accompanied by sand production and a rate surge to 6.3 bbls/day. Test B XII was also conducted at 2250 psi after it was impossible to load the sandpack to 3000 psi. A partial arch failure occurred in this test following a large increase in pressure drop. Drastic reduction in the pressure and rate did not affect the arch.

The initial cavity formed in test C I (table 21) was slightly smaller than those in the previous tests. It grew rapidly with increasing flow rate to more than 4 inches high by 1½ inches wide. Three minor arch failures occurred before the flow rate reached the maximum of 30.7 bbls/day. A major arch failure occurred in test C II at a flow rate of 22.4 bbls/day and 286 psi pressure drop.

The test data are shown in table 22. The failure was caused by a combination of pressure drop, flow rate, and skin effects. It was marked by both pressure and rate surges. The cavity enlarged to more than 4 inches when conditions stabilized. The cavity width was about 1 inch. Minor arch failures occurred during all tests conducted with the natural sand sample C except test C III conducted at 1000 psi stress level. Arch strengthening or load re-adjustments were observed in tests C IV and C VIII, as shown in tables 24 and 28, respectively. It was not possible to stress the sand to 2250 psi, the highest stress level at which tests were conducted with this sand was 1800 psi. (Maximum of 1960 psi was reached when stress-loading.)

The arch structures formed during tests conducted with natural sand sample D were generally more stable than those in the other sands, and cavity sizes were smaller. The maximum flow rates established in tests D I and D II (tables 30 and 31) were 2.04 bbls/day and 4.2 bbls/day, respectively, at about 350 psi pressure drop. Both tests, conducted at 500-psi stress level, were essentially stable. A major arch failure occurred in test D III which was also conducted at 500 psi. The failure occurred at a flow rate of 2.7 bbls/day and 137 psi pressure drop. It was also marked by both pressure and rate surges. Inlet pressure dropped while the outlet pressure increased, and the rate reached 7.05 bbls/day. The cavity size also enlarged beyond the 4 inches viewing area, and was 1 inch wide. All other tests with natural sand D were predominantly stable.

Summaries of cavity and failure data in all the tests are shown in tables 42 through 45, and table 46 through 49, respectively. More general reviews of the various observations, made during the tests, are presented in the following sections.

7.2 Cavity Formation

The cavities formed as the sandpacks were being stressed when the outlet valve was opened and fluid was flowing at low rates. Cavity formation resulted from the flow of fluid through the arch. Loose sand grains within the arch structure were carried by the drag force due to the flow, thereby creating a cavity. In test B II, the cavity did not form until the flow valve was opened.

The injection of water in the group A tests helped to initiate the formation of a cavity. The injection of water was found not necessary in order to initiate cavities in the natural sand samples. This was probably due to the high levels of water saturation in these sands. A comparison between the initial saturations in all the sandpacks is shown in table 51.

7.3 Cavity Growth

In all the tests, cavities developed above the perforation and extended upwards due to gravity. Cavity sizes increased as flow rate and pressure drop across the cell increased. Increases of cavity size resulted from increase of arch sizes, erosion, or failure of the inner grains of a stable arch structure. The initial cavity size was between ¼-inch to ½-inch high by ¼-inch to ½-inch wide. The largest cavity observed extended beyond the view area and was about 1½ inches wide. The shapes of the cavities were rather irregular and narrower at the bottom in most cases. The sizes reported were the maximum dimensions. In general cavity shapes were elliptical or rectangular after a major arch failure.

7.4 Arch Formation

Arch structures were formed around the perforation in response to stress load. It was not possible to examine the arch physically without destroying it, owing to equipment design. The formation of cavities during tests was observed by previous investigators to be evidence of arch formation. This is confirmed by this investigation. Arch formation also manifested itself by the readjustment of stresses around the perforation observed during tests.

There was no substantial sand production in any test during stress readjustment; only in two cases (tests B VI and C III, tables 14 and 13 respectively) were traces of sand observed. In tests B XI and C XI, one horizontal stress decreased as the sandpack was being stressed. This was an indication that the arches formed in the preceding tests were still stable. A formation of an arch across the cell was possible because of the cell geometry. This could also have affected the stresses in this manner. In tests B II and B VI, one horizontal stress was greater than the vertical stress as the result of a redistribution of the stress load by the arch. In test B VIII the arch collapsed under increasing stress load, causing sand to be produced, and the cavity to disappear.

7.5 Arch Failure

At least one major failure occurred in every sand used. The failures are described as 'major' because of the degree of instability generated at failure. All failures were accompanied by some sand production. In major failures the quantity of sand produced was quite high. At least about half of the volume of the separator (44 cubic inches) was produced before stability could be achieved. In test A III a complete arch collapse was observed and sand production was continuous as water reached the perforation. The major arch failure in test A IV reflected a weaker arch than that in test A I. The weakness of the arch was a result of the previous major failure in test A III. All other conditions of test were similar in tests A I and A IV. Sudden pressure drop resulted in the major arch failure in test B X, causing a significant flow rate surge. In test C II, the major arch failure was preceded by increasing skin. The failure caused tremendous rate and pressure surges. A similar situation occurred in test D III. The failure in this case was caused by a combination of skin and weakness of arch resulting from repeated tests.

Minor arch failures occurred in most other tests except those with natural sand sample D. These failures were accompanied by a slight drop in at least one of the stresses - predominantly the vertical stress and cavity enlargement. Sand D was more stable than either sands B or C. Sand C was stable at high stress levels, but rather unstable at 500 psi and 750 psi. Minor arch failure occurred at every stress level in tests with sand B. Arches restabilized in all cases except in test A III where failure resulted from water production. The arch in sand B restabilized more readily.

Chapter 8

ANALYSIS OF RESULTS

8.1 The experimental results have been analyzed with a view to identifying the various factors affecting the stability and failure of the sand arches formed during the tests. A number of such factors were identified as a result of the varying conditions under which tests were conducted at the same stress levels. The relationship between the various parameters measured during the test are examined graphically in figures 21 through 33. The in situ stress-load responses of some of the sands are shown in figures 34 through 37. The observed cavity sizes have also been plotted as functions of the flow rate and the pressure drop in figures 38 through 41, and figures 42 through 45, respectively. Points of arch failures are indicated on all the plots.

The stresses measured just before arch failures have also been examined in relation to the failure envelopes of the various sands. These are shown in figures 46 through 48. The sieve analyses of the produced sand following arch failures are compared with the analyses of the original samples in figures 49 through 52. The relationship between stress load, flow rate, and pressure drop at the conditions of arch failure are examined graphically for each sand in figures 53 through 58. The maximum stress changes at failure in each sand are shown in figure 59.

Although this does not quite accurately describe the behavior of the sands, poro-elasticity theory has been reviewed in Appendix A. Bratli, et al. (1979) remarked that theory of elasticity does not reflect sand arch behavior. Plastic deformation of the sands was in fact evident during the tests, as well as during the triaxial tests of the samples. Nevertheless, poro-elasticity theory combined with the actual failure envelope of the sand are considered valid bases of comparison of the stability and failure behavior of the sand arches. In their analysis Bratli, et al. (1979) assumed that the sand behaves elastically up to the level of Coulomb's failure criterion, and that the sand arch obeys Coulomb's failure criterion. With these simplifications, they developed a stability criterion for the sand arch, discussed in Chapter 3. This criterion has been examined in relation to the behavior of sand arches in this investigation. The comparison is shown in table 53.

The analysis was facilitated by the complex transformation shown in figure 60. A relationship between pressure drop per unit strength of flow and a dimensionless arch radius are developed and presented in figures 61 and 62.

Details of the theory are discussed in Appendix C. With the same approach, the permeability of the sandpack was estimated at the various stress levels during tests. These results are presented in figure 63 for each sand. The flow potential per unit strength of flow has also been calculated and presented in figure 64. A general behavior of all the sands at arch failure conditions is obtained from the dimensionless plots shown in figures 65 through 68. The figures show plots of dimensionless functions of pressure drop against dimensionless functions of stresses in the sandpack at failure conditions.

All these are reviewed in greater detail in the following sections.

8.2 Plots of Pressure Drop Versus Flow Rate

The pressure drop measured across the cell is plotted against flow rate for the tests with each sand, as shown in figures 21 through 26. Flow rate increased gradually to a maximum for a constant pressure drop. Owing to increasing skin effect, the rate tended to decline after reaching the maximum. Only the maximum steady flow rates are considered in these plots. All the plots are approximately linear at lower pressure drops. In most cases the plots deviate from linearity at higher pressure drop due to smaller rate responses. This may be attributed to increased skin effect owing to fine deposition around the perforation. Similar plots were obtained by Holman (1975), Bratli, et al. (1979), and Penberthy, et al. (1979). The latter showed that the slope of the straight line portion increases with the uniformity coefficient of the sandpack.

Figure 21 shows the test results from the Gopher State frac sand. The slope of the line is lowest in test A I and increases through test A III. Fine migration increased as the tests were repeated. The major arch failure in test A III eliminated any flow barrier resulting from fine deposition around the arch. This resulted in the improved flow performance observed in test A IV. Figures 22 through 24 show pressure drop versus flow rate measured in the natural sand sample B. The tests conducted at 1500 psi and 2250 psi are shown in figures 22 and 23, respectively. Figure 22 shows that the plots for tests B VI and B VII are essentially parallel. This indicates that the average sandpack permeability was lower in test B VII than in B VI. In figure 23, skin effect increased in test B X compared to test B IX. The improvement in test B XII was due to backflowing before the test. Comparative plots of the test results from sand B are shown in figure 24.

Plots of pressure drop versus flow rate for tests conducted with natural sand sample C are shown in figure 25. The slope of the straight portion increased with the overburden stress on the sandpack up to 1500 psi test stress level, but decreased at 2250 psi. Similar plots are made from test results with natural sand sample D, as shown in figure 26. In all cases, initial backflow before any test resulted in some flow improvement.

8.3 Plots of $\Delta P/Q$ Versus Q

Tippie (1973) showed that $\Delta P/Q$ is a measure of the skin effect. The inverse is a measure of the effective sandpack permeability as shown in Appendix C. Log-log plots of $\Delta P/Q$ versus Q for the different sands are shown in figures 27 through 30. The plots are shown on rectilinear coordinates in figures 31 through 33 for tests B II, C V, and C IX conducted at single pressure drops. The log-log plots are linear with a slope of -1 for a constant ΔP. The directions of increasing ΔP are indicated on the figures by arrows.

Figure 27 shows that arch failures in Sand A occurred at flow rates between 1.92 and 10.2 barrels per day, and at pressure drops between 33 psi and 123 psi. Arch failures in natural sand sample B did not occur at any flow rate lower than 1.5 barrels per day nor any pressure drop lower than 129 psi as shown in figure 63. The minimum flow rate at which arch failure occurred in sand C was 0.7 barrel per day, and the highest flow rate was 36 barrels per day. Arch failures occurred in this sand at pressure drops between 20 psi and 357 psi as shown in figure 75. The only arch failure in sand D was at a flow rate of 2.7 barrels per day and a pressure drop of 137 psi.

8.4 Cavity Data

Cavity size is defined by the product of the observed average width and height of the cavity. This is plotted against flow rate and pressure drop in figures 38 through 41 and figure 42 through 45, respectively. The plots are approximately linear with positive slopes. Cavity sizes increased with flow rate and pressure drop. The maximum cavity sizes decreased as overburden stress increased, in the absence of a major arch failure.

8.5 Failure Analysis

Stresses prevailing in the natural sands just before arch failures are represented by Mohr's circles in figures 46 through 48. The figures also show comparisons with the failure envelopes of the sand. The three orthogonal stresses measured during the tests are assumed to be approximately equal to the principal stresses in the arch structures. This assumption may not be strictly correct as the principal directions would possibly change during the tests.

The figures present a valuable comparative analysis of the behavior of arch structures in the different sands. Arch failures in sands C and D occurred under conditions that would be considered 'safe' for the sand, as shown in figures 47 and 48, respectively. This demonstrated that the arches were weaker than the sandpack under the conditions of failure.

In contrast, figure 46 shows that the arch failure at 1500 psi and the major failure that occurred at 2250 psi stress level in sand B were at conditions that would also cause the sand to fail. The arches therefore had better strengths than the sandpacks under those conditions. There was no evidence of grain crushing accompanying failure in both cases. Sieve analyses of the produced sands following arch failures are compared with the original samples in figures 49 through 52. A higher-percentage of coarse grains was produced following the major arch failure in sand B as shown in figure 50. Minor arch failures in other cases occurred under conditions that would be 'safe' for the sand.

The vertical stress load at failure is plotted against flow rate and pressure drop in figures 53 through 55 and figures 56 through 58, respectively, for sands A, B, and C.

Enough failure data were not available for similar plots for sand D. The failure conditions are bracketed by the curves shown in each of figures 53 and 56, and figures 54 and 57 for sands A and B, respectively. The stress levels reach maximum levels as flow rate and pressure drop at failure increase. The level of stress in the sandpack for failure at a given flow rate or pressure drop ranges between a minimum and a maximum value corresponding to the lower and upper curves. In contrast, the failure conditions in sand C lie along a single curve as shown in figures 55 and 58. Both figures show that the stress reaches a minimum value for increasing flow rate and pressure drop at failure.

Maximum stress changes at failure in all the sands are plotted against the vertical stress load in figure 132. The coefficient of linear correlation of the line is less than 0.1. Highest stress changes were obtained during major arch failure. Points of major arch failures are indicated by arrows and connected by dashed lines.

8.6 Theoretical Analysis

In making a theoretical analysis of the behavior of the sand arch developed during the tests, a simple spherical arch geometry was assumed. The theory of poro-elasticity discussed in Appendix A did not readily lend itself to the analysis because many of the various parameters involved were not accurately defined during the experiments. The analysis was therefore based on the simplified assumptions of Bratli, et al. (1979) and the theoretical development shown in Appendix C. Bratli and Risnes (1979) assumed that the spherical arch structure satisfied Lamé's equations of radial and tangential stresses. Combining these with the pressures due to fluid flow, and assuming Coulomb's criterion of failure, they obtained a stability criterion of the arch. In practical units, this stability criterion can be expressed as:

$$\frac{847.2\mu Q}{k_a R} \leq 4\frac{(T+1)}{T} \text{ So } \tan\alpha \qquad (8.1)$$

where μ = fluid viscosity (cp)

Q = flow rate (bbls/day)

k_a = arch permeability (md)

R = radius of the arch (inches)

So = shear strength of the sand (psi)

$T = 2(\tan^2\alpha - 1)$, $\alpha = \pi/4 + \phi/2$

ϕ = internal friction angle of the sand.

In Appendix C, by making a complex transformation shown in figure 59, an approximate relationship has been developed between the arch radius, the ratio of sandpack permeability to arch permeability, and the pressure drop across the cell. The relationship is only approximate because the effect of the casing simulator is neglected by assuming a circular cross-section of the cell. From this relationship the effects of arch radius on the pressure drop have been presented graphically in figures 60 and 61. In these figures, the abscissa is a dimensionless arch radius r, defined as the ratio of the arch radius to the diameter of the cell. The ordinate is the pressure drop per unit strength of the source and sink at steady state. In practical units:

$$\frac{\Delta P}{S} = \frac{\Delta P}{\frac{70.6Q\mu}{\bar{k}h}} = \left(\frac{\Delta P}{Q}\right)\left(\frac{\bar{k}h}{70.6\mu}\right) \quad (8.2)$$

where ΔP is the pressure drop in psi

Q is the flow rate in barrels per day

$\bar{k}$ is the average sandpack permeability in millidarcies

h is the average flow height in feet

μ is the fluid viscosity in centipoise

and S is the strength of the source and the sink.

From equation (8.2):

$$\bar{k} = \left[\frac{\Delta P}{S}\right]\left[\frac{70.6\mu}{h}\right]\left[\frac{1}{\Delta P/Q}\right] \quad (8.3)$$

The average permeability of the sandpack was evaluated at early flow times when the arch permeability was essentially the same as the sandpack permeability ($k_p/k_a = 1$). Since the initial cavity radius in all the tests varied between ¼ and ½ inch, the dimensionless arch radius at the time of cavity formation was assumed to vary between 0.0156 and 0.03125. (The diameter of the cell is 16 inches). From figure 134:

$$\text{For } r = 0.0156,\ \frac{\Delta P}{S} = 19.38$$

$$\text{and for } r = 0.03125,\ \frac{\Delta P}{S} = 16.57.$$

An average value of $\frac{\Delta P}{S}$ of 17.98 was used in evaluating equation (8.3). Assuming a fluid viscosity of 1.9cp, and an average flow height of 24 ft, equation (8.3) can be expressed as:

$$\bar{k} = \frac{100.49}{\Delta P/Q} \quad . \tag{8.4}$$

$\Delta P/Q$ values were determined from the slope of the straight line portion of the ΔP versus Q plots.

The values of $\frac{\Delta P}{S}$ at arch failure were determined from the experimental data. With the corresponding cavity size at failure, the ratio of the sandpack permeability to the arch permeability was obtained from figure 60 or 61. These are shown in table 54.

In order to complete this table, the shear strengths of the sand samples were determined from their failure envelopes. Estimate of the shear strength of the Gopher State frac sand was obtained from the failure envelope of similar 20-40 and 80-100 mesh Ottawa sand reported by Bratli, et al. (1970). The failure envelopes of the natural sands show that a single internal friction angle, ϕ, cannot be used to describe the sands. As a result, a range of values that contain the minimum and maximum points on the curves were used. A complete calculation of the parameters of equation (8.1) for the conditions of failure during the tests is shown in table 54. According to the criterion, a failure should occur when:

$$\frac{847.2\mu Q}{k_r D} \geq 4\frac{T+1}{T} \text{ So } \tan \alpha \qquad (8.5)$$

where r is a dimensionless arch radius, and D is the cell diameter.

The table shows that this criterion of failure was satisfied in almost all cases of arch failure with all the sands. The criterion did not distinguish between failure and non-failure satisfactorily, however. In many cases, the criterion for failure was met but failure did not occur. This difficulty is caused by the deviation of the true failure envelope from Bratli and Risnes' assumption of the simplified straight-line Mohr-Coulomb failure criterion, which is considerable in some stress ranges. Values of α and S_0 required by Bratli and Risnes' criterion are not defined by the true envelope.

The approach used in evaluating sandpack permeability in this analysis was also used to determine the sandpack permeability at different stress levels. The variation of dimensionless sandpack permeability with pseudo effective stress is plotted as shown in figure 62 for all sands. The results agree with published permeability variation with stress load in the literature. Similar results were obtained by Fatt (1953), Dobrynin (1962), and Vairogs, et al. (1972). The approach used in the analysis can therefore be justified.

Figure 63 shows equi-potential lines around the perforation calculated from equations (C1.4) and C1.7) of Appendix C. The elliptical or elongated shapes of the cavities formed during the tests can be explained as a reflection of the flow potential around the perforation as shown in the figure. The assumption of a spherical arch is only for the analytical convenience.

8.7 Dimensionless Pressure Drop Versus Dimensionless Stress

As discussed in Chapter 3, section 3.2.1, the net effective stress in a reservoir formation is the difference between the overburden stress and the reservoir pore pressure. In the model used in this investigation, pore pressure was not measured. The effective stress is considered to be the overburden stress less a certain fraction of the pressure drop: $\sigma_{effective} = \sigma_{ob} - A(P_{in} - P_{out})$.

For consistency with the previous investigators, the value of the constant A is assumed to be unity and the outlet pressure is neglected in relation to the inlet pressure. The resulting function $(\sigma_1 - P_{in})$ is called "pseudo effective stress" in this thesis. Dimensionless pressure drop functions are plotted against dimensionless stress functions in figures 65 through 68. The dimensionless quantities are defined as follows:

$$\text{(i)} \quad \Delta P_D' = \frac{\Delta P \cdot k_{max} R}{847.2 Q \mu}$$

$$\text{(ii)} \quad \Delta P_D = \frac{\Delta P \cdot k_{cor} R}{847.2 Q \mu} \tag{8.6}$$

$$\text{(iii)} \quad \sigma_{eD} = \frac{\sigma_1 - P_{in}}{\sigma_1}$$

$$\text{and (iv)} \quad \sigma_{fD} = \frac{\sigma_1 - P_{in}}{\sigma_1 - \Delta\sigma_{failure}} .$$

k_{max} is the estimated maximum permeability of the sandpack at any time during the tests in millidarcies, as shown in figure 63.

k_{cor} is the corrected sandpack permeability adjusted for the prevailing pseudo-effective stress at failure (also in millidarcies).

R is the average arch radius (inches) defined by the square root of the product of average maximum height and width of the cavity.

Q is the flow rate in barrels per day.

μ is the fluid viscosity in centipoise.

ΔP is the pressure drop across the cell (psi).

$(\sigma_1 - P_{in})$ is the pseudo effective stress defined above (psi).

and $\Delta\sigma_{failure}$ is the maximum change in sand stress when arch failed.

A plot of $\Delta P_D'$ against σ_{eD} is shown in figure 60. The failure data points satisfy the criterion:

$$\Delta P_D' \geq 5.023e^{-6.7986\sigma_{eD}} \tag{8.7}$$

83% of the data satisfy the condition:

$$\Delta P_D' \geq 984.08e^{-12.015\sigma_{eD}} \tag{8.8}$$

In figure 66, ΔP_D is plotted against σ_{eD}. The failure criterion established from this plot is

$$\Delta P_D \geq 15.56e^{-8.638\sigma_{eD}} \tag{8.9}$$

The dimensionless data points show a considerable scatter on the semi-log plot. In figure 67 the linear correlation coefficient of the data is -0.69, and the regression line is defined by:

$$\sigma_{eD} = 0.6426\Delta P_D^{-0.0778} \qquad (8.10)$$

for all conditions of failure

$$\sigma_{eD} \geq 0.4106\Delta P_D^{-0.1515}$$

$$\text{or } \Delta P_D \geq .002807\sigma_{eD}^{-6.601} \quad . \qquad (8.11)$$

The dimensionless stress function, σ_{fD}, is plotted against the dimensionless pressure drop, ΔP_D in figure 68. The regression line has been determined without considering the failure data resulting from water production, and the subsequent failure after desaturating (tests A III and A IV). The line is defined by

$$\sigma_{fD} = 0.6868\Delta P_D^{-0.07935} \quad , \qquad (8.12)$$

and the coefficient of correlation is -0.63. Failures occurred when:

$$\text{(i) } \sigma_{fD} \geq 0.5224\Delta P_D^{-0.1135}$$

$$\text{or (ii) } \Delta P_D \geq 0.003277\sigma_{fD}^{-8.8106} \quad . \qquad (8.13)$$

While accurate estimate of the in situ shear strength of cohesion which is required in using Bratli and Risnes' criterion may pose a problem the foregoing criteria do not require knowledge of formation cohesion. The application of these criteria to field data will therefore not involve the additional expense of soil testing.

Although none of the criteria has been tested in the field, equation (8.10) is believed to be superior for practical application. The parameters involved except the arch radius, R, are usually available from reservoir and production data. The arch radius may be estimated by the approach used in Appendix C.

The present failure criterion therefore has advantages over the criterion of Bratli and Risnes.

Chapter 9

SUMMARY AND CONCLUSIONS

9.1 Summary

Wellbore environment in a producing oil reservoir was simulated in the laboratory to study the behavior of arch structures formed around perforations by unconsolidated natural sands. The work was an extension of the sand-control studies carried out by Tippie (1973), Cleary (1978), Melvan (1978), and Wood (1979) using Gopher State frac sand. Producing natural sand formations were simulated inside a cylindrical pressure cell at overburden stresses of 500, 750, 1000, and 1800/2250 psi. Three natural sand samples with different physical and mechanical properties, but almost identical grain size distributions were used. X-ray diffraction analysis showed that about 1% by weight of each sand was composed of traces of various clay minerals. Additional properties of the sands were obtained from triaxial tests conducted at various confining pressures from 50 psi to 2000 psi.

A mixture of equal parts of 20-40 and 80-100 standard US mesh Gopher State frac sand was used for a series of tests conducted at 1500 psi overburden stress. The tests formed a contact between the previous and the present studies. The stability of a sand arch in a formation producing water was also examined with this sand.

In all other tests, kerosene was flowed through a stressed sandpack with "irreducible" level of water saturation. Stresses in the sandpack around the perforation measured in three orthogonal directions, were continuously monitored during the tests. The flow rate and pressures at the inlet and outlet of the cell were also continuously recorded.

Cavities formed around the perforation subsequent to arch formations. The growth and collapse of any cavity reflected the behavior of the arch that generated it. Constant visual observation of cavity and sand behavior around the perforations was achieved through a plexiglass viewing area. The relations between measured parameters and arch stability were analyzed. The stresses that resulted in failure of arch structures were compared with the failure envelope of the sand. The conditions at failure were compared with the stability criterion proposed by Bratli, et al. (1979). Dimensionless relationships between the various failure parameters for all the sands were presented graphically. From all these, the following conclusions are drawn on the behavior of arches and cavities in natural and Gopher State frac sands under the conditions of this study.

9.2 Conclusions

1. Sand arches formed around the perforation as a consequence of the stresses in the sandpack, and the cohesiveness of the sand.
2. Cavities developed due to the fluid drag force on the loose sand within stable arch structures. The size of a cavity reflected the inner radius of the arch that generated it.
3. In general, cavity size increased with respect to the flow rate and the pressure drop across the cell, and decreased with respect to the overburden stress.
4. The cavities extended upwards during growth as a result of gravity.
5. Arch instabilities developed due to:
   - (i) high flow rates
   - (ii) high pressure drop across the cell
   - (iii) flow restriction resulting from the deposition of fines around the perforation
   - (iv) structural weaknesses of the arch due to repeated tests
   - (v) sudden operational changes that might have caused rate and pressure surges
   - (vi) a combination of two or more of the above.

6. Cavity enlargement followed a minor arch failure. Much bigger cavities developed after major arch failures.
7. Sand arches would not develop with a funicular water saturation. Existing stable arches collapsed and sand produced continuously as water flowed out of the sandpack.
8. The criterion of arch failure in all the sands was:

$$\frac{\Delta P \cdot k_{cor} R}{847.2 Q \mu} \geq .002807 \left(\frac{\sigma_1 - P_{in}}{\sigma_1}\right)^{-6.601}$$

9. Natural sand sample D developed the most stable arches. Natural sand sample C formed arches that were very stable at 1000, 1500, and 1800 psi stress levels, but were rather unstable at 500 psi and 750 psi stress levels. Arches in sand B were less stable, but re-stabilized more readily after arch failures at all stress levels.
10. The sand arch structures were weaker at low stress levels (500 and 750 psi) and stronger at high stress levels (1500 and 2250 psi) than the sand bodies.

Chapter 10

SUGGESTIONS

10.1 Suggestions for Practical Application

The following suggestions based on the findings of this study should assist operators in dealing with sand problems.

1. Reservoir formation sand with adequate grain-to-grain stress, and cohesiveness, will form sand arches spanning over perforations when the wellbore is perforated under proper conditions permitting a stress relief. Formation cohesiveness may be from either the clay content or a pendular water saturation around the wellbore. Arches developed at all the stress levels of tests in this study.
2. The arch structure can give a sandfree production in reservoirs that will normally be expected to produce sand. Stable arches were formed at a flow rate of 37 barrels per day per perforation in the natural sand sample C.
3. The stability of the sand arch will depend on the formation overburden stress and the properties of the sand. In this study more stable arches were formed at 1500-, 1800-, and 2250-psi stress levels.

4. The failure criterion for practical application is of the form:

$$\frac{\Delta P \cdot kR}{Q\mu} \geq \alpha\left(\frac{\sigma_{effective}}{\sigma_{overburden}}\right)^{-\beta}$$

where α and β are constants.
The values of α and β should be established from test wells in a field. The parameters involved are readily available from reservoir and production data. (The arch radius R can be estimated by the approach used in Appendix C.)

5. Arch instability can be minimized by avoiding rapid operational changes like sudden opening and closing of flow valve which induces rate and pressure surges.
6. Skin buildup by the deposition of 'fines' around a stable arch may cause failure of the arch. Such failures should be anticipated if the formation contains a high percentage of 'fines'. The arch should restabilize readily. Improved flow performance may also occur following such restabilization.
7. Higher flow rates may be reached with a stable arch if drawdown is gradual.
8. Workover operations involving the injection of fluids will weaken a stable arch and might cause arch failure when flow resumes. Such workover operations should be

kept to a minimum when sand curtailment is entrusted to the formation of stable arches.

9. Stable sand arches cannot exist with funicular water saturation around the wellbore. Conventional sand control is recommended if there is a possibility of a future water cut.

10. The conditions for arches to form in an oil well are best achieved if the mud is slightly underweighted when perforating. This ensures a stress relief necessary for arch formation. This procedure also eliminates skin effect due to mud filtration which may cause arch instability.

10.2 Suggestions for Further Research

The following are areas that might be considered in future research work:

1. A comprehensive high pressure bleed-off test with varying outlet pressure.
2. A numerical simulation of the pressure cell model. (A groundwork for this is included in Appendix A through Appendix C.)
3. A two-perforation flow system showing flow interference effects on arch stability.
4. Arch stability in inclined wellbores.
5. Arch stability in a 2-phase gas-liquid system.

LITERATURE CITED

1. Bierbaumer, A. (1913): "Die Dimensionierung des Tunnelmauerwerkes", Leipzig, W. Engelmann.

2. Biot, M. A. (1941): "General Theory of Three-Dimensional Consolidation", Journal of Applied Physics, vol. 12, pp. 155-164.

3. Biot, M. A. (1955): "Theory of Elasticity and Consolidation for a Porous Anisotropic Solid", Journal of Applied Physics, Vol. 26, pp. 182-5.

4. Bishop, A. W. (1952): Ph.D. Thesis, Department of Civil Engineering, Imperial College, London.

5. Bishop, A. W. (1973): "The Influence of an Undrained Change in Stress on the Pore-Pressure in Porous Media of Low Compressibility", Geotechniques, Vol. 23, No. 3, pp. 435-442.

6. Böker, R. (1915): "Die Mechanik der bleibenden Formanderung in Kristallinisch aufgebauten, Korpern", Ver. dt. log Mitt. Forshl, Vol. 175, pp. 1-15.

7. Brace, W. F., and Byerlee, J. D. (1966): "Stick-slip as a Mechanism for Earthquakes", Science, Vol. 153, pp. 990-992.

8. Bratli, R. K., and Risnes, R. (1979): "Stability and Failure of Sand Arches", 54th Annual Fall Meeting, Las Vegas, Nevada, SPE Preprint No. 8427.

9. Caquot, A. (1934): "Equilibre des Massfis à Frottement Interne:, Paris, Gauthier-Villard.

10. Carpenter, C. B., and Spencer, G. B. (1940): "Measurements of Compressibility of Consolidated Oil-bearing Sandstones", U.S. Bureau of Mines, Rept. Invest. 3540.

11. Cleary, M. P. (1978): "The Effect of Fluid Properties on Arch Stability in Unconsolidated Sands", Thesis T-2072, Colorado School of Mines, Golden, Colorado.

12. Cleary, M.P., Melvan, J.J., and Kohlhaas, C.A.: "The Effect of Confining Stress and Fluid Properties of Arch Stability in Unconsolidated Sands", 54th Annual Fall Meeting, Las Vegas, Nevada, SPE Preprint No. 8426.

13. Coulomb, C.A. (1773): "Sur une Application des règles de Maximis et Minimis a Quelques Problèmes de Statique Relatifs à l'Architecture", Acad. Roy. des Sciences Memoires de Math. et de Physique par Divers Savans, Vol. 7, pp. 343-388.

14. Dobrynin, V.M. (1962): "Effect of Overburden Pressure on Some Preperties of Sandstones:, Society of Petroleum Engineers Journal, pp. 360-366.

15. Eaton, B.A. (1968): "Fracture Gradient Prediction and its Application in Oilfield Operations", 43rd Annual Fall Meeting, Houston, Texas, SPE Preprint No. 2163.

16. Engesser, F. (1882): "Über den Erddruck gegen innere Stützwände," Deut. Bauzeitg., Vol. 16, pp. 91-93.

17. Fairhurst, C. (1963)-editor: "Rock Mechanics", Pergamon Press.

18. Fatt, I. (1953): "The Effect of Overburden Pressure on Relative Permeability", AIME-SPE Transaction, Vol. 198, pp. 325-326.

19. Fatt, I. (1958): "Pore Volume Compressibilities of Sandstone Reservoir Rocks:, Journal of Petroleum Technology, pp. 64-66.

20. Gassman, F. (1951): "Elasticity of Porous Media", Vierteljahrsschr naturforsch Ges. Zurich, vol. 96, No. 1, pp. 1-21.

21. Geertsma, J. (1957): "The Effect of Fluid Pressure Decline on Volumetric Changes of Porous Rocks", AIME-SPE Transaction, Vol. 210, pp. 331-340.

22. Geertsma, J. (1973): "A Basic Theory of Subsidence Due to Reservoir Compaction: The Homogeneous Case:, Verhandelingen Kon. Ned. Geol. Mihnbouwk. Gen. Volume 28, pp. 43-62.

23. Gnirk, P.F. (1972): "The Mechanical Behavior of Uncased Wellbores Situated in Elastic/Plastic Media Under Hydrostatic Stress", AIME-SPE Transaction, vo. 253, pp. 49-59.

24. Hall, C. D. Jr., and Harrisberger, W. H. (1970): "Stability of Sand Arches: A Key to Sand Control", Journal of Petroleum Technology, pp. 821-829.

25. Hall, H. N. (1953): "Compressibility of Reservoir Rocks, AIME-SPE Transaction, Vol. 198, pp. 309-311.

26. Harrison, E., Kieschnick, W. F. Jr., and McGuire, W. J. (1954): "The Mechanics of Fracture Induction and Extension", AIME-SPE Transaction, Vol. 201, pp. 252-263.

27. Holman, G. B. (1975): "Evaluation of Control Techniques of Unconsolidated Silty Sands", 50th Annual Fall Meeting, Dallas Texas, SPE Preprint No. 5656.

28. Hughes, D. S., and Cooke, C. E. Jr., (1953): "The Effect of Pressure on the Reduction of Pore Volume of Consolidated Sandstones", Geophysics, vol. 18, pp. 298.

29. Jaeger, J. C., and Cook, N. G. W. (1969 & 1976): "Fundamentals of Rock Mechanics", John Wiley & Sons, Inc., New York.

30. Kohlhaas, C. A. (1976): "Evaluation of Well Completions in Southeast Asia for Sand Control", presented at Offshore Southeast Asia Conference, Singapore.

31. Lubinski, A. (1954): "The Theory of Elasticity for Porous Bodies Displaying a Strong Pore Structure", Proc. 2nd U.S. Congress on Applied Mechanics.

32. Melvan, J. J. (1978): "The Effect of Overburden Stress on the Formation and Stability of Arches in Unconsolidated Sands", Thesis T-2071, Colorado School of Mines, Golden, Colorado.

33. Mohr, O. (1900): "Welche Umstände bedingen die Elastizitätsgrenze und den Bruch eines Materials?" Z. ver. dt. lng., Vol. 44, pp. 1524-1530, and 1572-1577.

34. Morse, P. M. and Feshbach, H. (1953): "Methods of Theoretical Physics - Part II", McGraw-Hill Book Company, Inc., New York.

35. Penberthy, W. L. Jr., and Cope, B. J. (1979): "Design and Productivity of Gravel Packed Completions", 54th Annual Fall Meeting, Las Vegas, Nevada, SPE Preprint No. 8428.

36. Scot, P. P. Jr., Bearden, W. G., and Howard, G. C. (1953): "Rock Rupture as Affected by Fluid Properties", AIME-SPE Transaction Vol. 198, pp. 111-124.

37. Skempton, A. W. (1954): "The Pore Pressure Coefficients A and B", Geotechnique, vol. 4, No. 4, pp. 143-147.

38. Skempton, A. W. and Bishop, A. W. (1955): "The Gain in Stability due to Pore Pressure Dissipation in a Soft Clay Foundation", Proc. 5th Cong. Large Dams, Paris.

39. Spiegel, M. R. (1974): "Theory and Problems of Complex Variables with an Introduction to Conformal Mapping and its Applications", Schaum's Outline Series, McGraw-Hill Book Company, Inc., New York.

40. Stassi-D'Alia, F. (1959): "A Limiting Condition of Yielding and its Experimental Conformation", Industria Grafica Nazionale, Palermo.

41. Stein, N., and Hilchie, D. W. (1972): "Estimating the Maximum Production Rates Possible from Friable Sandstones Without Using Sand Control Measures", Journal of Petroleum Technology, Sept., pp. 1157-1160.

42. Stein, N., Odeh, A. S., and Jones, L. G. (1973): "Estimating Maximum Sand-Free Production Rates from Friable Sands for Different Well Completion Geometries", 48th Annual Fall Meeting, Las Vegas, Nevada, SPE Preprint No. 4534.

43. Suman, G. O. Jr. (1975): "Unconsolidated Sand Stabilization through Wellbore Stress State Control", 50th Annual Fall Meeting, Dallas, Texas, SPE Preprint No. 5717.

44. Terzaghi, K. (1936): "Stress Distribution in Dry and in Saturated Sand Above a Yielding Trap-Door", Proc. Intern. Conf. Soil Mechanics, Cambridge, Mass., Vol. 1, pp. 307-311.

45. Terzaghi, K. (1943): "Theoretical Soil Mechanics", John Wiley & Sons, Inc., New York, pp. 66-76.

46. Tippie, D. B. (1973): "The Effect of Producing Rate on the Formation of Arches in Unconsolidated Sands", Thesis T-1575, Colorado School of Mines, Golden, Colorado.

47. Tippie, D. B., and Kohlhaas, C. A. (1973): "Effect of Flow Rate on Stability of Unconsolidated Producing Sands", 48th Annual Fall Meeting, Las Vegas, Nevada, SPE Paper No. 4533.

48. Tippie, D. B., and Kohlhaas, C. A. (1974): "Variation of Skin Damage with Flow Rate Associated with Sand Flow or Stability in Unconsolidated Sand Reservoirs", 44th Annual California Regional Meeting, San Francisco, California, SPE Paper No. 4886.

49. Towle, G. F. (1976): "Stress Effects on Acoustic Velocities of Rocks", Thesis T-1702, Colorado School of Mines, Golden, Colorado.

50. Vairogs, J. and Rhoades, V. W. (1972): "Pressure Transient Tests in Formations Having Stress-Sensitive Permeability", 47th Annual Fall Meeting, San Antonio, Texas, SPE Preprint No. 5050.

51. Völlmy, A. (1937): "Eingebettete Rohre", Mitt. Inst. Baustatik, Eidgen-Tech. Hochschule, Zurich, Mitt. No. 8.

52. Von-Karman, T. (1911): "Festigkeitsversuche unter allseitigem Druck", Z. ver. dt. lng. Vol. 55, pp. 1749-1757.

53. Wood, D. C. (1979): "The Effect of Sand Size on Arch Stability in Unconsolidated Sands", Thesis T-2165, Colorado School of Mines, Golden, Colorado.

APPENDIX A

A 1 EQUATION OF PORO-ELASTICITY

The following describes the general elastic stress-strain behavior of a porous, permeable stressed material, subjected to changing pore pressure. This subject was discussed by Biot in 1941 and 1955, and by Geertsma in 1957 and 1973. Lubinski (1954) drew attention to the similarity between this and the subject of thermo-elasticity.

In a poroelastic material, Hooke's Law can be expressed as:

$$\tau_{ij} = 2G\left(e_{ij} + \frac{\nu}{1-2\nu}\, e\delta_{ij}\right) - (1-\beta)P\delta_{ij} \qquad \text{(A1.1)}$$

This is similar to the thermoelastic relation:

$$\tau_{ij} = 2G\left(e_{ij} + \frac{\nu}{1-2\nu} e\delta_{ij}\right) - \frac{2G(1+\nu)}{1-2\nu}\,\alpha T\delta_{ij}$$

where $e = e_{ii}$ (dilation)

P = Pore pressure

G = Bulk shear modulus

ν = Poisson's ratio

δ_{ij} = kronecker delta

β = cr/cb - the ratio of the compressibilities of rock matrix and rock bulk

α = thermal coefficient of material

and T = temperature of the material.

Equilibrium conditions are given by

$$\tau_{ij,j} + Fi = 0 \tag{A1.2}$$

where Fi denotes components of the body force.

The components of strains can be expressed in terms of displacements, u_i :

$$e_{ij} = \tfrac{1}{2}(u_{i,j} + u_{j,i}) \tag{A1.3}$$

$$e = U_{k,k} \quad . \tag{A1.4}$$

From equation (A1.1) through (A1.4):

$$G\ (u_{i,kk} + u_{k,ik}) + \frac{2G\nu}{1-2\nu}e{,}i - (1-\beta)P{,}i + Fi = 0 \tag{A1.5}$$

Also, by combining equations (A1.1) and (A1.2):

$$2G\ (e_{ij,j} + \frac{\nu}{1-2\nu}e{,}i) - (1-\beta)\ P{,}i + Fi = 0$$

Differentiating this and combining with equation (A1.3) gives:

$$\frac{2G(1-\nu)}{1-2\nu}\ e{,}ii - (1-\beta)P{,}ii + Fi{,}\ i = 0 \tag{A1.6}$$

Equations (A1.5) and (A1.6) are the general forms of poroelastic equation.

A 2. Solution of Poroelastic Equation

Substituting equation (A1.4) in equation (A1.5):

$$G(u_{i,kk} + u_{k,ik}) + \frac{2G\nu}{1-2\nu} u_{k,ki} - (1-\beta)P,i + Fi = 0 \quad \text{(A2.1)}$$

By expressing the displacements in terms of a displacement function ψ, such that

$$u_i = \psi,i \quad \text{and} \quad e = \psi,kk$$

and expressing the body force as a potential function, $-\Phi,i$, it can be shown from equation (A2.1) that:

$$\psi,_{ikk} = \frac{(1-\beta)(1-2\nu)}{2G(1-2\nu)} (P + \Phi),\, i \quad \text{(A2.2)}$$

Integrating equation (A2.2):

$$\psi,_{kk} = \frac{(1-\beta)(1-2\nu)}{2G(1-\nu)} (P + \Phi) + \text{constant.}$$

A particular solution to the differential equation is obtained by solving the Poisson's equation:

$$\psi,_{kk} = \frac{(1-\beta)(1-2\nu)}{2G(1-\nu)} (P + \Phi)$$

In terms of gravitational potential:

$$\psi = \frac{(1-\beta)(1-2\nu)}{4\pi G(1-\nu)} \iiint_V \frac{P+\Phi}{r} \, dV$$

A general solution is obtained by solving the equation: $e,_{kk} = 0$ which describes the displacement field in solid bodies. Thus a complete solution is obtained by adding the general solution to solid body elasticity to the particular solution above.

A 3. Equilibrium of a Spherical Arch

From equation (A1.5):

$$G\, u_{i,kk} + (G+\lambda)e_{,i} - (1-\beta)P_{,i} + F_i = 0 \qquad \text{(A3.1)}$$

where $\lambda = \dfrac{2G\nu}{1-2\nu}$

Assuming a solution in the form of:

$$u_i = x_i \psi(r) \qquad \text{(A3.2)}$$

where ψ is a displacement potential assumed to be a function of the radius of the sphere alone. Substituting equation (A3.2) in (A3.1) and neglecting the body forces:

$$(\lambda+2G)(\psi'' + \frac{4}{\gamma}\psi') - \frac{(1-\beta)}{\gamma}P' = 0 \qquad \text{(A3.3)}$$

$$\psi' = \frac{d\psi}{dr}, \quad \psi'' = \frac{d^2\psi}{dr^2} \quad \text{and} \quad P' = \frac{dP}{dr}$$

The general solution of equation (A3.3) is of the form:

$$\psi(r) = A_1 + \frac{A_2}{r^3} + \frac{(1-\beta)}{\lambda+2G}\psi_0(r)$$

$$\text{where } \psi_0(r) = \frac{1}{r^3}\int_{r_1}^{r} P(r)r^2 dr$$

A_1 and A_2 are constants.

Differentiating equation (A3.2), we have

$$u_{i,j} = \delta_{ij} + x_i \psi' \frac{x_j}{r}$$

and $$u_{i,i} = 3\psi + r\psi'$$

Substituting these in equation (A1.1):

$$\tau_{ij} = 2G(\psi\delta_{ij} + \frac{x_i x_j}{r}\psi') + \lambda(3\psi + r\psi') - (1-\beta)P\delta_{ij}$$

The radial and tangential stresses are:

$\sigma_r = \tau_{ij}\nu_i\nu_j$ and $\sigma_\theta = \tau_{ij}n_i n_j$ respectively.

where ν_i and ν_j are unit vectors

n_i and n_j are unit vectors normal to

ν_i and ν_j respectively.

Noting that $\nu_i = \frac{x_i}{r}$ in the radial direction,

$n_i n_i = 1$ and $n_i x_i = 0$, we have

$$\sigma_r = (3\lambda + 2G)\psi + (\lambda + 2G)r\psi' - (1-\beta)P \qquad \text{(A3.4)}$$

and $$\sigma_\theta = (3\lambda + 2G)\psi + \lambda r\psi' - (1-\beta)P \qquad \text{(A3.5)}$$

Substituting for ψ and ψ':

$$\sigma_r = (3\lambda + 2G)A_1 - \frac{4G}{r^3}A_2 - \frac{4G(1-\beta)}{\lambda+2G}\psi_0$$

and $$\sigma_\theta = (3\lambda + 2G)A_1 + \frac{2G}{r^3}A_2 + \frac{2G(1-\beta)}{\lambda+2G}(\psi_0 - P)$$

The constants A_1 and A_2 are eliminated by substituting proper boundary conditions.

APPENDIX B

EQUATION OF FLOW

B I. Three Dimensional Flow Equation

Suppose that a source and a sink in a cylinder are located at point (r_0, ϕ_0, z_0) and (r_1, ϕ_1, z_1), respectively, defined in a cylindrical coordinate. The Green's function of the interior of the cylinder is obtained by a series solution of the form:

$$\nabla^2\psi = -4\pi\delta_0(r_0, \phi_0, z_0) + 4\pi\delta_1(r_1, \phi_1, z_1) \quad \text{(B1.1)}$$

where δ_0 and δ_1 are both zero except at points (r_0, ϕ_0, z_0) and (r_1, ϕ_1, z), respectively.

Suppose there are no flow across the top, bottom and radial boundaries of the cylinder:

$$\frac{\partial\psi}{\partial z}\Big)_{z=0} = \frac{\partial\psi}{\partial z}\Big)_{z=\ell} = 0$$

and

$$\left\{\frac{\partial}{\partial r}\left[Jm\left(\frac{\pi\beta ms\,r}{re}\right)\right]\right\}_{r=re} = 0$$

The solution to equation (B1.1) is of the form (Morse and Fashbach, 1953):

$$\psi = \sum_{mns}^{\infty} A_{mns} \cos\left[m(\phi-\phi_0)\right]\cos\frac{n\pi z}{\ell} Jm\left(\frac{\pi\beta ms\,r}{r_e}\right)$$

$$- \sum_{mns}^{\infty} B_{mns} \cos\left[m(\phi-\phi_1)\right]\cos\frac{n\pi z}{\ell} Jm\left(\frac{\pi\beta ms\,r}{r_e}\right) \quad \text{(B1.2)}$$

where Jm(x) is the Bessel function of the first kind.

With the boundary condition we can obtain values of the constants Amns and Bmns:

$$Amns = \frac{G_2 \cos\left[m(\phi_0 - \phi_1)\right] - G_1}{\sin^2 m(\phi_0 - \phi_1)}$$

and

$$Bmns = \frac{G_1 \cos\left[m(\phi_0 - \phi_1)\right] - G_2}{\sin^2 m(\phi_0 - \phi_1)}$$

where

$$G_1 = \frac{16}{m^2 \ell \left(1 + \frac{n^2 re^2}{\ell^2 \beta^2 ms}\right)} \frac{1}{Jm^2}(\pi\beta_{ms}) \left[\cos \frac{n\pi z_0}{\ell} Jm\left(\frac{\pi\beta_{ms} r_0}{re}\right) - \cos m(\phi_0 - \phi_1) \cos \frac{n\pi z}{\ell} Jm\left(\frac{\pi\beta_{ms} r_1}{re}\right)\right]$$

and

$$G_2 = \frac{16}{m^2 \ell \left(1 + \frac{n^2 r_e^2}{ms}\right)} \frac{1}{Jm^2(\pi\beta_{ms})} \left[\cos m(\phi_0 - \phi_1) \cos \frac{n\pi z_0}{\ell} Jm\left(\frac{\pi\beta_{ms} r_0}{r_e}\right) - \cos \frac{n\pi z_1}{\ell} Jm\left(\frac{\pi\beta_{ms} r_1}{r_e}\right)\right]$$

B 2. Two Dimensional Steady-State Flow Equation

The flow equation discussed in appendix B 1 can be greatly simplified assuming a two-dimensional steady-state plane flow system. Consider a bounded stratum of porous medium, and suppose that an incompressible fluid of constant density, ρ, is flowing through at a steady state condition. Suppose also that there is no flow across the boundaries and the vertical direction x_3 is also a principal axis of permeability. The components of flow velocity in the three principal directions of permeability x_1, x_2 and x_3, are obtained from Darcy's law:

$$v_1 = -\frac{\rho}{\mu} k_1 \frac{\partial \Phi}{\partial x_1}, \quad v_2 = -\frac{\rho}{\mu} k_2 \frac{\partial \Phi}{\partial x_2} \quad \text{and} \quad v_3 = -\frac{\rho}{\mu} k_3 \frac{\partial \Phi}{\partial x_3} \qquad \text{(B 2.1)}$$

where k_1, k_2 and k_3 are the permeabilities in x_1, x_2 and x_3 directions,

and Φ is the flow potential defined as:

$$\Phi = \int_{P_1}^{P_2} \frac{dp}{\rho} + g\Delta x_3 \qquad \text{(B 2.2)}$$

P_1 is a reference pressure at a datum and P_2 is the pressure at any point - Δx_3 from the datum. Assuming no flow across the boundary, the component of velocity $v_3 = 0$, and

$$\frac{dp}{dx_3} = -\rho g$$

from continuity equation:

$$\frac{\partial v_1}{\partial x_1} + \frac{\partial v_2}{\partial x_2} = 0 \qquad \text{(B 2.3)}$$

Substituting equation (B 2.1) in (B 2.3):

$$k_1 \frac{\partial^2 p}{\partial x_1{}^2} + k_2 \frac{\partial^2 p}{\partial x_2{}^2} = 0 \qquad \text{(B 2.4)}$$

or

$$\frac{\partial^2 p}{\partial x^2} + \frac{\partial^2 p}{\partial y^2} = 0 \qquad \text{(B 2.5)}$$

where x and y are transformed coordinates:

$$x = x_1 \text{ and } y = x_2 \sqrt{\frac{k_1}{k_2}}$$

The x_1-x_2 and x-y coordinate systems are identical in an isotropic medium where $k_1 = k_2 (=k_3)$. In a cylindrical coordinate the Laplace equation (B 2.5) can be expressed as:

$$\frac{\partial^2 p}{\partial r^2} + \frac{1}{r}\frac{\partial p}{\partial r} + \frac{1}{r^2}\frac{\partial p}{\partial \phi^2} = 0$$

or

$$\frac{\partial^2 p}{\partial r'^2} + \frac{\partial^2 p}{\partial \phi^2} = 0 \qquad \text{(B 2.6)}$$

where $r' = \ln r$.

Equation (B 2.6) may be solved with the proper boundary conditions by numerical methods of either relaxation or iteration.

APPENDIX C

EFFECTS OF ARCH/CAVITY ON FLOW

Consider that the cell of a unit radius whose cross section is shown in figure 133 has a point source and a sink at points B and D respectively. Consider also that spherical arches of radii r_1 and r_2 are formed at B and D, respectively. Suppose that cavities are developed at both the inlet and outlet by fluid flow. The limiting radii of the cavities will be r_1 and r_2 at points B and D, respectively.

Consider the complex transformation of the cell cross section in the z-plane into the upper half of the w-plane. The linear fractional transformation of the unit circle in the z-plane into a circular band of infinite radius in the w-plane is of the form

$$z = \frac{\alpha w + \beta}{\gamma w + \delta} \qquad \text{(C 1.1)}$$

where $z = x + iy$; $w = u + iv$

$i = \sqrt{-1}$; α, β, γ , and δ are constants.

In figure 133,

(i) point A(0,0) in the z-plane is mapped into point A'(0,1) in the w-plane.

(ii) point C(0,1) in the z-plane is mapped into point

C'(∞,0) in the w-plane, and

(iii) point E(0, -1) in the z-plane is mapped into point E'(0,0) in the w-plane.

Substituting these point mapping and solving for α, β, γ and δ , equation (C 1.1) becomes:

$$z = \frac{w - i}{1 - iw} \tag{C 1.2}$$

By simple manipulation, equation (C 1.2) can be expressed as

$$w = \frac{z+i}{1+iz} = \frac{2x}{x^2+(1-y)^2} - \frac{i(x^2+y^2-1)}{x^2+(1-y)^2} \tag{C 1.3}$$

From equation (C 1.3):

$$u = \frac{2x}{x^2+(1-y)^2} \quad \text{and} \quad v = \frac{(x^2+y^2-1)}{x^2+(1-y)^2} \tag{C 1.4}$$

The complex potential Ω because of a combination of source and sink in the w-plane can be obtained from any standard text book of complex variable (ref. 39):

$$\Omega = -S\ln(w-1) + S\ln(w+1) \tag{C 1.5}$$

where S is the strength of the source and sink:

$$S = \frac{q\mu}{4\pi kh}$$

where q is the flow rate

μ is the fluid viscosity

k is the average sandpack permeability

and h is the average height of flow.

Equation (C 1.5) can also be expressed as:

$$\Omega = -\ S\ln\left[\frac{(u+1)^2 + v^2}{(u-1)^2 + v^2}\right] - iS\tan^{-1}\left[\frac{2v}{u^2 + v^2 - 1}\right] \qquad \text{(C 1.6)}$$

(Morse and Feshbach, page 1232)

Thus, the potential function Φ and the stream function Ψ are given by

$$\Phi = -\ S\ln\left[\frac{(u+1)^2 + v^2}{(u-1)^2 + v^2}\right] \qquad \text{(C 1.7)}$$

and

$$\Psi = -\ S\tan^{-1}\left[\frac{2v}{u^2 + v^2 - 1}\right] \qquad \text{(C 1.8)}$$

The potential function Φ_1 at point G at the inlet sandface can be obtained by combing equations (C 1.4) and (C 1.7), and substituting the transformed values when $x=1-r_1$ and $y=0.$, $(0<r_1 \leq 1)$

$$\Phi_1(z) = -\ S\ln\left[\frac{(4-4r_1+r_1^2)^2 + (2r_1-r_1^2)^2}{r_1^4 + (2r_1-r_1^2)^2}\right].$$

Similarly, the potential function Φ_2 at point F at the outlet sandface can be obtained by combining equations (C 1.4) and (C 1.8), and substituting the transformed values when $x = -1+r_2$, and $y=0.$, $(0<r_2\leq1)$

$$\Phi_2(z) = -\ S\ln\left[\frac{r_2^4 + (2r_2 - r_2^2)^2}{(4r_2-4-r_2^2) + (2r_2-r_2^2)^2}\right].$$

The potential difference between points G and F at the inlet and outlet of the cell is:

$$\Phi_1(Z) - \Phi_2(Z) = -S\ln\left[\frac{4-4r_1+r_1^2)^2 + (2r_1-r_1^2)^2}{r_1^4 + (2r_1-r_1^2)^2}\right] + S\ln\left[\frac{r_2^4 + (2r_2-r_2^2)^2}{4r_2-4-r_2^2)^2 + (2r_2-r_2^2)^2}\right]$$

$$= \Delta P \qquad \text{(C 1.9)}$$

Two cases are considered in completing the above analysis:

Case 1. Let $r_1 = r_2 = r$

where r is the radius of the arch.

By substituting this condition and simplifying equation (C 1.9) becomes:

$$\frac{\Delta P}{S} = -2\ \ln\left[\frac{r^2(r^2-2r+2)}{2(1-r)(2-r)^2}\right] \qquad \text{(C 1.10)}$$

Case 2. Let the effective cavity radius r_2 at the flow outlet be a function of the ratio of the sandpack permeability, k_p to the arch permeability, k_a.

Suppose $r_1 = r$; and $r_2 = re^{-(k_p/k_a\ -\ 1)}$

where r is the arch radius.

By substituting these in equation (C 1.9), we can express $\frac{\Delta P}{S}$ as a function of the arch radius, and the permeability ratio, k_p/k_a

$$\frac{\Delta P}{S} = f(r,\ k_p/k_a).$$

TABLE 1

Sand Sieve Analysis

Standard US Mesh Size	Grain Diameter (inches)	Cumulative Weight % Sand: Gopher State 20-40/80-100	Natural Sample B	Natural Sample C	Natural Sample D
10	0.0787	-	-	-	-
20	0.0331	0.25	19.24	36.62	27.14
40	0.0165	54.25	70.54	78.24	67.39
60	0.0098	64.56	93.72	96.00	90.34
80	0.0070	75.86	96.52	97.42	93.88
100	0.0059	92.09	97.96	98.16	96.02
120	0.0049	96.94	98.78	98.69	97.54
140	0.0041	98.29	99.01	98.86	98.12
170	0.0035	99.54	99.23	99.06	98.68
200	0.0029	100.00	99.42	99.22	99.11
400	0.0015	100.00	99.75	99.24	99.15
Fines	< 0.0015	100.00	100.00	100.00	100.00

TABLE 2

Statistical Parameters
Sand Sieve Analysis

Sand	Median Grain Size (inches)	Mean Grain Size (inches)	Standard Deviation (-)	Uniformity Coefficient (d_{40}/d_{90})
A	0.0175	0.0167	1.0174	3.471
B	0.0223	0.0234	0.7105	2.615
C	0.0260	0.0333	0.9150	2.583
D	0.0223	0.0263	1.000	2.385

TABLE 3

X-RAY DIFFRACTION MINERAL PERCENTAGES

PAGE 1 OF 1

LOCALITY: COLORADO SCHOOL OF MINES

T.S. NO.: 9693SJ

FORMATION: OUTCROP

CHARGE: 0265-68-01

AGE: N/A

	SAMPLE ID. NUMBER	QRTZ	FELD	CALC	DOLO	SIDR	ANHY	GYPS	PYRT	BARI	KAOL	ILLI MICA	CHLR	MONT	MXLR	HALI	ACTI
1	B	64	32								TRC	1		TRC			3
2	C	79	21	TRC							TRC	TRC		TRC			
3	D	70	30								TRC	TRC		TRC			

TABLE 4
CHEMICAL ANALYSIS OF SAMPLES

Percentage Elemental Constituent

Sand Sample	U.S. Mesh Size	SiO_2	Al_2O_3	Fe_2O_3	MgO	CaO	Na_2O	K_2O	TiO_2	P_2O_5	MnO	Loss on Ignition (900°C)
B	170-200	64.89	12.55	11.29	1.25	2.51	2.49	3.34	0.92	0.39	0.11	0.84
B	> 200	64.94	13.96	6.58	1.36	2.56	2.64	3.89	0.71	0.45	0.08	1.54
C	170-200	74.48	11.64	2.82	0.54	0.82	1.55	4.04	0.69	0.17	0.09	3.26
C	> 200	69.31	12.23	3.31	0.72	1.17	1.55	3.51	0.70	0.20	0.10	4.62
D	170-200	70.05	11.01	7.20	0.69	1.63	2.16	4.03	1.41	0.27	0.13	0.00
D	> 200	67.40	12.02	6.16	0.79	1.71	2.35	4.32	1.15	0.30	0.11	0.66

TEST NUMBER: A1

SAND: Gopher State
20-40/80-100 US Mesh.

STRESS LEVEL: 1500 psi

Time	EXPERIMENTAL DATA							CALCULATED DATA				
Time	Sand Stress			Pressure		Flow Rate, Q	ΔP	ΔP/Q	Pseudo Effective Stress			Comment
(hrs:min)	σ_1 (psi)	σ_2 (psi)	σ_3 (psi)	inlet (psi)	outlet (psi)	(Bbls/Day)	(psi)	(psi/bbls/day)	σ'_1 (psi)	σ'_2 (psi)	σ'_3 (psi)	
0:00	1500	-	-	34	5.3	1.50	28.7	19.13	1466	-	-	Injected 200cc of water to initiate cavity formation
0:12	1500	-	-	37	5.3	1.50	31.7	21.13	1463	-	-	
0:24	1500	-	-	34	4.5	1.50	29.5	19.67	1466	-	-	
0:36	1500	-	-	34	4.0	1.50	30.0	20.00	1466	-	-	Sand movement observed around perforation.
0:48	1490	-	-	36	4.3	2.78	31.7	11.40	1454	-	-	Cavity size: 1/2" x 3"
1:00	1480	-	-	37	4.0	3.04	33.0	10.86	1443	-	-	Visible loose sand movement
1:12	1445	-	-	37	4.0	4.46	33.0	7.40	1408	-	-	
1:24	1430	-	-	37	5.8	4.46	31.2	7.00	1393	-	-	Cavity shape changed: wider at the top.
1:36	1428	-	-	37	6.9	4.46	30.1	6.75	1391	-	-	
1:48	1425	-	-	40	7.0	4.46	33.0	7.40	1385	-	-	Size: 1/8 - 1/2 x 2 1/2"
2:00	1425	-	-	40	7.0	4.46	33.0	7.40	1385	-	-	Stable condition around perforation
2:12	1405	-	-	40	6.2	4.46	33.8	7.58	1365	-	-	
2:24	1395	-	-	40	7.0	5.50	33.0	6.00	1355	-	-	
2:36	1370	-	-	40	6.9	5.50	33.1	6.02	1330	-	-	Arch failed and restabilized
2:48	1370	-	-	39	6.9	5.50	32.1	5.84	1331	-	-	
3:00	1360	-	-	42	7.0	5.50	35.0	6.36	1318	-	-	Cavity size: 1/2" x 3 1/4"
3:12	1330	-	-	42	7.0	5.50	35.0	6.36	1288	-	-	
3:24	1300	-	-	42	7.0	5.50	35.0	6.36	1258	-	-	
3:36	1250	-	-	42	7.0	-	35.0	-	1208	-	-	
3:48	1220	-	-	42	7.0	-	35.0	-	1178	-	-	
4:00	1200	-	-	42	6.5	-	35.5	-	1158	-	-	Arch failed and cavity collapsed
4:12	1220	-	-	37	6.2	10.20	30.8	3.02	1183	-	-	

TABLE 3 (cont'd)

TEST NUMBER: AI

SAND: Gopher State
20-40/80-100 US Mesh.

STRESS LEVEL: 1500 psi

EXPERIMENTAL DATA | CALCULATED DATA

Time	Sand Stress			Pressure		Flow Rate, Q	ΔP	ΔP/Q	Pseudo Effective Stress			Comment
(hrs:min)	σ_1 (psi)	σ_2 (psi)	σ_3 (psi)	inlet (psi)	outlet (psi)	(Bbls/Day	(psi)	(psi/bbls/day)	σ'_1 (psi)	σ'_2 (psi)	σ'_3 (psi)	
4:24	1120	-	-	37	6.5	10.2	30.5	2.99	1083	-	-	Sand produced briefly
4:36	1110	-	-	32	6.5	10.2	25.5	2.50	1078	-	-	
4:48	1100	-	-	54	6.5	10.2	47.5	4.66	1046	-	-	
5:00	1090	-	-	90	6.5	10.2	83.5	8.19	1000	-	-	Arch failure;
5:12	1090	-	-	125	6.5	10.2	118.5	11.62	965	-	-	Sand movement
5:24	1000	-	-	160	6.5	10.2	153.5	15.05	835	-	-	around perforation
5:36	960	-	-	175	11.0	-	164.0	-	785	-	-	Cavity size: 1/2 - 1" x 4"
5:48	920	-	-	184	3.5	-	180.5	-	736	-	-	
6:00	920	-	-	200	5.9	7.2	194.1	26.96	720	-	-	
6:12	900	-	-	208	6.2	7.2	201.8	28.03	692	-	-	Re-stabilized condition
6:24	900	-	-	213	6.2	7.2	206.8	28.72	687	-	-	
6:36	900	-	-	220	5.9	6.32	214.1	33.88	680	-	-	Cavity size: 1" x 4"
6:48	855	-	-	220	5.8	5.49	214.2	39.02	635	-	-	
7:00	855	-	-	220	5.7	6.03	214.3	35.54	635	-	-	
7:12	855	-	-	252	5.2	7.30	246.8	33.81	603	-	-	
7:24	855	-	-	262	5.2	7.93	256.8	32.38	593	-	-	Stable condition
7:36	855	-	-	262	5.2	7.60	256.8	33.79	593	-	-	
7:48	840	-	-	262	5.2	6.80	256.8	37.76	578	-	-	
8:00	838	-	-	262	5.2	6.46	256.8	39.75	576	-	-	
8:12	838	-	-	262	5.2	6.13	256.8	41.89	576	-	-	
8:24	838	-	-	262	5.2	5.86	256.8	43.82	576	-	-	Stable condition
8:36	838	-	-	262	5.2	5.61	256.8	45.78	576	-	-	
8:48	838	-	-	262	5.2	5.46	256.8	47.03	576	-	-	

TEST NUMBER: A11

SAND: Gopher State
20-40/80-100 US Mesh

STRESS LEVEL: 1500 psi

Time	EXPERIMENTAL DATA: Sand Stress			Pressure		Flow Rate, Q	ΔP	CALCULATED DATA: ΔP/Q	Pseudo Effective Stress			Comment
(hrs:min)	σ_1 (psi)	σ_2 (psi)	σ_3 (psi)	inlet (psi)	outlet (psi)	(Bbls/Day	(psi)	(psi/bbls/day	σ'_1 (psi)	σ'_2 (psi)	σ'_3 (psi)	
0:00	810	-	-	46	3.5	0.27	42.5	157.4	764	-	-	
0:12	810	-	-	46	3.5	0.48	42.5	88.54	764	-	-	
0:24	810	-	-	46	3.5	0.46	42.5	92.39	764	-	-	Stable condition
0:36	810	-	-	56	3.5	0.94	52.5	55.85	754	-	-	
0:48	810	-	-	58	3.5	0.71	54.5	76.76	752	-	-	
1:00	810	-	-	60	3.5	0.62	56.5	91.13	750	-	-	Cavity size: 1" x >4"
1:12	810	-	-	61	3.5	0.60	57.5	95.83	749	-	-	
1:24	810	-	-	61	3.5	0.59	57.5	97.46	749	-	-	
1:36	810	-	-	73	3.5	1.30	69.5	53.46	737	-	-	Stable condition
1:48	810	-	-	75	3.5	1.24	71.5	57.66	735	-	-	
2:00	810	-	-	76	3.5	1.18	72.5	61.44	734	-	-	
2:12	810	-	-	76	3.5	1.13	72.5	64.16	734	-	-	Stable condition, no sand movement
2:24	810	-	-	95	3.4	2.09	91.6	43.83	715	-	-	
2:36	810	-	-	96	3.4	1.94	92.6	47.73	714	-	-	
2:48	810	-	-	98	3.4	1.91	94.6	49.53	712	-	-	
3:00	810	-	-	99	3.4	1.87	95.6	51.13	711	-	-	
3:12	810	-	-	100	3.4	1.81	96.6	53.37	710	-	-	
3:24	810	-	-	120	3.0	3.05	117.0	38.36	690	-	-	
3:36	810	-	-	123	3.0	3.02	120.0	39.74	687	-	-	
3:48	810	-	-	124	3.0	2.91	121.0	41.58	686	-	-	Stable condition
4:00	810	-	-	125	3.0	2.70	122.0	45.19	685	-	-	
4:12	810	-	-	127	3.0	2.62	124.0	47.33	683		-	

TABLE C (Cont'd)

TEST NUMBER: AII

SAND: Gopher State
20-40/80-100 US Mesh

STRESS LEVEL: 1500 psi

EXPERIMENTAL DATA — CALCULATED DATA

Time	Sand Stress			Pressure		Flow Rate, Q	ΔP	ΔP/Q	Pseudo Effective Stress			Comment
(hrs, min)	σ_1 (psi)	σ_2 (psi)	σ_3 (psi)	inlet (psi)	outlet (psi)	(Bbls/Day)	(psi)	(psi/bbls/day)	σ'_1 (psi)	σ'_2 (psi)	σ'_3 (psi)	
4:24	810	-	-	127	3.0	2.61	124.0	47.51	683	-	-	
4:36	810	-	-	150	2.6	3.76	147.4	39.20	660	-	-	
4:48	810	-	-	154	2.6	3.56	151.5	42.56	656	-	-	Stable condition
5:00	810	-	-	156	2.5	3.42	153.5	44.88	654	-	-	
5:12	810	-	-	156	2.4	3.33	153.6	46.13	654	-	-	
5:24	810	-	-	156	2.3	3.29	153.7	48.72	654	-	-	
5:36	810	-	-	182	2.3	4.83	179.7	37.20	628	-	-	
5:48	810	-	-	182	2.3	4.62	179.7	38.90	628	-	-	Stable condition
6:00	810	-	-	182	2.3	4.34	179.7	41.41	628	-	-	
6:12	810	-	-	185	2.3	4.17	182.7	43.81	625	-	-	
6:24	810	-	-	188	2.3	4.13	185.7	44.96	622	-	-	
6:36	810	-	-	198	2.3	4.29	195.7	45.62	612	-	-	
6:48	810	-	-	188	2.3	4.21	185.7	44.11	622	-	-	Stable condition
7:00	810	-	-	198	2.3	3.94	195.7	49.67	612	-	-	
7:12	810	-	-	213	2.3	4.19	210.7	50.29	597	-	-	
7:24	810	-	-	210	2.3	4.00	207.7	52.68	600	-	-	
7:36	810	-	-	213	2.3	3.94	210.7	53.48	597	-	-	
7:48	810	-	-	213	2.3	3.89	210.7	54.16	597	-	-	Stable condition
8:00	810	-	-	213	2.3	3.71	210.7	56.79	597	-	-	
8:12	810	-	-	212	2.3	3.70	209.7	56.68	598	-	-	
8:24	810	-	-	213	2.3	3.60	210.7	58.53	597	-	-	

TEST NUMBER: AII

SAND:

STRESS LEVEL:

EXPERIMENTAL DATA | CALCULATED DATA

Time	Sand Stress			Pressure		Flow Rate, Q	ΔP	ΔP/Q	Pseudo Effective Stress			Comment
(hrs:min)	σ_1 (psi)	σ_2 (psi)	σ_3 (psi)	inlet (psi)	outlet (psi)	(Bbls/Day)	(psi)	(psi/bbls/day)	σ'_1 (psi)	σ'_2 (psi)	σ'_3 (psi)	
8:36	810	-	-	217	2.3	3.57	214.7	60.14	593	-	-	
8:48	810	-	-	237	2.3	5.03	234.7	46.66	573	-	-	
9:00	810	-	-	237	2.3	4.74	234.7	49.51	573	-	-	
9:12	810	-	-	237	2.3	4.87	234.7	48.19	573	-	-	
9:24	810	-	-	237	2.3	4.70	234.7	49.94	573	-	-	Stable condition
9:36	810	-	-	237	2.3	4.51	234.7	52.04	573	-	-	
9:48	810	-	-	240	2.3	4.38	237.7	54.27	570	-	-	
10:00	810	-	-	240	2.3	4.20	237.7	56.60	570	-	-	
10:12	810	-	-	240	2.3	4.05	237.7	58.69	570	-	-	
10:24	810	-	-	240	2.3	4.00	237.7	59.43	570	-	-	
10:36	810	-	-	257	2.3	4.15	254.7	61.37	553	-	-	
10:48	810	-	-	257	2.3	4.17	254.7	61.08	553	-	-	Stable condition
11:00	810	-	-	257	2.3	4.00	254.7	63.68	553	-	-	
11:12	810	-	-	257	2.3	3.94	254.7	64.64	553	-	-	
11:24	810	-	-	245	2.3	5.04	242.7	48.15	565	-	-	
11:36	810	-	-	245	2.3	5.01	242.7	48.44	565	-	-	
11:48	810	-	-	245	2.3	4.71	242.7	51.53	565	-	-	
12:00	810	-	-	245	2.3	4.53	242.7	53.58	565	-	-	
12:12	810	-	-	245	2.3	4.34	242.7	55.92	565	-	-	Stable condition
12:24	810	-	-	245	2.3	4.29	242.7	56.57	565	-	-	
12:36	810	-	-	257	2.3	4.27	242.7	56.84	553	-	-	
12.48	810	-	-	257	2.3	4.21	242.7	57.65	553	-	-	

TEST NUMBER: AIII

SAND: Gopher State
20-40/80-100 US Mesh

STRESS LEVEL: 1500 psi

Time	EXPERIMENTAL DATA: Sand Stress			Pressure		Flow Rate, Q	ΔP	ΔP/Q	CALCULATED DATA: Pseudo Effective Stress			Comment
(hrs:min)	σ_1 (psi)	σ_2 (psi)	σ_3 (psi)	inlet (psi)	outlet (psi)	(Bbls/Day	(psi)	(psi/bbls/day)	σ'_1 (psi)	σ'_2 (psi)	σ'_3 (psi)	
0:00	810	-	-	70	2.0	0.86	68	79.07	740	-	-	Displacing kerosene by
0:04	810	-	-	73	2.0	0.88	71	80.68	737	-	-	water.
0:08	810	-	-	76	2.0	0.91	74	81.32	734	-	-	Stable condition.
0:12	810	-	-	78	2.0	0.95	76	89.41	732	-	-	Arch remained stable.
0:16	810	-	-	90	2.0	0.57	88	154.39	720	-	-	No change in Cavity.
0:20	810	-	-	90	2.0	0.58	88	151.72	720	-	-	Size: 1" x 3" Producing kerosene
0:24	810	-	-	83	2.0	0.59	81	137.29	727	-	-	
0:28	810	-	-	83	2.0	0.59	81	137.29	727	-	-	Stable condition
0:32	810	-	-	123	2.0	1.68	121	72.02	687	-	-	First drop of water
0:36	810	-	-	120	2.0	1.88	118	62.77	690	-	-	produced.
0:40	810	-	-	123	2.0	1.93	121	62.69	687	-	-	Complete arch collapse
0:44	370	-	-	125	2.0	1.85	123	66.49	245	-	-	followed. Excessive sand production: Terminated test.

TEST NUMBER: AIV

SAND: Gopher State 20-40/80-100 US Mesh

STRESS LEVEL: 1500 psi

	EXPERIMENTAL DATA								CALCULATED DATA				
Time	Sand Stress			Pressure		Flow Rate, Q	ΔP	ΔP/Q	Pseudo Effective Stress			Comment	
(hrs:min)	σ_1 (psi)	σ_2 (psi)	σ_3 (psi)	inlet (psi)	outlet (psi)	(Bbls/Day)	(psi)	(psi/bbls/day)	σ'_1 (psi)	σ'_2 (psi)	σ'_3 (psi)		
0:00	1520	-	-	62	2.3	0.45	59.7	132.67	1458	-	-	Injected 200 cc of water to initiate cavity	
0:12	1500	-	-	62	2.3	0.36	59.7	165.83	1438	-	-		
0:24	1485	-	-	62	2.3	0.36	59.7	165.83	1423	-	-		
0:36	1485	-	-	105	2.3	2.28	102.7	45.04	1380	-	-	Initial cavity Size: 1/2" x 1/2"	
0:48	1485	-	-	106	2.3	2.40	103.7	43.21	1379	-	-		
1:00	1450	-	-	106	2.3	2.47	103.7	41.98	1344	-	-	Arch failed, and restabilized. Cavity growth: 3/4" x 3/4". Sand produced. Stopped pump to clean up sand in flow line	
1:12	1450	-	-	108	2.3	2.57	105.7	41.13	1342	-	-		
1:24	1450	-	-	113	2.3	2.58	110.7	42.91	1337	-	-		
1:36	-	-	-	-	-	-	-	-	-	-	-		
1:48	1140	-	-	125	2.3	5.66	122.7	21.68	1015	-	-		
2:00	1000	-	-	125	2.3	5.94	122.7	20.66	875	-	-	Arch failed as flow started. Restabilized briefly and failed again. Complete arch failure with increasing sand production.	
2:12	780	-	-	127	2.3	5.95	124.7	20.96	653	-	-		
2:24	510	-	-	130	2.3	6.32	127.7	20.21	380	-	-		
2:36	490	-	-	135	2.3	6.31	132.7	21.03	355	-	-		
2:48	340	-	-	175	2.3	8.28	172.7	20.86	165	-	-		
3:00	160	-	-	184	2.3	8.57	181.7	21.20	-24	-	-	Arch finally restablished	
3:12	150	-	-	191	2.3	8.32	188.7	22.68	-41	-	-		
3:24	150	-	-	196	2.3	8.34	193.7	23.23	-46	-	-	Cavity size grew beyond view area: 1" x >4".	
3:36	150	-	-	223	2.3	7.69	220.7	28.70	-73	-	-		

TEST NUMBER: BI

SAND: Natural Sample B

STRESS LEVEL: 500 psi

Time	Sand Stress			Pressure		Flow Rate, Q	ΔP	ΔP/Q	Pseudo Effective Stress			Comment
(hrs:min)	σ_1 (psi)	σ_2 (psi)	σ_3 (psi)	inlet (psi)	outlet (psi)	(Bbls/Day)	(psi)	(psi/bbls/day)	σ'_1 (psi)	σ'_2 (psi)	σ'_3 (psi)	
0:00	450	280	250	18	2.4	1.30	15.6	12.0	432	262	232	No water was injected
0:12	440	260	230	18	2.4	1.50	15.6	10.4	422	242	212	
0:24	425	250	215	18	2.5	1.90	15.5	8.16	407	232	197	Cavity formed as
0:36	405	250	210	18	2.5	2.00	15.5	7.75	387	232	192	flow began
0:48	403	250	200	27	3.5	3.30	23.5	7.12	376	223	173	Cavity size: 1/2" x 1/2"
1:00	402	250	200	28	3.5	3.50	24.5	7.00	374	222	172	
1:12	402	250	200	28	3.5	3.55	24.5	6.90	374	222	172	
1:24	401	250	200	56	4.3	4.20	51.7	12.31	345	194	144	
1:36	401	250	190	65	4.5	4.68	60.5	12.93	336	185	125	Cavity grew.
1:48	400	250	190	65	4.5	4.85	60.5	12.47	335	185	125	Size: 1/2" x 1"
2:00	400	250	190	65	4.5	4.95	60.5	12.22	335	185	125	
2:12	390	250	190	65	4.5	5.04	60.5	12.00	325	185	125	Arch failure
2:24	380	250	190	65	4.8	5.06	60.2	11.90	315	185	125	
2:36	375	250	190	103	6.0	5.03	97.0	19.28	272	147	87	Cavity size: 1" x 3"
2:48	372	250	190	105	6.8	7.09	98.2	13.85	267	145	85	
3:00	360	250	190	105	7.0	7.09	98.0	13.82	255	145	85	
3:12	350	250	190	105	7.0	7.68	98.0	12.76	245	145	85	
3:24	340	250	190	138	9.0	8.50	129.0	15.18	202	112	52	Arch failure
3:36	335	250	190	138	10.0	8.92	128.0	14.35	197	112	52	
3:48	330	250	190	138	10.2	9.10	127.8	14.04	192	112	52	Cavity size: 1/2" x >4
4:00	330	250	190	138	10.7	9.26	127.3	13.75	192	112	52	
4:12	330	250	190	138	10.7	9.26	127.3	13.75	192	112	52	
4:24	330	250	190	180	11.0	9.26	169.0	18.25	150	70	10	
4:36	330	250	190	184	16.4	9.45	167.6	17.74	146	66	6	Restabilized condition
4:48	330	250	190	184	17.0	9.56	167.0	17.47	146	66	6	
5:00	330	250	190	184	16.8	9.61	167.2	17.40	146	66	6	
5:12	330	250	190	184	16.2	9.64	167.8	17.41	146	66	6	Cavity size 1 1/2" x > 4"
5:24	330	250	190	184	15.8	9.68	168.2	17.38	146	66	6	
5:36	330	250	190	184	15.8	9.68	168.2	17.38	146	66	6	
5:48	330	250	190	184	15.0	9.68	169.0	17.46	146	66	6	

EXPERIMENTAL DATA: Time through Flow Rate, Q; CALCULATED DATA: ΔP through Pseudo Effective Stress.

TABLE 10

TEST NUMBER: BII (Drawdown Test)

SAND: Natural
Sample B

STRESS LEVEL: 750 psi

Time	Sand Stress (EXPERIMENTAL DATA)			Pressure		Flow Rate, Q	ΔP	ΔP/Q (CALCULATED DATA)	Pseudo Effective Stress			Comment
(hr:min:sec)	σ_1 (psi)	σ_2 (psi)	σ_3 (psi)	inlet (psi)	outlet (psi)	(Bbls/Day)	(psi)	(psi/bbls/day)	σ'_1 (psi)	σ'_2 (psi)	σ'_3 (psi)	
0:00:00	750	420	860	14.0	3.0	0.60	11.0	18.33	736	406	846	Cavity formed almost
0:00:30	750	420	860	14.0	3.0	1.82	11.0	6.04	736	406	846	spontaneously as valve
0:01:00	745	420	860	14.0	3.0	2.20	11.0	5.00	731	406	846	was opened.
0:01:30	745	420	860	14.0	3.0	2.24	11.0	4.91	731	406	846	Cavity size: 1/2" x 1"
0:02:00	745	420	860	14.0	3.0	2.20	11.0	5.00	731	406	846	
0:02:30	745	420	860	14.0	3.0	2.09	11.0	5.26	731	406	846	Intense sand production
0:03:00	740	420	860	14.0	3.0	1.95	11.0	5.64	726	406	846	for a brief period.
0:03:30	740	420	860	14.0	3.0	1.82	11.0	6.04	726	406	846	
0:04:00	740	420	860	14.0	3.0	1.75	11.0	6.29	726	406	846	
0:04:30	740	420	860	14.0	3.0	1.63	11.0	6.75	726	406	846	
0:05:00	740	420	860	14.0	3.0	1.50	11.0	7.33	726	406	846	Stable condition
0:05:30	740	420	860	14.0	3.0	1.36	11.0	8.09	726	406	846	
0:06:00	740	420	860	14.0	2.5	1.33	11.5	8.65	726	406	846	
0:06:30	740	420	860	14.0	2.5	1.23	11.5	9.35	726	406	846	
0:07:00	740	420	860	14.0	2.5	1.15	11.5	10.00	726	406	846	
0:07:30	740	420	860	14.0	2.5	1.10	11.5	10.45	726	406	846	
0:08:00	740	420	860	14.0	2.3	1.02	11.7	11.47	726	406	846	Conditions remained
0:08:30	740	420	860	14.0	2.3	0.93	11.7	12.58	726	406	846	stable
0:09:00	740	420	860	14.0	2.3	0.88	11.7	13.30	726	406	846	
0:09:30	740	420	860	14.0	2.3	0.83	11.7	14.10	726	406	846	
0:10:00	740	420	860	14.0	2.3	0.78	11.7	15.00	726	406	846	

TABLE B (Cont'd)

TEST NUMBER: BII (Drawdown Test)

SAND: Natural Sample B

STRESS LEVEL: 750 psi

Time	Sand Stress (EXPERIMENTAL DATA)			Pressure		Flow Rate, Q	ΔP	ΔP/Q (CALCULATED DATA)	Pseudo Effective Stress			Comment
(hrs:min:sec)	σ_1 (psi)	σ_2 (psi)	σ_3 (psi)	inlet (psi)	outlet (psi)	(Bbls/Day)	(psi)	(psi/bbls/day)	σ'_1 (psi)	σ'_2 (psi)	σ'_3 (psi)	
0:10:30	740	420	860	14.0	2.3	0.74	11.7	15.81	726	406	846	
0:11:00	740	420	860	14.0	2.3	0.69	11.7	16.96	726	406	846	
0:11:30	740	420	860	14.0	2.3	0.61	11.7	19.18	726	406	846	Stable condition
0:12:00	740	420	860	14.0	2.3	0.60	11.7	19.50	726	406	846	
0:12:30	740	420	860	14.0	2.3	0.55	11.7	21.27	726	406	846	
0:13:00	740	420	860	14.0	2.3	0.51	11.7	22.94	726	406	846	
0:13:30	740	420	860	14.0	2.3	0.46	11.7	25.43	726	406	846	
0:14:00	740	420	860	14.0	2.3	0.45	11.7	26.00	726	406	846	
0:14:30	740	420	860	14.0	2.3	0.42	11.7	27.86	726	406	846	
0:15:00	740	420	860	14.0	2.3	0.40	11.7	29.25	726	406	846	
0:15:30	740	420	860	14.0	2.3	0.39	11.7	30.00	726	406	846	
0:16:00	740	420	860	14.0	2.3	0.38	11.7	30.79	726	406	846	
0:16:30	740	420	860	14.0	2.3	0.32	11.7	36.56	726	406	846	
0:17:00	740	420	860	14.0	2.3	0.32	11.7	36.56	726	406	846	
0:17:30	740	420	860	14.0	2.3	0.31	11.7	37.74	726	406	846	
0:18:00	740	420	860	14.0	2.3	0.31	11.7	37.74	726	406	846	Stable condition
0:18:30	740	420	860	14.0	2.3	0.30	11.7	39.00	726	406	846	
0:19:00	740	420	860	14.0	2.3	0.30	11.7	39.00	726	406	846	
0:19:30	740	420	860	14.0	2.3	0.26	11.7	45.00	726	406	846	
0:20:00	740	420	860	14.0	2.3	0.26	11.7	45.00	726	406	846	
0:20:30	740	420	860	14.0	2.3	0.26	11.7	45.00	726	406	846	
0:21:00	740	420	860	14.0	2.3	0.26	11.7	45.00	726	406	846	
0:21:30	740	420	860	14.0	2.3	0.24	11.7	48.75	726	406	846	
0:22:00	740	420	860	14.0	2.3	0.24	11.7	48.75	726	406	846	
0:22:30	740	420	860	14.0	2.3	0.22	11.7	53.18	726	406	846	
0:23:00	740	420	860	14.0	2.3	0.22	11.7	53.18	726	406	846	
0:23:30	740	420	860	14.0	2.3	0.20	11.7	58.50	726	406	846	Stable condition
0:24:00	740	420	860	14.0	2.3	0.18	11.7	65.56	726	406	846	

TEST NUMBER: BII

SAND: Natural
Sample B

STRESS LEVEL: 750 psi

EXPERIMENTAL DATA | CALCULATED DATA

Time	Sand Stress			Pressure		Flow Rate, Q	ΔP	ΔP/Q	Pseudo Effective Stress			Comment
(hr:min)	σ_1 (psi)	σ_2 (psi)	σ_3 (psi)	inlet (psi)	outlet (psi)	(Bbls/Day)	(psi)	(psi/bbls/day)	σ'_1 (psi)	σ'_2 (psi)	σ'_3 (psi)	
0:00	780	500	700	35	3.5	1.13	31.5	27.88	745	465	665	Arch formed during
0:04	780	500	700	36	4.5	1.75	31.5	18.00	744	464	664	test BII remained
0:08	780	500	700	36	4.5	2.20	31.5	14.32	743	463	663	stable
0:12	780	500	700	39	5.1	2.42	33.9	14.01	741	461	661	Cavity size: 1/2" x 1 1/2"
0:16	780	500	700	41	5.6	2.62	35.4	13.51	739	459	659	Stable arch
0:20	780	500	700	42	5.6	2.75	36.4	13.24	738	458	658	condition
0:24	780	500	700	42	5.9	2.80	36.1	12.89	738	458	658	
0:28	780	500	700	42	5.9	2.90	36.1	12.45	738	458	658	Traces of Sand
0:32	780	500	700	42	5.9	2.98	36.1	12.11	738	458	658	
0:36	780	500	700	42	5.9	2.99	36.1	12.07	738	458	658	
0:40	780	500	700	42	5.9	3.00	36.1	12.03	738	458	658	
0:44	780	500	700	42	5.9	3.00	36.1	12.03	738	458	658	
0:48	780	500	700	83	6.3	4.24	76.7	18.09	697	417	617	
0:52	780	500	700	88	6.8	5.00	81.2	16.24	692	412	612	Stable condition
0:56	780	500	700	90	7.0	5.45	83.0	15.23	690	410	610	Cavity size: 1/2" x 2"
1:00	780	500	700	91	7.0	5.80	84.0	14.48	689	409	609	
1:04	780	500	700	92	7.0	6.00	85.0	14.17	688	408	608	
1:08	780	500	700	93	7.0	6.11	86.0	14.08	687	407	607	Stable arch condition
1:12	780	500	700	95	7.8	6.18	87.2	14.11	685	405	605	
1:16	780	500	700	98	9.0	6.20	89.0	14.35	682	402	602	Cavity size: 1" x 3"
1:20	780	500	700	98	10.0	-	88.0	-	682	402	602	
1:24	780	500	700	98	10.7	6.32	87.3	13.81	682	402	602	
1:28	780	500	700	98	11.2	6.55	86.8	13.25	683	402	602	Traces of sand.
1:32	780	500	700	99	12.0	7.42	87.0	11.73	681	401	601	
1:36	780	500	700	100	12.3	7.80	87.7	11.24	680	400	600	
1:40	780	500	700	103	13.0	8.00	90.0	11.25	677	397	597	
1:44	780	500	700	135	13.3	8.10	121.7	15.02	645	365	565	
1:48	780	500	700	140	13.4	8.12	126.6	15.59	640	360	560	Stable arch remained

TEST NUMBER: BIV

SAND: Natural Sample B

STRESS LEVEL: 750 psi

EXPERIMENTAL DATA | CALCULATED DATA

Time	Sand Stress			Pressure		Flow Rate, Q	ΔP	ΔP/Q	Pseudo Effective Stress			Comment
(hrs:min)	σ_1 (psi)	σ_2 (psi)	σ_3 (psi)	inlet (psi)	outlet (psi)	(Bbls/Day)	(psi)	(psi/bbls/day)	σ'_1 (psi)	σ'_2 (psi)	σ'_3 (psi)	
0:00	750	320	560	360	3.5	0.90	356.5	396.10	390	-40	200	Stable arch remained
0:04	740	320	560	385	3.5	1.20	381.5	317.92	355	-65	175	(from previous
0:08	720	320	550	410	4.0	1.40	406.0	290.00	310	-90	140	test)
0:12	720	320	550	429	4.0	1.53	425.0	277.80	291	-109	121	Slight failure,
0:16	720	320	550	453	4.2	1.53	448.8	293.30	267	-133	97	Traces of sand
0:20	720	320	550	475	4.5	1.53	470.5	307.52	245	-155	75	Cavity size: 1" x > 4"
0:24	710	300	550	490	4.5	1.53	485.5	317.32	220	-190	60	Re-stabilized
0:28	710	300	540	500	4.5	1.53	495.5	323.86	210	-200	40	condition
0:32	710	300	540	500	4.5	1.53	495.5	323.86	210	-200	40	
0:36	710	300	540	500	4.5	1.53	495.5	323.86	210	-200	40	
0:40	710	300	540	850	4.5	2.50	845.5	338.20	-140	-650	-310	Stable condition
0:44	710	300	540	1000	4.5	2.90	995.5	343.28	-290	-700	-460	
0:48	705	300	540	1050	4.5	3.05	1045.5	342.79	-345	-750	-510	
0:52	705	300	540	1100	5.0	3.45	1095.0	317.39	-395	-800	-560	Possible flow
0:56	705	300	540	1450	5.0	4.80	1445.0	301.04	-745	-1150	-910	impairment suspected
1:00	705	300	540	1500	5.2	5.35	1494.8	279.40	-795	-1200	-960	
1:04	705	300	540	1500	6.5	5.70	1493.5	262.02	-795	-1200	-960	
1:08	705	280	540	1500	7.0	-	1493.0	-	-795	-1220	-960	
1:12	700	280	540	1250	3.0	4.65	1247.0	268.17	-550	-970	-710	
1:16	700	280	540	1250	3.0	5.65	1247.0	220.71	-550	-970	-710	
1:20	700	280	540	1250	4.5	6.39	1245.5	194.91	-550	-970	-710	
1:24	700	280	540	1270	6.2	6.70	1263.8	188.63	-570	-990	-730	Stable condition
1:28	700	280	540	1270	7.0	6.95	1263.0	181.73	-570	-990	-730	
1:32	700	280	540	1300	8.0	7.00	1292.0	184.57	-600	-1020	-760	
1:36	700	280	540	1350	8.0	7.00	1342.0	191.71	-650	-1070	-810	
1:40	700	280	540	1500	8.0	7.40	1492.0	201.62	-800	-1220	-960	Stable condition
1:44	700	280	540	1600	8.0	8.50	1592.0	187.29	-900	-1320	-1060	
1:48	700	280	540	1650	8.0	9.00	1642.0	182.40	-950	-1370	-1110	
1:52	700	280	540	1650	8.0	9.00	1642.0	182.40	-950	-1370	-1110	Pump breakdown
1:56	700	280	540	1650	8.0	9.00	1642.0	182.40	-950	-1370	-1110	

TABLE 13

TEST NUMBER: BV

SAND: Natural
Sample B

STRESS LEVEL: 1000 psi

EXPERIMENTAL DATA / CALCULATED DATA

Time (hrs:min)	Sand Stress σ_1 (psi)	σ_2 (psi)	σ_3 (psi)	Pressure inlet (psi)	outlet (psi)	Flow Rate, Q (Bbls/Day)	ΔP (psi)	ΔP/Q (psi/bbls/day)	Pseudo Effective Stress σ'_1 (psi)	σ'_2 (psi)	σ'_3 (psi)	Comment
0:00	960	680	550	212	8.0	7.38	204.0	27.64	748	468	338	No water injected.
0:04	950	670	540	212	7.8	6.78	204.2	30.12	738	458	328	Initial arch formation
0:08	950	670	540	212	7.0	6.30	205.0	32.54	738	458	328	Cavity observed
0:12	950	670	540	212	7.0	5.90	205.0	34.75	738	458	328	Size: 1/2" x 1/2"
0:16	950	670	540	212	6.8	5.75	205.2	35.69	738	458	328	
0:20	950	670	540	212	6.4	5.61	205.6	36.65	738	459	328	Traces of sand.
0:24	950	670	540	212	6.2	5.52	205.8	37.28	738	458	328	
0:28	950	670	540	212	6.2	5.45	205.8	37.76	738	458	328	Cavity size: 1/2" x 1"
0:32	950	670	540	212	6.1	5.39	205.9	38.20	738	458	328	
0:36	950	670	540	212	6.0	5.30	206.0	38.87	738	458	328	
0:40	950	670	540	212	6.0	5.30	206.0	38.87	738	458	328	
0:44	950	670	540	215	6.0	5.24	206.0	39.31	735	455	325	
0:48	940	660	530	217	6.0	5.22	211.0	40.42	723	443	313	Minor arch failure
0:52	940	660	530	217	5.8	5.24	211.2	40.31	723	443	313	Restabilized arch
0:56	960	660	530	217	5.8	5.17	211.2	40.85	743	443	313	Arch strengthened.
1:00	960	665	530	217	5.8	5.10	211.2	41.41	743	448	313	(Load adjustment)
1:04	960	660	530	217	5.8	5.05	211.2	41.82	743	443	313	Cavity size: 3/4" x 1 1/2"
1:08	960	660	530	217	5.8	5.05	211.2	41.82	743	443	313	
1:12	950	660	530	217	5.8	4.95	211.2	42.67	733	443	313	
1:16	960	660	530	217	5.8	4.90	211.2	43.10	743	443	313	

TABLE 13 (cont'd)

TEST NUMBER: BV

SAND: Natural Sample B

STRESS LEVEL: 1000 psi

EXPERIMENTAL DATA / CALCULATED DATA

Time	Sand Stress			Pressure		Flow Rate, Q	ΔP	ΔP/Q	Pseudo Effective Stress			Comment
(hrs:min)	σ_1 (psi)	σ_2 (psi)	σ_3 (psi)	inlet (psi)	outlet (psi)	(Bbls/Day)	(psi)	(psi/bbls/day)	σ'_1 (psi)	σ'_2 (psi)	σ'_3 (psi)	
1:20	960	660	530	217	5.8	4.88	211.2	43.28	743	443	313	Cavity size: 1" x 2"
1:24	900	640	530	217	5.6	4.74	211.4	44.60	683	423	313	Arch failure and
1:28	900	640	530	217	5.6	4.74	211.4	44.60	683	423	313	restabilization
1:32	900	640	530	217	5.6	4.70	211.4	44.98	683	423	313	
1:36	900	630	520	217	5.6	4.68	211.4	45.17	683	413	303	Cavity size: 1" x 2 1/2"
1:40	890	620	510	223	5.6	4.68	217.4	46.45	667	397	287	
1:44	890	620	510	223	5.6	4.60	217.5	47.28	667	397	287	
1:48	890	620	510	223	5.3	4.53	217.7	48.06	667	397	287	
1:52	890	620	510	223	5.2	4.49	217.8	48.51	667	397	287	
1:56	890	620	510	242	5.1	4.65	236.9	50.95	667	378	268	
2:00	890	620	510	242	5.1	4.84	236.9	48.95	648	378	268	
2:04	890	620	510	242	5.2	4.90	236.8	48.33	648	378	268	
2:08	890	620	510	242	5.3	4.85	236.7	48.80	648	378	268	
2:12	880	620	510	242	5.5	4.85	236.5	48.76	638	378	268	
2:16	880	620	510	242	5.5	4.85	236.5	48.76	638	378	268	Cavity size: 1" x 3"
2:20	870	610	510	242	5.5	4.85	236.5	48.76	628	368	268	
2:24	870	610	510	267	5.7	5.05	261.3	51.74	603	343	243	
2:28	870	610	510	267	5.8	5.25	261.2	49.75	603	343	243	
2:32	870	600	510	267	5.8	5.39	261.2	48.46	603	333	243	
2:36	875	600	510	267	5.8	5.40	261.2	48.37	608	333	243	

TABLE 13 (cont'd)

TEST NUMBER: BV

SAND: Natural Sample B

STRESS LEVEL: 1000 psi

	EXPERIMENTAL DATA							CALCULATED DATA				
Time	Sand Stress			Pressure		Flow Rate, Q	ΔP	$\Delta P/Q$	Pseudo Effective Stress			Comment
(hrs:min)	σ_1 (psi)	σ_2 (psi)	σ_3 (psi)	inlet (psi)	outlet (psi)	(Bbls/Day)	(psi)	(psi/bbls/day)	σ'_1 (psi)	σ'_2 (psi)	σ'_3 (psi)	
2:40	850	580	510	267	5.8	5.40	261.2	48.37	583	313	243	
2:44	850	580	510	267	5.8	5.40	261.2	48.37	583	313	243	
2:48	855	580	505	292	6.0	5.75	286.0	49.74	563	288	213	
2:52	855	580	500	292	6.1	5.95	285.9	48.05	563	288	208	Cavity size: 1" x 3"
2:56	860	580	500	292	6.0	6.02	285.9	47.49	568	288	208	
3:00	865	580	500	292	6.1	6.03	285.9	47.41	573	288	208	
3:04	870	585	500	292	6.1	6.03	285.9	47.41	578	293	208	Stable condition
3:08	870	585	500	310	6.0	6.34	304.0	47.95	560	275	190	
3:12	875	585	505	310	6.0	6.50	304.0	46.77	565	275	195	
3:16	890	590	505	310	5.9	6.39	304.1	47.59	580	280	195	
3:20	890	590	505	310	5.9	6.10	304.1	49.85	580	280	195	
3:24	880	590	500	310	5.9	5.54	304.1	54.89	570	280	190	
3:28	890	590	500	310	5.8	5.30	304.2	57.40	580	280	190	Cavity size: 1" x 3"
3:32	870	590	500	310	5.8	5.06	304.2	60.12	560	280	190	
3:36	870	590	500	302	5.8	4.80	296.2	61.71	568	288	198	
3:40	880	590	500	305	5.2	4.40	299.8	68.14	575	285	195	
3:44	890	590	500	306	5.0	4.23	301.0	71.16	584	284	194	
3:48	870	590	500	307	5.0	4.00	302.0	75.50	563	283	193	
3:52	875	590	500	307	4.6	3.80	302.4	79.58	568	283	193	
3:56	875	590	500	307	4.6	3.65	302.4	82.85	568	283	193	
4:00	885	590	500	306	4.6	3.42	301.4	88.13	579	284	194	Stable condition
4:04	870	590	500	306	4.6	3.24	301.4	93.02	564	284	194	
4:08	880	590	500	360	4.6	3.24	301.4	93.02	574	284	194	

TABLE 14

TEST NUMBER: BVI

SAND: Natural
Sample B

STRESS LEVEL: 1500 psi

EXPERIMENTAL DATA | CALCULATED DATA

Time	Sand Stress			Pressure		Flow Rate, Q	ΔP	ΔP/Q	Pseudo Effective Stress			Comment
(hrs:min)	σ_1 (psi)	σ_2 (psi)	σ_3 (psi)	inlet (psi)	outlet (psi)	(Bbls/Day)	(psi)	(psi/bbls/day)	σ'_1 (psi)	σ'_2 (psi)	σ'_3 (psi)	
0:00	1410	360	1290	179	9.6	7.7	169.4	22.00	1231	181	1111	Existing arch from pre-
0:04	1240	315	1280	179	8.2	7.25	170.8	23.56	1061	136	1101	vious test failed, as
0:08	1220	310	1280	183	8.0	6.70	175.0	26.12	1037	127	1097	sand pack was being
0:12	1220	300	1280	183	7.2	6.35	175.8	27.69	1037	117	1097	stressed.
0:16	1205	300	1280	183	7.0	6.00	176.0	29.33	1022	117	1097	Cavity collapsed and
0:20	1205	300	1280	183	6.5	5.70	176.5	30.96	1022	117	1097	sand produced.
0:24	1205	280	1280	184	6.3	5.40	177.7	32.91	1021	96	1096	Condition stabilized
0:28	1205	280	1280	184	6.0	5.20	178.0	34.23	1021	96	1096	New cavity formed.
0:32	1205	280	1280	184	5.8	4.89	178.2	36.44	1021	96	1096	Size: 1/2" x 1/2"
0:36	1205	280	1280	184	5.8	4.80	178.2	37.13	1021	96	1096	
0:40	1205	280	1280	184	5.8	4.70	178.2	37.91	1021	96	1096	
0:44	1215	280	1280	184	5.6	4.56	178.4	39.12	1031	96	1096	Arch strengthening
0:48	1220	280	1280	184	5.6	4.49	178.4	39.73	1036	96	1096	
0:52	1220	280	1280	184	5.6	4.40	178.4	40.55	1036	96	1096	Stable condition
0:56	1220	280	1280	184	5.6	4.30	178.4	41.49	1036	96	1096	
1:00	1215	280	1280	184	5.6	4.20	178.4	42.48	1031	96	1096	Traces of sand
1:04	1200	280	1280	202	5.2	4.36	196.8	45.14	998	78	1078	Cavity size: 1/2" x 3/4"
1:08	1200	280	1280	202	5.2	4.44	196.8	44.32	998	78	1078	
1:12	1200	280	1280	202	5.2	4.44	196.8	44.32	998	78	1078	
1:16	1210	280	1280	202	5.2	4.44	196.8	44.32	1008	78	1078	

TABLE 14 (cont'd)

TEST NUMBER: BVI

SAND: Natural
Sample B

STRESS LEVEL: 1500 psi

Time	Sand Stress			Pressure		Flow Rate, Q	ΔP	ΔP/Q	Pseudo Effective Stress			Comment
(hrs:min)	σ_1 (psi)	σ_2 (psi)	σ_3 (psi)	inlet (psi)	outlet (psi)	(Bbls/Day)	(psi)	(psi/bbls/day)	σ'_1 (psi)	σ'_2 (psi)	σ'_3 (psi)	
1:20	1200	280	1280	202	5.2	4.42	196.8	44.52	998	78	1078	
1:24	1190	280	1280	202	5.2	4.35	196.8	45.24	988	78	1078	
1:28	1190	280	1270	202	5.2	4.30	196.8	45.77	988	78	1068	Stable condition
1:32	1190	280	1270	202	5.2	4.25	196.8	46.31	988	78	1068	
1:36	1190	280	1270	202	5.2	4.15	196.8	47.42	988	78	1068	
1:40	1190	280	1270	202	5.2	4.14	196.8	47.54	988	78	1068	
1:44	1190	280	1270	214	5.2	4.12	208.8	50.68	976	66	1056	
1:48	970	280	1270	214	5.2	4.20	208.8	49.71	756	66	1056	Arch failed and
1:52	1190	280	1270	214	5.2	4.20	208.8	49.71	976	66	1056	restabilized
1:56	1190	280	1270	214	5.2	4.20	208.8	49.71	976	66	1056	1/2" x 1/2"
2:00	1200	280	1270	230	5.2	4.40	224.8	51.09	970	50	1040	
2:04	1195	280	1270	230	5.2	4.49	224.8	50.07	965	50	1040	Cavity size: 1/2" x 1"
2:08	1195	280	1270	230	5.2	4.50	224.8	49.96	965	50	1040	
2:12	1190	280	1270	230	5.2	4.50	224.8	49.96	960	50	1040	
2:16	1180	280	1270	230	5.2	4.50	224.8	49.96	950	50	1040	
2:20	1180	280	1270	230	5.2	4.40	224.8	51.09	950	50	1040	
2:24	1185	280	1270	230	5.2	4.40	224.8	51.09	955	50	1040	
2:28	1190	280	1270	230	5.2	4.40	224.8	51.09	960	50	1040	
2:32	1190	280	1270	240	5.2	4.40	234.8	53.36	950	40	1030	
2:36	1190	280	1270	240	5.2	4.50	234.8	52.18	950	40	1030	
2:40	1190	280	1270	252	5.2	4.55	246.8	54.24	938	28	1018	

TABLE 14(cont'd)

TEST NUMBER: BVI

SAND: Natural
Sample B

STRESS LEVEL: 1500 psi

EXPERIMENTAL DATA | CALCULATED DATA

Time	Sand Stress			Pressure		Flow Rate, Q	ΔP	ΔP/Q	Pseudo Effective Stress			Comment
(hrs:min)	σ_1 (psi)	σ_2 (psi)	σ_3 (psi)	inlet (psi)	outlet (psi)	(Bbls/Day)	(psi)	(psi/bbls/day)	σ'_1 (psi)	σ'_2 (psi)	σ'_3 (psi)	
2:44	1145	280	1270	252	5.2	4.60	246.8	53.65	893	28	1018	Arch failed and
2:48	1190	280	1270	252	5.2	4.60	246.8	53.65	938	28	1018	restabilized
2:52	1190	280	1270	252	5.2	4.60	246.8	53.65	938	28	1018	
2:56	1170	280	1270	252	5.2	4.60	246.8	53.65	918	28	1018	Cavity size: 1/2" x 2"
3:00	1120	280	1270	252	5.2	4.60	246.8	53.65	868	28	1018	Arch failed again, and
3:04	1160	280	1270	267	5.2	4.72	261.8	55.47	893	13	1003	restabilized
3:08	1170	280	1270	267	5.2	4.82	261.8	54.32	903	13	1003	
3:12	1190	280	1270	267	5.2	4.90	261.8	53.43	923	13	1003	Cavity size 1" x 2"
3:16	1190	280	1270	267	5.2	4.92	261.8	53.21	923	13	1003	
3:20	1160	280	1270	267	5.2	4.95	261.8	53.10	893	13	1003	
3:24	1160	280	1270	306	5.2	5.10	300.8	58.98	854	-26	964	Cavity growth:
3:28	1170	280	1270	306	5.6	5.58	300.4	53.84	864	-26	964	Size: 1" x 3"
3:32	1180	280	1270	306	6.0	5.83	300.0	51.46	874	-26	964	
3:36	1190	280	1270	306	6.0	5.95	300.0	50.42	884	-26	964	
3:40	1190	280	1270	306	6.0	5.96	300.0	50.34	884	-26	964	
3:44	1190	280	1270	306	6.0	5.98	300.0	50.17	884	-26	964	
3:48	1170	280	1270	306	6.0	6.00	300.0	50.00	864	-26	964	
3:52	1170	280	1270	306	6.0	5.95	300.0	50.42	864	-26	964	
3:56	1180	280	1270	306	6.0	5.90	300.0	50.85	874	-26	964	
4:00	1190	280	1270	306	6.0	5.88	300.0	51.02	884	-26	964	
4:04	1200	280	1270	306	6.0	5.80	300.0	51.72	894	-26	964	Cavity size: 1" x 3 1/3"
4:08	1180	280	1270	306	6.0	5.70	300.0	52.63	874	-26	964	
4:12	1150	280	1270	306	6.0	5.61	300.0	53.48	844	-26	964	Failure
4:16	1110	280	1270	306	6.0	5.60	300.0	53.57	804	-26	964	

TABLE 15

TEST NUMBER: BVII

SAND: Natural
Sample B

STRESS LEVEL: 1500 psi

	EXPERIMENTAL DATA								CALCULATED DATA			
Time	Sand Stress			Pressure		Flow Rate, Q	ΔP	ΔP/Q	Pseudo Effective Stress			Comment
(hrs:min)	σ_1 (psi)	σ_2 (psi)	σ_3 (psi)	inlet (psi)	outlet (psi)	(Bbls/Day)	(psi)	(psi/bbls/day)	σ'_1 (psi)	σ'_2 (psi)	σ'_3 (psi)	
0:00	1340	400	1290	40	4.0	1.20	36.0	30.00	1300	360	1250	
0:04	1340	400	1290	40	3.8	1.00	36.2	36.20	1300	360	1250	
0:08	1340	400	1290	40	3.6	0.90	36.4	40.44	1300	360	1250	Stable arch remained
0:12	1340	400	1290	40	3.5	0.82	36.5	44.51	1300	360	1250	
0:16	1340	395	1290	40	3.5	0.80	36.5	45.63	1300	355	1250	
0:20	1330	395	1290	75	3.5	0.72	71.5	99.31	1255	320	1215	
0:24	1330	390	1290	75	3.5	0.80	71.5	89.38	1255	315	1215	
0:28	1325	390	1290	75	3.5	0.82	71.5	87.20	1250	315	1215	Cavity size: 1" x 4"
0:32	1325	380	1290	75	3.5	0.88	71.5	81.25	1250	305	1215	
0:36	1320	380	1290	125	3.6	1.25	121.4	97.12	1195	255	1165	
0:40	1320	280	1290	126	3.7	1.41	122.3	86.74	1194	254	1164	
0:44	1320	380	1290	126	3.8	1.50	122.2	81.47	1194	254	1164	
0:48	1320	380	1290	127	3.8	1.52	123.2	81.05	1193	253	1163	
0:52	1320	380	1290	127	3.8	1.52	123.2	81.05	1193	253	1163	Stable arch condition
0:56	1320	380	1290	127	3.8	1.52	123.2	81.05	1193	253	1163	
1:00	1320	380	1290	127	4.0	1.51	123.0	81.46	1193	253	1163	No sand produced
1:04	1320	380	1290	127	4.0	1.51	123.0	81.46	1193	253	1163	
1:08	1320	380	1290	127	4.0	1.49	123.0	82.55	1193	253	1163	
1:12	1300	380	1290	127	4.0	1.43	123.0	86.01	1173	253	1163	Minor arch failure
1:16	1295	380	1290	127	4.0	1.42	123.0	86.62	1168	253	1163	Arch restabilization
1:20	1295	380	1290	127	4.0	1.41	123.0	87.23	1168	253	1163	Traces of sand

TABLE 15(cont'd)

TEST NUMBER: BVII

SAND: Natural
Sample B

STRESS LEVEL: 1500 psi

Time	Sand Stress (EXPERIMENTAL DATA)			Pressure		Flow Rate, Q	ΔP	ΔP/Q	Pseudo Effective Stress (CALCULATED DATA)			Comment
(hrs:min)	σ_1 (psi)	σ_2 (psi)	σ_3 (psi)	inlet (psi)	outlet (psi)	(Bbls/Day)	(psi)	(psi/bbls/day)	σ'_1 (psi)	σ'_2 (psi)	σ'_3 (psi)	
1:24	1300	380	1290	189	4.5	1.82	184.5	101.37	1111	191	1101	
1:28	1310	280	1290	189	4.6	2.13	184.4	86.57	1121	191	1101	Arch restabilization
1:32	1320	380	1290	189	4.6	2.25	184.4	81.96	1131	191	1101	
1:36	1320	280	1290	189	4.6	2.34	184.4	78.80	1131	191	1101	
1:40	1320	380	1290	189	4.6	2.34	184.4	78.80	1131	191	1101	Stable arch condition
1:44	1320	380	1290	208	4.6	2.42	203.4	84.05	1112	172	1082	
1:48	1320	380	1290	206	4.6	2.55	201.4	78.98	1114	174	1084	
1:52	1320	380	1290	206	4.6	2.60	201.4	77.46	1114	174	1084	
1:56	1320	380	1290	206	4.6	2.60	201.4	77.46	1114	174	1084	
2:00	1330	380	1290	225	4.6	2.68	220.4	82.24	1105	155	1065	
2:04	1330	380	1290	225	4.6	2.75	220.4	80.15	1105	155	1065	
2:08	1340	380	1290	225	4.6	2.80	220.4	78.71	1115	155	1065	
2:12	1330	380	1290	225	4.6	2.80	220.4	78.71	1105	155	1065	Stable arch condition.
2:16	1330	380	1290	225	4.6	2.80	220.4	78.71	1105	155	1065	
2:20	1330	380	1290	225	4.6	2.80	220.4	78.71	1105	155	1065	
2:24	1330	380	1290	225	4.6	2.80	220.4	78.71	1105	155	1065	
2:28	1320	380	1290	225	4.6	2.80	220.4	78.71	1095	155	1065	
2:32	1320	380	1290	225	4.6	2.80	220.4	78.71	1095	155	1065	
2:36	1340	380	1290	242	4.6	2.80	237.4	84.79	1098	138	1048	Load adjustment.
2:40	1345	380	1290	242	4.6	2.80	237.4	84.79	1103	138	1048	
2:44	1340	380	1290	242	4.6	2.90	237.4	81.86	1098	138	1048	

TEST NUMBER: BVII

SAND: Natural
Sample B

STRESS LEVEL: 1500 psi

EXPERIMENTAL DATA | CALCULATED DATA

Time	Sand Stress			Pressure		Flow Rate, Q	ΔP	$\Delta P/Q$	Pseudo Effective Stress			Comment
(hrs:min)	σ_1 (psi)	σ_2 (psi)	σ_3 (psi)	inlet (psi)	outlet (psi)	(Bbls/Day)	(psi)	(psi/bbls/day)	σ'_1 (psi)	σ'_2 (psi)	σ'_3 (psi)	
2:48	1320	380	1290	242	4.6	2.91	237.4	81.58	1078	138	1048	
2:52	1320	380	1290	242	4.6	2.93	237.4	81.02	1078	138	1048	
2:56	1320	380	1290	242	4.6	2.90	237.4	81.86	1078	138	1048	
3:00	1320	380	1290	267	4.6	2.90	262.4	90.48	1053	113	1023	Minor arch failure
3:04	1320	380	1290	267	4.6	2.90	262.4	90.48	1053	113	1023	
3:08	1300	380	1290	267	4.7	3.18	262.3	82.48	1033	113	1023	
3:12	1320	370	1290	267	4.7	3.30	262.3	79.48	1053	103	1023	
3:16	1300	370	1290	267	4.7	3.38	262.3	77.60	1033	103	1023	
3:20	1310	370	1290	267	4.7	3.40	262.3	77.15	1043	103	1023	Arch restabilization
3:24	1320	360	1290	302	5.1	3.40	296.9	87.32	1018	58	988	
3:28	1320	360	1290	302	5.2	3.72	296.8	79.78	1018	58	988	
3:32	1320	360	1290	302	5.2	4.00	296.8	74.20	1018	58	988	Stable arch condition
3:36	1320	360	1290	302	5.5	4.16	296.5	71.27	1018	58	988	
3:40	1320	360	1290	302	5.5	4.25	296.5	69.76	1018	58	988	
3:44	1320	360	1290	302	5.5	4.30	296.5	68.95	1018	58	988	
3:48	1320	360	1290	302	5.5	4.32	296.5	68.63	1018	58	988	
3:52	1320	360	1290	302	5.5	4.32	296.5	68.63	1018	58	988	Stable arch condition
3:56	1330	360	1290	302	5.5	4.32	296.5	68.63	1028	58	980	
4:00	1330	360	1290	302	5.5	4.32	296.5	68.63	1028	58	988	
4:04	1330	360	1290	302	5.5	4.32	296.5	68.63	1028	58	988	Cavity size: 1" x >4"
4:08	1330	360	1290	302	5.5	4.30	296.5	68.95	1028	58	988	
4:12	1325	360	1290	302	5.5	4.28	296.5	69.27	1023	58	988	
4:16	1325	360	1290	302	5.5	4.22	296.5	70.26	1023	58	988	
4:20	1320	360	1290	302	5.5	4.21	296.5	70.43	1018	58	988	Stable arch condition
4:24	1320	360	1290	302	5.5	4.20	296.5	70.60	1018	58	988	
4:28	1325	360	1290	302	5.5	4.20	296.5	70.60	1023	58	988	
4:32	1340	360	1290	302	5.5	4.15	296.5	71.45	1038	58	988	

TABLE 16

TEST NUMBER: BVIII (Stress Loading)

SAND: Natural Sample B

STRESS LEVEL: 1340-2320 psi

EXPERIMENTAL DATA / CALCULATED DATA

Time	Sand Stress			Pressure		Flow Rate, Q	ΔP	ΔP/Q	Pseudo Effective Stress			Comment
(hrs:min)	σ_1 (psi)	σ_2 (psi)	σ_3 (psi)	inlet (psi)	outlet (psi)	(Bbls/Day)	(psi)	(psi/bbls/day)	σ'_1 (psi)	σ'_2 (psi)	σ'_3 (psi)	
0:00	1340	350	1220	155	3.0	0.42	152.0	361.90	1185	195	1065	Arch failed under
0:01	1720	580	1320	145	3.4	0.88	141.6	160.91	1575	435	1175	increasing stress load.
0:02	1640	430	1315	143	3.5	1.30	139.5	107.31	1497	287	1172	
0:03	1780	600	1360	140	4.0	1.70	136.0	80.00	1640	460	1220	Sand produced briefly
0:04	1840	620	1390	138	4.3	2.08	133.7	64.28	1702	482	1252	
0:05	1900	640	1400	136	4.5	2.94	131.5	44.73	1764	504	1264	Cavity disappeared
0:06	1935	645	1420	135	4.9	3.20	130.1	40.66	1800	510	1285	
0:07	1990	660	1440	135	5.1	3.50	129.9	37.11	1855	525	1305	
0:08	2020	680	1445	135	5.6	3.86	129.4	33.52	1885	545	1310	Restabilized condition
0:09	2060	685	1460	135	5.8	4.00	129.2	32.30	1925	550	1325	
0:10	2120	710	1470	135	5.9	4.23	129.1	30.52	1985	575	1335	Restabilized condition
0:11	2150	725	1485	134	6.1	4.50	127.9	28.42	2016	591	1351	
0:12	2170	740	1490	132	6.2	4.72	125.8	26.65	2038	608	1358	Small cavity developing
0:13	2200	760	1500	132	6.3	4.91	125.7	25.60	2068	628	1368	about 1/4" x 1/4"
0:14	2235	765	1520	131	6.7	5.10	124.3	24.37	2104	634	1389	
0:15	2240	780	1520	130	6.9	5.24	123.1	23.49	2110	650	1390	
0:16	2260	800	1530	130	7.0	5.31	123.0	23.16	2130	670	1400	Rams "knocking"
0:18	2320	830	1530	130	7.0	5.30	123.0	23.21	2190	700	1400	

TABLE 17

TEST NUMBER: BIX

SAND: Natural Sample B

STRESS LEVEL: 2250 psi

	EXPERIMENTAL DATA								CALCULATED DATA			
Time	Sand Stress			Pressure		Flow Rate, Q	ΔP	ΔP/Q	Pseudo Effective Stress			Comment
(hrs:min)	σ_1 (psi)	σ_2 (psi)	σ_3 (psi)	inlet (psi)	outlet (psi)	(Bbls/Day)	(psi)	(psi/bbls/day)	σ'_1 (psi)	σ'_2 (psi)	σ'_3 (psi)	
0:00	2320	830	1530	130	7.0	5.30	123.0	23.21	2190	700	1400	No water injected
0:04	2150	720	1500	130	7.0	5.05	123.0	24.36	2020	590	1370	
0:08	2110	715	1500	131	6.8	5.00	124.2	24.86	1979	584	1369	Cavity formed
0:12	2080	710	1500	132	6.5	4.95	125.5	25.35	1948	578	1368	
0:16	2055	705	1500	132	6.2	4.90	125.8	25.67	1923	573	1368	
0:20	2040	680	1500	133	6.2	4.82	126.8	26.31	1907	547	1367	
0:24	2035	680	1500	135	6.0	4.79	129.0	26.93	1900	545	1365	
0:28	2015	680	1500	135	5.6	4.72	129.4	27.42	1880	545	1365	
0:32	2005	680	1500	135	5.6	4.65	129.4	27.83	1870	545	1365	
0:36	2000	675	1500	135	5.6	4.62	129.4	28.01	1865	540	1365	
0:40	2000	670	1500	135	5.6	4.56	129.4	28.38	1865	535	1365	
0:44	1995	660	1500	135	5.6	4.52	129.4	28.63	1860	525	1365	
0:48	1990	660	1500	135	5.5	4.50	129.5	28.78	1855	525	1365	
0:52	1970	660	1500	135	5.5	4.44	129.5	29.17	1835	525	1365	Arch failure
0:56	1965	650	1500	135	5.2	4.40	129.8	29.50	1830	515	1365	Cavity size: 1/4" x 3/4"
1:00	1965	650	1500	135	5.1	4.35	129.9	29.86	1830	515	1365	
1:04	1965	650	1500	135	5.1	4.30	129.9	30.21	1830	515	1365	
1:08	1965	650	1500	136	5.1	4.20	130.9	31.17	1829	514	1364	
1:12	1940	650	1500	136	5.1	4.20	130.9	31.17	1804	514	1364	Arch failure
1:16	1930	640	1500	137	5.1	4.72	131.9	27.94	1793	513	1363	Cavity size: 1/2" x 3/4"
1:20	1930	640	1500	245	5.1	5.52	239.9	43.46	1685	395	1255	

TEST NUMBER: BIX

SAND: Natural Sample B

STRESS LEVEL: 2250 psi

EXPERIMENTAL DATA | CALCULATED DATA

Time	Sand Stress			Pressure		Flow Rate, Q	ΔP	ΔP/Q	Pseudo Effective Stress			Comment
(hrs:min)	σ_1 (psi)	σ_2 (psi)	σ_3 (psi)	inlet (psi)	outlet (psi)	(Bbls/Day)	(psi)	(psi/bbls/day)	σ'_1 (psi)	σ'_2 (psi)	σ'_3 (psi)	
1:24	1930	640	1500	247	5.1	5.80	241.9	41.71	1683	393	1253	
1:28	1930	640	1500	248	5.1	5.95	242.9	40.82	1682	392	1252	
1:32	1920	640	1500	250	5.7	6.00	244.3	40.72	1670	390	1250	Arch failure
1:36	1920	640	1500	250	6.3	6.00	243.7	40.62	1670	390	1250	Cavity size: 3/4" x 3/4"
1:40	1915	640	1500	252	6.3	6.00	245.7	40.95	1663	388	1248	
1:44	1915	640	1500	252	6.3	6.00	245.7	40.95	1663	388	1248	
1:48	1920	640	1500	292	6.3	6.51	285.7	43.89	1628	348	1208	
1:52	1920	640	1500	292	6.4	6.62	285.6	43.14	1628	348	1208	
1:56	1930	640	1500	292	7.0	6.63	285.0	42.99	1638	348	1208	Arch strengthening
2:00	1930	640	1500	292	7.0	6.63	285.0	42.99	1638	348	1208	
2:04	1930	640	1500	296	7.0	6.63	289.0	43.59	1634	344	1204	Restabilized condition
2:08	1930	640	1500	296	7.0	6.63	289.0	43.59	1634	344	1204	
2:12	1930	640	1500	302	7.0	6.63	295.0	44.49	1628	338	1198	
2:16	1930	640	1500	302	7.0	6.61	295.0	44.63	1628	338	1198	
2:20	1930	640	1500	302	7.0	6.60	295.0	44.70	1628	338	1198	
2:24	1925	640	1500	302	7.0	6.52	295.0	45.25	1623	338	1198	
2:28	1930	640	1500	302	7.0	6.46	295.0	45.67	1628	338	1198	
2:32	1930	640	1500	302	6.9	6.41	295.1	46.04	1628	338	1198	Stable condition
2:36	1930	640	1500	302	6.9	6.35	295.1	46.47	1628	338	1198	
2:40	1930	640	1500	302	6.9	6.33	295.1	46.62	1628	338	1198	
2:44	1930	640	1500	302	6.9	6.26	295.1	47.14	1628	338	1198	
2:48	1935	630	1500	302	6.8	6.20	295.2	47.61	1633	328	1198	
2:52	1935	630	1500	302	6.5	6.14	295.2	48.08	1633	328	1198	
2:56	1935	630	1500	296	6.5	6.02	295.2	49.04	1639	334	1204	
3:00	1935	630	1500	296	6.5	5.95	289.5	48.66	1639	334	1204	
3:04	1930	620	1500	292	6.5	5.82	285.5	49.05	1638	328	1208	
3:08	1940	620	1500	292	6.5	5.79	285.5	49.31	1648	328	1208	
3:12	1940	620	1500	292	6.2	5.71	285.8	50.05	1648	328	1208	Stable condition
3:16	1940	620	1500	292	6.2	5.70	285.8	50.14	1648	328	1208	
3:20	1940	620	1500	292	6.1	5.62	285.9	50.87	1648	328	1208	Cavity size: 3/4" x 3/4"
3:24	1935	620	1500	292	6.0	5.60	286.0	51.07	1643	328	1208	
3:28	1935	620	1500	292	6.0	5.56	286.0	51.44	1643	328	1208	
3:32	1935	620	1500	292	6.0	5.51	286.0	51.91	1643	328	1208	

TABLE 18

TEST NUMBER: BX

SAND: Natural
Sample B

STRESS LEVEL: 2250 psi

Time	EXPERIMENTAL DATA							CALCULATED DATA				
	Sand Stress			Pressure		Flow Rate, Q	ΔP	ΔP/Q	Pseudo Effective Stress			Comment
(hrs:min)	σ_1 (psi)	σ_2 (psi)	σ_3 (psi)	inlet (psi)	outlet (psi)	(Bbls/Day)	(psi)	(psi/bbls/day)	σ'_1 (psi)	σ'_2 (psi)	σ'_3 (psi)	
0:00	2270	660	1560	65	3.0	0.65	62.0	95.38	2205	595	1495	
0:04	2205	640	1540	65	4.0	1.52	61.0	40.13	2140	575	1475	
0:08	2180	620	1530	86	4.6	1.72	81.4	47.33	2094	534	1444	
0:12	2160	600	1530	86	4.6	1.70	81.4	47.88	2074	514	1444	Stable arch condition
0:16	2150	600	1530	86	4.6	1.77	81.4	45.99	2064	514	1444	remained
0:20	2150	600	1530	86	4.6	1.82	81.4	44.73	2064	514	1444	
0:24	2140	600	1530	294	4.6	1.85	289.4	156.43	1846	306	1236	
0:28	2140	600	1530	294	4.6	1.95	289.4	148.41	1846	306	1236	Closed bypass valve
0:32	2140	600	1530	294	5.0	2.30	289.0	125.65	1846	306	1236	completely.
0:36	2150	600	1530	294	5.1	2.61	288.9	110.69	1856	306	1236	
0:40	2140	600	1530	294	5.6	2.95	288.4	97.76	1846	306	1236	
0:44	2140	560	1530	294	5.6	3.10	288.4	93.03	1846	266	1236	Major arch failure
0:48	1800	560	1500	294	6.0	3.90	288.0	73.85	1506	266	1206	Instantaneous rate
0:52	1780	565	1490	294	5.8	3.38	288.2	85.27	1486	271	1196	increase to 6.3B/D.
0:56	1880	560	1490	294	5.5	3.30	288.5	87.42	1586	266	1196	Sand produced.
1:00	1780	560	1490	294	5.3	3.30	288.7	87.48	1486	266	1196	
1:04	1760	560	1490	294	5.4	3.30	288.6	87.45	1466	266	1196	Arch restabilized
1:08	1755	560	1490	294	5.1	3.30	288.9	87.55	1461	266	1196	
1:12	1760	560	1490	294	5.1	3.22	288.9	89.72	1466	266	1196	Arch restabilized condi-
1:16	1755	560	1490	294	5.1	3.22	288.9	89.72	1461	266	1196	tion
1:20	1755	560	1490	294	5.1	3.22	288.9	89.72	1461	266	1196	

TABLE 10(cont'd)

TEST NUMBER: BX

SAND: Natural Sample B

STRESS LEVEL: 2250 psi

	EXPERIMENTAL DATA								CALCULATED DATA			
Time	Sand Stress			Pressure		Flow Rate, Q	ΔP	ΔP/Q	Pseudo Effective Stress			Comment
(hrs:min)	σ_1 (psi)	σ_2 (psi)	σ_3 (psi)	inlet (psi)	outlet (psi)	(Bbls/Day)	(psi)	(psi/bbls/day)	σ'_1 (psi)	σ'_2 (psi)	σ'_3 (psi)	
1:24	1755	555	1490	294	4.9	3.22	289.1	89.78	1461	261	1196	
1:28	1755	555	1490	294	4.9	3.12	289.1	92.66	1461	261	1196	
1:32	1755	555	1490	294	4.9	3.12	289.1	92.66	1461	261	1196	
1:36	1755	550	1490	294	4.9	3.09	289.1	93.56	1461	256	1196	Stable arch condition
1:40	1760	550	1490	294	4.9	3.06	289.1	94.48	1466	256	1196	
1:44	1760	550	1490	294	4.5	3.04	289.5	95.23	1466	256	1196	
1:48	1765	550	1490	294	4.5	3.00	289.5	96.50	1471	256	1196	
1:52	1765	550	1490	294	4.5	3.00	289.5	96.50	1471	256	1196	
1:56	1765	550	1490	294	4.5	2.99	289.5	96.82	1471	256	1196	Cavity size: 1" x >4"
2:00	1760	550	1490	294	4.5	2.98	289.5	97.15	1466	256	1196	
2:04	1755	550	1490	294	4.5	2.94	289.5	98.47	1461	256	1196	Stable arch condition
2:08	1760	550	1490	294	4.5	2.90	289.5	99.83	1466	256	1196	
2:12	1760	550	1490	294	4.5	2.90	289.5	99.83	1466	256	1196	
2:16	1760	550	1490	294	4.5	2.89	289.5	100.17	1466	256	1196	
2:20	1760	550	1490	294	4.5	2.88	289.5	100.52	1466	256	1196	

TABLE 19

TEST NUMBER: BXI

SAND: Natural Sample B

STRESS LEVEL: 780-2280 psi

EXPERIMENTAL DATA / CALCULATED DATA

Time	Sand Stress			Pressure		Flow Rate, Q	ΔP	ΔP/Q	Pseudo Effective Stress			Comment
(hrs:min)	σ_1 (psi)	σ_2 (psi)	σ_3 (psi)	inlet (psi)	outlet (psi)	(Bbls/Day)	(psi)	(psi/bbls/day)	σ'_1 (psi)	σ'_2 (psi)	σ'_3 (psi)	
0:00	780	80	1260	56	4.5	1.73	51.5	29.77	724	24	1204	
0:04	730	80	1260	56	7.0	4.50	49.0	10.89	674	24	1204	
0:08	760	85	1260	56	7.2	5.20	48.8	9.38	704	29	1204	
0:12	1110	190	1240	56	7.9	5.30	48.1	9.08	1054	134	1184	Arch collapsed under
0:16	1520	360	1200	57	7.9	5.41	49.1	9.08	1463	303	1143	load.
0:20	1640	390	1120	59	7.8	5.52	51.2	9.28	1581	331	1061	Cavity disappeared.
0:24	1710	450	1150	59	7.0	5.05	52.0	10.30	1651	391	1091	
0:28	1850	560	1200	59	6.9	4.90	52.1	10.63	1791	501	1141	
0:32	2120	720	1240	59	6.5	4.70	52.5	11.17	2061	661	1181	
0:36	2120	740	1215	61	5.8	3.29	55.2	16.78	2059	679	1154	
0:40	2080	720	1215	61	5.8	3.65	55.2	15.12	2019	659	1154	
0:44	2240	840	1260	61	5.8	3.63	55.2	15.21	2179	779	1199	
0:48	2300	875	1310	61	5.8	3.39	55.2	16.28	2239	814	1249	Hydraulic line pressure
0:52	2230	840	1280	62	5.6	3.29	56.4	17.14	2168	778	1218	≈ 10,000 psi
0:56	2280	890	1350	62	5.6	3.32	56.4	16.99	2218	828	1288	Stress load decline
1:00	2240	860	1320	62	5.6	3.45	56.4	16.35	2178	798	1258	
1:04	2280	920	1380	62	5.2	3.28	56.8	17.32	2218	858	1318	Rams "knocking"
1:08	2220	860	1360	63	5.2	3.28	57.8	17.62	2157	797	1297	

TABLE 20

TEST NUMBER: BXII

SAND: Natural Sample B

STRESS LEVEL: 2250 psi

EXPERIMENTAL DATA | CALCULATED DATA

Time	Sand Stress			Pressure		Flow Rate, Q	ΔP	ΔP/Q	Pseudo Effective Stress			Comment
(hrs:min)	σ_1 (psi)	σ_2 (psi)	σ_3 (psi)	inlet (psi)	outlet (psi)	(Bbls/Day)	(psi)	(psi/bbls/day)	σ'_1 (psi)	σ'_2 (psi)	σ'_3 (psi)	
0:00	2230	875	1360	63	5.2	3.28	57.8	17.62	2167	812	1297	
0:04	2120	800	1360	63	5.2	3.10	57.8	18.65	2057	737	1297	Cavity formed without
0:08	2060	760	1360	62	5.0	2.90	57.0	19.66	1998	698	1298	injecting water
0:12	2040	720	1360	62	4.6	2.80	57.4	20.50	1978	658	1298	Size: 1/2" x 1/2"
0:16	2000	720	1360	62	4.6	2.75	57.4	20.87	1938	658	1298	
0:20	1990	710	1360	62	4.6	2.75	57.4	20.87	1928	648	1298	
0:24	1965	680	1360	62	4.6	2.70	57.4	21.26	1903	618	1298	
0:28	1960	680	1360	62	4.6	2.70	57.4	21.26	1898	618	1298	Stable arch condition
0:32	1950	680	1360	62	4.6	2.61	57.4	21.99	1888	618	1298	Cavity size: 1/2" x 3/4"
0:36	1930	675	1360	62	4.6	2.61	57.4	21.99	1868	613	1298	
0:40	1920	675	1360	62	4.6	2.61	57.4	21.99	1858	613	1298	
0:44	1900	670	1360	62	4.6	2.61	57.4	21.99	1838	608	1298	
0:48	1890	670	1360	62	4.6	2.59	57.4	22.16	1828	608	1298	
0:52	1880	640	1360	62	4.6	2.59	57.4	22.16	1818	578	1298	
0:56	1880	640	1360	62	4.6	2.59	57.4	22.16	1818	578	1298	
1:00	1860	640	1360	62	4.6	2.59	57.4	22.16	1798	578	1298	
1:04	1855	640	1360	62	4.6	2.59	57.4	22.16	1793	578	1298	
1:08	1850	640	1350	62	4.6	2.59	57.4	22.16	1793	578	1288	
1:12	1845	640	1350	65	2.2	0.60	62.8	104.67	1780	575	1285	Closed and opened out-
1:16	1840	640	1350	65	4.0	2.10	61.0	29.05	1775	575	1285	let valve to create a
1:20	1820	630	1350	65	4.5	2.62	60.5	23.09	1755	565	1285	disturbance.

TABLE 20(cont'd)

TEST NUMBER: BXII

SAND: Natural Sample B

STRESS LEVEL: 2250 psi

EXPERIMENTAL DATA | CALCULATED DATA

Time	Sand Stress			Pressure		Flow Rate, Q	ΔP	$\Delta P/Q$	Pseudo Effective Stress			Comment
(hrs:min)	σ_1 (psi)	σ_2 (psi)	σ_3 (psi)	inlet (psi)	outlet (psi)	(Bbls/Day)	(psi)	(psi/bbls/day)	σ'_1 (psi)	σ'_2 (psi)	σ'_3 (psi)	
1:24	1820	620	1350	65	4.6	2.75	60.4	21.96	1755	555	1285	Stable conditions
1:28	1815	620	1350	65	4.6	2.80	60.4	21.57	1750	555	1285	remained
1:32	1815	620	1350	65	4.6	2.80	60.4	21.57	1750	555	1285	
1:36	1750	580	1320	296	10.0	>8.20	286.0	<34.88	1454	284	1024	Closed bypass valve,
1:40	1720	560	1320	296	10.0	8.20	286.0	34.88	1424	264	1024	sudden P in increase:
1:44	1710	560	1320	296	9.5	8.20	286.5	34.94	1414	264	1024	Arch failed.
1:48	1710	560	1310	296	9.0	8.20	287.0	35.00	1414	264	1014	Sand produced briefly
1:52	1710	560	1310	296	9.0	>8.20	287.0	<35.00	1414	264	1014	Arch restabilized.
1:56	1710	560	1310	296	3.0	13.50	293.0	21.70	1414	264	1014	Switched manometer to
2:00	1700	560	1310	64	2.5	7.50	61.5	8.20	1635	496	1246	monitor higher flow
2:04	1700	560	1310	64	2.5	7.50	61.5	8.20	1636	496	1246	rate.
2:08	1690	560	1310	64	2.5	7.80	61.5	7.90	1626	496	1246	Opened bypass valve.
2:12	1685	550	1310	64	2.5	8.80	61.5	6.99	1621	486	1246	
2:16	1685	550	1310	296	3.6	11.00	292.4	26.58	1389	254	1014	
2:20	1685	550	1300	296	3.6	11.00	292.4	26.58	1389	254	1004	Stable condition
2:24	1685	550	1300	296	3.6	11.00	292.4	26.58	1389	254	1004	remained.
2:28	1675	550	1300	296	3.6	11.00	292.4	26.58	1379	254	1004	
2:32	1675	550	1300	296	3.6	11.00	292.4	26.58	1379	254	1004	

TABLE 21

TEST NUMBER: CI

SAND: Natural
Sample C

STRESS LEVEL: 500 psi

EXPERIMENTAL DATA | CALCULATED DATA

Time	Sand Stress			Pressure		Flow Rate, Q	ΔP	ΔP/Q	Pseudo Effective Stress			Comment
(hrs:min)	σ_1 (psi)	σ_2 (psi)	σ_3 (psi)	inlet (psi)	outlet (psi)	(Bbls/Day)	(psi)	(psi/bbls/day)	σ'_1 (psi)	σ'_2 (psi)	σ'_3 (psi)	
-	500	320	-	-	-	-	-	-	-	-	-	No water injected.
0:00	480	300	800	25	3.0	-	23.0	-	455	275	775	Initial arch formed.
0:04	475	300	800	28	8.0	7.3	20.0	2.74	447	272	772	Cavity observed:
0:08	440	290	800	27	3.6	14.8	23.4	1.58	413	263	773	Size 1/4" x 1/2"
0:12	430	280	800	27	3.5	13.5	23.5	1.74	403	253	773	Initial arch failure
0:16	420	280	800	28	3.5	13.5	24.5	1.81	392	252	772	Arch restabilized
0:20	405	280	800	32	3.5	12.8	28.5	2.23	373	248	768	Cavity size: 1/4" x 2"
0:24	405	275	800	35	3.5	12.7	31.5	2.48	370	240	765	Arch failure:
0:28	400	275	800	36	3.5	11.9	32.5	2.73	364	239	764	Cavity size: 1/4" x 3"
0:32	390	270	800	36	3.5	11.8	32.5	2.75	354	234	764	Cavity size: 1/2" x 4"
0:36	370	265	800	42	3.5	11.8	38.5	3.26	328	223	758	Cavity size: 1" x 4"
0:40	365	260	800	50	3.5	11.8	46.5	3.94	315	210	750	Arch failure
0:44	355	250	800	52	3.5	14.8	48.5	3.28	303	198	748	Sand produced
0:48	350	250	800	53	3.5	13.5	49.5	3.67	297	197	747	Cavity partly filled with
0:52	350	250	800	54	3.5	13.5	50.5	3.74	296	196	746	sand.
0:56	350	250	800	56	4.0	11.8	52.0	4.41	294	194	744	Cavity size: 1 1/2" x > 4"
1:00	350	250	800	65	4.0	14.8	61.0	4.12	285	185	735	Arch failure
1:04	315	250	800	110	7.0	28.5	103.0	3.61	205	140	690	Sand produced
1:08	300	250	800	115	7.0	30.7	108.0	3.52	185	135	685	
1:12	300	250	800	120	7.0	30.4	113.0	3.72	180	130	680	Arch restabilized
1:16	290	250	800	125	6.3	28.5	118.7	4.16	165	125	675	
1:20	280	250	800	130	7.0	29.8	123.0	4.13	150	120	670	Cavity size: 1 3/4" x > 4"
1:24	260	240	800	133	7.0	29.8	126.0	4.23	127	107	667	
1:28	260	240	800	135	7.0	29.8	128.0	4.30	125	105	665	Stable arch
1:32	265	240	800	138	7.0	29.8	131.0	4.40	127	102	662	
1:36	500	360	980	350	4.5	19.8	345.5	17.45	150	10	630	Arch stress adjustments
1:40	490	360	980	353	4.5	20.5	348.5	17.00	137	7	627	No sand produced.
1:44	480	360	980	353	4.5	20.5	348.5	17.00	127	7	627	Increased skin: Inlet pressure increased to 350 psi.

TABLE 22

TEST NUMBER: CII

SAND: Natural Sample C

STRESS LEVEL: 750 psi

Time	Experimental Data: Sand Stress			Pressure		Flow Rate, Q	ΔP	Calculated Data: ΔP/Q	Pseudo Effective Stress			Comment
(hrs:min)	σ_1 (psi)	σ_2 (psi)	σ_3 (psi)	inlet (psi)	outlet (psi)	(Bbls/Day)	(psi)	(psi/bbls/day)	σ'_1 (psi)	σ'_2 (psi)	σ'_3 (psi)	
-	750	450	860	-	-	-	-	-	-	-	-	No water injected
0:00	735	440	860	37	3.0	8.9	34.0	3.82	698	403	826	Cavity formation:
0:04	730	420	860	38	4.4	2.71	33.6	12.40	692	382	822	Size: 1/2" x 1/2"
0:08	710	415	860	39	5.0	3.60	34.0	9.44	671	376	821	
0:12	700	415	860	39	5.2	3.81	33.8	8.87	661	376	821	
0:16	700	415	860	41	5.2	3.90	35.8	9.18	659	374	819	Stable condition
0:20	700	415	860	41	5.2	3.90	35.8	9.18	659	374	819	
0:24	700	415	860	41	5.3	3.82	35.7	9.35	659	374	819	
0:28	700	415	860	46	5.5	4.02	40.5	10.07	654	369	814	
0:32	700	410	865	51	5.6	4.15	45.4	10.94	649	359	814	
0:36	700	410	865	51	5.7	4.40	45.3	10.30	649	359	814	
0:40	700	410	865	60	5.8	4.70	54.2	11.53	640	350	805	Stable condition
0:44	700	410	865	61	6.0	5.01	55.0	10.98	639	349	804	
0:48	700	410	865	61	6.0	5.01	55.0	10.98	639	349	804	
0:52	700	410	865	68	6.0	5.18	62.0	11.97	632	342	797	
0:56	700	405	870	70	6.4	5.42	63.6	11.73	630	340	800	
1:00	700	405	870	70	6.4	5.45	64.1	11.76	630	335	800	
1:04	700	405	870	78	6.8	5.40	71.2	13.19	622	327	792	
1:08	700	405	870	79	7.0	5.82	72.0	12.37	621	326	791	
1:12	700	405	870	80	7.0	5.88	73.0	12.41	620	325	790	Cavity size: 1/2" x 1"
1:16	700	405	870	81	7.0	5.80	73.0	12.59	619	324	789	

TEST NUMBER: CII

SAND: Natural
Sample C

STRESS LEVEL: 750 psi

Time	Sand Stress (EXPERIMENTAL DATA)			Pressure		Flow Rate, Q	ΔP	ΔP/Q	Pseudo Effective Stress (CALCULATED DATA)			Comment
(hrs:min)	σ_1 (psi)	σ_2 (psi)	σ_3 (psi)	inlet (psi)	outlet (psi)	(Bbls/Day)	(psi)	(psi/bbls/day)	σ'_1 (psi)	σ'_2 (psi)	σ'_3 (psi)	
1:20	700	405	870	90	7.4	6.30	82.6	13.11	610	315	780	
1:24	700	405	870	93	7.4	6.54	85.6	13.09	607	312	777	Stable arch condition
1:28	700	405	870	95	7.4	6.55	87.6	13.37	605	310	775	
1:32	700	405	870	108	8.4	6.89	99.6	14.46	592	297	762	
1:36	700	405	870	111	9.0	7.73	102.0	13.20	589	294	759	Cavity size: 3/4" x 2"
1:40	700	405	870	113	9.2	7.92	103.8	13.11	587	292	757	
1:44	700	405	870	115	9.2	7.95	105.8	13.31	585	290	755	
1:48	695	405	870	111	3.3	7.95	107.7	13.55	584	294	759	Switched mnometer
1:50	700	405	890	236	4.0	15.50	232.0	14.97	464	169	654	Increasing skin build-up.
1:52	710	410	910	255	4.6	19.10	250.4	13.11	455	155	655	Major arch failure
1:54	730	415	920	275	4.9	21.00	270.1	12.86	455	140	645	Observed pressure and rate
1:56	735	415	930	291	5.1	22.40	285.9	12.76	444	124	639	surges
-	645	405	860	252	16.2	33.0	235.8	7.15	393	163	608	Produced sand - 1/2
2:00	620	405	860	257	6.0	25.3	251.0	9.92	363	148	603	'separator' - full
2:04	605	400	860	261	5.9	24.5	255.1	10.41	344	139	599	
2:06	605	400	860	266	5.9	24.3	260.1	10.70	339	134	594	Cavity size: 1" x >4"
2:08	595	400	860	326	8.5	33.7	317.5	9.42	269	74	534	
2:12	570	400	860	336	9.1	37.0	326.9	8.84	234	64	524	
2:16	560	400	860	340	9.1	37.0	330.9	8.94	220	60	520	
2:20	535	400	860	346	9.1	36.0	336.9	9.36	189	54	514	
2:24	520	400	860	346	9.0	35.0	337.0	9.63	174	54	514	
2:28	515	400	860	348	9.0	34.2	339.0	9.91	167	52	512	
2:32	510	395	850	349	8.0	33.3	341.0	10.24	161	46	501	Restabilized condition
2:36	510	395	850	350	8.0	32.6	342.0	10.49	160	47	500	

TEST NUMBER: CIII

SAND: Natural
Sample C

STRESS LEVEL: 1000 psi

EXPERIMENTAL DATA | CALCULATED DATA

Time	Sand Stress			Pressure		Flow Rate, Q	ΔP	ΔP/Q	Pseudo Effective Stress			Comment
(hrs:min)	σ_1 (psi)	σ_2 (psi)	σ_3 (psi)	inlet (psi)	outlet (psi)	(Bbls/Day)	(psi)	(psi/bbls/day)	σ'_1 (psi)	σ'_2 (psi)	σ'_3 (psi)	
0:00	1005	710	480	45	4.5	0.7	40.5	57.86	960	665	435	No water injected
0:04	1000	700	480	46	4.5	1.2	41.5	34.58	954	654	434	No immediate cavity
0:08	1000	680	480	46	4.5	1.38	41.5	30.07	954	634	434	observed
0:12	1000	680	480	46	4.5	1.49	41.5	27.85	954	634	434	
0:16	980	680	490	46	4.6	1.59	41.4	26.04	934	634	444	Stable condition
0:20	980	680	490	46	4.6	1.63	41.4	25.40	934	634	444	
0:24	980	680	490	46	5.0	1.64	41.0	25.00	934	634	444	
0:28	970	680	490	51	5.0	1.64	46.0	28.05	919	629	439	No sand produced
0:32	970	680	490	51	5.0	1.69	46.0	27.22	919	629	439	
0:36	960	670	520	51	5.0	1.70	46.0	27.06	909	619	469	
0:40	960	670	525	51	5.0	1.74	46.0	26.44	909	619	474	
0:44	960	670	530	56	5.0	1.75	46.0	26.29	904	614	474	
0:48	960	670	540	56	5.0	1.80	46.0	25.56	904	614	484	
0:52	960	670	550	65	5.0	1.83	60.0	32.79	895	605	485	
0:56	960	660	560	65	5.0	1.93	60.0	31.09	895	595	495	
1:00	960	660	560	65	5.0	2.00	60.0	30.00	895	595	495	
1:04	960	660	560	65	5.0	2.02	60.0	29.70	895	595	495	Stable condition
1:08	960	660	560	65	5.0	1.92	60.0	31.25	895	595	495	
1:12	960	660	560	75	5.5	1.98	69.5	35.10	885	585	485	
1:16	960	660	560	76	5.5	2.10	70.5	33.57	884	584	484	No sand produced
1:20	960	660	560	76	5.5	2.14	70.5	32.94	884	584	484	

TEST NUMBER: CIII

SAND: Natural
Sample C

STRESS LEVEL: 1000 psi

Time	Sand Stress (EXPERIMENTAL DATA)			Pressure		Flow Rate, Q	ΔP	ΔP/Q (CALCULATED DATA)	Pseudo Effective Stress			Comment
(hrs:min)	σ_1 (psi)	σ_2 (psi)	σ_3 (psi)	inlet (psi)	outlet (psi)	(Bbls/Day)	(psi)	(psi/bbls/day)	σ'_1 (psi)	σ'_2 (psi)	σ'_3 (psi)	
1:24	960	660	560	87	5.5	2.20	81.5	37.05	873	573	473	
1:28	960	660	560	87	5.5	2.30	81.5	35.43	873	573	473	
1:32	960	660	560	87	5.5	2.34	81.5	34.83	873	573	473	
1:36	960	660	560	88	5.5	2.35	82.5	35.11	872	572	472	
1:40	960	660	560	88	5.5	2.35	82.5	35.11	872	572	472	
1:41	960	660	560	88	5.5	2.35	82.5	35.11	872	572	472	
1:18	960	655	560	105	5.5	2.42	99.5	41.12	855	550	455	
1:52	960	655	560	106	5.5	2.62	100.5	38.36	854	549	454	
1:56	960	655	560	106	5.5	2.70	100.5	37.22	854	549	454	
2:00	960	655	560	106	5.5	2.70	100.5	37.22	854	549	454	
2:04	960	655	560	106	5.6	2.68	100.4	37.46	854	549	454	
2:08	960	655	560	125	5.6	2.75	119.4	43.42	835	530	435	
2:12	960	655	560	127	5.6	3.00	121.4	40.47	833	528	433	
2:16	960	655	560	130	5.6	3.12	124.4	39.87	830	525	430	
2:20	960	655	560	130	5.6	3.12	124.4	39.87	830	525	430	
2:24	960	655	560	130	5.6	3.12	124.4	39.87	830	525	430	1/2" x 1/2" cavity observed
2:28	980	660	560	194	5.6	4.05	188.4	46.52	786	466	366	
2:32	980	660	560	199	5.6	4.50	193.4	42.98	781	461	361	
2:36	980	660	560	201	5.6	4.56	195.4	42.85	779	459	359	Slight cavity growth
2:40	980	660	560	204	6.1	4.56	197.9	43.40	776	456	356	Size: 1/2" x 3/4"
2:44	1000	670	560	204	7.0	4.50	197.0	43.78	796	466	356	
2:48	1000	680	560	256	7.0	5.30	249.0	46.98	744	424	304	Arch stress re-adjustment.
2:52	1000	680	560	262	7.0	5.40	255.0	47.22	738	418	298	Only traces of sand.
2:56	1000	680	560	265	7.0	5.15	258.0	50.10	735	415	295	
3:00	1000	680	560	270	7.2	4.95	264.8	53.49	730	410	290	
3:04	1000	680	560	358	7.2	5.75	350.8	61.01	642	322	202	Stable condition
3:08	1000	680	560	358	7.0	5.90	351.0	59.49	642	322	202	
3:12	1000	680	560	358	7.0	5.75	351.0	61.04	642	322	202	
3:16	1000	680	560	360	7.5	5.50	352.5	64.09	640	320	200	Cavity size: 1/2" x 1"
3:20	990	680	560	360	7.5	5.18	352.5	68.05	640	320	200	
3:24	990	680	560	360	7.5	5.00	352.5	70.50	640	320	200	

TABLE 24

TEST NUMBER: CIV

SAND: Natural
Sample C

STRESS LEVEL: 1500 psi

EXPERIMENTAL DATA | CALCULATED DATA

Time	Sand Stress			Pressure		Flow Rate, Q	ΔP	ΔP/Q	Pseudo Effective Stress			Comment
(hrs:min)	σ_1 (psi)	σ_2 (psi)	σ_3 (psi)	inlet (psi)	outlet (psi)	(Bbls/Day)	(psi)	(psi/bbls/day)	σ'_1 (psi)	σ'_2 (psi)	σ'_3 (psi)	
-	1500	1000	600	-	-	-	-	-	-	-	-	No water injected
0:00	1445	960	630	46	4.0	0.30	42.0	140.00	1399	914	584	Cavity formed as flow
0:04	1405	930	640	46	4.0	0.38	42.0	110.53	1359	884	594	began
0:08	1400	925	640	46	4.0	0.49	42.0	85.71	1354	879	594	Cavity size: 1/4" x 1/4"
0:12	1395	920	640	56	4.0	0.51	52.0	101.96	1339	864	594	
0:16	1390	890	640	56	4.0	0.58	52.0	89.66	1334	834	594	
0:20	1370	890	640	56	4.5	0.61	51.5	84.43	1314	834	594	
0:24	1370	890	640	56	4.5	0.69	51.5	74.64	1314	834	594	
0:28	1370	890	640	56	4.5	0.72	51.5	71.53	1314	834	594	Stable condition
0:32	1370	890	640	64	4.5	0.78	59.5	76.28	1306	826	576	
0:36	1370	890	640	64	4.5	0.81	59.5	73.46	1306	826	576	
0:40	1370	890	640	64	4.5	0.85	59.5	70.00	1306	826	576	Stable condition
0:44	1370	890	640	64	4.5	0.90	59.5	66.11	1306	826	576	
0:48	1370	890	640	64	4.5	0.95	59.5	62.63	1306	826	576	
0:52	1370	890	640	64	4.5	1.00	59.5	59.50	1306	826	576	No sand produced
0:56	1360	885	640	64	4.5	1.02	59.5	58.33	1296	821	576	
1:00	1360	885	640	74	4.5	1.18	69.5	58.90	1286	811	566	Cavity size 1/2" x 1/2"
1:04	1360	885	640	74	4.5	1.24	69.5	56.05	1286	811	566	
1:08	1360	885	640	74	4.5	1.24	69.5	56.05	1286	811	566	
1:12	1355	880	640	74	4.5	1.24	69.5	56.05	1281	806	566	
1:16	1355	880	640	74	4.5	1.24	69.5	56.05	1281	806	566	Stable condition

TABLE 24 (cont'd)

TEST NUMBER: CIV

SAND: Natural
Sample C

STRESS LEVEL: 1500 psi

	EXPERIMENTAL DATA								CALCULATED DATA			
Time	Sand Stress			Pressure		Flow Rate, Q	ΔP	ΔP/Q	Pseudo Effective Stress			Comment
(hrs:min)	σ_1 (psi)	σ_2 (psi)	σ_3 (psi)	inlet (psi)	outlet (psi)	(Bbls/Day)	(psi)	(psi/bbls/day)	σ'_1 (psi)	σ'_2 (psi)	σ'_3 (psi)	
1:20	1355	880	640	74	4.5	1.24	69.5	56.05	1281	806	566	
1:24	1350	880	640	74	4.5	1.24	69.5	56.05	1276	806	566	
1:28	1350	880	640	74	4.5	1.25	69.5	55.60	1276	806	566	
1:32	1350	880	640	74	4.5	1.28	69.5	54.30	1276	806	566	
1:36	1350	880	640	85	4.5	1.33	80.5	60.53	1265	795	555	
1:40	1350	880	640	85	4.5	1.33	80.5	60.53	1265	795	555	Cavity size: 1/2" x 3/4"
1:44	1350	880	640	85	4.5	1.33	80.5	60.53	1265	795	555	
1:48	1350	870	640	103	4.5	1.50	98.5	65.67	1247	767	537	
1:52	1350	870	640	104	4.5	1.56	99.5	63.78	1246	766	536	
1:56	1350	870	640	105	4.5	1.60	99.5	62.19	1245	765	535	
2:00	1350	870	640	105	4.5	1.63	100.5	61.66	1245	765	535	
2:04	1350	870	640	105	4.5	1.63	100.5	61.66	1245	765	535	
2:08	1350	870	640	105	4.5	1.63	100.5	61.66	1245	765	535	
2:12	1350	870	640	105	4.5	1.63	100.5	61.66	1245	765	535	
2:16	1350	870	640	121	4.5	1.78	116.5	65.45	1229	749	519	
2:20	1350	870	640	122	4.5	1.88	117.5	62.50	1228	748	518	
2:24	1340	860	640	122	4.5	1.89	117.5	62.17	1218	738	518	Cavity size 1/2" x 3/4"
2:28	1340	860	640	122	4.5	1.89	117.5	62.17	1218	738	518	
2:32	1340	860	640	123	4.5	1.89	118.5	62.70	1217	737	517	
2:36	1340	860	640	124	4.5	1.90	119.5	62.89	1216	736	516	
2:40	1340	860	640	125	4.5	1.90	120.5	63.42	1215	735	515	

TABLE 24 (cont'd)

TEST NUMBER: CIV

SAND: Natural
Sample C

STRESS LEVEL: 1500 psi

Time	Sand Stress (EXPERIMENTAL DATA)			Pressure		Flow Rate, Q	ΔP	$\Delta P/Q$	Pseudo Effective Stress (CALCULATED DATA)			Comment
(hrs:min)	σ_1 (psi)	σ_2 (psi)	σ_3 (psi)	inlet (psi)	outlet (psi)	(Bbls/Day)	(psi)	(psi/bbls/day)	σ'_1 (psi)	σ'_2 (psi)	σ'_3 (psi)	
2:44	1350	860	650	156	4.5	1.92	151.5	78.91	1194	704	494	
2:48	1350	860	650	159	5.0	2.18	154.0	70.64	1191	701	491	
2:52	1350	860	660	159	5.0	2.36	154.0	65.25	1191	701	501	
2:56	1350	860	660	161	5.0	2.41	156.0	64.73	1189	699	499	
3:00	1350	860	660	161	5.0	2.41	156.0	64.73	1189	699	499	
3:04	1370	860	680	219	5.1	2.84	213.9	75.32	1151	641	461	
3:08	1370	860	680	223	5.8	3.24	217.2	67.04	1147	637	457	
3:12	1370	860	680	225	5.8	3.39	219.2	64.66	1145	635	455	
3:16	1370	860	680	225	5.8	3.40	219.2	64.47	1145	635	455	No failures
3:20	1370	860	680	276	5.8	3.60	270.2	75.06	1094	584	404	No sand produced
3:24	1370	860	680	280	5.8	3.71	274.2	73.91	1090	580	400	
3:28	1370	860	680	280	5.8	3.71	274.2	73.91	1090	580	400	
3:32	1370	860	680	282	5.8	3.68	276.2	75.05	1088	578	398	Stable condition
3:36	1380	860	680	282	5.8	3.60	276.2	76.72	1098	578	398	
3:40	1390	880	680	350	6.2	4.35	343.8	79.03	1040	530	330	Cavity size: 1/2" x 1"
3:44	1390	880	680	350	6.2	4.57	343.8	75.23	1040	530	330	Arch strengthening
3:48	1390	880	680	350	6.2	4.57	343.8	75.23	1040	530	330	
3:52	1390	880	680	360	6.2	4.56	353.8	77.59	1030	520	320	
3:56	1390	880	680	360	6.0	4.50	353.8	78.62	1030	520	320	
4:00	1390	880	680	360	5.8	4.35	354.2	81.43	1030	520	320	
4:04	1390	880	680	360	5.8	4.22	254.2	83.93	1030	520	320	

TEST NUMBER: CV

SAND: Natural
Sample C

STRESS LEVEL: 1500 psi

EXPERIMENTAL DATA / CALCULATED DATA

Time	Sand Stress			Pressure		Flow Rate, Q	ΔP	ΔP/Q	Pseudo Effective Stress			Comment
(hrs:min)	σ_1 (psi)	σ_2 (psi)	σ_3 (psi)	inlet (psi)	outlet (psi)	(Bbls/Day)	(psi)	(psi/bbls/day)	σ'_1 (psi)	σ'_2 (psi)	σ'_3 (psi)	
0:00	1440	920	800	360	3.5	1.00	356.5	356.50	1080	560	440	Arch failed and sand
0:04	1440	920	805	360	3.5	1.00	356.5	356.50	1080	560	445	produced (1/2 separator
0:08	1280	790	640	360	12.0	1.50	348.0	232.00	920	430	280	- full)
0:12	1275	790	640	360	5.0	1.90	355.0	186.84	915	430	280	Cavity size: 1" x >4"
0:16	1275	790	640	360	5.5	2.40	354.5	147.71	915	430	280	
0:20	1275	790	640	360	5.6	2.69	354.4	131.75	915	430	280	
0:24	1275	790	640	360	5.6	3.00	354.4	118.13	915	430	280	
0:28	1275	790	640	360	5.6	3.30	354.4	107.39	915	430	280	
0:32	1275	790	640	360	5.9	3.50	354.1	101.17	915	430	280	Restabilized arch
0:36	1275	790	640	360	6.0	3.65	354.0	96.99	915	430	280	
0:40	1275	790	640	360	6.1	3.85	353.9	91.92	915	430	280	
0:44	1275	790	640	360	6.9	4.09	353.1	86.33	915	430	280	
0:48	1275	790	640	360	6.9	4.22	353.1	83.67	915	430	280	
0:52	1275	790	640	360	7.0	4.40	353.0	80.23	915	430	280	
0:56	1275	790	640	360	7.0	4.56	353.0	77.41	915	430	280	
1:00	1275	790	640	360	7.0	4.70	353.0	75.11	915	430	280	
1:04	1275	790	640	360	7.0	4.83	353.0	73.08	915	430	280	
1:08	1275	790	640	360	7.0	4.90	353.0	72.04	915	430	280	
1:12	1275	790	640	360	7.1	5.00	352.9	70.58	915	430	280	
1:16	1275	790	640	360	7.2	5.10	352.8	69.18	915	430	280	
1:20	1275	790	640	360	7.5	5.24	352.5	67.27	915	430	280	

TABLE 23(cont'd)

TEST NUMBER: CV

SAND: Natural
Sample C

STRESS LEVEL: 1500 psi

	EXPERIMENTAL DATA							CALCULATED DATA				
Time	Sand Stress			Pressure		Flow Rate, Q	ΔP	ΔP/Q	Pseudo Effective Stress			Comment
(hrs:min)	σ_1 (psi)	σ_2 (psi)	σ_3 (psi)	inlet (psi)	outlet (psi)	(Bbls/Day)	(psi)	(psi/bbls/day)	σ'_1 (psi)	σ'_2 (psi)	σ'_3 (psi)	
1:24	1275	790	640	360	7.5	5.40	352.5	65.28	915	430	280	
1:28	1275	790	640	360	7.9	5.50	352.2	64.02	915	430	280	
1:32	1275	790	640	360	8.0	5.60	352.0	62.86	915	430	280	
1:36	1275	790	640	360	8.0	5.70	352.0	61.75	915	430	280	
1:40	1275	790	640	360	8.0	5.80	353.0	60.69	915	430	280	
1:44	1275	790	640	360	8.0	5.85	352.0	60.17	915	430	280	Stable condition
1:48	1275	790	640	360	8.0	5.90	352.0	59.66	915	430	280	
1:52	1275	790	640	360	8.0	5.95	352.0	59.16	915	430	280	
1:56	1275	790	640	360	8.0	5.96	352.0	59.06	915	430	280	
2:00	1275	790	640	360	8.0	6.00	352.0	58.67	915	430	280	
2:04	1275	790	640	360	8.0	6.00	352.0	58.67	915	430	280	Stable condition prevailed
2:08	1275	790	640	360	8.0	6.01	352.0	58.57	915	430	280	
2:12	1275	790	640	360	8.0	6.02	352.0	58.47	915	430	280	
1:16	1275	790	640	360	8.0	6.02	352.0	58.47	915	430	280	

TEST NUMBER: CVI (Stress Loading)

SAND: Natural
Sample C

STRESS LEVEL: 130-1600 psi

EXPERIMENTAL DATA | CALCULATED DATA

Time	Sand Stress			Pressure		Flow Rate, Q	ΔP	ΔP/Q	Pseudo Effective Stress			Comment
(hrs:min)	σ_1 (psi)	σ_2 (psi)	σ_3 (psi)	inlet (psi)	outlet (psi)	(Bbls/Day)	(psi)	(psi/bbls/day)	σ'_1 (psi)	σ'_2 (psi)	σ'_3 (psi)	
0:00	130	120	990	25	3.5	0.3	21.5	71.67	105	95	965	
0:04	130	120	990	25	4.5	1.65	20.5	12.42	105	95	965	
0:08	130	120	990	25	5.2	2.60	19.8	7.62	105	95	965	
0:12	130	120	990	25	5.2	2.50	19.8	7.92	105	95	965	
0:16	130	120	990	25	5.2	2.50	19.8	7.92	105	95	965	
0:20	440	280	900	25	5.2	2.90	19.8	6.83	415	255	875	
0:24	860	520	800	25	5.2	2.45	19.8	8.08	835	495	775	
0:28	1150	720	740	25	4.5	2.14	20.5	9.58	1125	695	715	
0:32	1340	840	730	25	4.5	1.89	20.5	10.85	1315	815	705	
0:36	1440	900	720	25	4.5	1.75	20.5	11.71	1415	875	659	
0:40	1500	930	720	25	4.5	1.63	20.5	12.58	1475	905	695	
0:44	1560	980	720	25	4.5	1.55	20.5	13.23	1535	955	695	9000 psi hydraulic line
0:46	1600	1000	720	25	4.5	-	20.5	-	1575	975	695	pressure.
0:48	1570	980	725	25	4.5	1.42	20.5	14.44	1545	955	700	Stopped pneumatic pump.
0:50	1520	960	680	25	4.5	-	20.5	-	1495	935	655	Rams "knocking"
0:52	1460	930	720	25	4.0	1.24	21.0	16.94	1435	905	695	
0:56	1440	920	730	25	4.0	1.12	21.0	18.75	1415	895	705	
1:00	1420	900	720	25	4.0	1.02	21.0	20.59	1395	875	695	
1:04	1410	900	720	25	4.0	1.01	21.0	20.79	1385	875	695	
1:08	1400	900	720	25	4.0	1.01	21.0	20.79	1375	875	695	
1:12	1390	890	720	25	4.0	0.96	21.0	21.88	1365	865	695	
1:16	1380	890	720	25	4.0	0.94	21.0	22.34	1255	865	695	
1:20	1370	880	720	25	4.0	0.92	21.0	22.83	1345	855	695	
1:24	1370	880	720	-	3.5	0.55	-	-	-	-	-	
1:28	1370	870	720	-	3.5	0.45	-	-	-	-	-	Stopped fluid pump
1:32	1370	870	720	-	3.5	0.41	-	-	-	-	-	
1:36	1365	870	720	-	3.5	0.32	-	-	-	-	-	
1:40	1360	870	720	-	3.5	0.30	-	-	-	-	-	
1:44	1355	870	720	-	3.5	0.26	-	-	-	-	-	
1:48	1355	870	720	-	3.5	0.26	-	-	-	-	-	
1:52	1355	860	720	-	3.5	0.26	-	-	-	-	-	
1:56	1355	860	720	-	3.5	0.26	-	-	-	-	-	

TABLE 27

TEST NUMBER: CVII (Stress Loading)

SAND: Natural
Sample C

STRESS LEVEL: 1200-1710 psi

Time	EXPERIMENTAL DATA: Sand Stress			Pressure		Flow Rate, Q	ΔP	CALCULATED DATA: ΔP/Q	Pseudo Effective Stress			Comment
(hrs:min)	σ_1 (psi)	σ_2 (psi)	σ_3 (psi)	inlet (psi)	outlet (psi)	(Bbls/Day)	(psi)	(psi/bbls/day)	σ'_1 (psi)	σ'_2 (psi)	σ'_3 (psi)	
0:00	1200	1040	725	26	2.3	0.22	23.7	107.73	1174	1014	699	24 hours after CVI
0:02	1220	1045	720	26	3.0	0.22	23.0	104.55	1194	1019	694	
0:04	1500	1270	680	26	3.2	0.24	22.8	95.00	1474	1244	654	
0:06	1600	1360	685	26	3.5	0.26	22.5	86.54	1574	1334	659	
0:08	1640	1380	710	26	3.7	0.26	22.3	85.77	1614	1354	684	
0:10	1680	1390	710	26	4.0	0.26	22.0	84.62	1654	1364	684	
0:12	1710	1400	710	26	4.5	0.38	21.5	56.58	1684	1374	684	
0:14	1730	1430	730	26	4.5	0.38	21.5	56.58	1704	1404	704	
0:16	1740	1440	730	26	4.7	0.55	21.3	38.73	1714	1414	704	
0:18	1750	1440	740	26	4.7	0.70	21.3	30.43	1724	1414	714	
0:20	1700	1380	740	26	4.7	0.72	21.3	29.58	1674	1354	714	Stopped stress loading
0:22	1680	1370	750	26	4.7	0.72	21.3	29.58	1654	1344	724	
0:24	1675	1365	750	26	4.7	0.72	21.3	29.58	1649	1339	724	
0:26	1670	1360	750	26	4.7	0.72	21.3	29.58	1644	1334	724	Rams "knocking"
0:28	1710	1380	720	26	4.7	0.72	21.3	29.58	1684	1354	694	
0:30	1680	1365	730	26	4.7	0.72	21.3	29.58	1654	1339	704	
0:32	1675	1360	730	26	4.7	0.72	21.3	29.58	1649	1334	704	

TABLE 28

TEST NUMBER: CVIII

SAND: Natural
Sample C

STRESS LEVEL: 1800 psi

	EXPERIMENTAL DATA								CALCULATED DATA			
Time	Sand Stress			Pressure		Flow Rate, Q	ΔP	ΔP/Q	Pseudo Effective Stress			Comment
(hrs:min)	σ_1 (psi)	σ_2 (psi)	σ_3 (psi)	inlet (psi)	outlet (psi)	(Bbls/Day)	(psi)	(psi/bbls/day)	σ_1 (psi)	σ_2 (psi)	σ_3 (psi)	
0:00	1760	1130	660	26	4.6	0.73	21.4	29.32	1734	1104	634	Cavity formed without
0:04	1690	1065	720	26	4.6	0.73	21.4	29.32	1664	1039	694	injecting water
0:08	1660	1040	730	26	4.6	0.73	21.4	29.32	1634	1014	704	Size: 1/4" x 1/2"
0:12	1640	1030	730	26	4.6	0.73	21.4	29.32	1614	1004	704	
0:16	1640	1020	730	26	4.6	0.73	21.4	29.32	1614	994	704	
0:20	1640	1020	730	26	4.5	0.70	21.5	30.71	1614	994	704	
0:24	1620	1020	740	26	4.5	0.70	21.5	30.71	1594	994	714	Slight arch failure
0:28	1610	1020	740	46	4.5	1.14	41.5	36.40	1564	974	694	
0:32	1600	1010	750	46	5.0	1.33	41.5	31.20	1554	964	704	Traces of sand
0:36	1600	1000	750	56	5.0	1.33	51.0	38.35	1544	944	694	
0:40	1600	1000	750	56	5.0	1.59	51.0	32.08	1544	944	694	Restabilized condition
0:44	1600	1000	750	56	5.0	1.62	51.0	31.48	1544	944	694	
0:48	1600	1000	750	56	5.0	1.62	51.0	31.58	1544	944	694	
0:52	1600	1000	750	65	5.0	1.85	60.0	32.43	1535	935	685	
0:56	1600	1000	750	65	5.5	1.92	59.5	30.99	1535	935	685	
1:00	1600	995	750	65	5.5	1.92	59.5	30.99	1535	930	685	
1:04	1600	990	750	76	5.5	1.99	70.5	35.43	1524	914	674	
1:08	1595	990	750	76	5.5	2.05	70.5	34.39	1519	914	674	
1:12	1595	990	760	76	5.5	2.05	70.5	34.39	1519	914	684	
1:16	1595	980	760	76	5.5	2.05	70.5	34.39	1519	904	684	
1:20	1590	980	760	88	5.5	2.20	82.5	37.50	1502	892	672	

TABLE 28(cont'd)

TEST NUMBER: CVIII

SAND: Natural
Sample C

STRESS LEVEL: 1800 psi

Time	Sand Stress (Experimental Data)			Pressure		Flow Rate, Q	ΔP	ΔP/Q	Pseudo Effective Stress (Calculated Data)			Comment
(hrs:min)	σ_1 (psi)	σ_2 (psi)	σ_3 (psi)	inlet (psi)	outlet (psi)	(Bbls/Day)	(psi)	(psi/bbls/day)	σ_1 (psi)	σ_2 (psi)	σ_3 (psi)	
1:24	1590	980	760	88	5.5	2.34	82.5	35.11	1502	892	672	
1:28	1590	980	760	88	5.5	2.34	82.5	35.11	1502	892	672	Stable condition
1:32	1590	980	760	88	5.5	2.34	82.5	35.11	1502	892	672	
1:36	1590	980	760	104	5.5	2.42	98.5	40.70	1486	876	656	
1:40	1590	980	760	104	5.5	2.62	98.5	37.60	1486	876	656	
1:44	1590	980	760	104	5.5	2.62	98.5	37.60	1486	876	656	
1:48	1590	980	760	104	5.5	2.60	98.5	37.88	1486	876	656	
1:52	1590	980	760	104	5.5	2.52	98.5	39.09	1486	876	656	
1:56	1590	980	760	122	5.5	2.80	116.5	41.61	1468	858	638	Stable condition
2:00	1580	980	760	122	5.5	2.95	116.5	39.49	1458	858	638	
2:04	1580	980	760	122	5.5	2.95	116.5	39.49	1458	858	638	
2:08	1580	980	760	159	6.7	3.14	152.3	48.50	1421	821	601	
2:12	1580	980	760	161	6.8	3.85	154.2	40.05	1419	819	599	Stable condition remained
2:16	1580	980	760	161	6.8	3.85	154.2	40.05	1419	819	599	
2:20	1580	980	770	247	7.5	3.80	239.5	63.03	1333	733	523	
2:24	1580	980	770	257	7.5	4.72	249.5	52.86	1323	723	513	
2:28	1580	980	770	261	8.0	4.85	253.0	52.16	1319	719	509	Cavity size: 1/2" x 1"
2:32	1580	980	770	360	8.0	5.62	352.0	62.63	1220	620	410	
2:36	1590	980	770	360	8.0	6.05	352.0	58.18	1230	620	410	Strengthened arch
2:40	1590	980	770	360	7.5	5.97	352.5	59.05	1230	620	410	
2:44	1590	980	770	360	7.5	5.80	352.5	60.78	1230	620	410	Stable condition
2:48	1590	980	770	360	7.5	5.61	352.5	62.83	1230	620	410	Cavity size: 1/2" x 1"

TABLE 29

TEST NUMBER: CIX

SAND: Natural Sample C

STRESS LEVEL: 1800 psi

EXPERIMENTAL DATA / CALCULATED DATA

Time	Sand Stress			Pressure		Flow Rate, Q	ΔP	ΔP/Q	Pseudo Effective Stress			Comment
(hrs:min)	σ_1 (psi)	σ_2 (psi)	σ_3 (psi)	inlet (psi)	outlet (psi)	(Bbls/Day)	(psi)	(psi/bbls/day)	σ_1 (psi)	σ_2 (psi)	σ_3 (psi)	
0:00	1960	1400	750	27	3.5	-	23.5	-	1933	1373	723	Stressed sandpack to
0:04	1710	1210	900	27	3.5	-	23.5	-	1683	1183	873	1960 psi (maximum
0:08	1710	1210	900	360	4.0	1.20	356.0	296.7	1350	850	540	attainable)
0:12	1710	1210	900	360	5.9	3.56	354.1	99.47	1350	850	540	No water injected
0:16	1710	1210	900	360	6.5	4.47	353.5	79.08	1350	850	540	Cavity formed
0:20	1710	1210	900	360	6.5	4.60	353.5	76.85	1350	850	540	Size: 1/2" x 1/2"
0:24	1710	1210	900	360	6.5	4.60	353.5	76.85	1350	850	540	Cavity size: 1/2" x 1"
0:28	1710	1210	900	360	6.5	4.55	353.5	77.69	1350	850	540	
0:32	1710	1210	900	360	6.5	4.49	353.5	78.73	1350	850	540	
0:36	1710	1200	900	360	6.5	4.45	353.5	79.44	1350	840	540	Stable condition
0:40	1710	1200	900	360	6.0	4.40	354.0	80.45	1350	840	540	
0:44	1710	1200	900	360	5.9	4.35	354.1	81.40	1350	840	540	
0:48	1710	1200	900	360	5.9	4.30	354.1	82.35	1350	840	540	
0:52	1710	1200	900	360	5.9	4.24	354.1	83.51	1350	840	540	
0:56	1710	1200	900	360	5.9	4.20	354.1	84.31	1350	840	540	Stopped test for 15 hours.

TABLE 29(cont'd

TEST NUMBER: CIX

SAND: Natural
Sample C

STRESS LEVEL: 1800 psi

Time	EXPERIMENTAL DATA: Sand Stress			Pressure		Flow Rate, Q	ΔP	CALCULATED DATA: ΔP/Q	Pseudo Effective Stress			Comment
(hrs:min)	σ_1 (psi)	σ_2 (psi)	σ_3 (psi)	inlet (psi)	outlet (psi)	(Bbls/Day)	(psi)	(psi/bbls/day)	σ_1 (psi)	σ_2 (psi)	σ_3 (psi)	
15:00	1580	1140	920	360	2.5	0.50	357.5	715.00	1220	780	560	Test continued after
15:04	1580	1140	920	360	4.5	2.40	355.5	148.13	1220	780	560	15 hours.
15:08	1580	1140	920	360	5.0	3.20	355.0	110.94	1220	780	560	(Maximum ΔP imposed)
15:12	1580	1140	920	360	5.5	3.40	354.5	104.26	1220	780	560	
15:16	1590	1140	920	360	5.5	3.48	354.5	101.87	1230	780	560	Conditions remained stable
15:20	1590	1140	920	360	5.5	3.48	354.5	101.87	1230	780	560	
15:24	1600	1140	920	360	5.5	3.44	354.5	103.05	1240	780	560	
15:28	1600	1140	920	360	5.5	3.39	354.5	104.57	1240	780	560	Cavity size: 1/2" x 1"
												Stopped test
30:32	1600	1140	920	360	3.5	0.83	356.5	429.52	1240	780	560	Test continued after
30:36	1600	1140	920	360	4.5	2.80	355.5	126.96	1240	780	560	15 hours
30:40	1600	1140	920	360	5.0	3.20	355.0	110.94	1240	780	560	
30:44	1600	1140	920	360	5.2	3.22	354.8	110.19	1240	780	560	Conditions remained stable.
30:48	1600	1140	920	360	5.2	3.20	354.8	110.88	1240	780	560	
30:52	1600	1140	920	360	5.2	3.10	354.8	114.45	1240	780	560	

TABLE 30

TEST NUMBER: DI

SAND: Natural
Sample D

STRESS LEVEL: 500 psi

EXPERIMENTAL DATA | CALCULATED DATA

Time	Sand Stress			Pressure		Flow Rate, Q	ΔP	ΔP/Q	Pseudo Effective Stress			Comment
(hrs:min)	σ_1 (psi)	σ_2 (psi)	σ_3 (psi)	inlet (psi)	outlet (psi)	(Bbls/Day)	(psi)	(psi/bbls/day)	σ'_1 (psi)	σ'_2 (psi)	σ'_3 (psi)	
0:00	480	220	110	46	5.8	1.35	40.2	29.78	434	174	64	No water injected
0:04	470	220	110	46	5.8	1.45	40.2	27.72	424	174	64	Initial cavity formed.
0:08	460	220	110	46	5.8	1.49	40.2	26.98	414	174	64	Size: 1/2" x 1/4"
0:12	460	220	110	52	5.8	1.49	46.2	31.01	402	168	58	
0:16	460	220	110	52	5.8	1.49	46.2	31.01	402	168	58	Water droplets showing.
0:20	460	220	110	52	5.8	1.44	46.2	32.08	402	168	58	
0:24	460	220	110	52	5.8	1.42	46.2	32.54	402	168	58	
0:28	450	220	110	56	5.8	1.33	50.2	37.74	394	164	54	Cavity size
0:32	450	220	110	56	5.8	1.33	50.2	37.74	394	164	54	increased: 1/2" x 1/2"
0:36	450	220	110	56	5.8	1.33	50.2	37.74	394	164	54	
0:40	450	220	110	56	5.8	1.33	50.2	37.74	394	164	54	
0:44	450	200	110	62	5.8	1.33	56.2	42.26	388	138	48	
0:48	450	200	110	62	5.8	1.33	56.2	42.26	388	138	48	Cavity size: 1/2" x 1"
0:52	450	200	110	62	5.9	1.33	56.1	42.18	388	138	48	
0:56	450	200	110	70	6.2	1.33	63.8	47.97	380	130	40	
1:00	450	200	115	70	6.5	1.40	63.5	45.36	380	130	45	
1:04	450	200	115	70	6.5	1.40	63.5	45.36	380	130	45	
1:08	450	210	120	78	6.2	1.40	71.8	51.29	372	132	42	
1:12	450	210	120	79	6.2	1.40	72.8	52.00	371	131	41	Stable condition
1:16	450	210	120	80	6.2	1.40	73.8	52.71	370	130	40	
1:20	450	210	120	80	6.2	1.40	73.8	52.71	370	130	40	

TEST NUMBER: DI

SAND: Natural
Sample D

STRESS LEVEL: 500 psi

EXPERIMENTAL DATA | CALCULATED DATA

Time	Sand Stress			Pressure		Flow Rate, Q	ΔP	ΔP/Q	Pseudo Effective Stress			Comment
(hrs:min)	σ_1 (psi)	σ_2 (psi)	σ_3 (psi)	inlet (psi)	outlet (psi)	(Bbls/Day)	(psi)	(psi/bbls/day)	σ'_1 (psi)	σ'_2 (psi)	σ'_3 (psi)	
1:24	450	220	120	85	6.2	1.38	78.8	57.10	365	135	35	
1:28	450	220	120	85	7.0	1.38	78.0	56.52	365	135	35	
1:32	450	220	120	85	7.0	1.41	78.0	55.32	365	135	35	
1:36	450	220	120	90	7.0	1.42	83.0	58.45	360	130	30	
1:40	455	220	120	90	7.0	1.48	83.0	56.08	365	130	30	Stable condition
1:44	455	220	120	90	7.0	1.48	83.0	56.08	365	130	30	
1:48	455	220	120	90	6.5	1.44	83.5	57.99	365	130	30	
1:52	455	220	120	90	7.0	1.42	83.0	58.45	365	130	30	
1:56	460	220	125	100	7.0	1.43	93.0	65.03	360	120	25	
2:00	460	220	125	110	7.0	1.52	93.0	61.18	360	120	25	
2:04	460	220	125	100	7.0	1.52	93.0	61.18	360	120	25	
2:08	460	220	130	110	7.4	1.50	102.6	68.40	350	110	20	
2:12	475	220	130	113	4.5	1.62	108.5	66.98	362	107	17	Open separator valve fully.
2:16	475	220	135	113	4.5	1.72	108.5	63.08	362	107	22	
2:20	480	220	135	125	4.5	1.62	120.5	74.38	355	95	10	
2:24	480	220	140	127	4.5	1.72	122.5	71.22	353	93	13	
2:28	485	220	140	127	4.5	1.70	122.5	72.06	358	93	13	
2:32	490	220	140	150	4.5	2.04	145.5	71.32	340	70	-10	
2:36	500	225	145	150	4.5	2.00	145.5	72.50	350	75	-5	Stable arch condition
2:40	510	225	150	152	4.5	1.84	147.5	80.16	358	73	-2	
2:44	555	245	160	208	4.5	1.93	203.5	105.44	347	37	-48	
2:48	555	245	200	213	4.5	2.00	208.5	104.25	342	32	-13	
2:52	555	245	200	213	4.5	1.89	208.5	110.32	342	32	-13	
2:56	555	245	200	213	4.5	1.80	208.5	115.83	342	32	-13	
3:00	595	270	200	282	4.5	1.90	277.5	146.05	313	-12	-82	
3:04	590	270	220	287	4.5	1.80	282.5	156.94	303	-17	-67	
3:08	585	270	220	289	4.5	1.60	284.5	177.81	296	-19	-69	
3:12	565	270	220	360	4.5	1.42	285.5	201.06	275	-20	-70	No sand produced
3:16	595	280	230	360	4.5	1.71	355.5	207.89	235	-80	-130	
3:20	580	270	240	360	4.5	1.74	355.5	204.31	220	-90	-120	
3:24	560	270	240	360	4.5	1.75	355.5	203.14	200	-90	-160	
3:28	555	250	240	360	4.5	1.70	355.5	209.12	195	-110	-165	

TEST NUMBER: DII

SAND: Natural
Sample D

STRESS LEVEL: 500 psi

Time	Sand Stress			Pressure		Flow Rate, Q	ΔP	ΔP/Q	Pseudo Effective Stress			Comment
(hrs:min)	σ_1 (psi)	σ_2 (psi)	σ_3 (psi)	inlet (psi)	outlet (psi)	(Bbls/Day)	(psi)	(psi/bbls/day)	σ'_1 (psi)	σ'_2 (psi)	σ'_3 (psi)	
	EXPERIMENTAL DATA							CALCULATED DATA				
0:00	500	240	370	44	5.0	0.60	39.0	65.00	456	196	326	Backflowed to clean-up skin around perforation
0:04	510	240	370	47	5.2	1.08	41.8	38.70	463	193	323	
0:08	510	240	370	49	5.2	1.33	43.8	32.93	461	191	321	
0:12	510	240	370	49	5.2	1.38	43.8	31.74	461	191	321	
0:16	510	240	370	59	5.2	1.41	53.8	38.16	451	181	311	
0:20	520	240	370	61	5.2	1.62	55.8	34.44	459	179	309	
0:24	520	240	370	61	5.2	1.69	55.8	33.02	459	179	309	
0:28	520	240	370	61	5.3	1.69	55.7	32.96	459	179	309	
0:32	520	240	370	67	5.3	1.80	61.7	34.28	453	173	303	Cavity size: 1" x 1 1/4"
0:36	520	240	370	67	5.3	1.82	61.7	33.90	453	173	303	
0:40	520	240	325	67	5.3	1.82	61.7	33.90	453	173	258	
0:44	520	245	325	77	5.3	1.89	71.7	37.94	443	163	248	
0:48	520	245	325	78	5.4	1.95	72.6	37.23	442	167	247	
0:52	520	245	325	78	5.6	1.95	72.4	37.13	442	167	247	
0:56	525	250	280	96	5.8	1.95	90.2	46.26	429	154	184	
1:00	530	250	200	103	5.8	2.42	97.2	40.17	427	147	97	Cavity size: 1" x 1 1/2"
1:04	530	250	200	103	5.8	2.50	97.2	38.88	427	147	97	
1:08	530	250	200	103	5.8	2.50	97.2	38.88	427	147	97	
1:12	570	265	220	159	6.2	3.39	152.8	45.08	411	106	61	Arch strengthening.
1:16	570	265	220	159	6.4	3.55	152.6	42.99	411	106	61	
1:20	570	265	220	159	6.4	3.55	152.6	42.99	411	106	61	
1:24	570	265	220	159	6.4	3.55	152.6	42.99	411	106	61	
1:28	620	285	220	360	7.0	4.14	353.0	85.27	260	-75	-140	
1:30	610	280	220	360	7.0	4.20	353.0	84.05	250	-80	-40	Cavity was partly filled with sand.
1:32	600	280	220	360	7.0	4.14	353.0	85.27	240	-80	-140	
1:36	595	280	220	370	7.0	3.80	363.0	95.53	225	-90	-150	
1:40	595	280	220	370	7.0	3.61	363.0	100.55	225	-90	-150	Cavity size increase: 1" x 1 3/4"
1:44	595	280	220	370	6.5	3.38	363.5	107.54	225	-90	-150	
1:48	595	280	220	370	6.2	3.19	363.8	114.04	225	-90	-150	
1:52	580	275	220	380	6.2	3.00	373.8	124.60	200	-105	-160	
1:56	570	275	220	380	4.5	-	375.5	-	190	-105	-160	

TABLE 32

TEST NUMBER: DIII

SAND: Natural
Sample D

STRESS LEVEL: 500 psi

EXPERIMENTAL DATA | CALCULATED DATA

Time (hrs:min)	Sand Stress σ_1 (psi)	Sand Stress σ_2 (psi)	Sand Stress σ_3 (psi)	Pressure inlet (psi)	Pressure outlet (psi)	Flow Rate, Q (Bbls/Day)	ΔP (psi)	ΔP/Q (psi/bbls/day)	Pseudo Effective Stress σ'_1 (psi)	Pseudo Effective Stress σ'_2 (psi)	Pseudo Effective Stress σ'_3 (psi)	Comment
0:00	485	200	380	46	3.5	0.12	42.5	354.17	439	154	334	Backflowed.
0:04	485	200	380	46	4.2	0.38	41.8	110.00	439	154	334	No water injected
0:08	485	200	400	46	4.5	0.60	41.5	69.17	439	154	354	New cavity observed
0:12	485	200	405	46	5.0	1.00	41.0	41.00	439	154	359	Size: 1/2" x 1/2"
0:16	485	200	410	46	5.0	1.02	41.0	40.20	439	154	364	
0:20	520	250	420	91	5.2	1.20	85.8	71.50	429	159	329	
0:24	520	250	430	93	5.8	1.74	87.2	50.11	427	157	337	Increased cavity
0:28	520	250	440	93	5.8	1.80	87.2	48.44	427	157	347	size: 1/2" x 3/4"
0:32	520	250	450	93	5.8	1.82	87.2	47.91	427	157	357	
0:36	520	250	460	93	5.8	1.82	87.2	47.91	427	157	367	Cavity size: 1/2" x 1"
0:40	555	265	460	142	5.8	2.49	136.2	54.70	413	123	318	
0:44	555	265	460	143	5.8	2.60	137.2	52.77	412	122	317	
0:48	555	265	470	143	5.8	2.63	137.2	52.17	412	122	327	
0:50	460	265	460	143	5.8	2.70	137.2	50.81	317	122	317	Major arch failure
-	460	210	460	112	18.5	7.05	93.5	13.26	348	153	348	Sand produced
0:52	460	210	460	122	9.0	6.82	113.0	16.57	338	88	338	(1/2 -separator- full)
0:52	460	210	460	126	8.0	6.14	117.0	19.06	335	85	335	Cavity size: 1" x >4"
0:56	460	210	460	127	7.8	5.50	119.2	21.67	333	83	333	
0:58	460	210	460	130	7.0	5.02	123.0	24.50	330	80	330	
1:00	460	210	460	132	7.0	4.68	125.0	26.71	328	78	328	
1:04	460	210	460	135	6.2	4.20	128.8	30.67	325	75	325	
1:08	460	210	460	135	6.0	3.89	129.0	33.16	325	75	325	
1:12	460	210	460	137	5.8	3.74	131.2	35.08	323	73	323	Restabilized condition
1:16	460	210	460	139	5.8	3.55	133.5	37.52	321	71	321	

TABLE 5.2 (cont'd)

TEST NUMBER: DIII

SAND: Natural
Sample D

STRESS LEVEL: 500 psi

EXPERIMENTAL DATA | CALCULATED DATA

Time	Sand Stress			Pressure		Flow Rate, Q	ΔP	ΔP/Q	Pseudo Effective Stress			Comment
(hrs:min)	σ_1 (psi)	σ_2 (psi)	σ_3 (psi)	inlet (psi)	outlet (psi)	(Bbls/Day)	(psi)	(psi/bbls/day)	σ'_1 (psi)	σ'_2 (psi)	σ'_3 (psi)	
1:20	460	210	460	140	5.8	3.42	134.2	39.24	320	70	320	
1:24	460	210	460	140	5.6	3.30	134.4	40.73	320	70	320	
1:28	460	210	460	140	5.5	3.12	134.5	43.11	320	70	320	
1:32	460	210	460	140	5.2	3.03	134.8	44.49	320	70	320	
1:36	460	210	460	141	5.2	2.94	135.8	46.19	319	69	319	
1:38	460	210	460	198	5.3	3.22	192.7	59.84	262	12	262	Restabilized condition
1:40	460	210	460	200	6.0	4.15	194.0	46.75	260	10	260	
1:44	460	210	460	206	6.2	4.70	199.8	42.51	254	4	254	
1:48	460	210	460	208	6.2	4.52	201.8	44.65	252	2	252	
1:52	460	210	460	210	6.0	4.30	204.0	47.44	250	0	250	
1:56	460	210	460	213	5.8	4.10	207.2	50.54	247	-3	247	
2:00	460	210	460	214	5.8	3.93	208.2	52.98	246	-4	246	
2:04	460	210	460	215	5.8	3.86	209.2	54.20	245	-5	245	
2:08	460	210	460	215	5.6	3.72	209.4	56.29	245	-5	245	
2:12	460	210	460	215	5.5	3.62	209.5	57.87	245	-5	245	Stable condition
2:14	460	210	460	360	7.0	4.89	353.0	72.19	100	-150	100	
2:16	460	210	460	360	7.0	5.35	353.0	65.98	100	-150	100	
2:20	460	210	460	360	7.0	5.33	353.0	66.23	100	-150	100	
2:24	460	210	460	360	6.2	5.05	353.8	70.06	100	-150	100	
2:28	460	210	460	360	6.0	4.80	354.0	73.75	100	-150	100	
2:32	460	210	460	360	5.8	4.65	354.2	76.17	100	-150	100	
2:36	460	210	460	360	5.8	4.36	354.2	81.24	100	-150	100	

TABLE 55

TEST NUMBER: DIV

SAND: Natural
Sample D

STRESS LEVEL: 750 psi

Time	EXPERIMENTAL DATA: Sand Stress			Pressure		Flow Rate, Q	ΔP	CALCULATED DATA: Δ P/Q	Pseudo Effective Stress			Comment
(hrs:min)	σ_1 (psi)	σ_2 (psi)	σ_3 (psi)	inlet (psi)	outlet (psi)	(Bbls/Day)	(psi)	(psi/bbls/day)	σ'_1 (psi)	σ'_2 (psi)	σ'_3 (psi)	
0:00	750	350	500	39	4.0	1.02	35.0	34.31	711	311	461	No water injected.
0:04	730	340	500	41	5.0	2.31	36.0	15.58	689	299	459	
0:08	720	330	500	43	5.0	2.42	38.0	15.70	677	287	457	
0:12	715	320	500	45	5.0	2.30	40.0	17.39	670	275	455	Cavity formed
0:16	710	320	500	45	4.5	2.02	40.5	20.05	665	275	455	size: 1/4" x 1/2"
0:20	700	320	500	61	4.5	2.24	56.5	25.22	639	259	439	
0:24	700	320	500	61	4.5	2.24	56.5	25.22	639	259	439	
0:28	700	320	500	61	4.5	2.12	56.5	26.65	639	259	439	
0:32	700	320	500	85	4.5	2.52	80.5	31.94	615	235	415	Stable condition
0:36	700	320	500	90	4.5	2.59	85.5	33.01	610	230	410	
0:40	700	315	500	90	4.5	2.52	85.5	33.01	610	225	410	
0:44	700	315	500	90	4.5	2.52	85.5	33.93	610	225	410	
0:48	700	310	500	118	4.8	2.94	113.2	38.50	582	192	382	
0:52	700	310	500	119	5.0	3.14	114.0	36.31	581	191	381	
0:56	700	310	500	120	5.0	3.02	115.0	38.08	580	190	380	
1:00	700	300	500	122	4.5	2.80	117.5	41.96	578	178	378	
1:04	700	300	500	124	4.5	2.62	119.5	45.61	576	176	376	
1:08	700	300	500	156	4.5	3.04	151.5	49.84	544	144	344	Cavity size: 1/2" x 3/4"
1:12	700	300	500	156	4.8	3.48	151.2	43.45	544	144	344	
1:16	700	300	500	163	4.8	3.42	158.2	46.26	537	137	337	
1:20	700	300	500	165	4.5	3.20	160.5	50.16	535	135	335	

TABLE 33 (cont'd)

TEST NUMBER: DIV

SAND: Natural
Sample D

STRESS LEVEL: 750 psi

Time	EXPERIMENTAL DATA							CALCULATED DATA				
Time	Sand Stress			Pressure		Flow Rate, Q	ΔP	$\Delta P/Q$	Pseudo Effective Stress			Comment
(hrs:min)	σ_1 (psi)	σ_2 (psi)	σ_3 (psi)	inlet (psi)	outlet (psi)	(Bbls/Day)	(psi)	(psi/bbls/day)	σ'_1 (psi)	σ'_2 (psi)	σ'_3 (psi)	
1:24	700	300	500	240	4.5	3.30	235.5	71.36	460	60	260	
1:28	700	300	500	248	5.8	4.65	242.2	52.09	452	52	252	
1:32	700	300	500	257	5.8	4.70	251.2	53.45	443	43	243	Stable condition
1:36	700	300	500	258	5.8	4.50	252.2	56.04	442	42	242	
1:40	700	300	500	265	5.5	4.22	259.5	61.49	435	35	235	
1:44	700	300	500	270	5.2	3.90	264.8	67.90	430	30	230	
1:48	700	300	500	338	5.8	4.84	332.2	68.64	362	-38	162	
1:52	700	300	500	340	6.0	5.14	334.0	64.98	360	-40	160	Cavity size: 1/2" x 1"
1:56	700	300	500	345	5.8	5.00	339.2	67.84	355	-45	155	
2:00	700	300	500	383	5.8	4.60	377.2	82.00	317	-83	117	
2:04	700	300	500	380	5.5	4.40	374.5	85.11	320	-80	120	Stable condition
2:08	700	300	500	380	5.2	4.20	374.8	89.24	320	-80	120	
2:12	700	300	500	380	5.4	4.00	374.6	93.65	320	-80	120	
2:16	700	300	500	380	4.8	3.80	375.2	98.74	320	-80	120	

TEST NUMBER: DV

SAND: Natural
Sample D

STRESS LEVEL: 750 psi

EXPERIMENTAL DATA | CALCULATED DATA

Time	Sand Stress			Pressure		Flow Rate, Q	ΔP	ΔP/Q	Pseudo Effective Stress			Comment
(hrs:min)	σ_1 (psi)	σ_2 (psi)	σ_3 (psi)	inlet (psi)	outlet (psi)	(Bbls/Day)	(psi)	(psi/bbls/day)	σ'_1 (psi)	σ'_2 (psi)	σ'_3 (psi)	
0:00	750	400	600	45	3.5	1.42	41.5	29.23	705	355	555	Backflowed before test
0:04	740	400	500	45	3.5	2.24	41.5	18.53	695	355	455	started.
0:08	740	410	500	46	3.5	2.20	42.5	19.32	694	364	454	Previous arch remained
0:12	740	400	500	46	3.5	1.94	42.5	21.91	694	364	454	stable.
0:16	740	380	500	46	3.5	1.75	42.5	24.29	694	334	454	
0:20	740	380	500	46	3.5	1.60	42.5	26.56	694	334	454	Stable condition
0:24	740	380	500	46	3.5	1.43	42.5	29.72	694	334	454	
0:28	740	380	500	70	3.5	1.80	66.5	36.94	670	310	430	
0:32	740	380	500	70	3.5	1.95	66.5	34.10	670	310	430	No sand produced.
0:36	735	350	500	72	3.5	1.92	68.5	35.68	663	278	428	
0:40	735	350	500	72	3.5	1.80	68.5	38.06	663	278	428	Cavity size: 1/2" x 1"
0:44	735	350	500	72	3.5	1.70	68.5	40.29	663	278	428	
0:48	735	350	500	122	3.5	1.55	118.5	76.45	613	228	378	Stable condition
0:52	735	350	500	122	3.6	2.10	118.4	56.38	608	228	378	
0:56	730	350	500	122	4.0	2.62	118.0	45.04	608	228	378	
1:00	720	350	500	123	4.0	2.62	119.0	45.42	597	227	377	
1:04	720	350	500	125	4.0	2.35	121.0	51.49	595	225	375	
1:08	720	350	500	223	4.6	3.00	218.4	72.80	497	127	277	
1:12	720	350	500	248	4.6	3.22	243.4	75.59	472	102	252	Stable condition
1:16	720	350	500	257	4.0	2.62	253.0	96.56	463	93	243	
1:20	720	350	500	262	3.6	2.10	258.4	123.05	458	88	238	
1:24	720	350	500	262	3.5	1.82	258.5	142.03	458	88	238	
1:28	720	350	500	360	3.6	2.92	356.4	122.05	360	-10	140	Cavity size: 1/2" x 1"
1:32	720	350	500	360	3.6	2.84	356.4	125.49	360	-10	140	
1:36	720	350	500	360	3.6	2.62	356.4	136.03	360	-10	140	
1:40	720	350	500	360	3.6	2.42	356.4	147.27	360	-10	140	

TABLE 35

TEST NUMBER: DVI

SAND: Natural
Sample D

STRESS LEVEL: 750 psi

EXPERIMENTAL DATA / CALCULATED DATA

Time	Sand Stress			Pressure		Flow Rate, Q	ΔP	ΔP/Q	Pseudo Effective Stress			Comment
(hrs:min)	σ_1 (psi)	σ_2 (psi)	σ_3 (psi)	inlet (psi)	outlet (psi)	(Bbls/Day)	(psi)	(psi/bbls/day)	σ'_1 (psi)	σ'_2 (psi)	σ'_3 (psi)	
0:00	700	440	130	42	2.5	0.6	39.5	65.83	658	398	88	
0:02	700	440	150	44	3.2	1.32	40.8	30.91	656	396	106	Existing arch remained
0:04	700	440	290	45	3.5	1.55	41.5	26.77	655	395	245	stable.
0:08	700	440	310	46	3.5	1.63	42.5	26.07	654	394	264	Cavity size: 1/2" x 1"
0:12	700	440	320	46	3.5	1.63	42.5	26.07	654	394	274	
0:16	700	440	320	46	3.5	1.63	42.5	26.07	654	394	274	
0:20	700	440	320	360	4.0	2.70	356.0	131.85	340	80	-20	
0:24	700	400	320	360	3.8	2.24	356.2	159.02	340	40	-20	
0:28	700	400	350	360	3.5	1.93	356.5	184.72	340	40	-20	Stable arch condition
0:32	700	400	350	360	3.5	1.75	356.5	203.71	340	40	-20	prevailed
0:36	700	400	350	360	3.5	1.58	356.5	225.63	340	40	-20	
0:40	700	365	360	360	3.5	1.49	356.5	239.26	340	5	-20	
0:44	700	350	360	360	3.4	1.40	356.6	254.71	340	-10	-20	
0:48	700	350	360	360	3.4	1.34	356.6	266.12	340	-10	-20	No sand produced
0:52	700	350	370	360	3.2	1.29	356.8	276.59	340	-10	-20	
0:56	700	350	395	360	3.2	1.24	356.8	287.74	340	-10	-20	No failures
1:00	700	350	410	360	3.2	1.13	356.8	315.75	340	-10	-20	
1:04	700	350	410	360	3.2	1.10	356.8	324.36	340	-10	-20	
1:08	700	350	410	360	3.2	1.04	356.8	343.08	340	-10	-20	

TEST NUMBER: DVII

SAND: Natural
Sample D

STRESS LEVEL: 1000 psi

EXPERIMENTAL DATA | CALCULATED DATA

Time	Sand Stress			Pressure		Flow Rate, Q	ΔP	ΔP/Q	Pseudo Effective Stress			Comment
(hrs:min)	σ_1 (psi)	σ_2 (psi)	σ_3 (psi)	inlet (psi)	outlet (psi)	(Bbls/Day)	(psi)	(psi/bbls/day)	σ'_1 (psi)	σ'_2 (psi)	σ'_3 (psi)	
0:00	1005	560	400	22	4.0	2.42	18.0	7.44	983	538	378	Existing arch collapsed
0:04	965	560	400	42	4.0	2.24	38.0	16.96	923	518	358	during stress-loading.
0:08	960	530	460	42	4.0	2.63	38.0	14.45	918	488	358	Cavity disappeared
0:12	950	530	460	43	4.0	2.63	39.0	14.83	907	487	417	New arch developed as flow
0:16	940	530	460	43	4.0	2.52	39.0	15.48	897	487	417	began: 1/4" x 1/4".
0:20	930	515	460	43	4.0	2.41	39.0	16.18	887	472	417	Cavity observed (0:04 hour)
0:24	925	515	460	43	4.0	2.30	39.0	16.96	882	472	417	
0:28	925	490	460	72	4.6	3.0	67.4	22.47	853	443	388	
0:32	925	480	460	75	4.6	3.10	70.4	22.71	850	430	385	
0:36	925	480	460	75	4.6	3.03	70.4	23.23	850	405	385	
0:40	925	480	460	76	4.6	2.90	71.4	24.62	849	404	384	Cavity size: 1/2" x 2"
0:44	925	480	460	130	4.6	3.22	125.4	38.94	795	350	330	
0:48	925	460	460	135	4.6	3.58	130.4	36.42	790	325	325	
0:52	925	460	460	136	4.6	3.55	131.4	37.01	789	325	325	
0:56	925	460	460	140	4.6	3.40	135.4	39.82	785	325	325	
1:00	920	460	460	140	4.6	3.20	135.4	42.31	780	320	320	
1:04	920	460	460	233	4.8	3.80	228.2	60.05	687	227	227	
1:08	920	460	460	243	5.0	4.15	238.0	57.35	677	217	217	
1:12	920	460	460	250	5.0	3.90	245.0	62.82	670	210	210	
1:16	920	460	460	255	4.8	3.52	250.2	71.08	665	205	205	
1:20	920	460	460	257	4.6	3.20	252.4	78.88	663	203	203	
1:24	920	460	460	260	4.5	2.98	255.5	85.74	660	200	200	
1:28	920	460	460	262	4.0	2.82	258.0	91.49	658	198	198	
1:32	920	460	460	263	4.0	2.70	259.0	95.93	657	197	197	Stable condition
1:36	920	460	460	263	4.0	2.60	259.0	99.62	657	197	197	
1:40	920	460	460	263	4.0	2.49	259.0	104.02	657	197	197	Cavity size: 1/2" x 2"
1:44	920	460	460	360	4.6	3.72	355.4	95.54	560	100	100	
1:48	920	460	460	360	4.6	3.82	355.4	93.04	560	100	100	
1:52	920	460	460	360	4.6	3.65	355.4	97.37	560	100	100	
1:56	920	460	460	360	4.6	3.45	355.4	103.01	560	100	100	
2:00	920	460	460	360	4.6	3.18	355.4	111.76	560	100	100	

TABLE 57

TEST NUMBER: DVIII

SAND: Natural
Sample D

STRESS LEVEL: 1000 psi

Time (hrs:min)	EXPERIMENTAL DATA: Sand Stress σ_1 (psi)	σ_2 (psi)	σ_3 (psi)	Pressure inlet (psi)	Pressure outlet (psi)	Flow Rate, Q (Bbls/Day)	ΔP (psi)	CALCULATED DATA: $\Delta P/Q$ (psi/bbls/day)	Pseudo Effective Stress σ'_1 (psi)	σ'_2 (psi)	σ'_3 (psi)	Comment
0:00	890	560	580	360	2.8	0.28	357.2	1275.71	530	200	220	
0:02	890	560	580	360	3.0	1.24	357.0	287.90	530	200	220	Conditions remained stable
0:04	890	560	570	360	3.5	1.45	356.5	245.86	530	200	210	
0:06	890	560	560	360	3.5	1.48	356.5	240.88	530	200	200	No sand produced
0:08	890	560	560	360	3.5	1.48	356.5	240.88	530	200	200	
0:10	890	560	560	360	3.5	1.42	356.5	251.06	530	200	200	Cavity size: 1/2" x 2"
0:12	890	560	560	360	3.5	1.35	356.5	264.07	530	200	200	
0:14	890	560	560	360	3.5	1.30	356.5	274.23	530	200	200	
0:16	890	560	560	360	3.0	1.24	357.0	287.90	530	200	200	
0:18	890	560	560	360	3.0	1.20	357.0	297.50	530	200	200	
0:20	890	560	560	360	3.0	1.12	357.0	318.75	530	200	200	
0:22	890	560	560	360	3.0	1.02	357.0	350.00	530	200	200	Stable condition
0:24	890	560	560	360	3.0	1.01	357.0	353.47	530	200	200	
0:26	890	560	560	360	3.0	1.00	357.0	357.00	530	200	200	
0:28	890	560	560	360	3.0	0.92	357.0	388.04	530	200	200	
0:30	890	560	560	360	3.0	0.90	357.0	396.67	530	200	200	

TABLE 30

TEST NUMBER: DIX

SAND: Natural
Sample D

STRESS LEVEL: 1500 psi

EXPERIMENTAL DATA | CALCULATED DATA

Time	Sand Stress			Pressure		Flow Rate, Q	ΔP	ΔP/Q	Pseudo Effective Stress			Comment
(hrs:min)	σ_1 (psi)	σ_2 (psi)	σ_3 (psi)	inlet (psi)	outlet (psi)	(Bbls/Day)	(psi)	(psi/bbls/day)	σ'_1 (psi)	σ'_2 (psi)	σ'_3 (psi)	
0:00	1520	760	680	21	4.0	2.14	17.0	7.94	1499	739	659	Cavity observed
0:04	1450	740	620	21	3.6	1.92	17.4	9.06	1429	719	599	Size: 1/4" x 1/4"
0:08	1440	720	590	21	3.5	1.80	17.5	9.72	1419	699	569	
0:12	1420	700	560	21	3.5	1.70	17.5	10.29	1399	679	539	
0:16	1420	690	560	21	3.5	1.60	17.5	10.94	1399	669	539	
0:20	1420	680	540	21	3.5	1.52	17.5	11.51	1399	659	519	
0:24	1410	680	520	42	3.5	1.92	38.5	20.05	1368	638	478	
0:28	1405	680	520	42	3.5	2.14	38.5	17.99	1363	638	478	Cavity growth
0:32	1400	680	520	42	3.5	2.15	38.5	17.91	1358	638	478	Size: 1/2" x 1/4"
0:36	1400	680	520	70	3.5	2.15	66.5	30.93	1330	610	450	
0:40	1400	670	520	75	4.0	2.71	71.0	26.20	1325	595	445	Observed cavity growth
0:44	1400	670	520	75	4.0	2.76	71.0	25.72	1325	595	445	Size: 1/2" x 1/2"
0:48	1395	660	520	76	4.0	2.71	72.0	26.57	1319	584	444	
0:52	1395	660	520	77	4.0	2.68	73.0	27.24	1318	583	443	
0:56	1395	660	520	77	4.0	2.42	73.0	30.17	1318	583	443	
1:00	1395	650	520	130	4.2	2.99	125.8	42.07	1265	520	390	
1:04	1390	640	520	134	4.2	3.04	129.8	42.70	1256	506	386	Cavity size: 1/2" x 3/4"
1:08	1380	640	520	135	4.2	2.90	130.8	45.10	1245	505	385	
1:12	1380	640	520	137	4.0	2.70	133.0	49.26	1243	503	383	
1:16	1380	640	520	140	4.0	2.50	136.0	54.40	1240	500	380	
1:20	1380	640	520	177	4.0	2.88	173.0	60.07	1203	463	343	

TABLE 58 (cont'd)

TEST NUMBER: DIX

SAND: Natural Sample D

STRESS LEVEL: 1500 psi

	EXPERIMENTAL DATA								CALCULATED DATA			
Time	Sand Stress			Pressure		Flow Rate, Q	ΔP	ΔP/Q	Pseudo Effective Stress			Comment
(hrs:min)	σ_1 (psi)	σ_2 (psi)	σ_3 (psi)	inlet (psi)	outlet (psi)	(Bbls/Day)	(psi)	(psi/bbls/day)	σ'_1 (psi)	σ'_2 (psi)	σ'_3 (psi)	
1:24	1380	640	520	181	4.0	2.95	177.0	60.00	1199	459	339	
1:28	1380	640	520	181	4.2	3.00	176.8	58.93	1199	459	339	
1:32	1380	640	520	181	4.2	2.98	176.8	58.33	1199	459	339	Stable condition
1:36	1380	640	520	184	4.2	2.80	179.8	64.21	1196	456	336	
1:40	1380	640	520	291	4.5	3.42	286.5	83.77	1089	349	229	
1:44	1380	640	520	302	4.5	3.50	297.5	85.00	1078	338	218	
1:48	1380	640	520	306	4.5	3.38	301.5	89.20	1074	334	214	
1:52	1380	640	520	310	4.5	3.00	305.5	101.83	1070	330	210	
1:56	1380	640	520	360	4.4	2.80	355.6	127.00	1020	280	160	
2:00	1380	640	520	360	4.2	3.10	355.8	114.71	1020	280	160	
2:04	1380	640	520	360	4.2	3.04	355.8	117.04	1020	280	160	
2:08	1380	640	520	360	4.2	2.95	355.8	120.61	1020	280	160	
2:12	1380	640	520	360	4.2	2.80	355.8	127.07	1020	280	160	
2:16	1380	640	520	360	4.2	2.62	355.8	135.80	1020	280	160	Stable condition
2:20	1380	640	520	360	4.2	2.49	355.8	142.89	1020	280	160	
2:24	1380	640	520	360	4.0	2.32	356.0	153.45	1020	280	160	

TEST NUMBER: DX

SAND: Natural
Sample D

STRESS LEVEL: 2250 psi

EXPERIMENTAL DATA — CALCULATED DATA

Time	Sand Stress			Pressure		Flow Rate, Q	Δ P	Δ P/Q	Pseudo Effective Stress			Comment
(hrs:min)	σ_1 (psi)	σ_2 (psi)	σ_3 (psi)	inlet (psi)	outlet (psi)	(Bbls/Day)	(psi)	(psi/bbls/day)	σ'_1 (psi)	σ'_2 (psi)	σ'_3 (psi)	
0:00	2260	1840	1040	64	5.8	3.45	58.2	16.87	2196	1776	976	Ram "knocked" as stress-
0:04	2240	1840	1040	64	5.8	3.00	58.2	19.40	2176	1776	976	load stopped jumped to
0:08	2230	1840	1040	68	5.2	2.50	62.8	25.12	2162	1772	972	2500 psi. A second "knock"
0:12	2195	1820	1040	70	4.8	2.13	65.2	30.61	2125	1750	970	occurred shortly after.
0:16	2180	1810	1040	75	4.6	1.90	69.4	36.53	2105	1735	965	Initial cavity observed -
0:20	2160	1800	1040	75	4.6	1.75	70.4	40.23	2085	1725	965	Size: 1/2" x 1/2"
0:24	2180	1805	1040	75	4.6	1.61	70.4	43.73	2105	1730	965	No water was injected.
0:28	2170	1800	1040	75	4.5	1.50	70.5	47.00	2095	1725	965	Cavity growth
0:32	2155	1780	1040	75	4.5	1.40	70.5	50.36	2080	1705	965	Size: 1/2" x 3/4"
0:36	2150	1760	1030	75	4.3	1.32	70.7	53.56	2075	1685	955	Arch strengthened
0:40	2140	1750	1030	75	4.2	1.26	70.8	56.19	2065	1675	955	Cavity grew to 1/2" x 1"
0:44	2130	1750	1020	75	4.0	1.22	71.0	58.20	2055	1675	945	Cavity size: 1" x 2"
0:48	2130	1750	1020	75	4.0	1.15	71.0	61.74	2055	1675	945	
0:52	2130	1750	1020	140	5.2	2.90	134.8	46.48	1990	1610	880	Cavity size: 1" x 2"
0:56	2125	1750	1015	152	5.8	3.50	146.2	41.77	1973	1598	863	
1:00	2120	1745	1010	155	5.8	3.55	149.2	42.03	1965	1590	855	
1:04	2120	1740	1005	165	5.8	3.46	159.2	46.01	1955	1575	840	
1:08	2120	1740	1000	165	5.8	3.46	159.2	46.01	1955	1575	835	
1:12	2120	1740	1000	165	5.5	3.42	159.5	46.64	1955	1575	835	Cavity size: 1" x 2 1/2"
1:16	2120	1740	1000	170	5.5	3.39	164.5	48.53	1950	1570	830	
1:20	2115	1735	995	170	5.5	3.29	164.5	50.00	1945	1565	825	
1:24	2110	1735	990	287	7.3	5.85	279.7	47.81	1823	1448	703	
1:28	2105	1730	980	312	7.5	6.20	304.5	49.11	1793	1418	668	
1:32	2100	1720	970	325	7.3	5.95	317.7	53.39	1775	1395	645	
1:36	2100	1710	970	360	7.0	5.70	353.0	61.93	1740	1350	610	Cavity size: 1" x 3"
1:40	2090	1700	960	360	3.5	6.70	356.5	53.21	1730	1340	600	Switched manometer
1:44	2090	1700	950	360	3.5	6.70	356.5	53.21	1730	1340	590	

TEST NUMBER: DXI

SAND: Natural Sample D

STRESS LEVEL: 2250 psi

EXPERIMENTAL DATA / CALCULATED DATA

Time	Sand Stress			Pressure		Flow Rate, Q	ΔP	ΔP/Q	Pseudo Effective Stress			Comment
(hrs:min)	σ_1 (psi)	σ_2 (psi)	σ_3 (psi)	inlet (psi)	outlet (psi)	(Bbls/Day)	(psi)	(psi/bbls/day)	σ'_1 (psi)	σ'_2 (psi)	σ'_3 (psi)	
0:00	2235	1255	1150	44	3.0	0.42	41.0	97.62	2191	1211	1106	
0:04	2195	1250	1145	44	3.0	0.60	41.0	68.33	2151	1206	1101	Arch remained stable.
0:08	2180	1250	1145	44	3.0	0.69	41.0	59.42	2136	1206	1101	Cavity size: 1/2" x 3"
0:12	2170	1245	1140	44	3.0	0.70	41.0	58.57	2126	1201	1096	
0:16	2160	1245	1140	56	3.0	0.70	53.0	75.71	2104	1189	1084	
0:20	2160	1235	1140	56	3.0	0.82	53.0	64.63	2104	1179	1084	
0:24	2160	1235	1140	59	3.0	0.83	56.0	67.47	2101	1176	1081	
0:28	2160	1230	1140	59	3.0	0.83	56.0	67.47	2101	1171	1081	
0:32	2160	1220	1130	59	3.0	0.83	56.0	67.47	2101	1161	1071	Stable condition
0:36	2150	1220	1130	82	3.0	0.91	79.0	86.81	2068	1138	1048	
0:40	2150	1220	1130	82	3.2	1.06	78.8	74.34	2068	1138	1048	
0:44	2140	1210	1130	82	3.2	1.10	78.8	71.64	2058	1128	1048	
0:48	2140	1210	1130	93	3.2	1.14	89.8	78.77	2047	1117	1037	
0:52	2140	1195	1130	115	3.5	1.39	111.5	80.22	2025	1080	1015	
0:56	2140	1195	1130	115	3.5	1.43	111.5	77.97	2025	1080	1015	
1:00	2140	1190	1130	127	3.5	1.49	123.5	82.89	2013	1063	1003	
1:04	2140	1170	1130	130	3.5	1.52	126.5	83.22	2010	1040	1000	
1:08	2130	1150	1130	130	3.5	1.52	126.5	83.22	2000	1020	1000	
1:12	2120	1150	1130	165	3.5	1.92	161.5	84.11	1955	985	965	Stable condition
1:16	2120	1150	1130	165	3.8	2.16	161.2	74.63	1955	985	965	
1:20	2120	1110	1120	165	3.8	2.22	161.2	72.61	1955	945	955	
1:24	2120	1110	1120	165	3.8	2.22	161.2	72.61	1955	945	955	
1:28	2120	1110	1120	243	4.5	2.80	238.5	85.18	1877	867	877	
1:32	2120	1110	1120	255	4.5	2.90	250.5	86.38	1865	855	865	
1:36	2120	1110	1120	262	4.5	2.90	257.5	88.79	1858	848	858	Traces of sand
1:40	2120	1110	1120	394	5.0	4.05	389.0	96.05	1726	716	726	
1:44	2120	1110	1120	415	5.6	4.80	409.4	85.29	1705	695	705	Stable condition
1:48	2120	1110	1120	394	5.6	4.90	388.4	79.27	1726	716	726	
1:52	2120	1110	1120	415	5.6	4.56	409.4	89.78	1705	695	705	Cavity size: 1/2" x 3"

TEST NUMBER: DXII

SAND: Natural
Sample D

STRESS LEVEL: 2250 psi

EXPERIMENTAL DATA | CALCULATED DATA

Time	Sand Stress			Pressure		Flow Rate, Q	ΔP	ΔP/Q	Pseudo Effective Stress			Comment
(hrs:min)	σ_1 (psi)	σ_2 (psi)	σ_3 (psi)	inlet (psi)	outlet (psi)	(Bbls/Day)	(psi)	(psi/bbls/day)	σ'_1 (psi)	σ'_2 (psi)	σ'_3 (psi)	
0:00	2250	1190	1150	41	3.0	0.60	38.0	63.33	2209	1149	1109	
0:04	2230	1180	1150	41	3.0	0.73	38.0	52.05	2189	1139	1109	
0:08	2220	1180	1130	41	3.0	0.75	38.0	50.67	2179	1139	1089	Stable arch prevailed.
0:12	2200	1170	1120	41	3.0	0.75	38.0	50.67	2159	1129	1079	
0:16	2200	1160	1120	41	3.0	0.75	38.0	50.67	2159	1119	1079	
0:18	2195	1160	1120	41	3.0	0.75	38.0	50.67	2154	1119	1079	
0:20	2195	1160	1120	409	5.0	1.42	404.0	284.51	1786	751	711	
0:22	2195	1160	1120	482	5.5	3.62	476.5	131.63	1713	678	638	
0:24	2195	1160	1120	500	6.0	4.80	494.0	102.92	1695	660	620	Cavity size: 1/2" x 3"
0:26	2195	1160	1120	500	7.0	5.45	493.0	90.46	1695	660	620	
0:28	2195	1160	1120	500	7.2	6.14	492.8	80.26	1695	660	620	
0:30	2195	1160	1120	750	8.0	6.89	742.0	107.69	1445	410	370	
0:32	2195	1160	1120	750	8.5	7.55	741.5	98.21	1445	410	370	Traces of sand
0:34	2195	1160	1120	750	9.0	7.92	741.0	93.56	1445	410	370	
0:36	2195	1160	1120	750	9.0	8.00	741.0	92.63	1445	410	370	
0:38	2195	1160	1120	214	8.6	8.14	205.4	25.23	1981	946	906	Essentially stable condition
0:40	2195	1160	1120	222	7.0	5.96	215.0	36.07	1973	938	898	
0:42	2195	1160	1120	228	6.0	4.84	222.0	45.87	1967	932	892	Stable condition
0:44	2195	1160	1120	245	5.2	4.15	239.8	57.78	1950	915	875	
0:46	2195	1160	1120	252	5.1	3.72	246.9	66.37	1943	908	868	
0:48	2195	1160	1120	260	4.8	3.43	255.2	74.40	1935	900	860	
0:50	2195	1160	1120	268	4.6	3.14	263.4	83.89	1927	892	852	
0:52	2195	1160	1120	273	4.6	2.94	268.4	91.29	1922	887	847	Stable condition
0:54	2195	1160	1120	277	4.6	2.80	272.4	97.29	1918	883	843	
0:56	2195	1160	1120	287	4.6	2.71	282.4	104.21	1908	873	833	Cavity size: 1/2" x 3"
0:58	2195	1160	1120	294	4.6	2.65	289.4	109.21	1901	866	826	
1:00	2195	1160	1120	294	4.6	2.59	289.4	111.74	1901	866	826	

TABLE: 42

CAVITY DATA

Gopher State Frac Sand
(20-40/80-100 Mixture)

Test Number	Stress (psi)	Flow Rate (Bbls/Day)	Pressure Drop ΔP (psi)	Cavity Size Width (inches)	Cavity Size Length (inches)	Comment
AI	1500	1.5	30.0	1/8	3	Formation
		4.46	33.0	1/8-1/2	2 1/2	
		5.50	35.0	1/2	3 1/4	
		10.2	30.8	1/2	3 1/4	Failure
		10.2	164.0	1/2-1	4	
		6.32	214.0	1	4	
AIV	1500	2.28	103.0	1/2	1/2	Formation
		2.40	104.0	1/2	1/2	
		2.58	111.0	3/4	3/4	
		5.95	123.0	3/4	3/4	Failure
		7.69	221.0	1	4	

TABLE: 43

CAVITY DATA

Natural Sand - Sample B

Test Number	Stress (psi)	Flow Rate (Bbls/Day)	ΔP (psi)	Cavity Size Width (inches)	Cavity Size Length (inches)	Comment
B I	500	1.30	16	1/2	1/2	Formation
		3.30	16	1/2	1/2	
		4.68	61	1/2	1	
		4.95	61	1/2	1	
		5.03	97	1	3	
		7.68	98	1	3	
		8.50	129	1	3	Failure
		9.10	128	1	4	
		9.64	168	1 1/2	4	
B II	750	0.60	11	1/2	1	Formation
		2.24	11	1/2	1	
B III	750	2.42	34	1/2	1 1/2	
		5.45	83	1/2	2	
		6.20	89	1	3	
B IV	750	1.53	471	1	4	
B V	1000	-	205	1/2	1/2	
		-	206	1/2	1	
		-	211	1/2	1	Failure
		-	211	3/4	1 1/2	
		4.88	211	1	2	
		4.74	211	1/2	2	
		4.68	211	1/2	2 1/2	
		4.85	237	1	3	
		6.10	286	1	3	
		5.90	304	1	3	
B VI	1500	-	178	1/2	1/2	Formation
		-	197	1/2	3/4	
		4.20	207	1/2	3/4	Failure
		4.20	209	1/2	1/2	
		4.49	225	1/2	1	
		4.55	247	1/2	1	
		4.60	247	1/2	1	Failure
		4.60	247	1/2	2	
		4.90	262	1	2	
		5.58	300	1	3	
		5.80	300	1	3 1/3	
		5.60	300	1	3 1/3	Failure
B VII	1500	0.82	72	1	4	
		4.32	297	1	4	

TABLE: 43

CAVITY DATA

Natural Sand - Sample B

Test Number	Stress (psi)	Flow Rate (Bbls/Day)	ΔP (psi)	Cavity Size Width (inches)	Cavity Size Length (inches)	Comment
BIX	2250	-	124.0	1/4	1/4	Formation
		4.50	130.0	1/4	1/4	
		4.40	130.0	1/4	1/4	Failure
		4.40	130.0	1/4	3/4	
		4.20	131.0	1.4	3/4	
		4.72	132.0	1/2	3/4	
		5.95	243.0	1/2	3/4	
		6.00	244.0	3/4	3/4	Failure
BX	2250	3.90	288.0	3/4	3/4	
		6.30	289.0	1	4	
BXII	2250	2.90	57.0	1/2	1/2	
		2.70	57.0	1/2	3/4	
		2.80	60.0	1/2	3/4	
		11.00	292.0	1/2	3/4	

TABLE: 44
CAVITY DATA

Natural Sand-Sample C

Test Number	Stress (psi)	Flow Rate (Bbls/Day)	ΔP (psi)	Cavity Size Width (inches)	Cavity Size Length (inches)	Comment
CI	500	7.30	20.0	1/4	1/2	Formation
		14.80	23.4	1/4	1/4	Failure
		13.50	24.5	1/4	2	
		12.80	28.5	1/4	2	
		11.90	32.5	1/4	4	
		11.80	32.8	1	4	
		11.80	38.5	1	4	Failure
		28.50	103.0	1	4	Failure
		28.50	118.7	1 3/4	4	
CII	750	2.70	33.6	1/2	1/2	
		5.88	23.0	1/2	1	
		7.73	102.0	3/4	2	
		22.40	286.0	3/4	2	Major failure
		24.30	260.0	1	4	
		36.00	337.0	1	4	Failure
CIII	1000	3.12	124.0	1/2	1/2	Formation
		4.56	198.0	1/4	3/4	
		5.75	351.0	1/2	1	
CIV	1500	0.49	42.0	1/4	1/4	Formation
		1.24	70.0	1/2	1/2	
		1.33	81.0	1/2	3/4	
		3.60	276.0	1/2	1	
CV	1500	1.50	348.0	1	4	
CVIII	1800	0.73	21.0	1/4	1/2	Formation
		5.62	352.0	1/2	1	
		5.80	353.0	1/2	1	
CIX	1800	3.56	354.0	1/2	1/2	
		4.60	354.0	1/2	1	

TABLE: 45
CAVITY DATA

Natural Sand-Sample D

Test Number	Stress (psi)	Flow Rate (Bbls/Day)	ΔP (psi)	Cavoty Size Width (inches)	Length (inches)	Comment
DI	500	1.45	40.0	1/2	1/4	Formation
		1.42	46.0	1/2	1/2	
		1.33	50.0	1/2	1	
DII	500	1.69	56.0	1	1 1/4	
		3.61	363.0	1	1 3/4	
DIII	500	0.38	42.0	1/2	1/2	
		1.80	87.0	1/2	3/4	
		1.82	87.0	1/2	1	
		2.70	137.0	1/2	1	Major failure
		5.50	119.0	1	4	
DIV	750	2.30	40.0	1/4	1/2	Formation
		3.48	151.0	1/2	3/4	
		5.14	334.0	1/2	1	
DV	750	1.80	69.0	1/2	1	
DVI	750	1/63	43.0	1/2	1	
DVII	1000	2.41	39.0	1/4	1/4	Formation
		2.90	71.0	1/2	2	
		2.60	259.0	1/2	2	
DVIII	1000	1.42	357	1/2	2	
DIX	1500	2.14	17.0	1/4	1/4	Formation
		2.14	39.0	1/2	1/4	
		2.76	71.0	1/2	1/2	
		3.04	130	1/2	3/4	
DX	2250	2.13	65.0	1/2	1/2	Formation
		1.75	70.0	1/2	3/4	
		1.50	71.0	1/2	1	
		2.90	135.0	1	2	
		3.42	160.0	1	2 1/2	
		5.95	318.0	1	3	
DXI	2250	0.69	41.0	1/2	3	
		4.56	409.0	1/2	3	
DXII	2250	3.62	447.0	1/2	3	

TABLE 46
FAILURE DATA

Gopher State Frac Sand
20-40/80-100 US Mesh Mixture

Test Number	Stress Level (psi)	ΔP (psi)	Q (Bbls/day)	Sand Stress σ_1 (psi)	σ_2 (psi)	σ_3 (psi)	$\Delta\sigma_{max}$ (psi)	Comment
AI	1500	33	5.50	1395	-	-	25	
	1500	35	10.20	1250	-	-	30-50	
	1500	84	10.20	1100	-	-	40	
AII	1500	-	-	-	-	-	-	No failures
AIII	1500	121	1.93	810	-	-	440	Major failure due to water production
AIV	1500	104	2.40	1485	-	-	35	
	1500	123	5.66	1140	-	-	140-360	
	1500	173	5.95-8.28	780/340			190-630	Major arch failure

TABLE 47
FAILURE DATA

Natural Sand - Sample B

Test Number	Stress Level (psi)	ΔP (psi)	Q (Bbls/day)	Sand Stress σ_1 (psi)	σ_2 (psi)	σ_3 (psi)	$\Delta\sigma_{max}$ (psi)	Comment
BI	500	61	5.04	390	250	190	10-15	
		129	8.50	340	250	190	5-10	
BII	750	-	-	-	-	-	-	No failures
BIII	750	-	-	-	-	-	-	No failures
BIV	750	382	1.20	740	320	560	20	
BV	1000	206	5.24	950	670	540	10	
	1000	211	4.88	960	660	530	60	
BVI	1500	209	4.12	1190	280	1270	220	
	1500	247	4.55	1190	280	1270	45	
	1500	247	4.60	1170	280	1270	20-60	
	1500	300	5.70	1180	280	1270	30-70	
BVII	1500	123	1.49	1320	380	1290	20-25	
	1500	262	2.90	1320	380	1290	20	
BIX	2250	130	4.50	1990	660	1500	20-25	
	2250	243	5.95	1930	640	1500	10-15	
BX	2250	288	3.10	2140	560	1530	360	Major failure

TABLE 48

FAILURE DATA

Natural Sand-Sample C

Test Number	Stress Level (psi)	ΔP (psi)	Q (Bbls/day)	Sand Stress σ_1 (psi)	σ_2 (psi)	σ_3 (psi)	$\Delta\sigma_{max}$ (psi)	Comment
C I	500	20	7.30	475	300	800	35-45	
	500	25	13.5	420	280	800	15	
	500	33	11.80	390	270	800	20-25	
	500	61	14.80	350	250	800	35-45	
C II	750	286	22.40	735	415	930	90-115	Major failure
C III	1000							No failures
C IV	1500							No failures
C V	1500	357	1.00	1440	920	800	165	
C VII	1800	22	0.70	1640	1020	730	20	

TABLE 49
FAILURE DATA

Natural Sand - Sample D

Test Number	Stress Level (psi)	ΔP (psi)	Q (Bbls/day)	Sand Stress σ_1 (psi)	σ_2 (psi)	σ_3 (psi)	$\Delta\sigma_{max}$ (psi)	Comment
DI	500	-	-	-	-	-	-	No failures
DII	500	-	-	-	-	-	-	No failures
DIII	500	137	2.70	460	265	460	95	Major arch failure
DIV	750	-	-	-	-	-	-	No failures
DV	750	-	-	-	-	-	-	No failures
DVI	750	-	-	-	-	-	-	No failures
DVII	1000	-	-	-	-	-	-	No failure
DIX	1500	-	-	-	-	-	-	No failure
DX	2250	-	-	-	-	-	-	No failures

TABLE 50

Sand Pack Parameters

Sand	Porosity (%)	Initial Water Saturation (%)
A	39.0	16.5
B	32.4	30.5
C	31.1	33.0
D	32.5	31.3

TABLE 51

Flow Test

Sand	Porosity (%)	Permeability (darcy)
A	31.0	15.35
B	37.0	20.1
C	39.2	30.4
D	33.0	2.14

TABLE 52

Fluid Properties

	Viscosity @ 70° F (cp)	Density @ 70° F gms/cc
Kerosene	1.9	0.81
Water	1.0	1.00

Table 53. Comparison of Failure Conditions with Bratli, et al.'s Stability Criterion.

Test Number	Slope (ΔP Vs Q)	Sandpack Permeability k_{avg} (md)	$\left[\frac{\Delta P}{S}\right]$ failure	r' failure	$\frac{k_p}{k_a}$	k_a (md)	$\frac{847.2\mu Q}{k_a r_f D}$	$4\frac{T+1}{T}$ So $\tan\alpha$
A I	92.63	1.08	1.16	0.156	1.0	1.08	3284	24.4-26.5
			0.69	0.200	1.0	1.08	4751	
			6.97	0.200	1.0	1.08	4751	
A III	91.85	1.09	12.22	0.200	1.2	0.91	1067	
A IV	21.23	4.73	36.68	0.031	9.6	0.49	15895	
			18.39	0.047	1.3	3.64	3328	
			24.89	0.047	4.6	1.03	12428	
B I	18.06	5.56	12.04	0.0625	1.0	5.56	1459*	714-956
			15.09	0.1875	2.5	2.22	2054*	
B IV	109.60	0.92	52.40	0.031	17.5	0.05	77888	
B V	43.30	2.32	16.32	0.156	2.75	0.84	4023	
			17.95	0.1875	3.9	0.59	4438	
B VI	64.62	1.56	14.16	0.0469	1.0	1.56	5665	
			15.15	0.0625	1.0	1.56	4695	
			14.99	0.0625	1.0	1.56	4746	
			14.69	0.0125	1.0	1.56	29408	

Table 53. Continued.

Test Number	Slope (ΔP VsQ)	Sandpack Permeability k_{avg} (md)	$\left[\frac{\Delta P}{S}\right]_{failure}$	r' failure	$\frac{k_p}{k_a}$	k_a (md)	$\frac{847.2\mu Q}{k_a r_f D}$	$4\frac{T+1}{T}$So tanα
B VII	62.71	1.60	23.64	0.250	7.35	0.22	2725	
			25.86	0.250	8.45	0.19	6142	
B IX	62.22	1.62	8.37	0.016	1.0	1.62	17914	
			11.83	0.047	1.0	1.62	7879	
B X	140.00	0.72	11.97	0.047	1.0	0.72	9236	
C I	4.73	21.25	10.42	0.031	1.0	21.25	1106*	829-1312
			10.63	0.031	1.0	21.25	1802	
			15.68	0.031	1.0	21.25	2260	
C II	16.96	5.93	13.55	0.125	1.0	5.93	3040	
C V	35.00	2.87	183.43	0.125	>50	<0.06	>13414	
C VIII	50.00	2.01	11.30	0.031	1.0	2.01	1130*	
D III	58.00	1.73	15.71	0.125	1.97	0.88	2469	756-1344

* Failure condition that does not obey Bratli, et al.'s criterion.

Table 54. Sand Characteristics

Sand	Cohesive Strength, So (psi)	Angle of Internal Friction ϕ (deg)	Angle of Failure α(deg.) $\alpha = 45^{o}+\phi/2$
A	2.83	29.6-37	59.8-63.5
B	85	23.4-47.7	56.7-68.85
C	90	13.6-58.0	51.8-74
D	90	23.3-58.8	56.65-74.4

Figure 1.

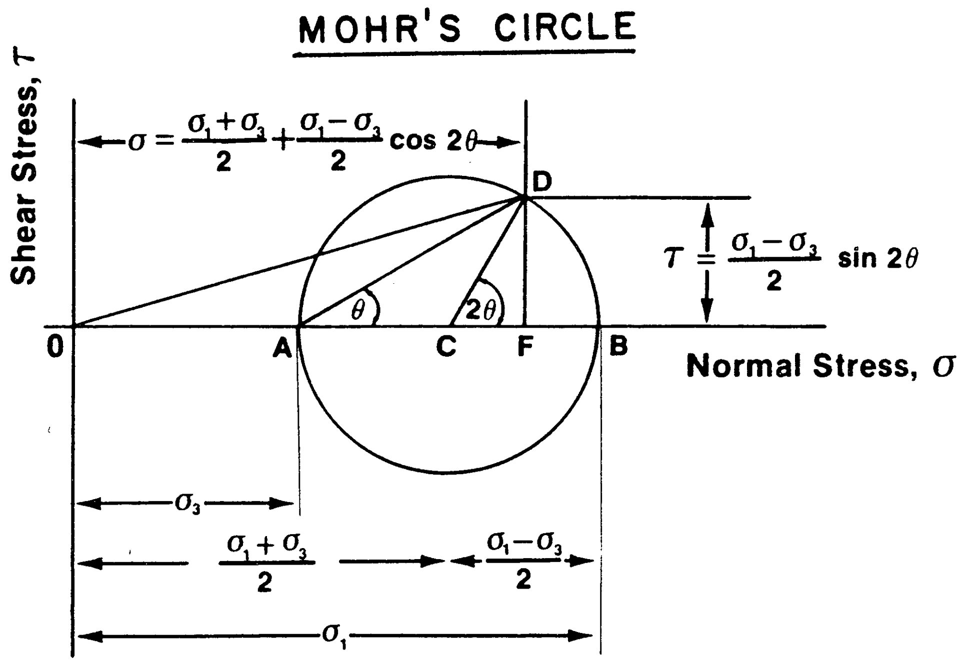

Figure 2.

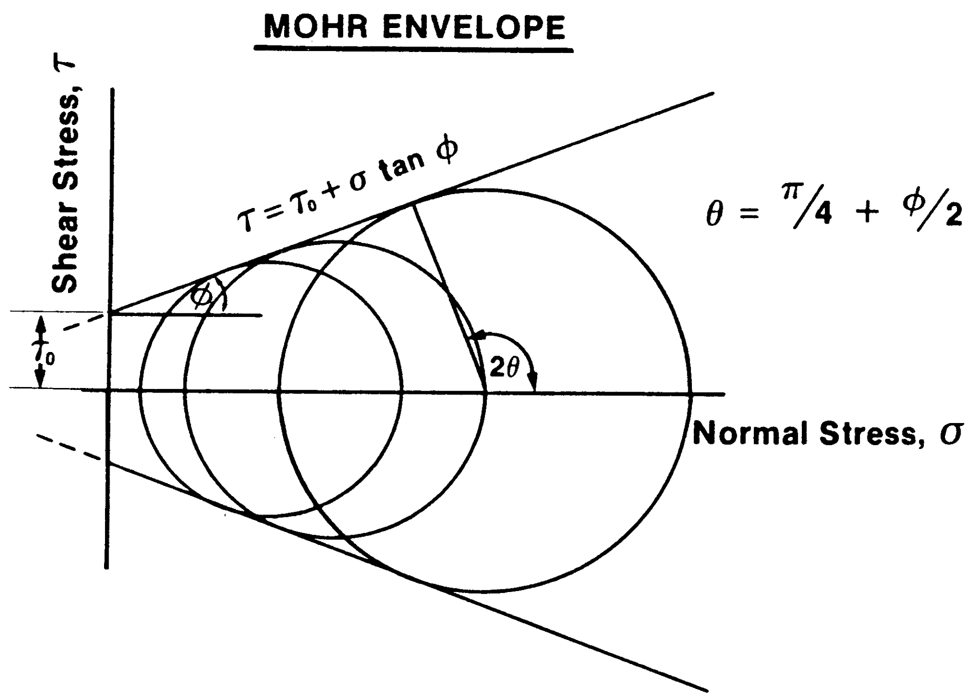

Figure 3.

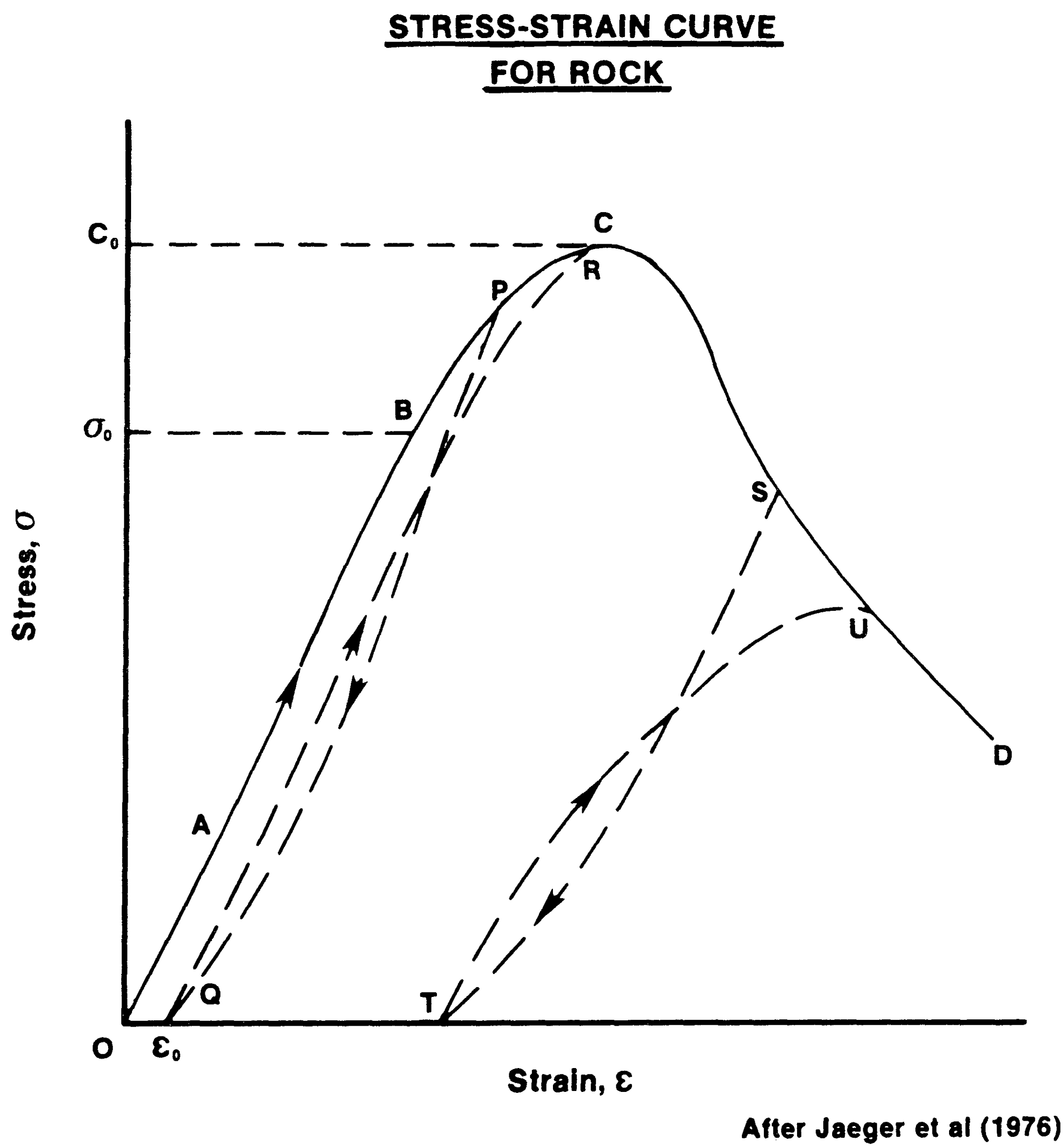
STRESS-STRAIN CURVE
FOR ROCK
C
R
P
B
S
U
D
A
Q
T
C_0
σ_0
Stress, σ
O
ε_0
Strain, ε
After Jaeger et al (1976)

Figure 4a.

DEVIATOR STRESS VS VOLUMETRIC STRAIN
(20 -40 MESH OTTAWA SAND)

DILATION

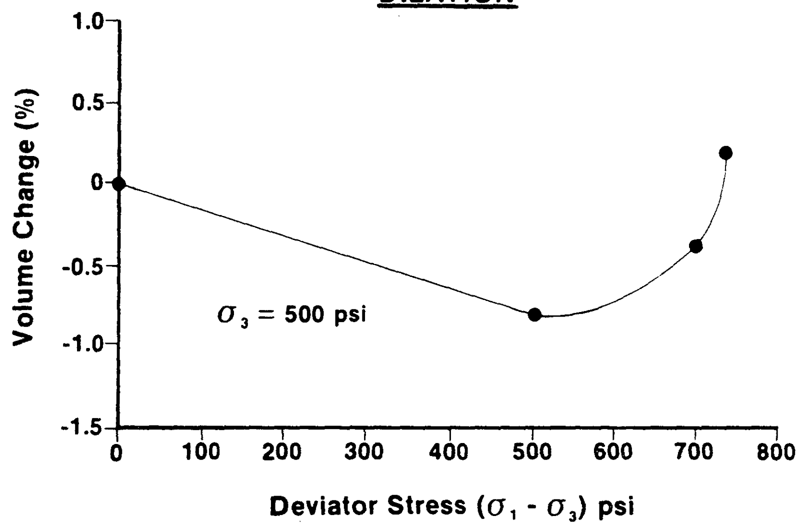

Figure 4b.

DEVIATOR STRESS VS VOLUMETRIC STRAIN
(20 - 40 MESH OTTAWA SAND)

CONTRACTION

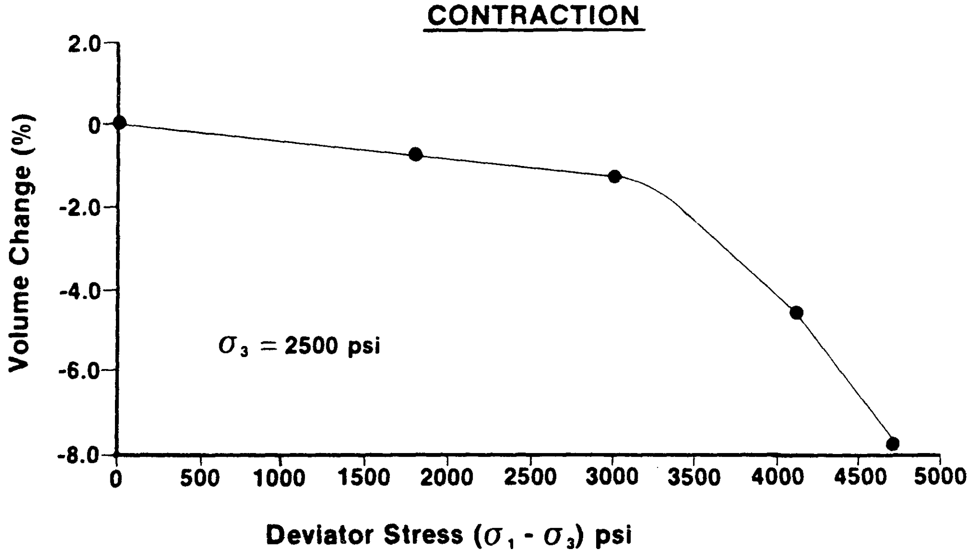

After Hall & Harrisberger (1970)

Figure 5. **A CROSS SECTIONAL VIEW OF THE PRESSURE CELL**

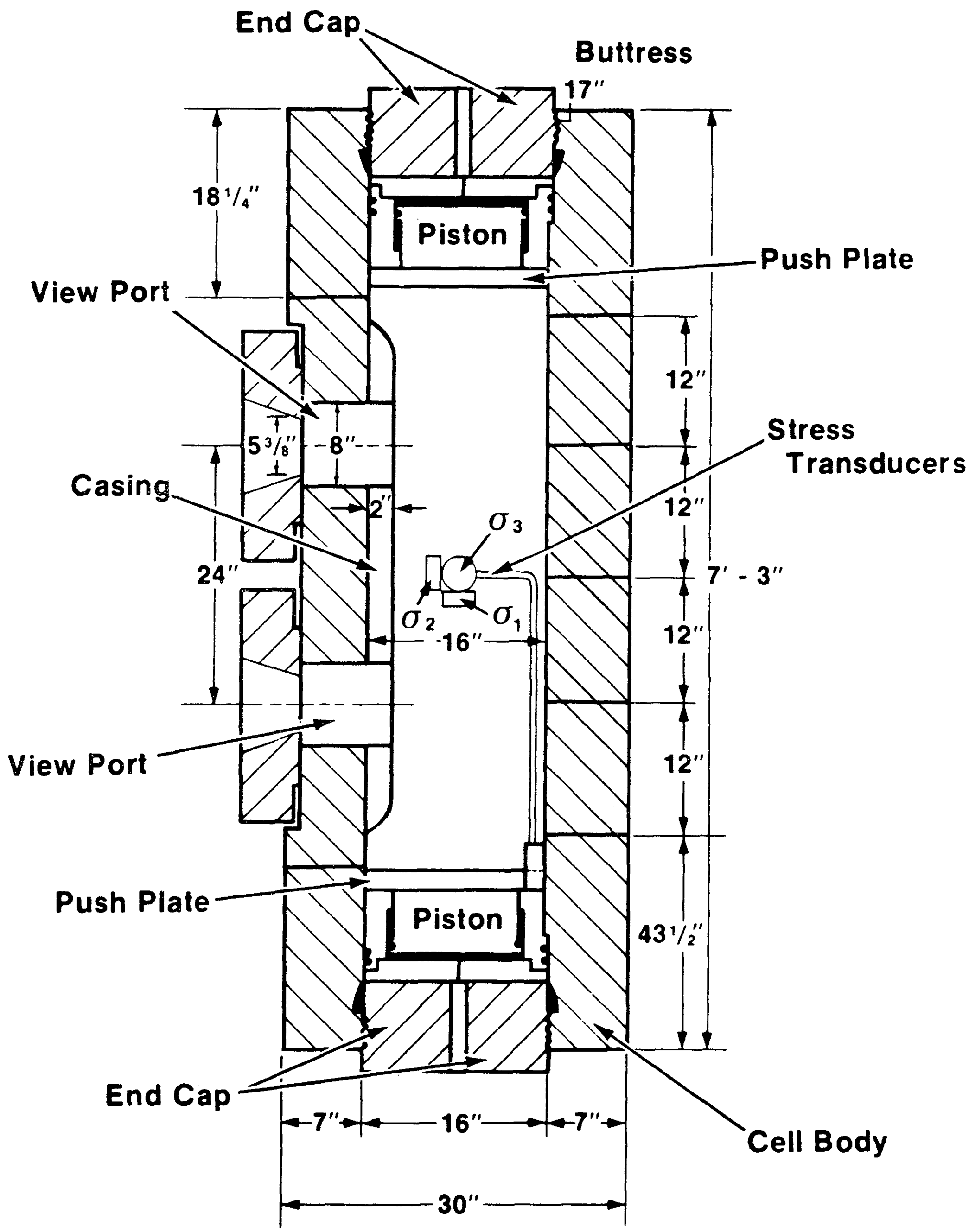

Figure 6.

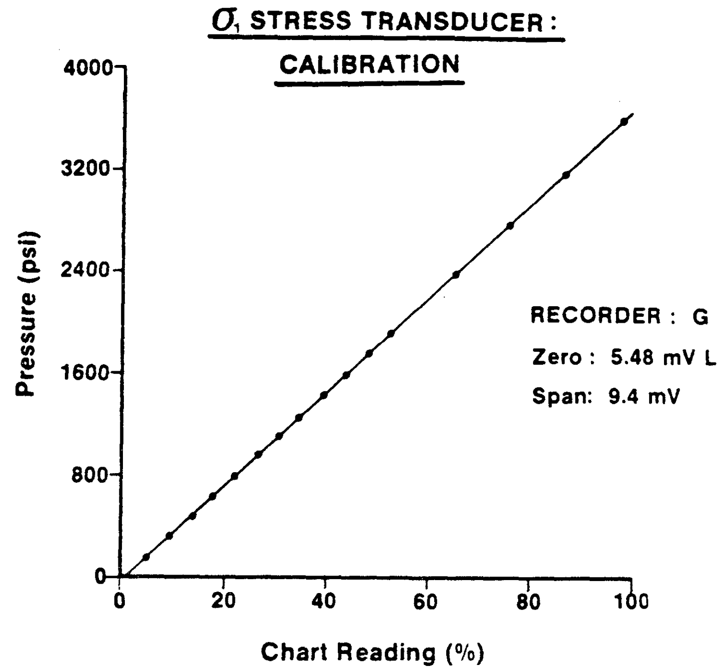

Figure 7.

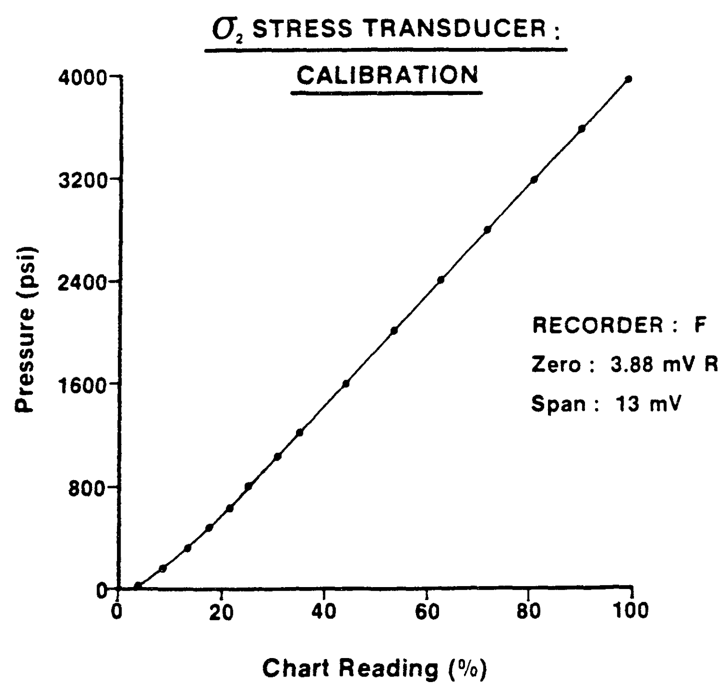

Figure 8.

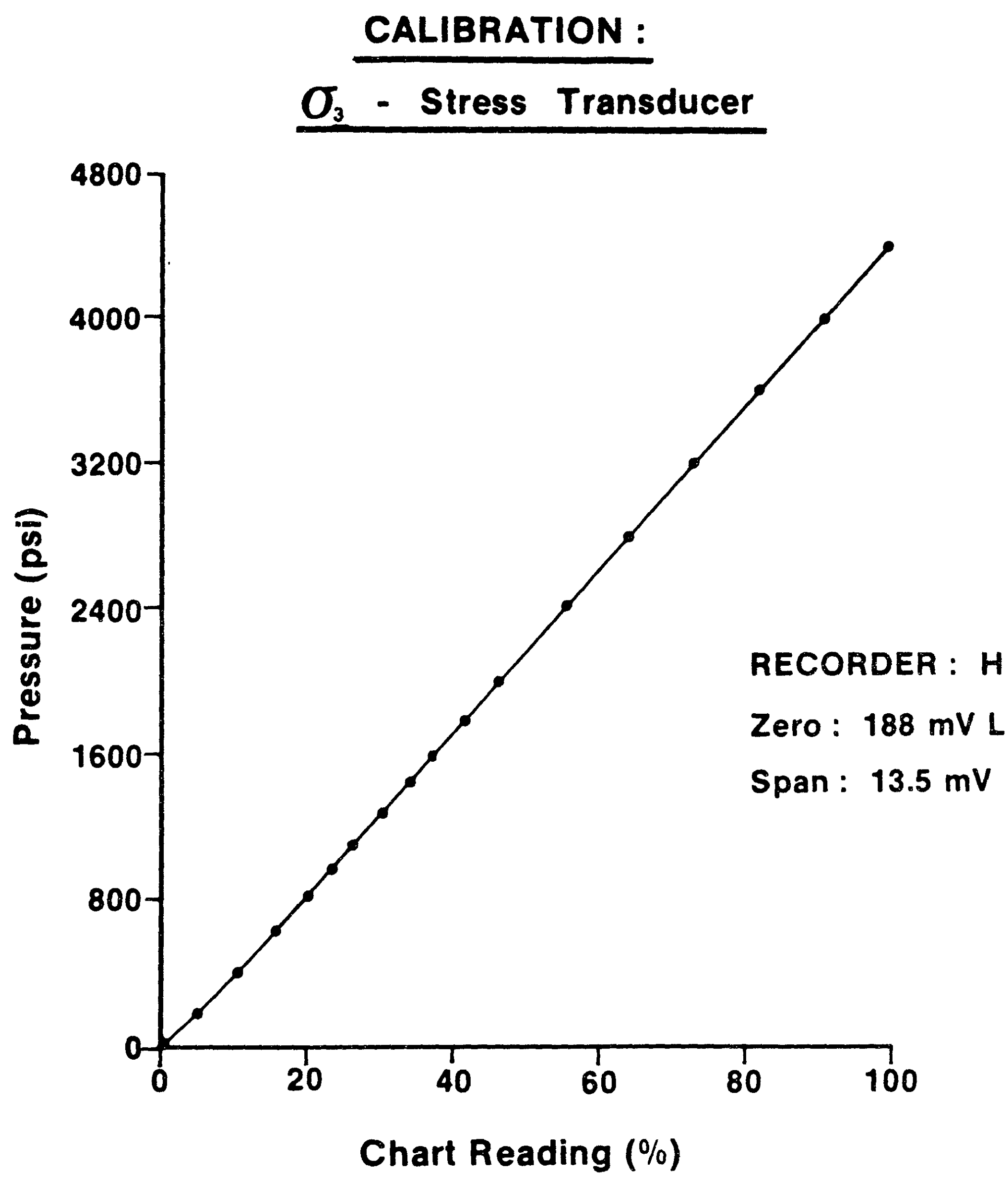
CALIBRATION :
σ_3 - Stress Transducer
4800
4000
3200
2400
1600
800
0
Pressure (psi)
0
20
40
60
80
100
Chart Reading (%)
RECORDER : H
Zero : 188 mV L
Span : 13.5 mV

Figure 9.

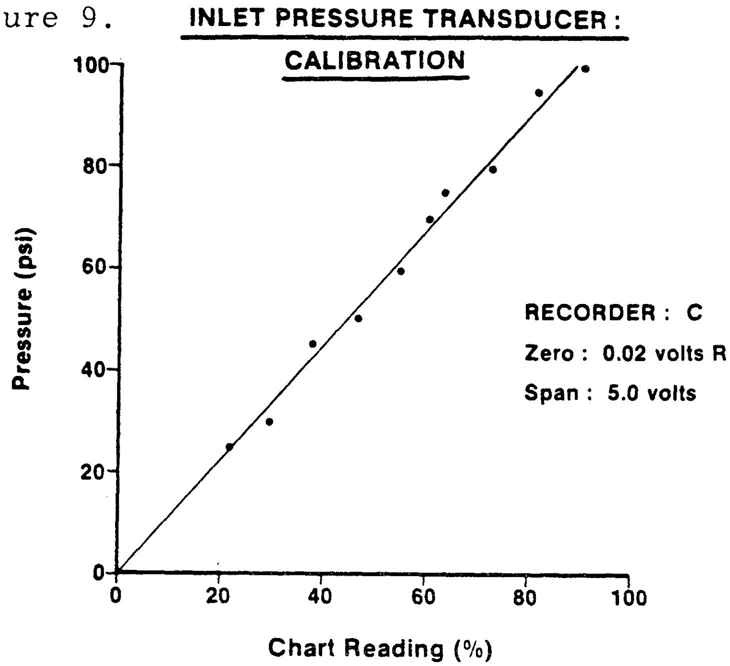

Figure 10.

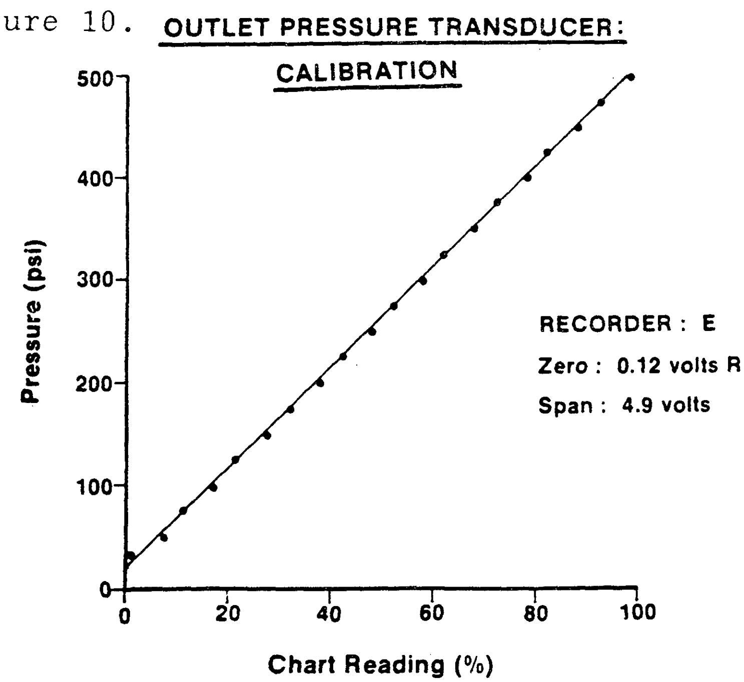

Figure 11.

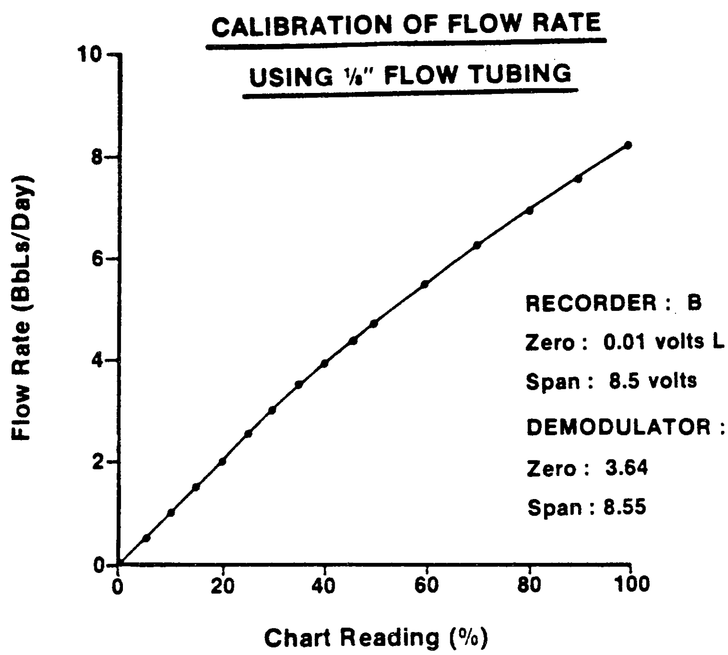

Figure 12.

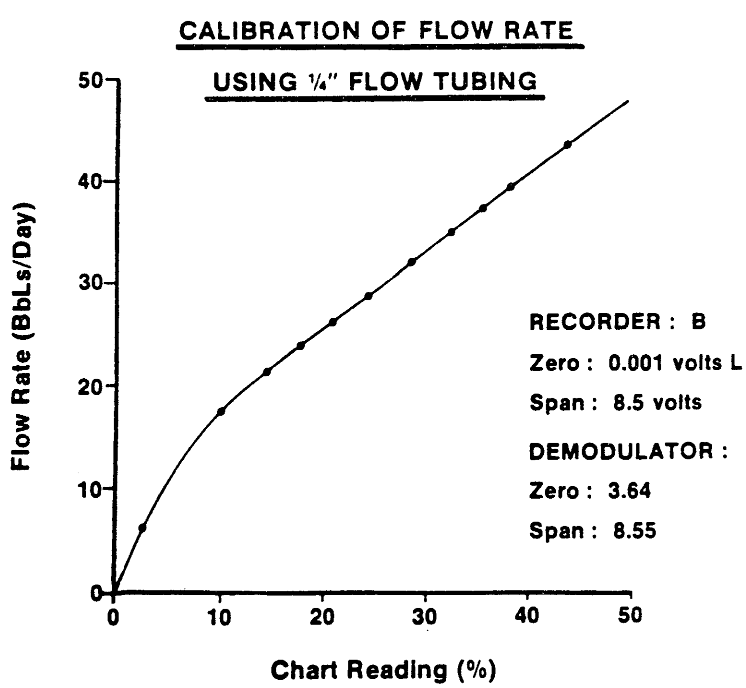

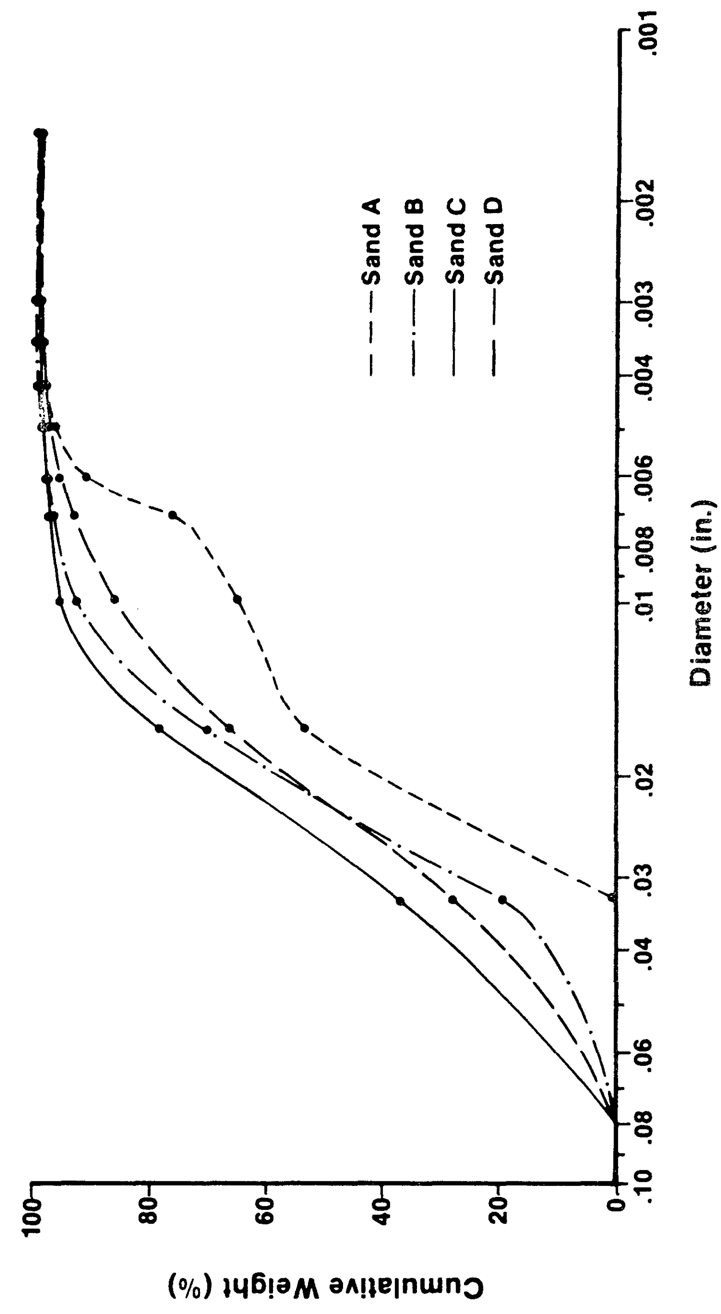

Figure 13.

SAND SIEVE ANALYSIS

Figure 14.

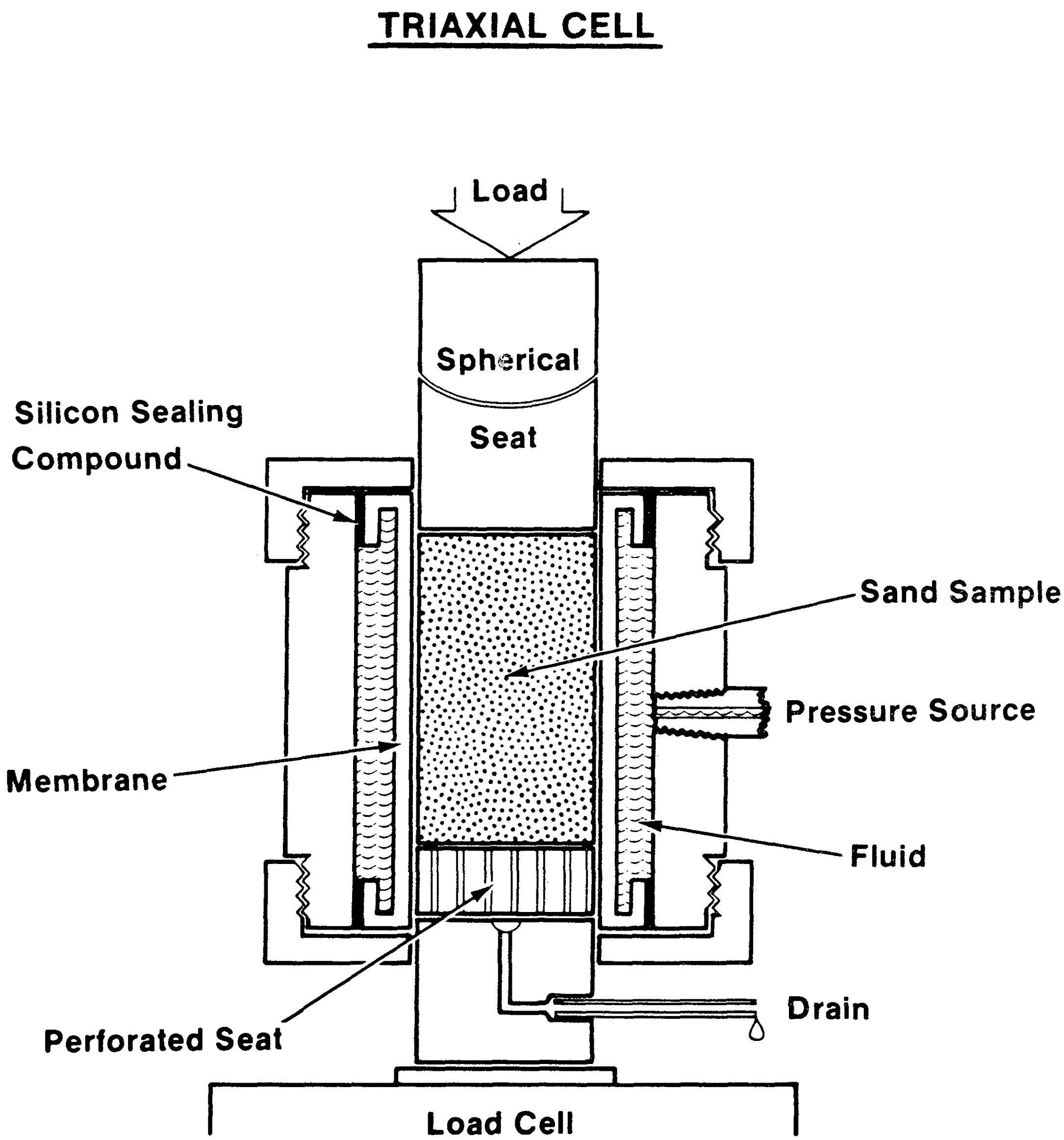
TRIAXIAL CELL
Load
Spherical
Seat
Silicon Sealing
Compound
Sand Sample
Pressure Source
Membrane
Fluid
Drain
Perforated Seat
Load Cell

Figure 15.

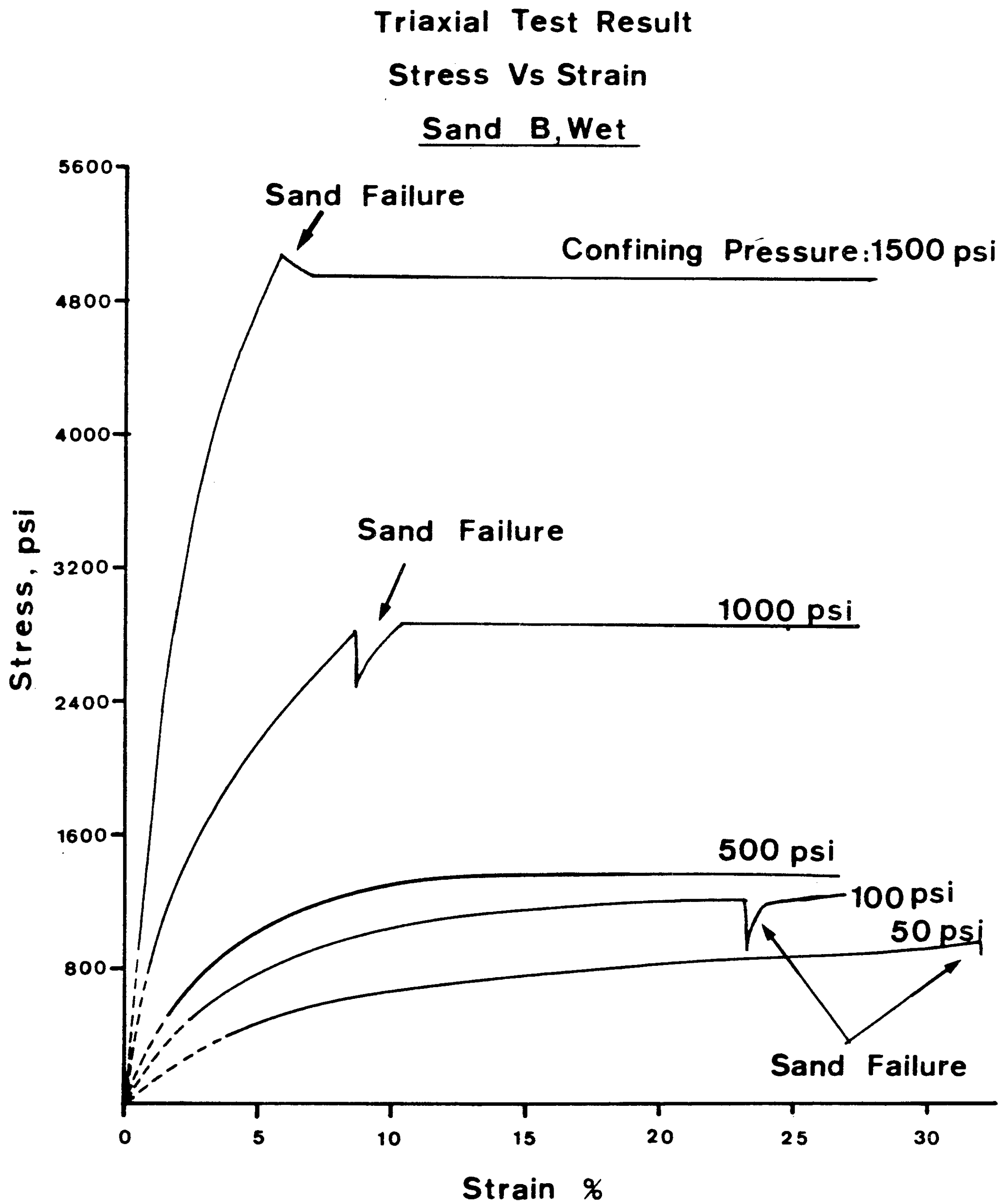
Triaxial Test Result
Stress Vs Strain
Sand B, Wet
Sand Failure
Confining Pressure:1500 psi
Sand Failure
1000 psi
500 psi
100 psi
50 psi
Sand Failure
Stress, psi
5600
4800
4000
3200
2400
1600
800
0
5
10
15
20
25
30
Strain %

Figure 16. **Triaxial Test Result**

Stress Vs Strain

Sand C, Wet

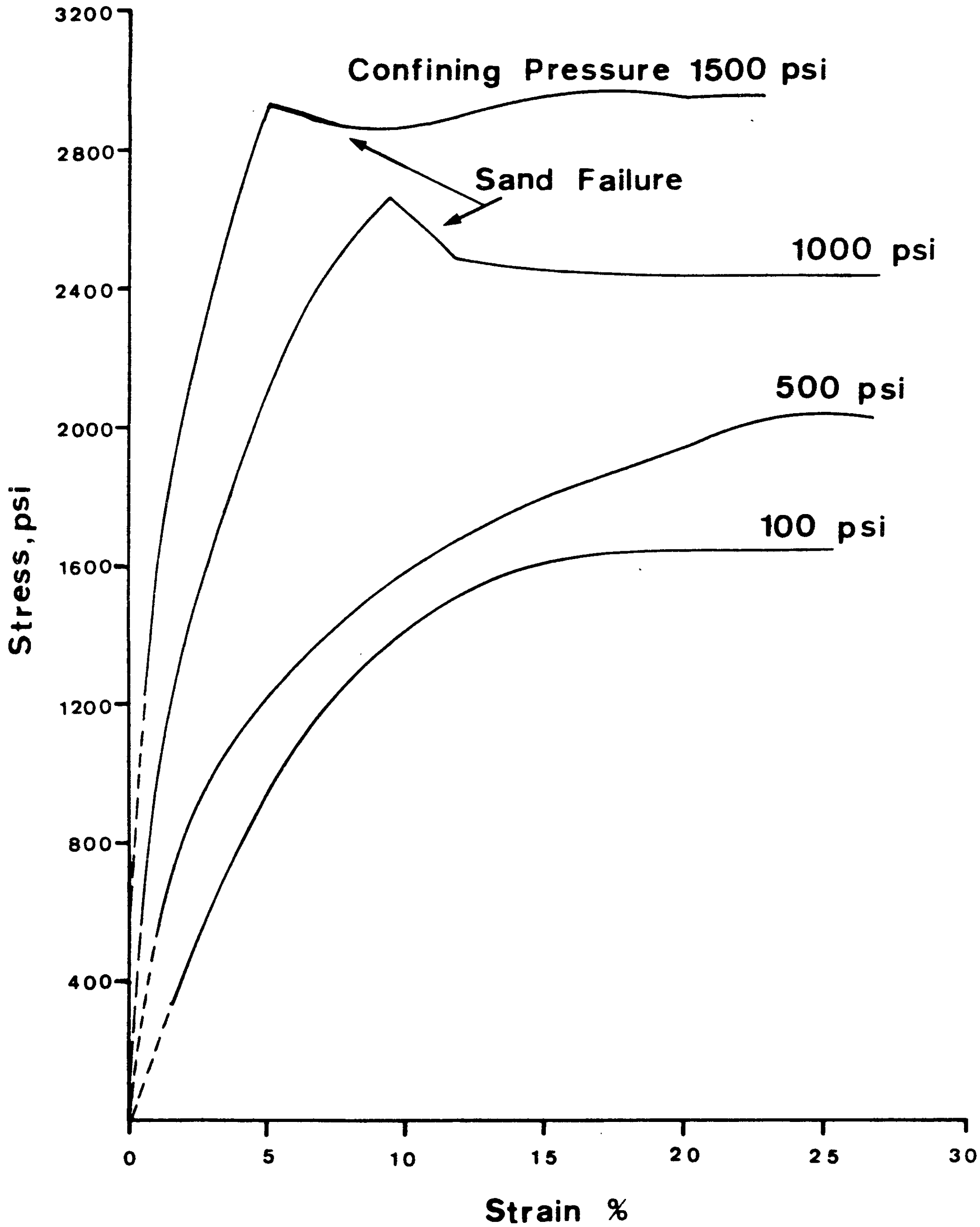

Figure 17. **Triaxial Test Result**

Stress Vs Strain

Sand D, Wet

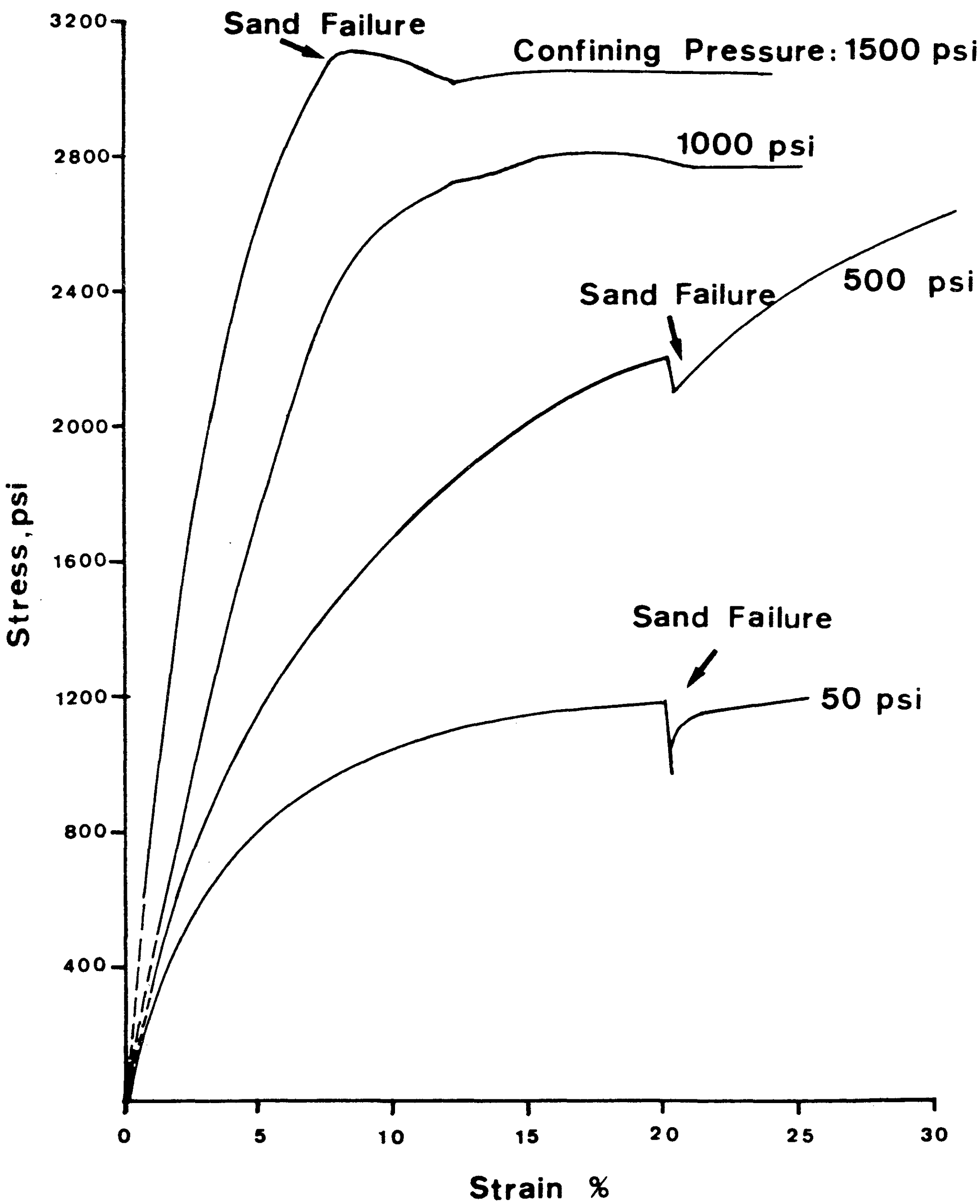

Figure 18a. MOHR FAILURE ENVELOPE

Sand A

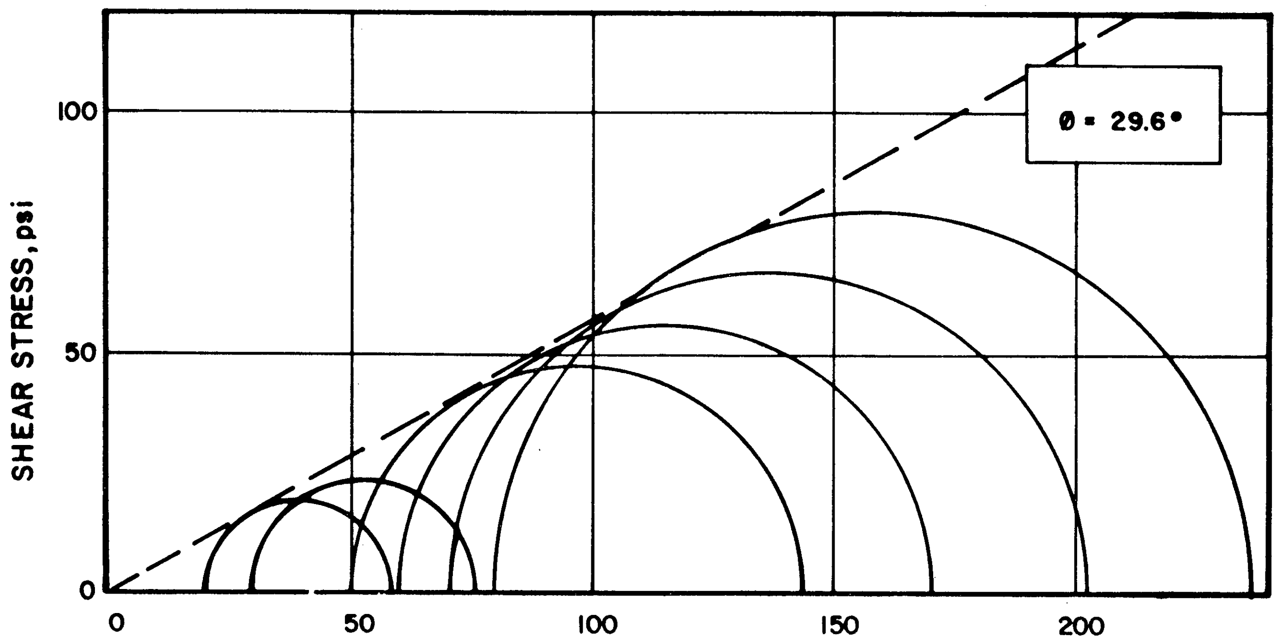

* AFTER TIPPIE (1973)

Figure 18b. **Mohr Failure Envelope**

Sand B

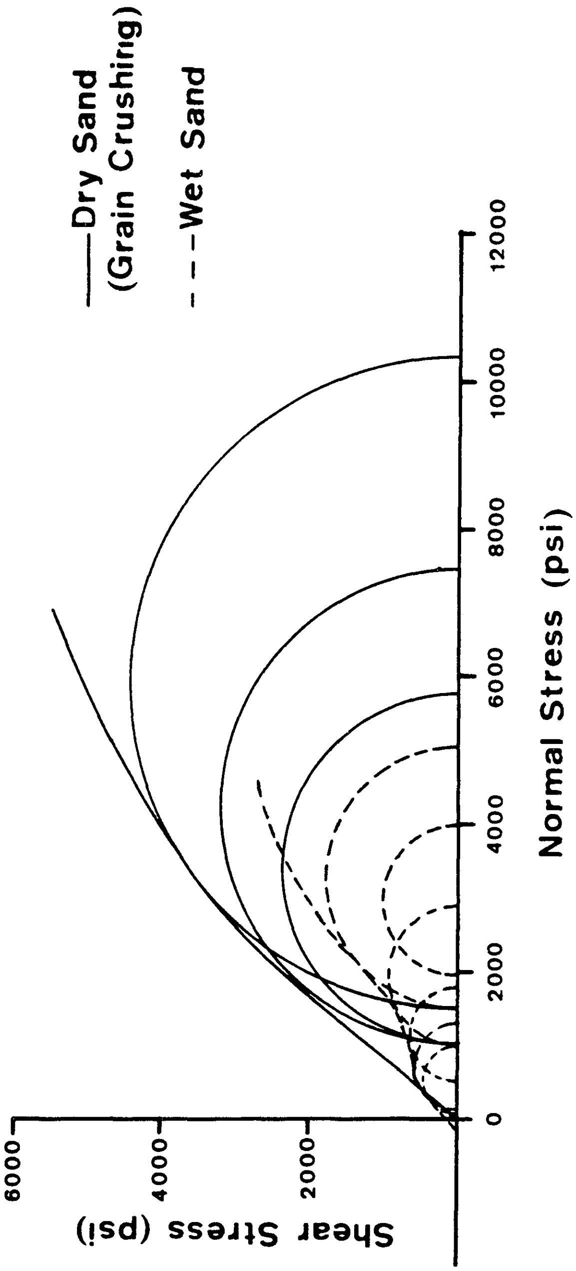

Figure 19. Mohr Failure Envelope

Sand C

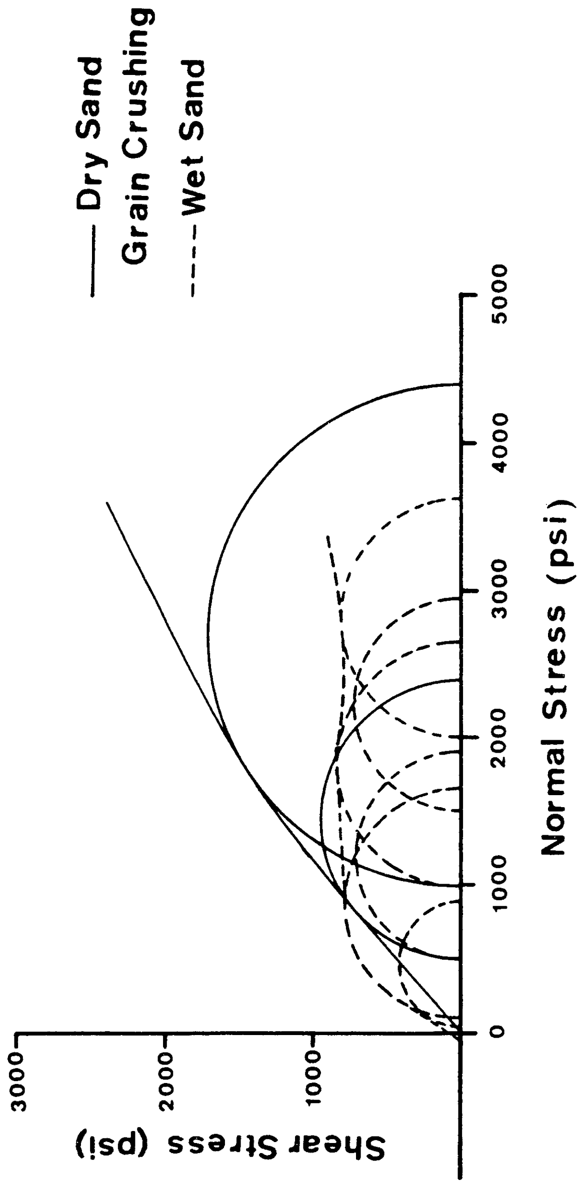

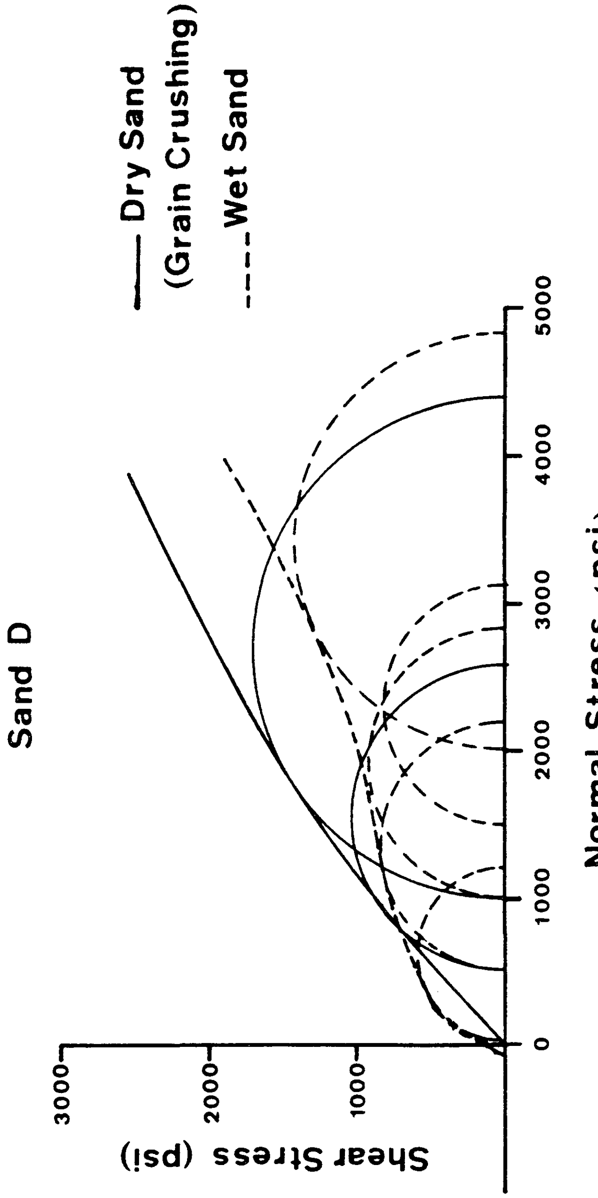
Mohr Failure Envelope
Sand D
Shear Stress (psi)
3000
2000
1000
0
1000
2000
3000
4000
5000
Normal Stress (psi)
Dry Sand
(Grain Crushing)
Wet Sand

Figure 20.

Figure 21. **PRESSURE DROP VS FLOW RATE**

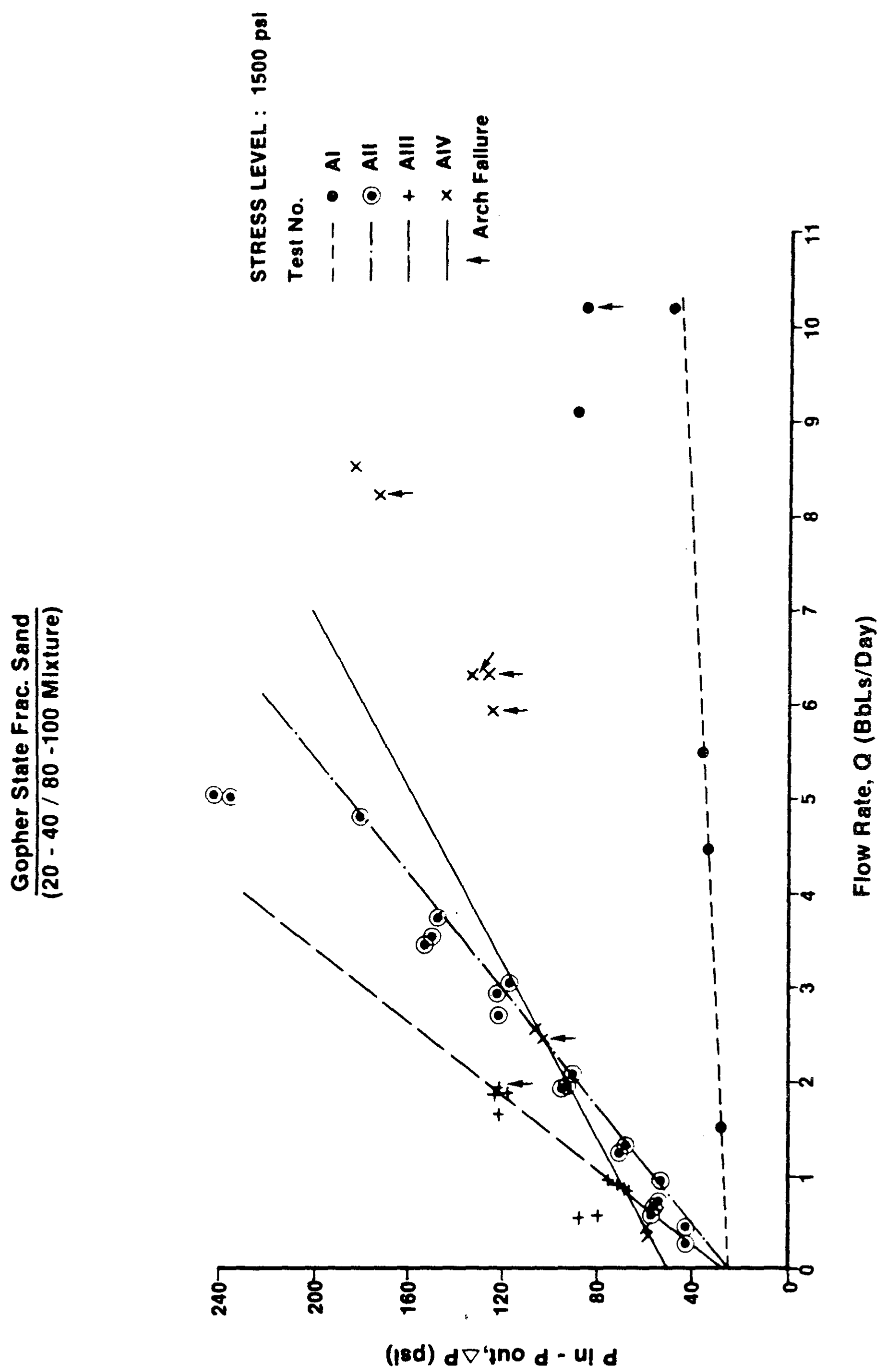

Figure 22.

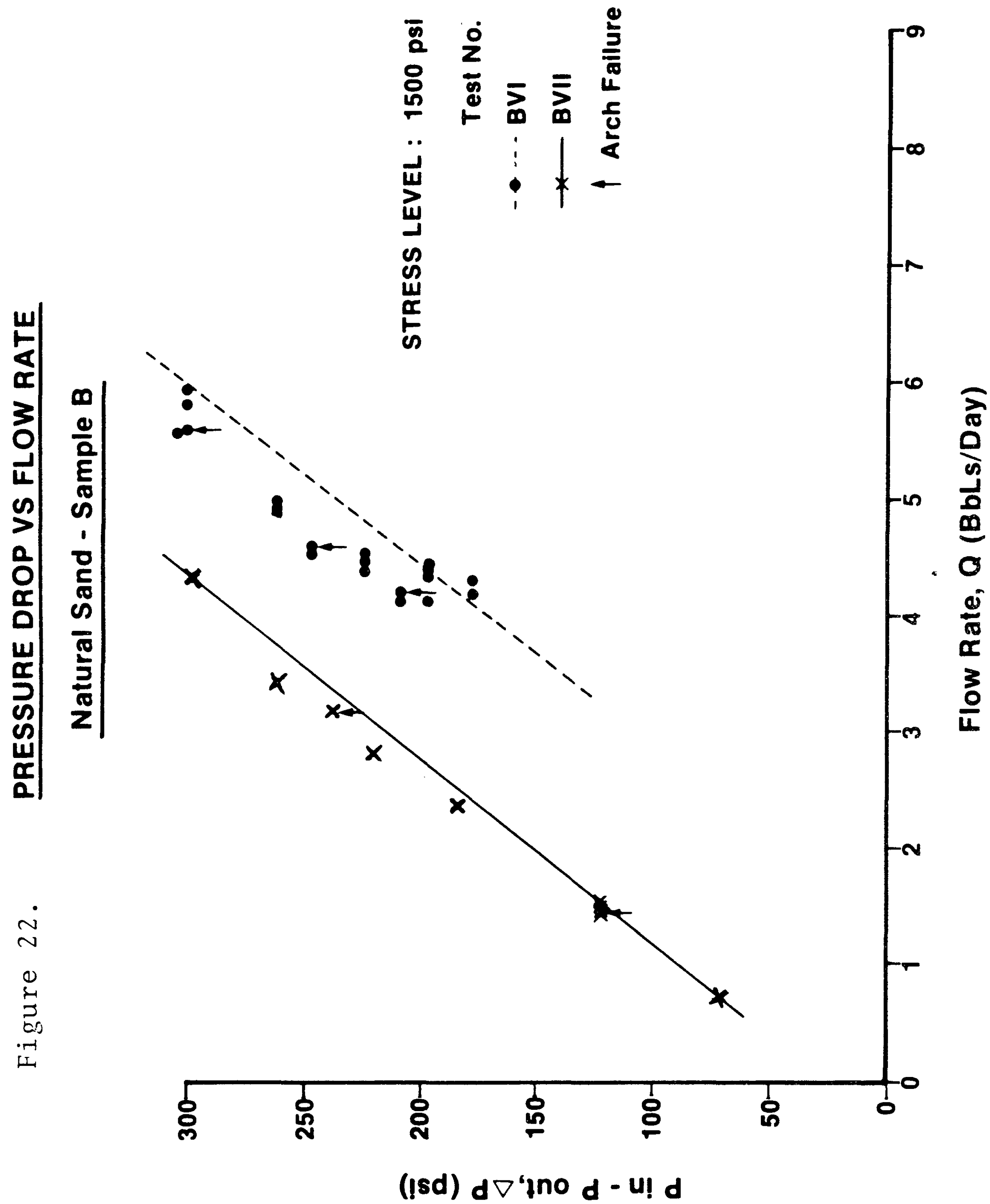
PRESSURE DROP VS FLOW RATE
Natural Sand - Sample B
STRESS LEVEL : 1500 psi
Test No.
BVI
BVII
Arch Failure
P in - P out, △P (psi)
Flow Rate, Q (BbLs/Day)
0
50
100
150
200
250
300
1
2
3
4
5
6
7
8
9

Figure 23.

PRESSURE DROP VS FLOW RATE

Natural Sand - Sample B

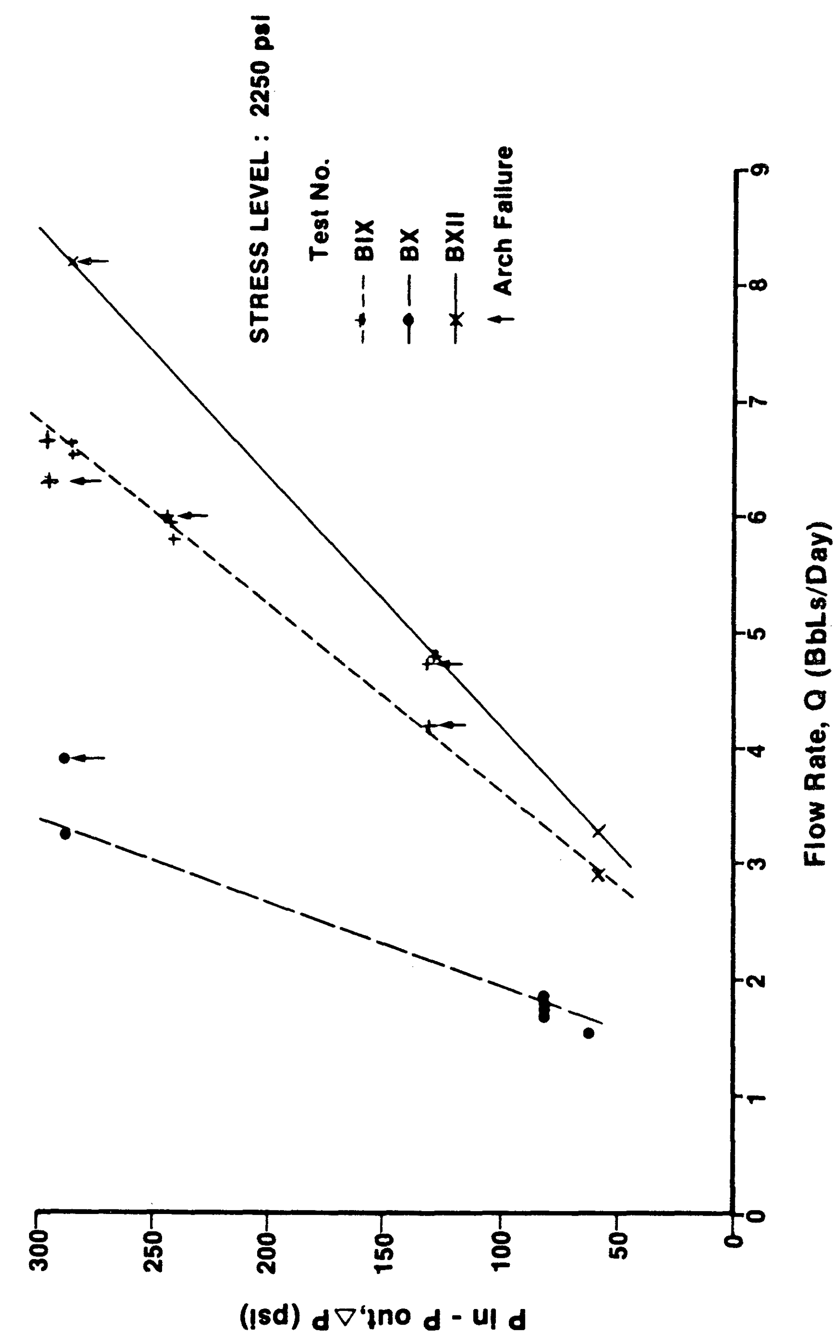

Figure 24. **PRESSURE DROP VS FLOW RATE**

Natural Sand - Sample B

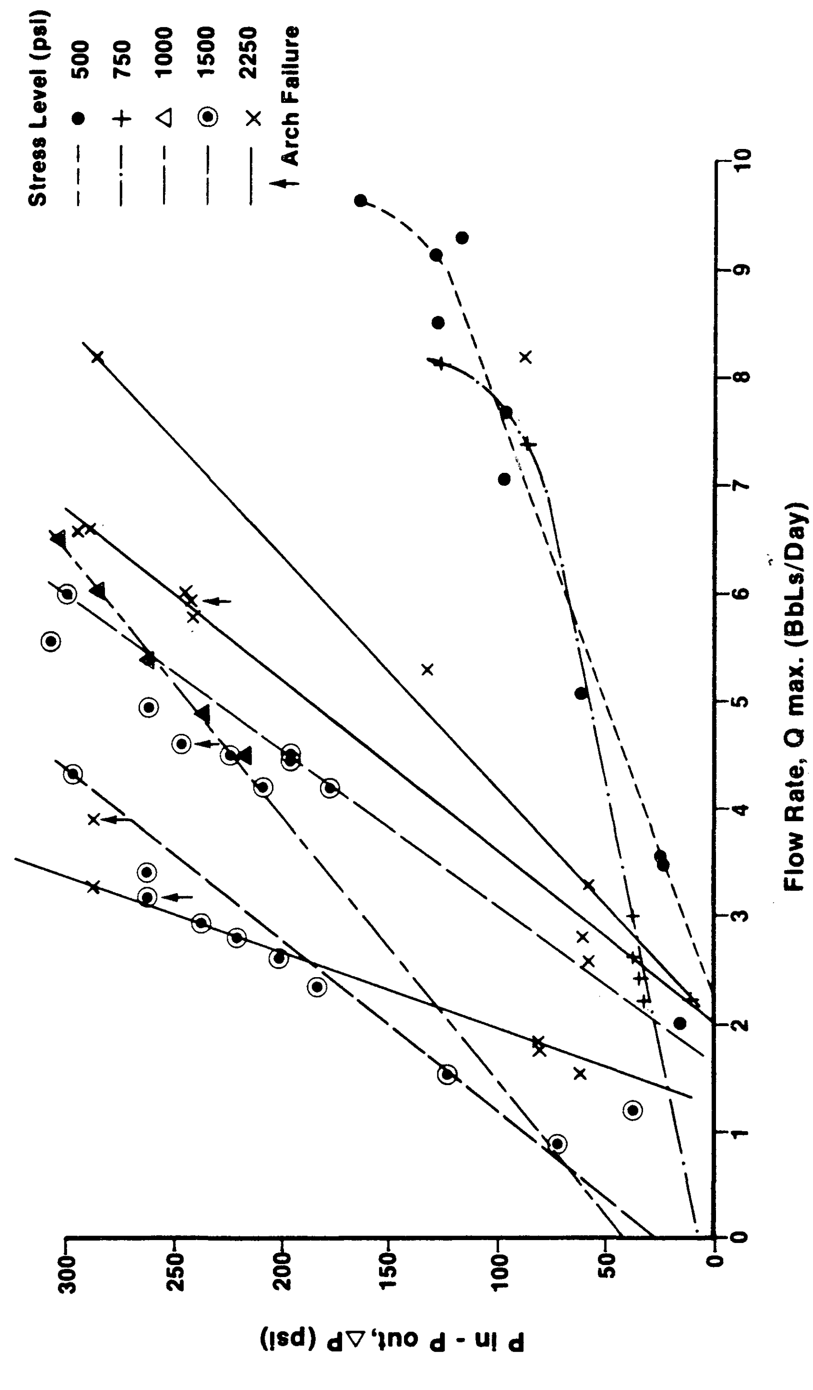

Figure 25. **PRESSURE DROP VS FLOW RATE**

Natural Sand - Sample C

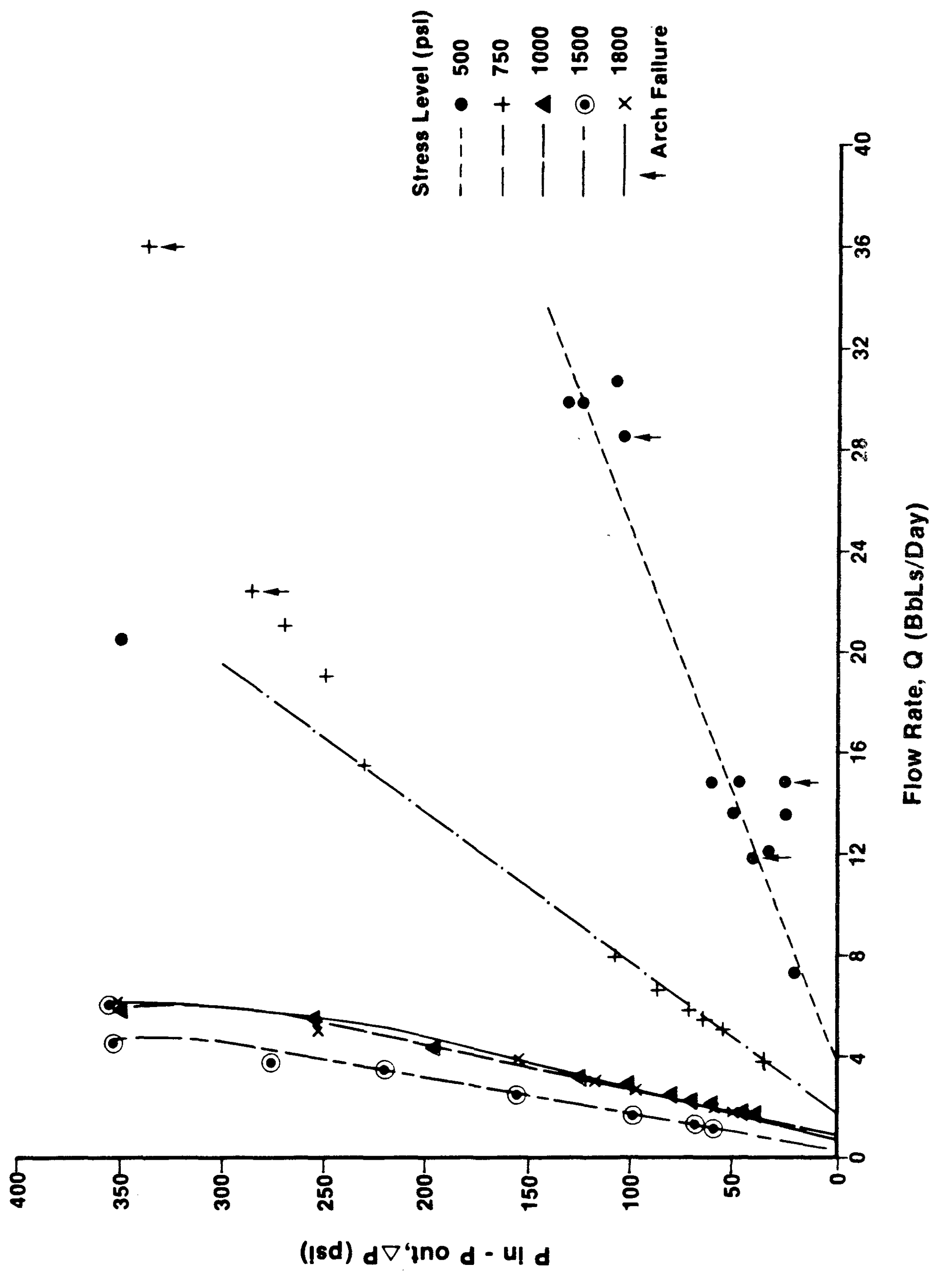

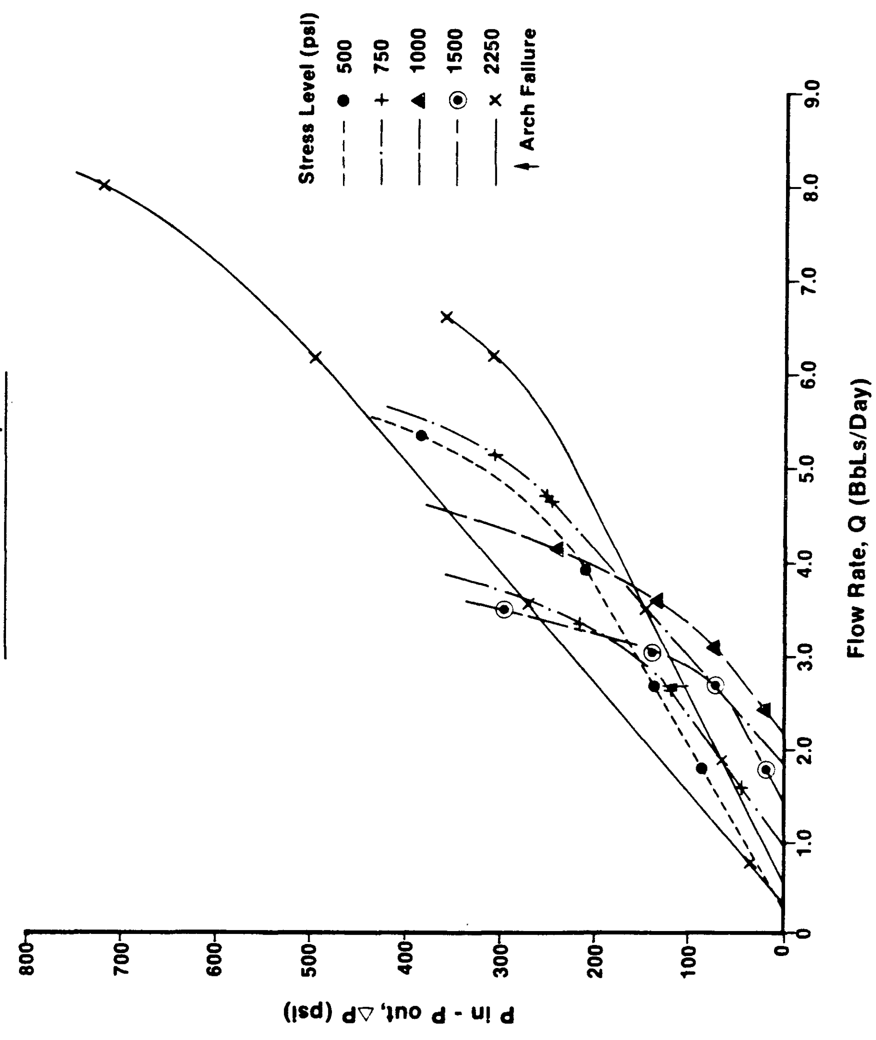

Figure 26. **PRESSURE DROP VS FLOW RATE**

Natural Sand - Sample D

Figure 27.

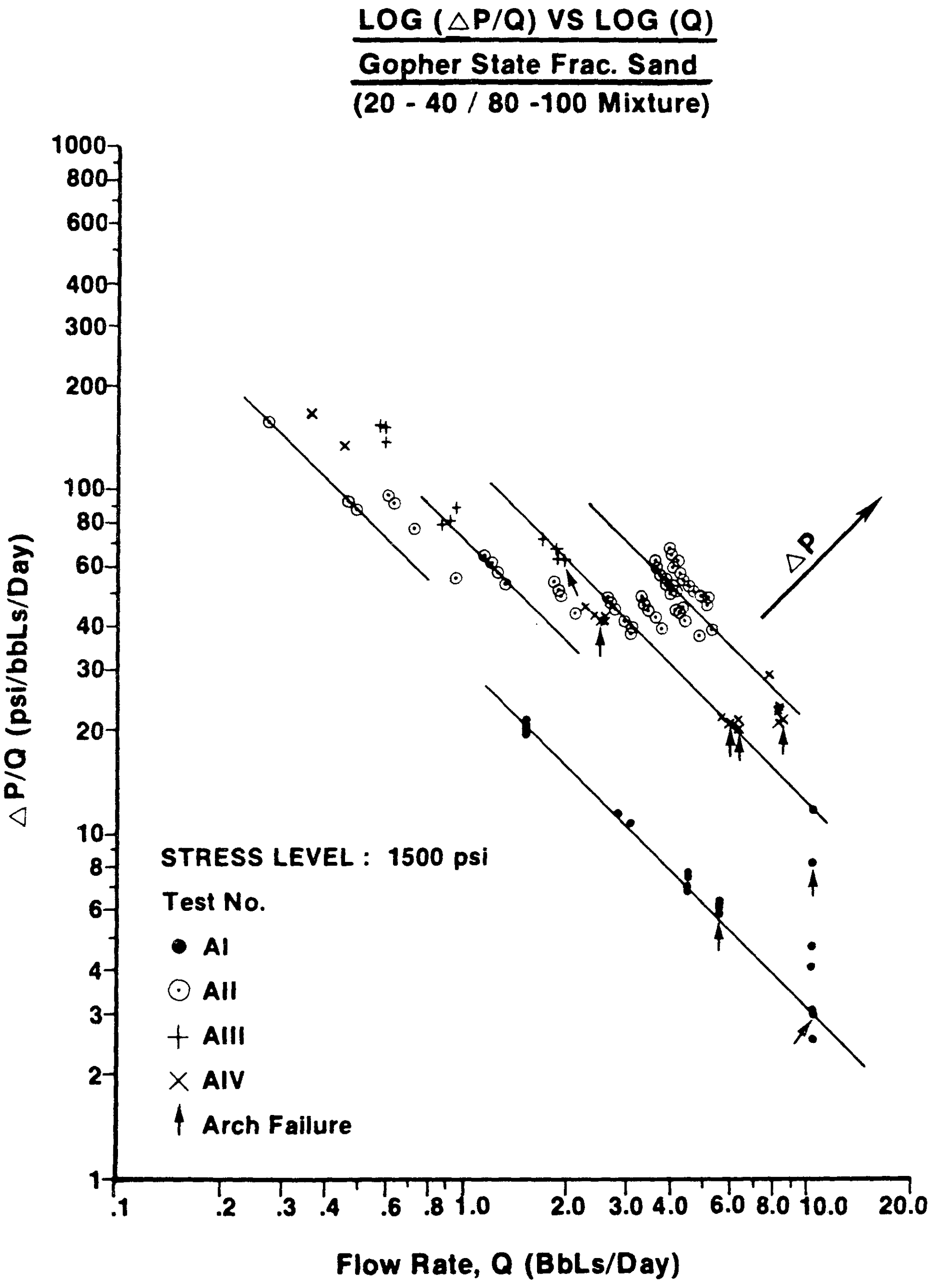
LOG (△P/Q) VS LOG (Q)
Gopher State Frac. Sand
(20 - 40 / 80 -100 Mixture)
△P/Q (psi/bbLs/Day)
1000
800
600
400
300
200
100
80
60
40
30
20
10
8
6
4
3
2
1
△P
STRESS LEVEL : 1500 psi
Test No.
AI
AII
AIII
AIV
Arch Failure
.1
.2
.3
.4
.6
.8
1.0
2.0
3.0
4.0
6.0
8.0
10.0
20.0
Flow Rate, Q (BbLs/Day)

Figure 28.

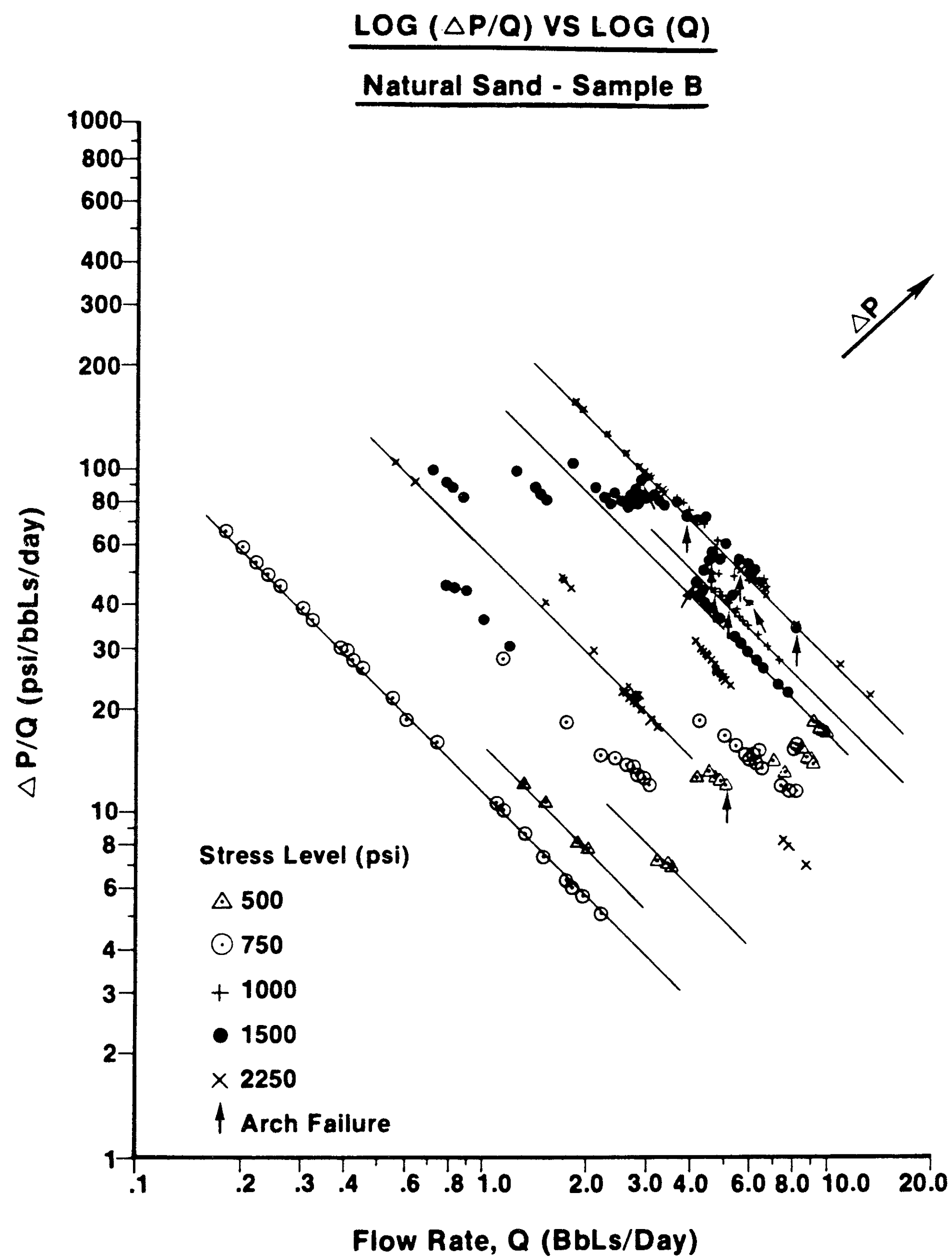
LOG (△P/Q) VS LOG (Q)
Natural Sand - Sample B
△P
△ P/Q (psi/bbLs/day)
1000
800
600
400
300
200
100
80
60
40
30
20
10
8
6
4
3
2
1
Stress Level (psi)
500
750
1000
1500
2250
Arch Failure
.1
.2
.3
.4
.6
.8
1.0
2.0
3.0
4.0
6.0
8.0
10.0
20.0
Flow Rate, Q (BbLs/Day)

Figure 29.

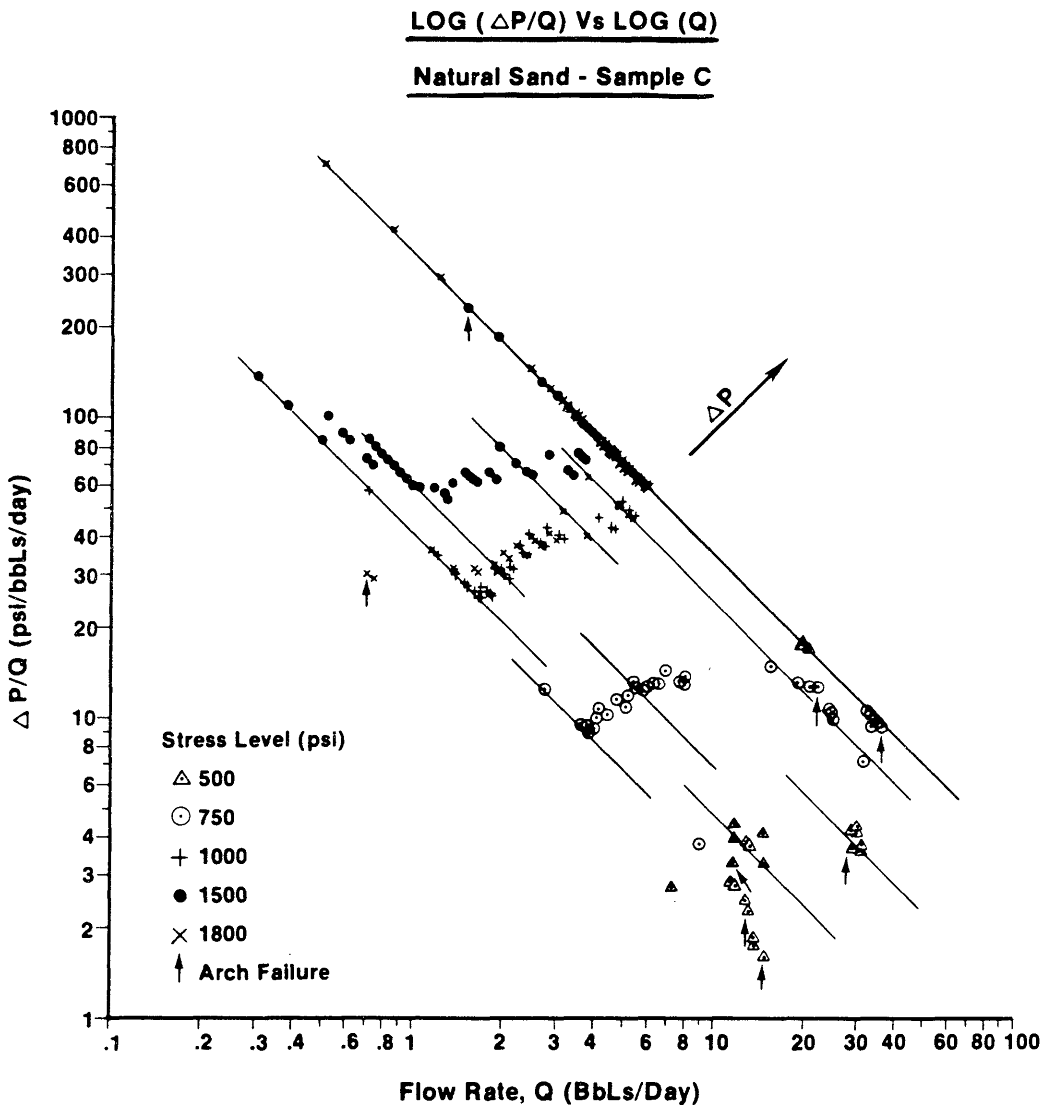
LOG (△P/Q) Vs LOG (Q)
Natural Sand - Sample C
△P
△ P/Q (psi/bbLs/day)
Flow Rate, Q (BbLs/Day)
Stress Level (psi)
500
750
1000
1500
1800
Arch Failure
1000
800
600
400
300
200
100
80
60
40
30
20
10
8
6
4
3
2
1
.1
.2
.3
.4
.6
.8
1
2
3
4
6
8
10
20
30
40
60
80
100

Figure 30.

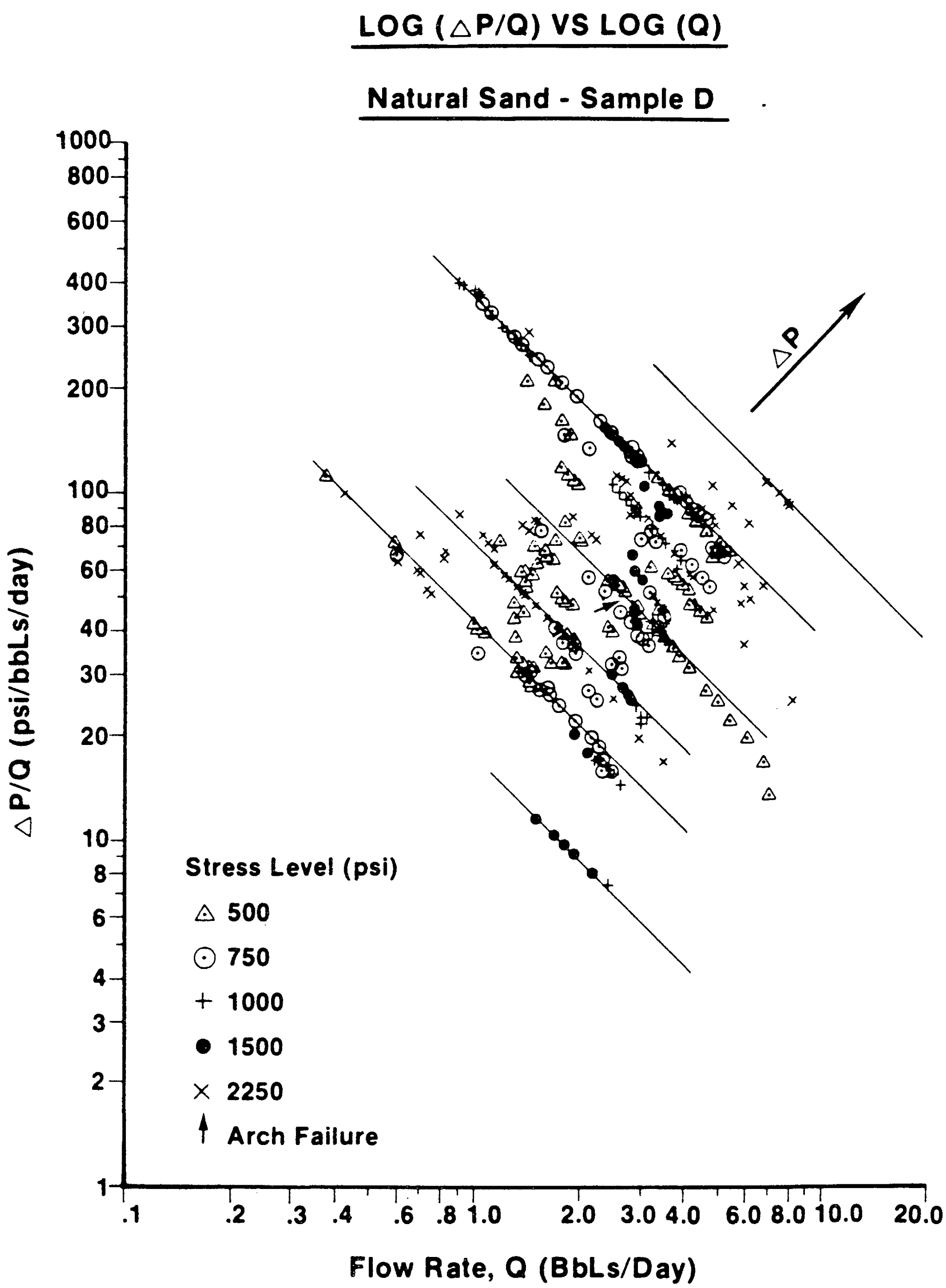
LOG (△P/Q) VS LOG (Q)
Natural Sand - Sample D
1000
800
600
400
300
200
100
80
60
40
30
20
10
8
6
4
3
2
1
△P/Q (psi/bbLs/day)
△P
Stress Level (psi)
500
750
1000
1500
2250
Arch Failure
.1
.2
.3
.4
.6
.8
1.0
2.0
3.0
4.0
6.0
8.0
10.0
20.0
Flow Rate, Q (BbLs/Day)

Figure 31.

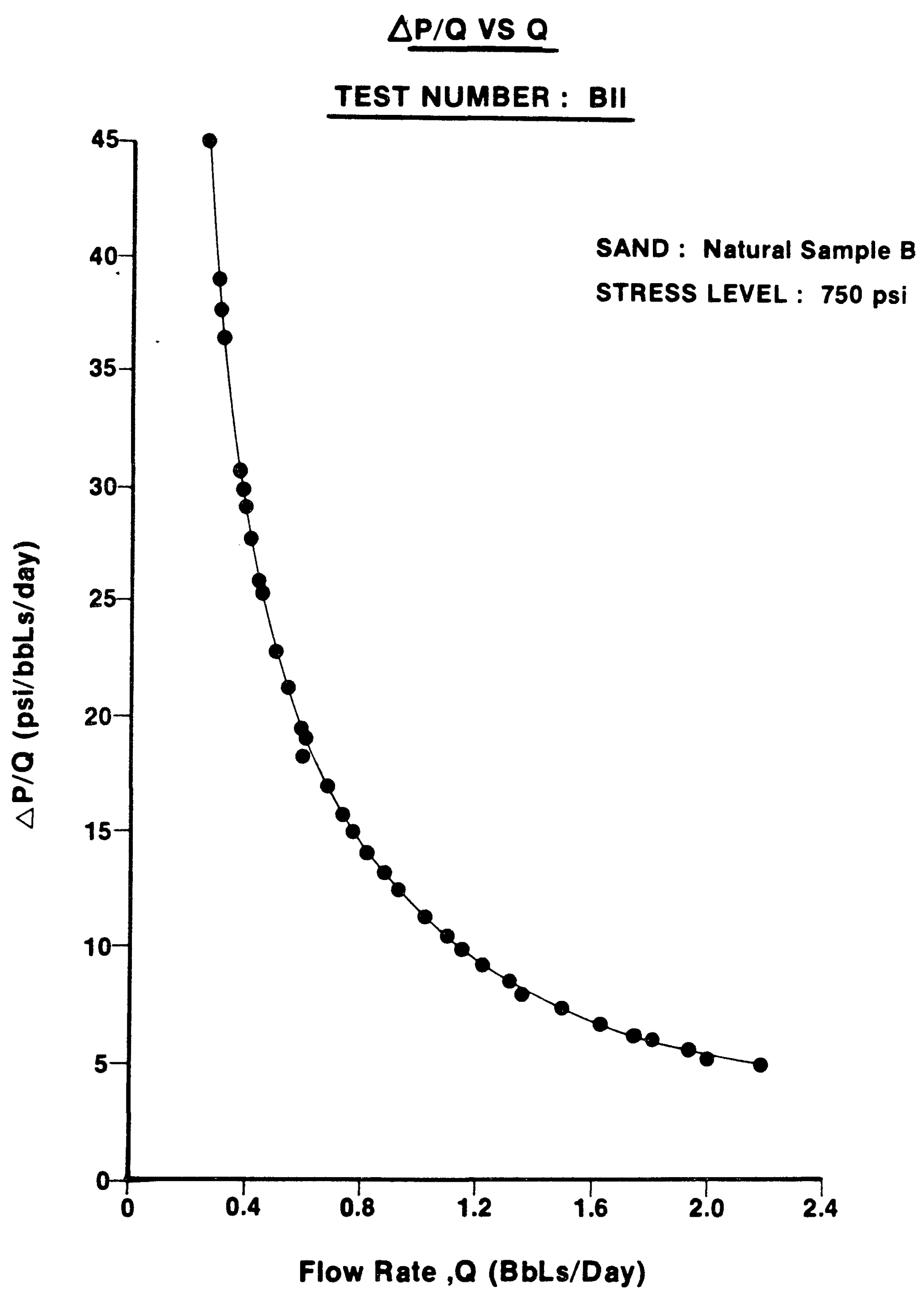
ΔP/Q VS Q
TEST NUMBER : BII
SAND : Natural Sample B
STRESS LEVEL : 750 psi
ΔP/Q (psi/bbLs/day)
45
40
35
30
25
20
15
10
5
0
0
0.4
0.8
1.2
1.6
2.0
2.4
Flow Rate ,Q (BbLs/Day)

Figure 32.

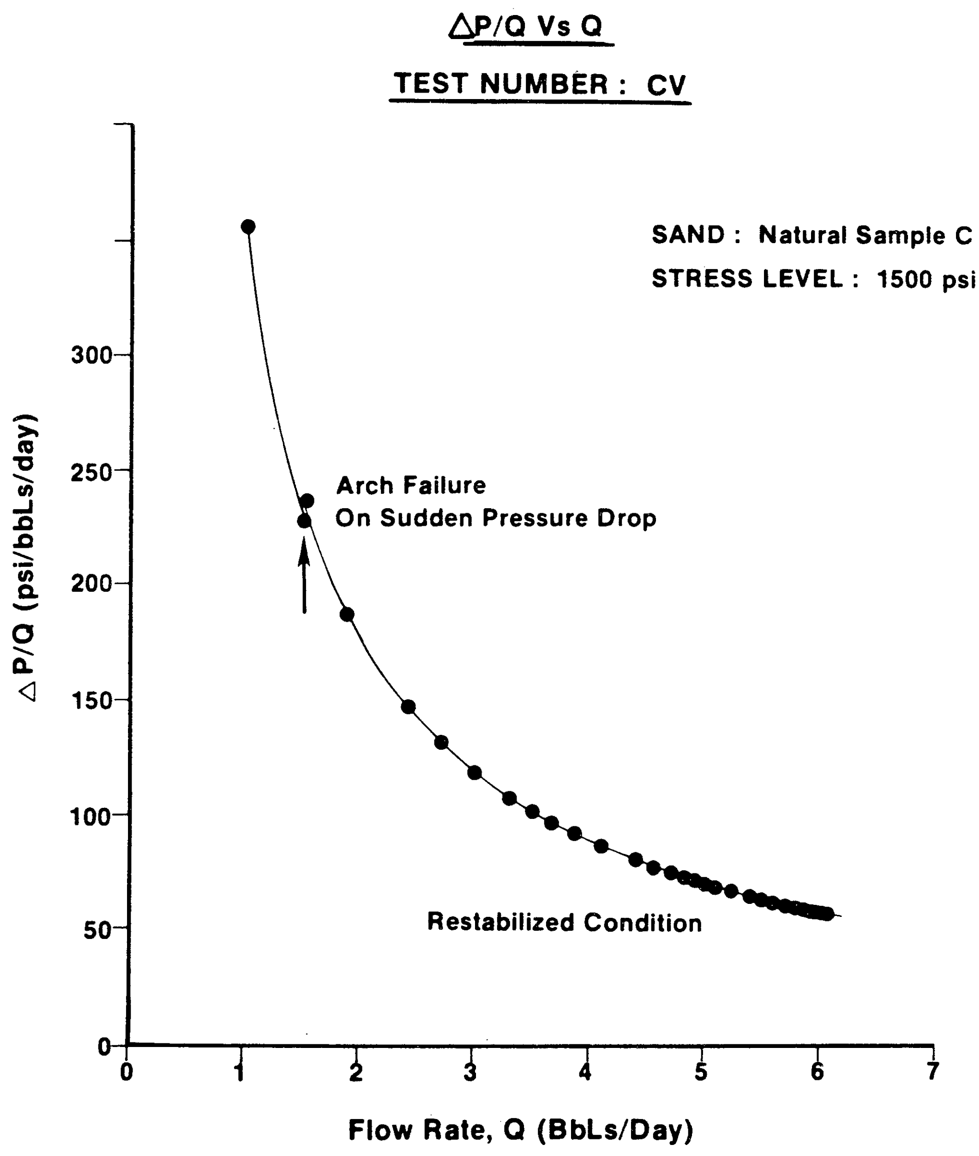
ΔP/Q Vs Q
TEST NUMBER : CV
SAND : Natural Sample C
STRESS LEVEL : 1500 psi
Arch Failure
On Sudden Pressure Drop
Restabilized Condition
ΔP/Q (psi/bbLs/day)
300
250
200
150
100
50
0
0
1
2
3
4
5
6
7
Flow Rate, Q (BbLs/Day)

Figure 33.

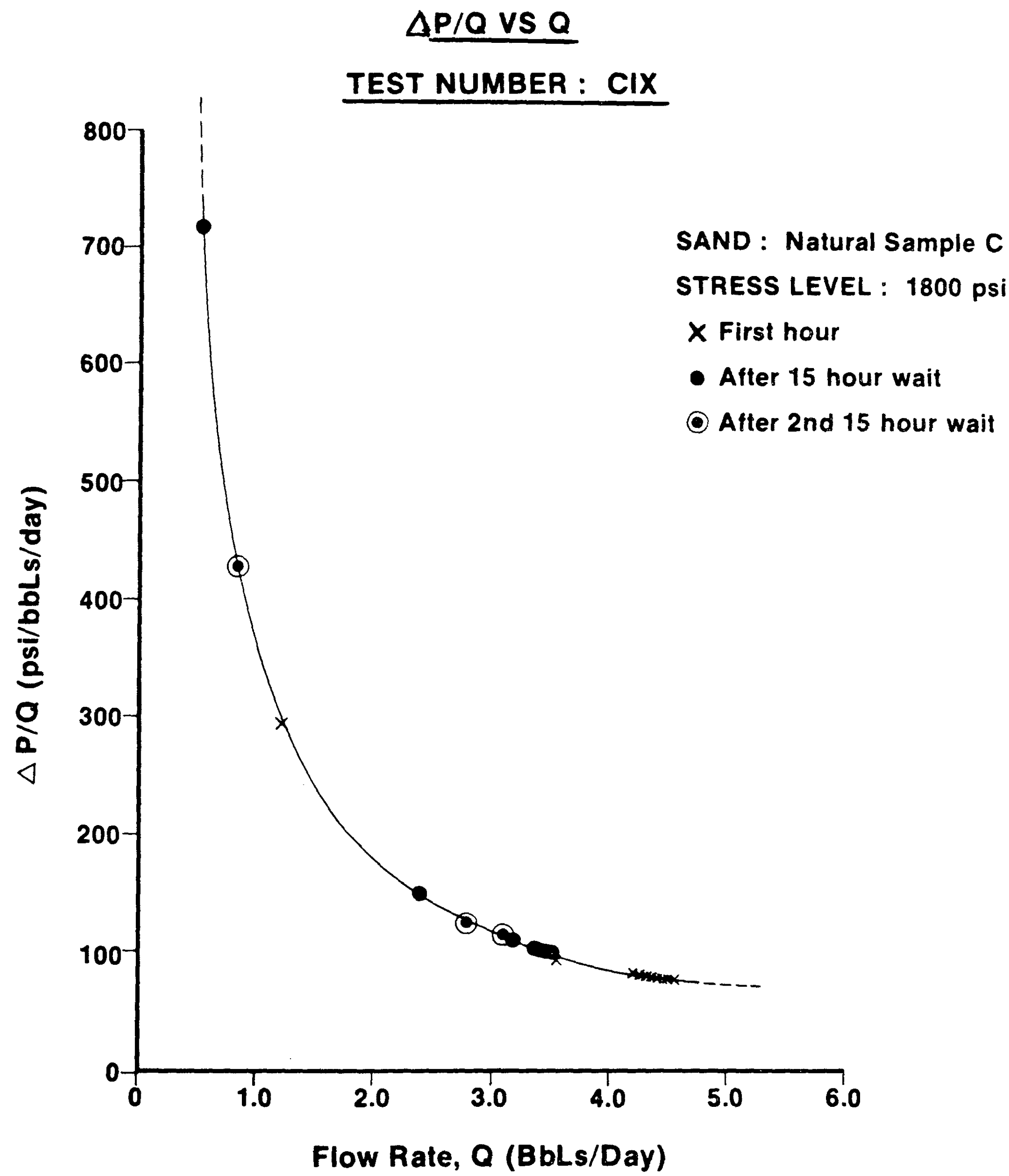
ΔP/Q VS Q
TEST NUMBER : CIX
SAND : Natural Sample C
STRESS LEVEL : 1800 psi
X First hour
After 15 hour wait
After 2nd 15 hour wait
Δ P/Q (psi/bbLs/day)
800
700
600
500
400
300
200
100
0
1.0
2.0
3.0
4.0
5.0
6.0
Flow Rate, Q (BbLs/Day)

Figure 34.

TEST NUMBER : BVIII

IN - SITU STRESS BEHAVIOR

STRESS VS TIME (CONSTANT PUMP RATE)

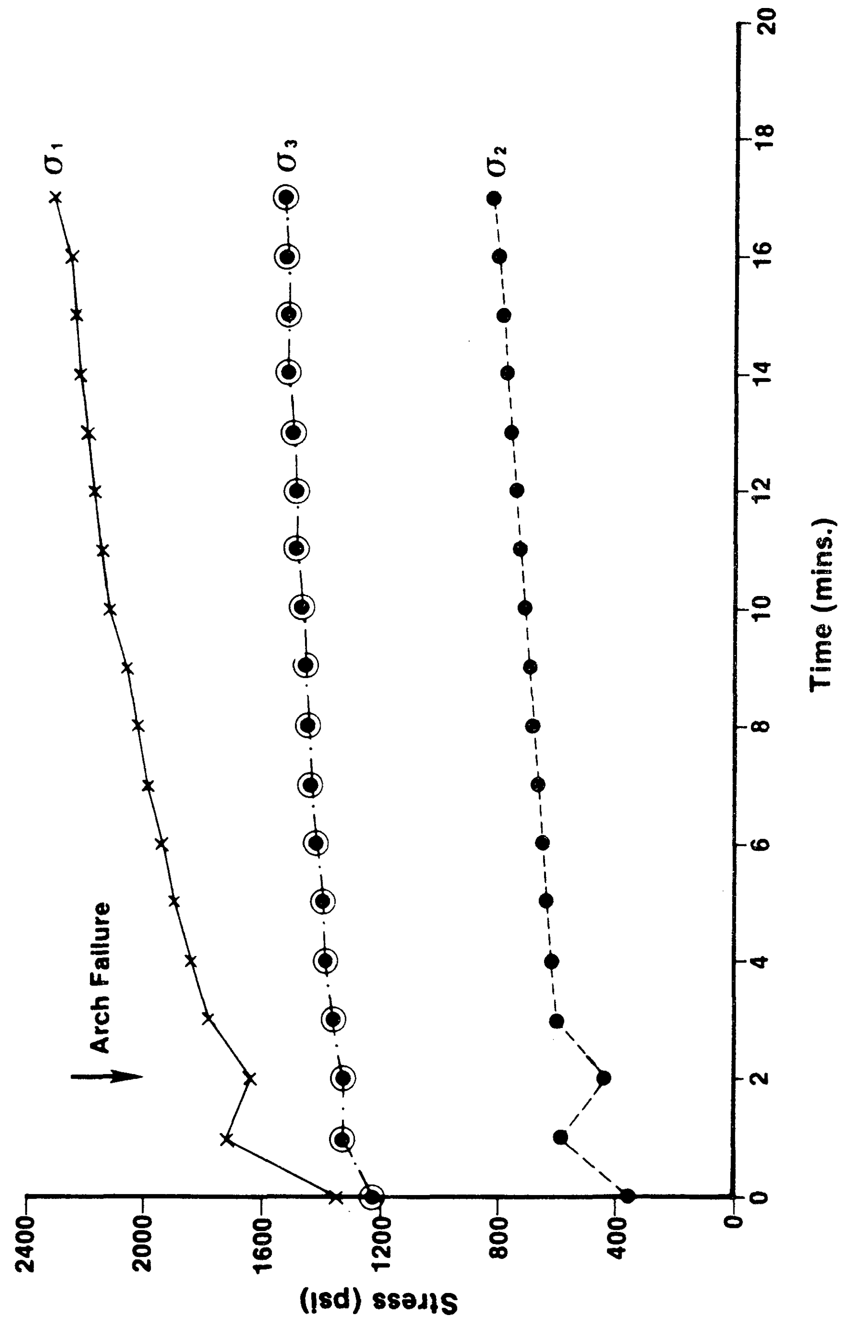

Figure 35.

TEST NUMBER : BXI

IN-SITU STRESS BEHAVIOR

STRESS VS TIME (CONSTANT PUMP RATE)

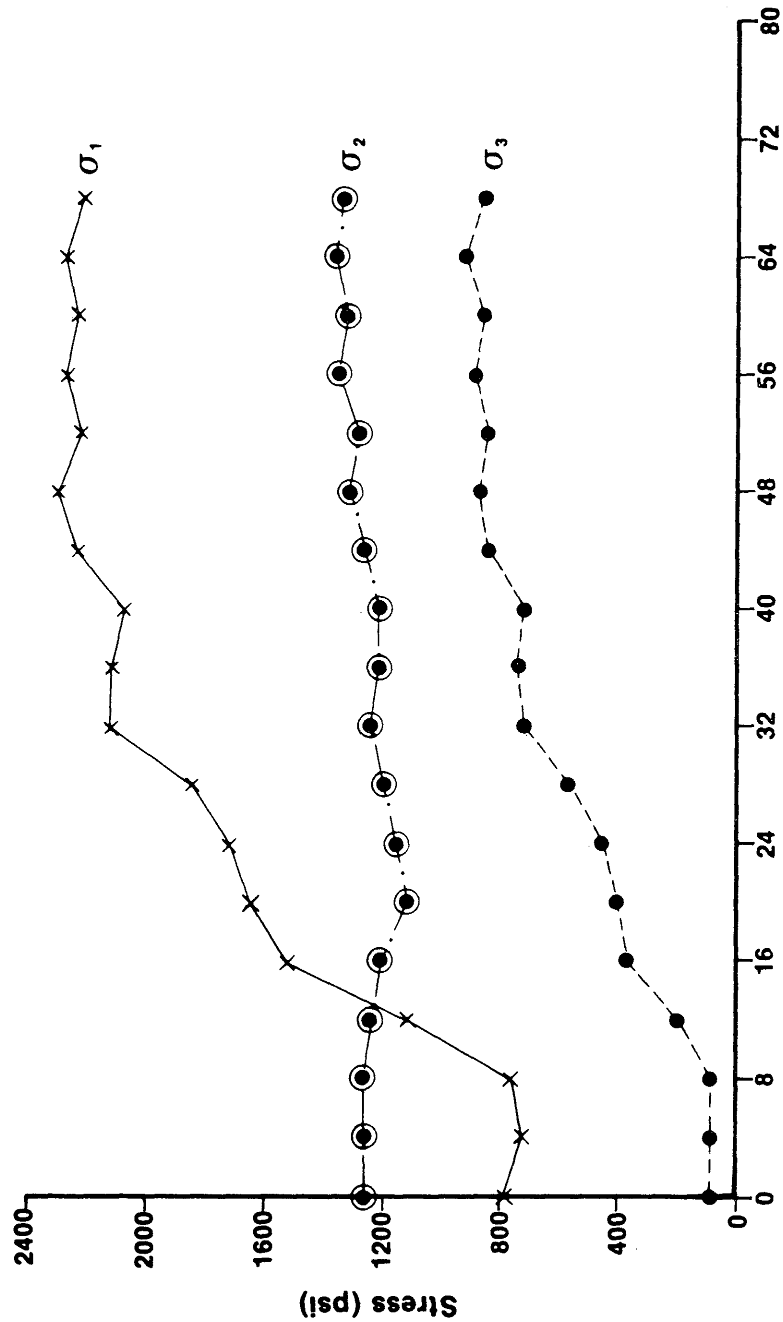

Figure 36.

TEST NUMBER : CVI

IN-SITU STRESS BEHAVIOR

STRESS VS TIME

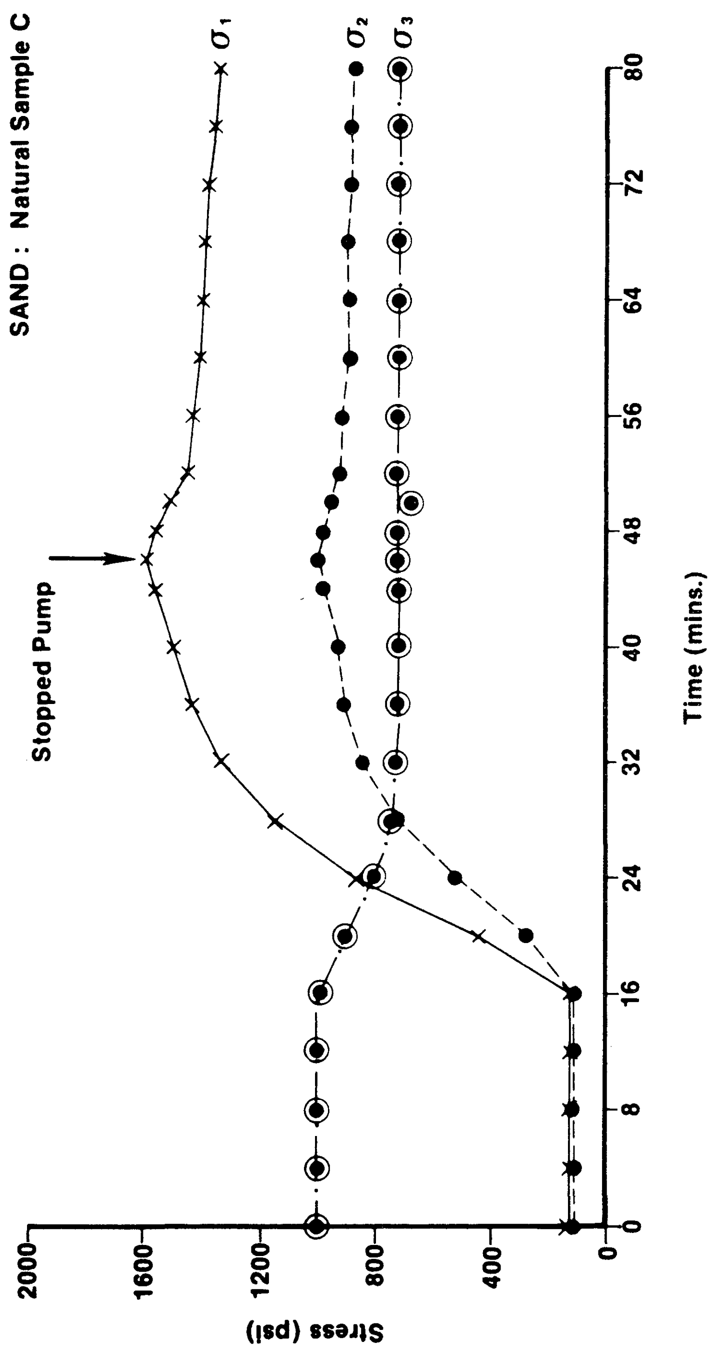

Figure 37.

TEST NUMBER : CVII
IN-SITU STRESS BEHAVIOR

STRESS VS TIME

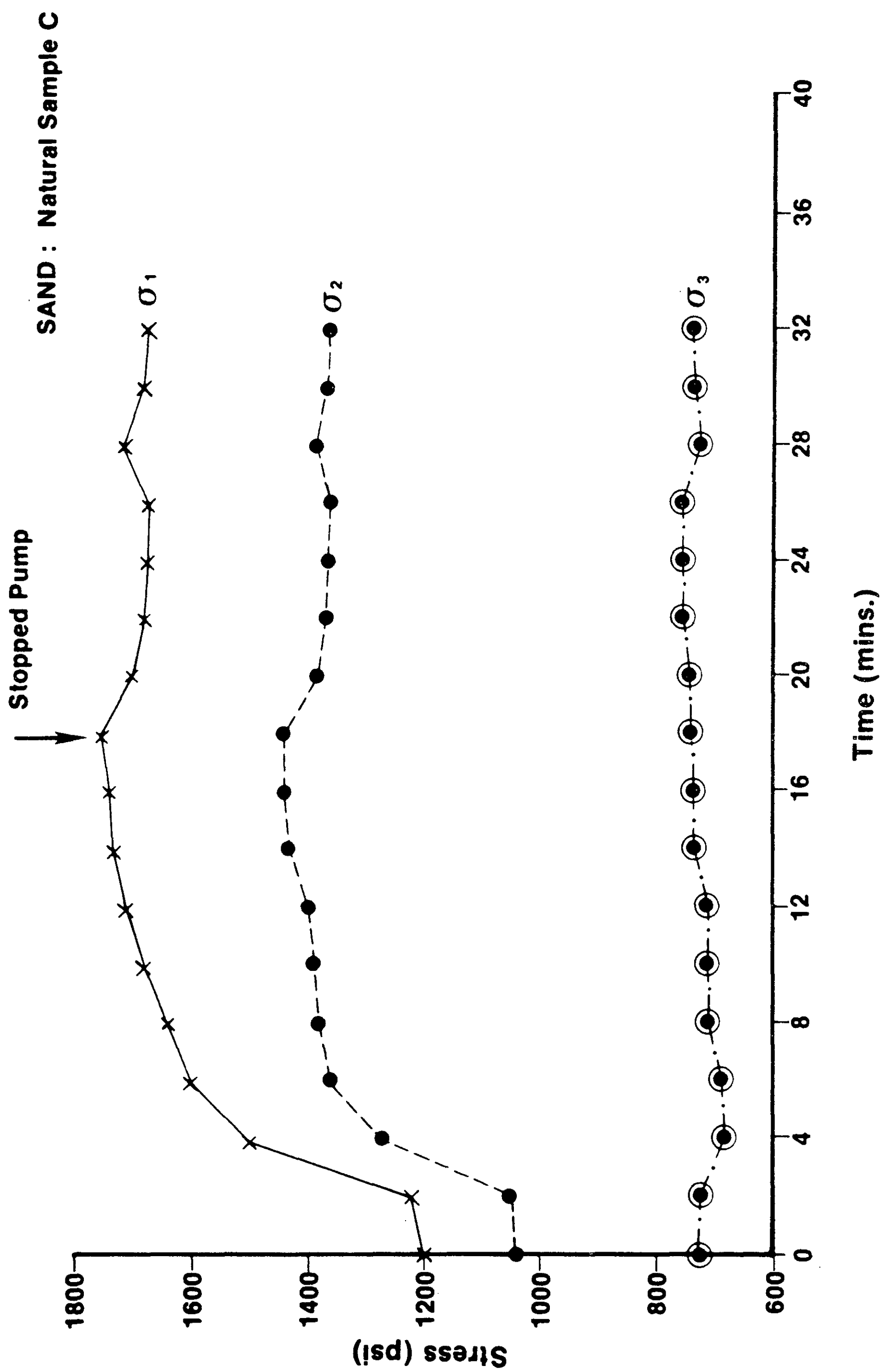

Figure 38. Cavity Size Vs Flow Rate
Gopher State Frac. Sand
(20-40/80-100 Mixture)

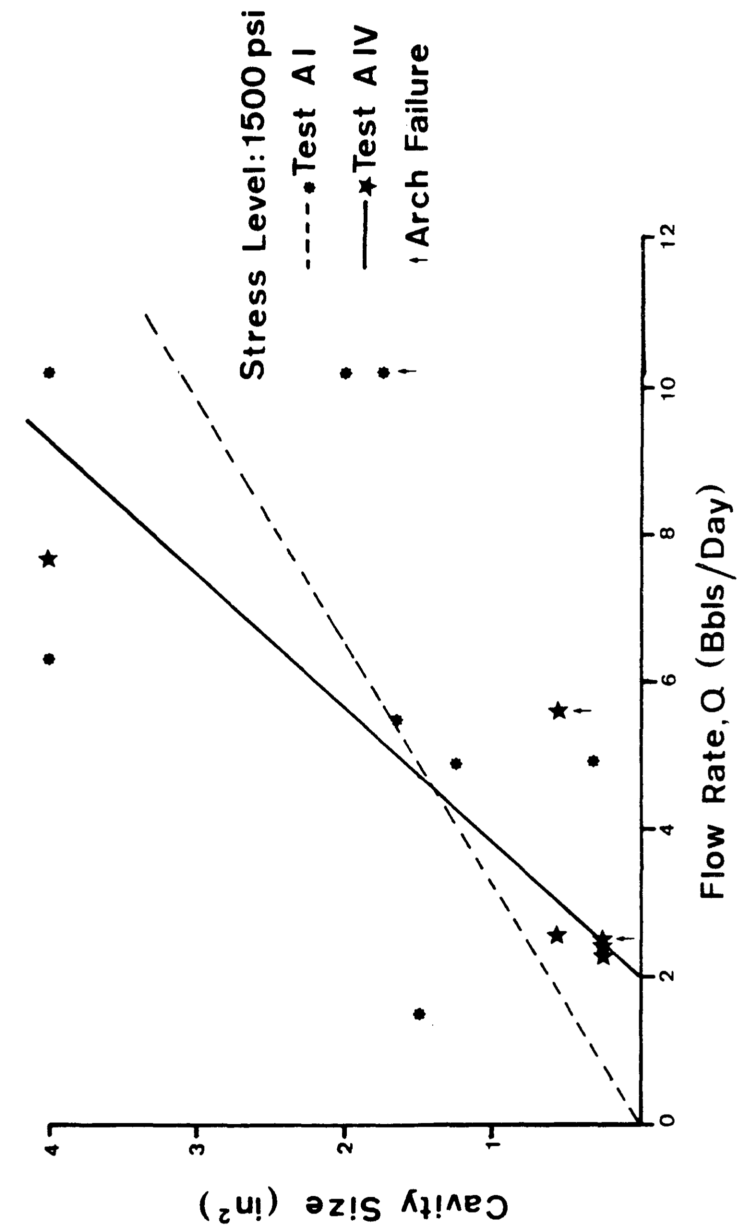

Figure 39. **CAVITY SIZE VS FLOW RATE**

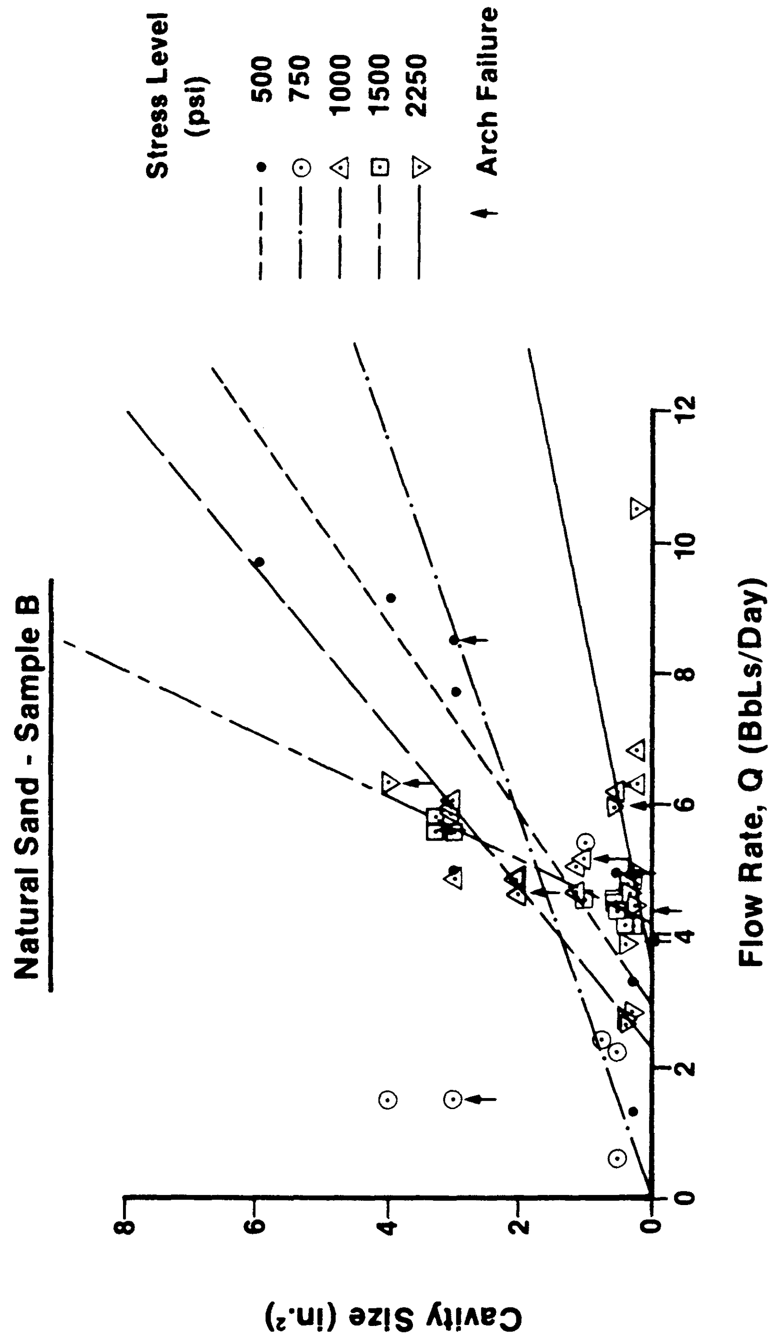

Figure 40. **CAVITY SIZE VS FLOW RATE**

Natural Sand - Sample C

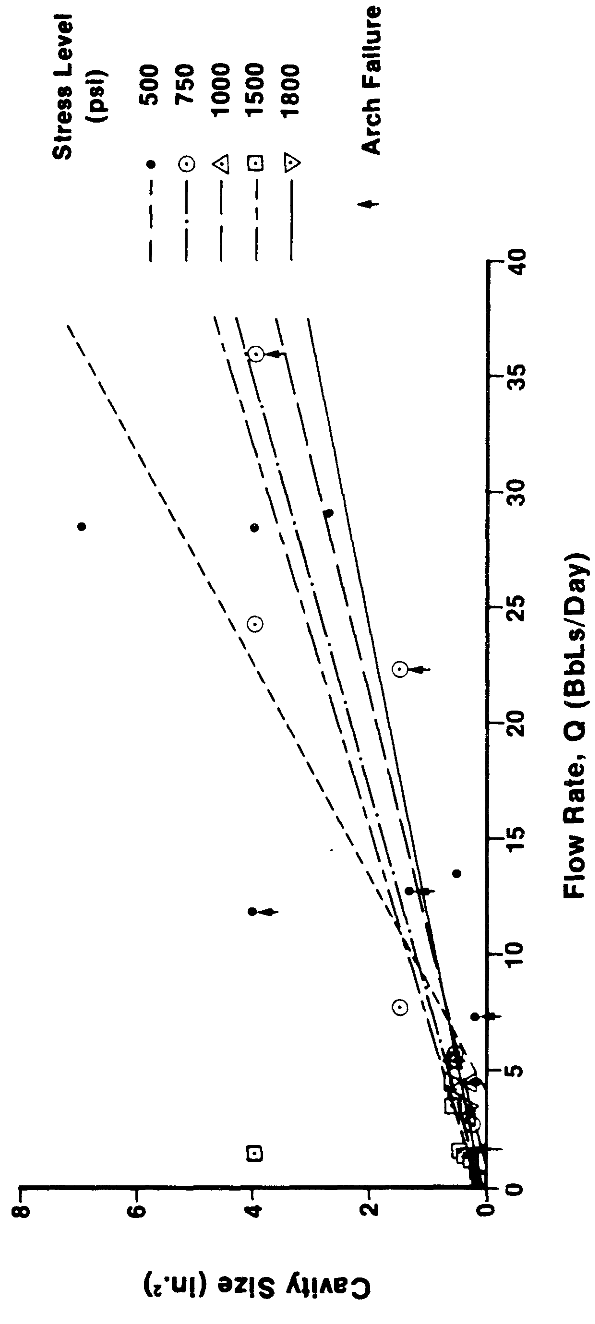

Figure 41. **CAVITY SIZE VS FLOW RATE**

Natural Sand - Sample D

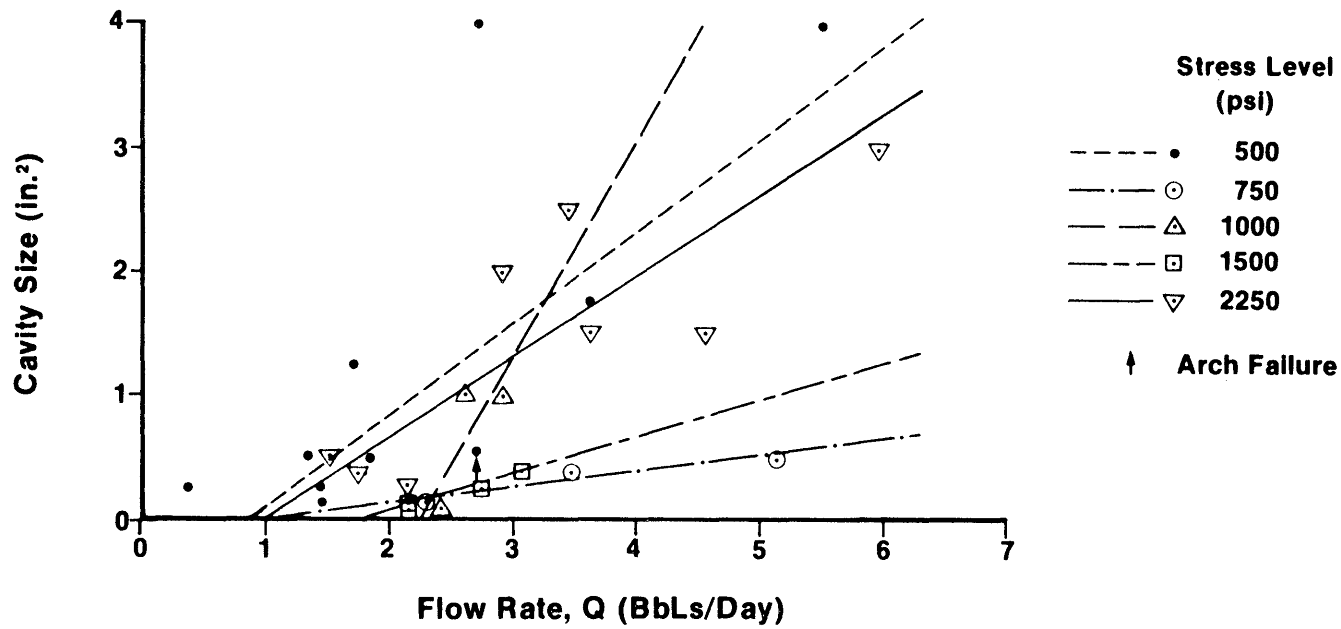

Figure 42. **Cavity Size Vs Pressure Drop**
Gopher State Frac. Sand
(20-40/80-100 Mixture)

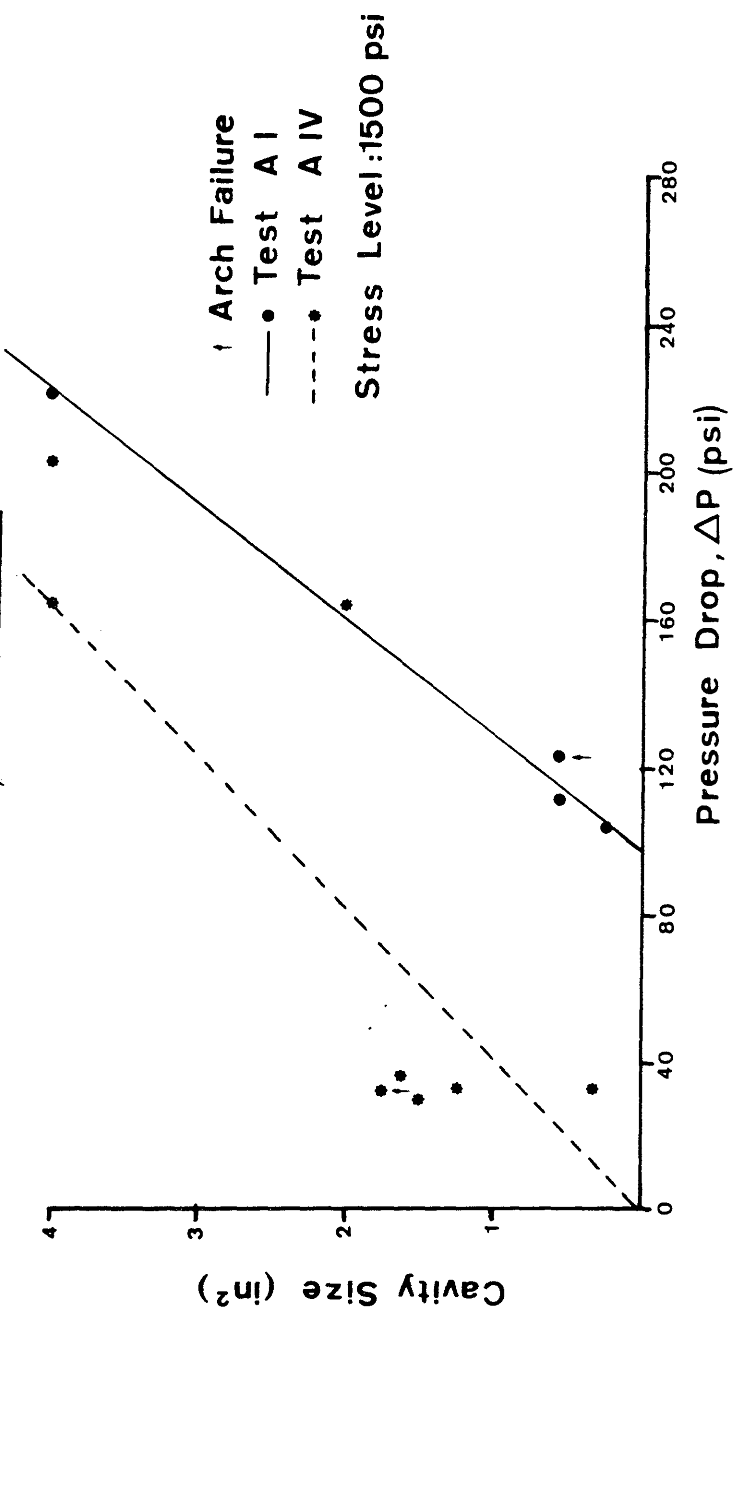

Figure 43.

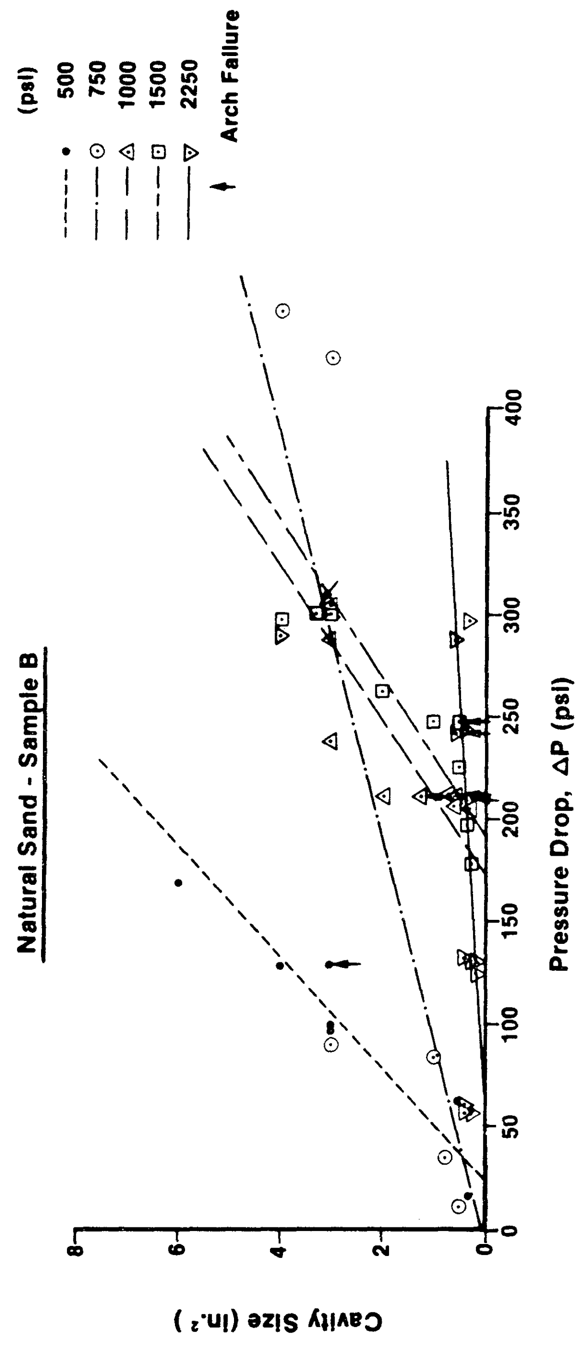
CAVITY SIZE VS PRESSURE DROP
Natural Sand - Sample B
Stress Level
(psi)
500
750
1000
1500
2250
Arch Failure
Cavity Size (in.²)
0
2
4
6
8
0
50
100
150
200
250
300
350
400
Pressure Drop, ΔP (psi)

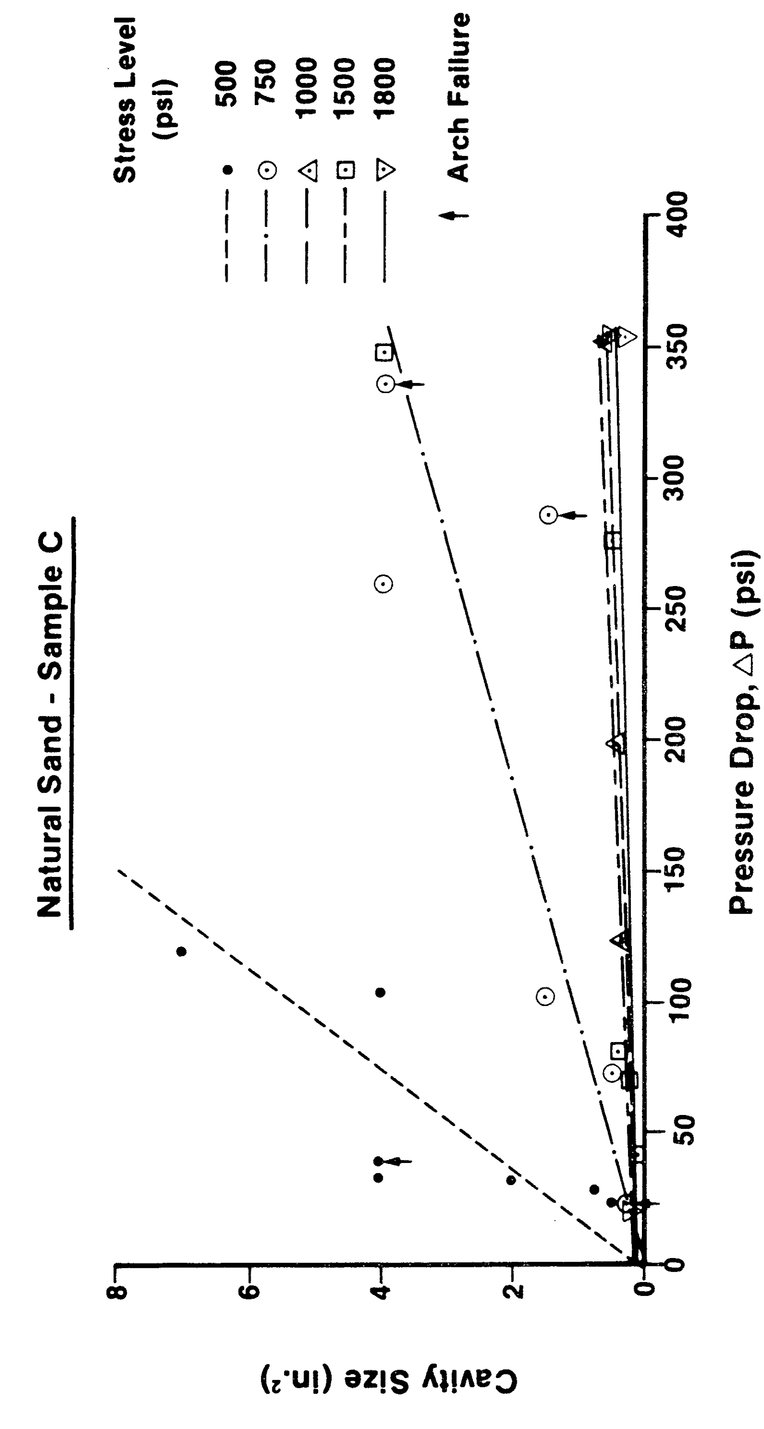
CAVITY SIZE VS PRESSURE DROP
Natural Sand - Sample C
Cavity Size (in.²)
Pressure Drop, ΔP (psi)
Stress Level (psi)
500
750
1000
1500
1800
Arch Failure
0
2
4
6
8
50
100
150
200
250
300
350
400

Figure 44.

Figure 45. Cavity Size Vs Pressure Drop
Natural Sand-Sample D

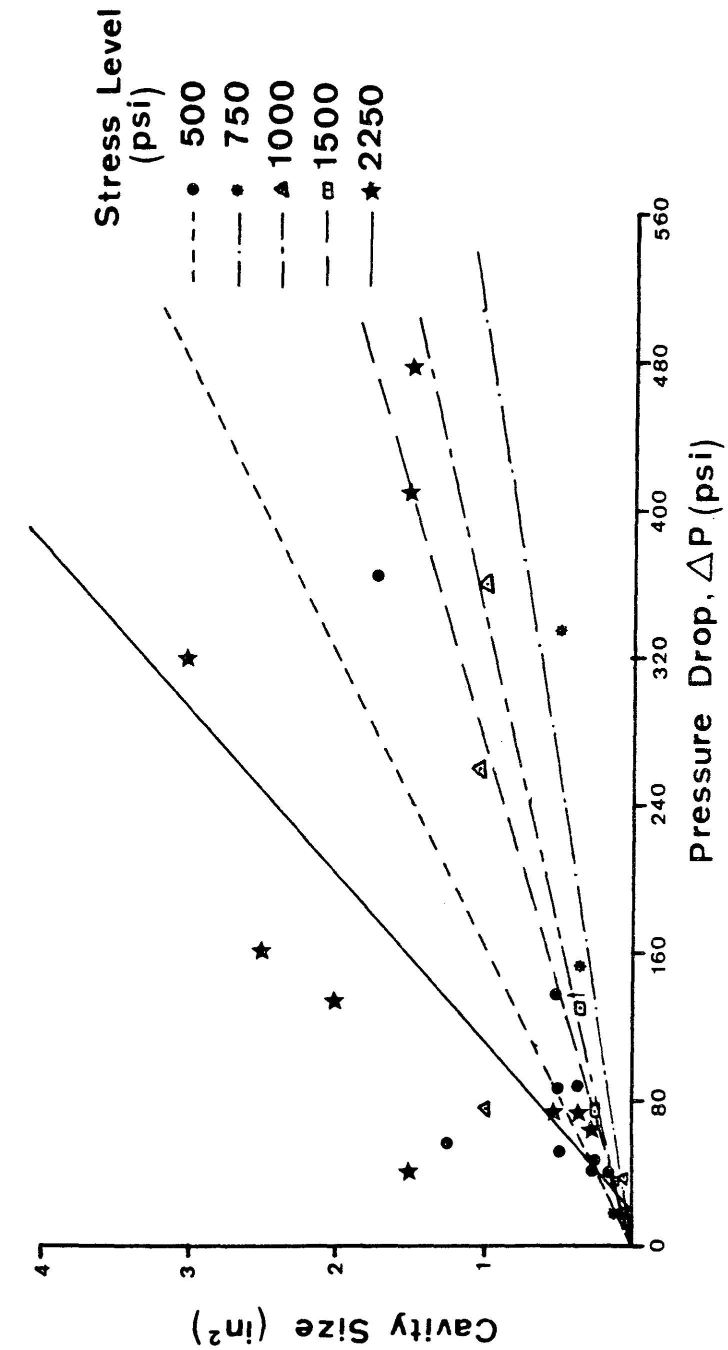

Figure 46. **Mohr's Circles At Arch Failure Natural Sand - Sample B**

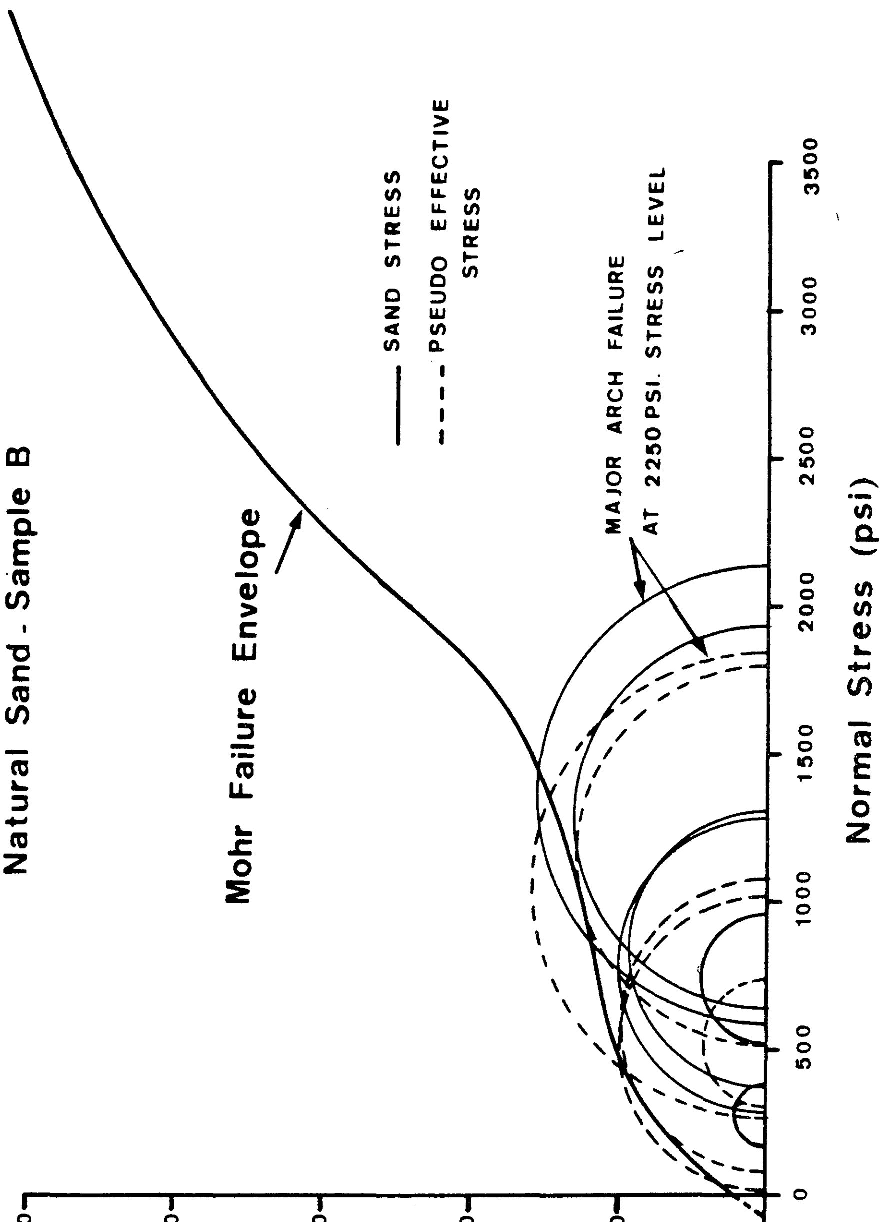

Figure 47. **Mohr's Circles At Arch Failure Natural Sand-Sample C**

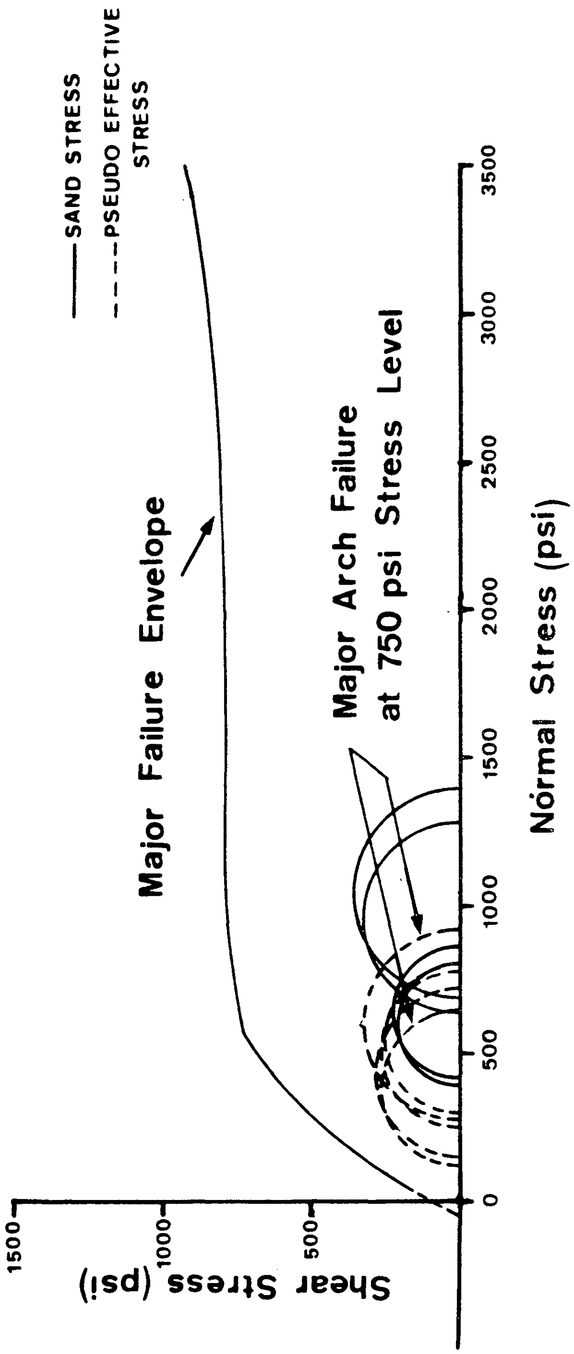

Figure 48. **Mohr's Circles At Arch Failure Natural Sand-Sample D**

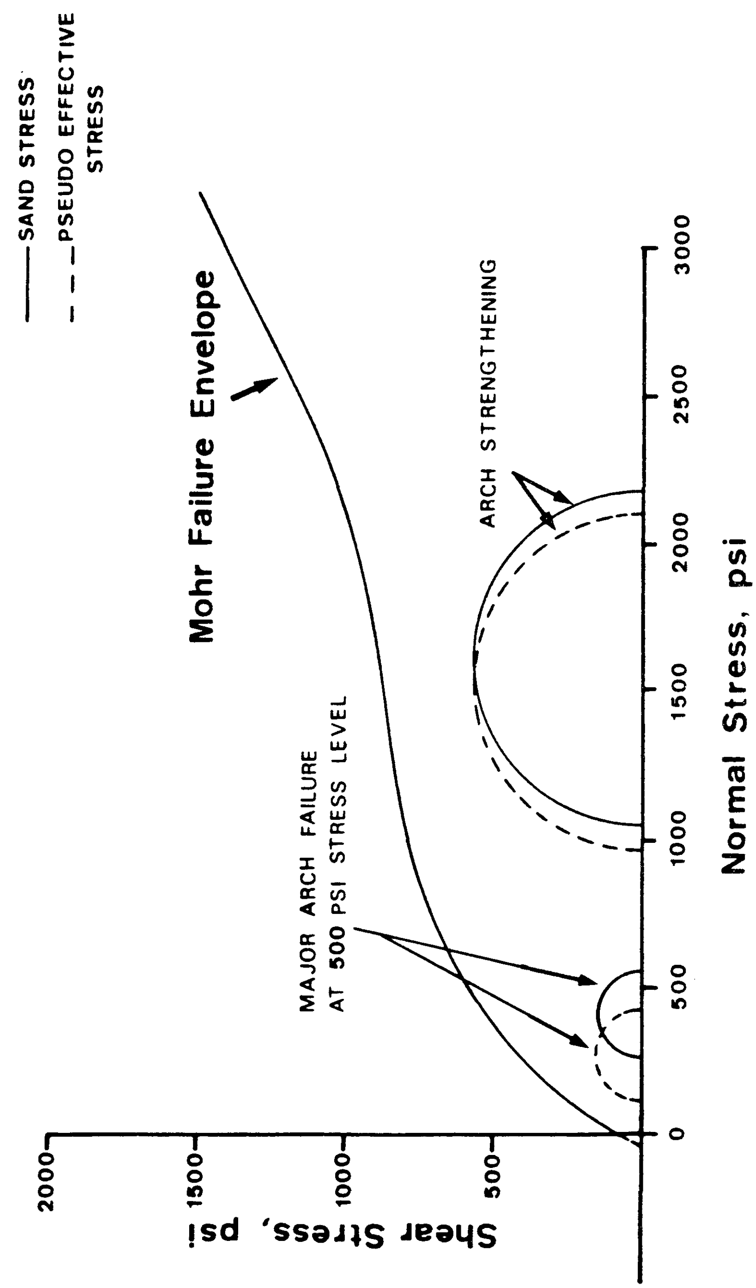

Figure 49.

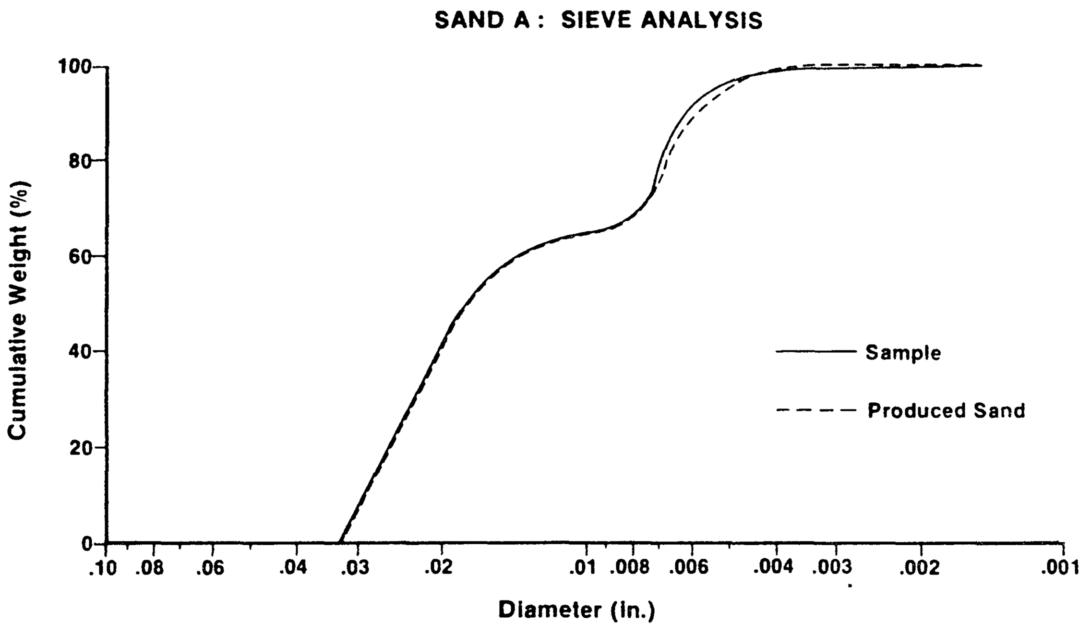

Figure 50.

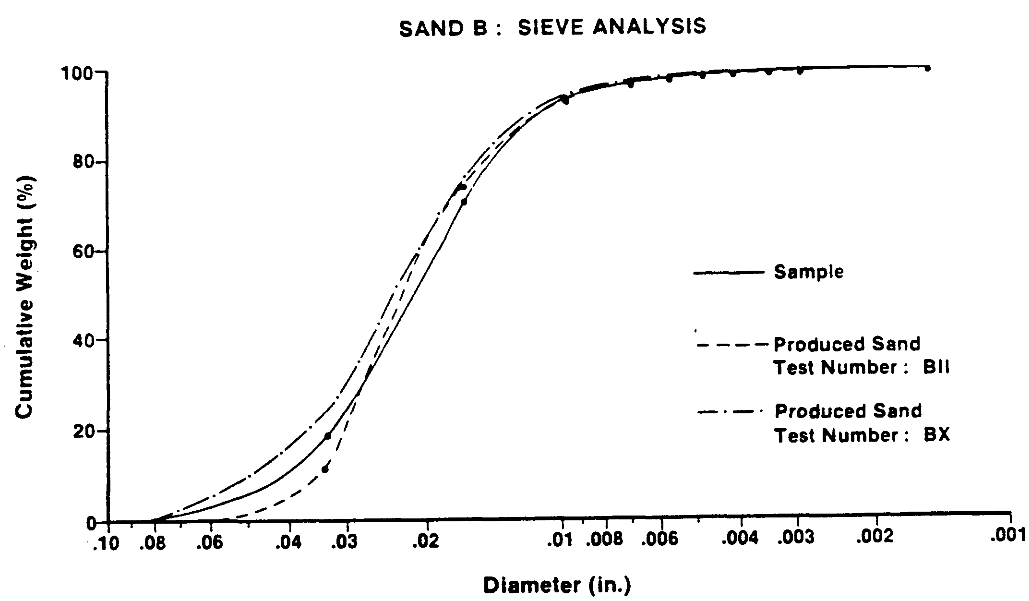

Figure 51.

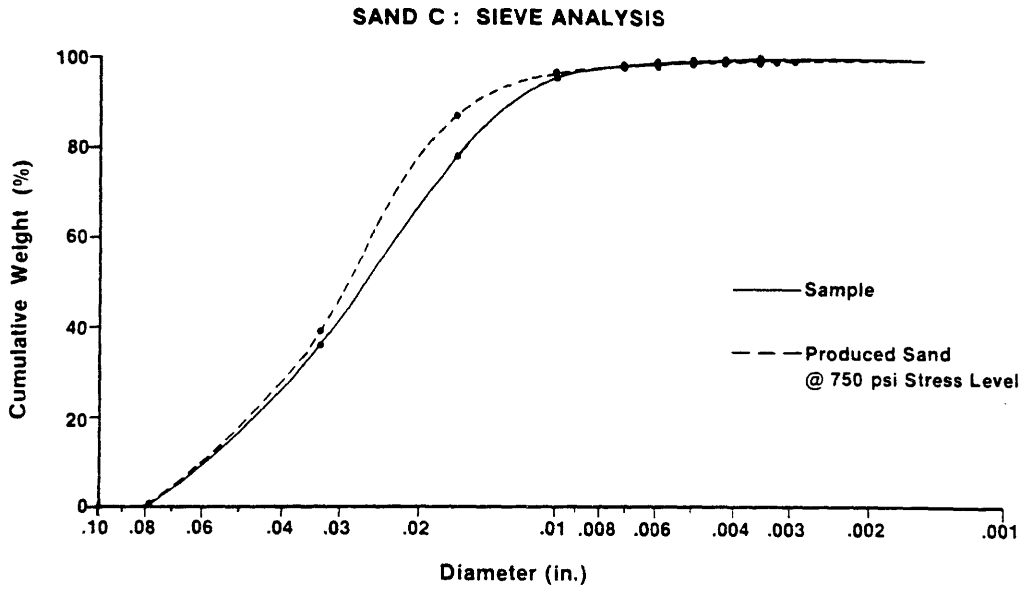

Figure 52.

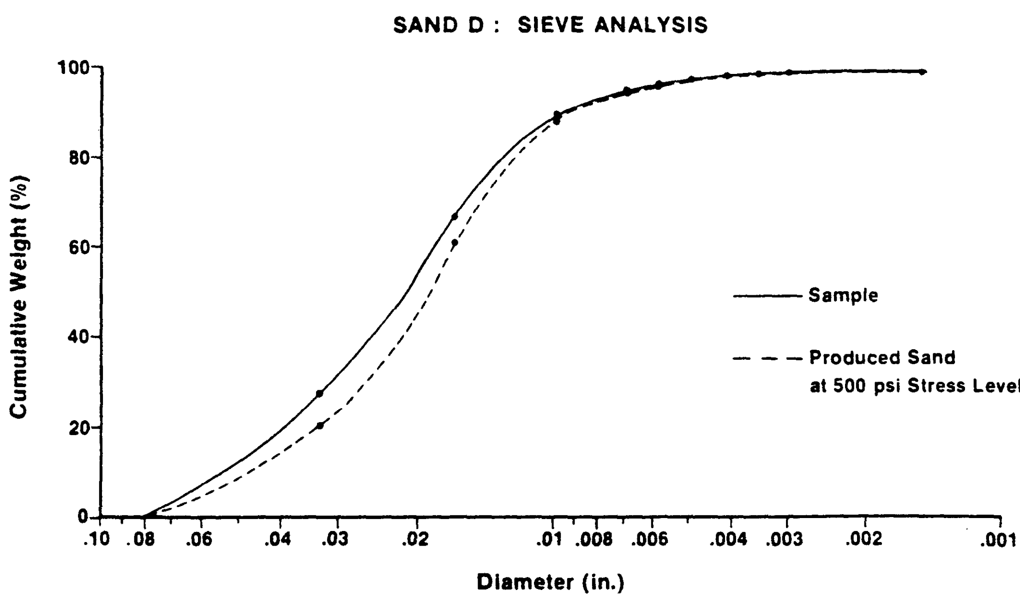

Figure 53. ARCH FAILURE CONDITION

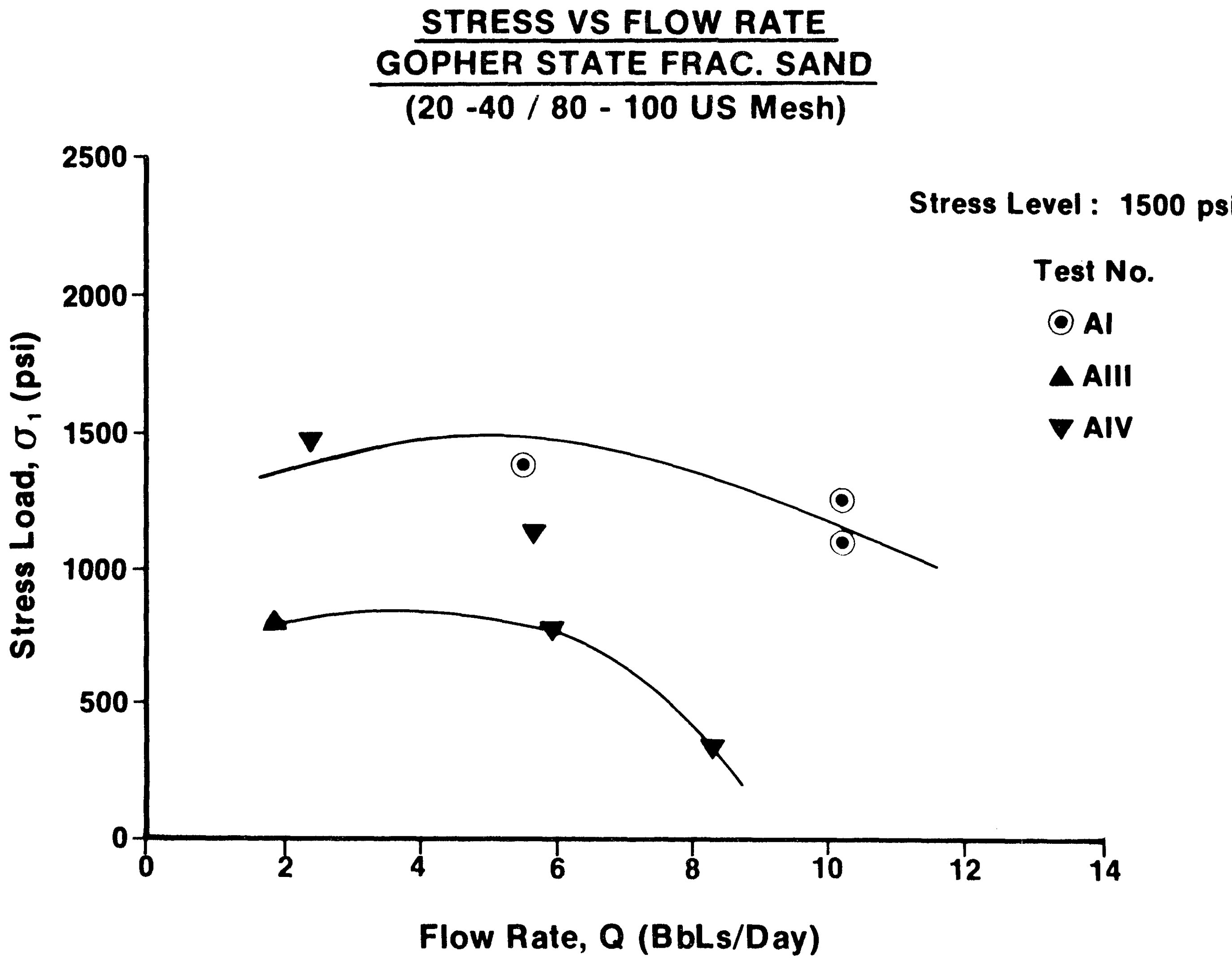

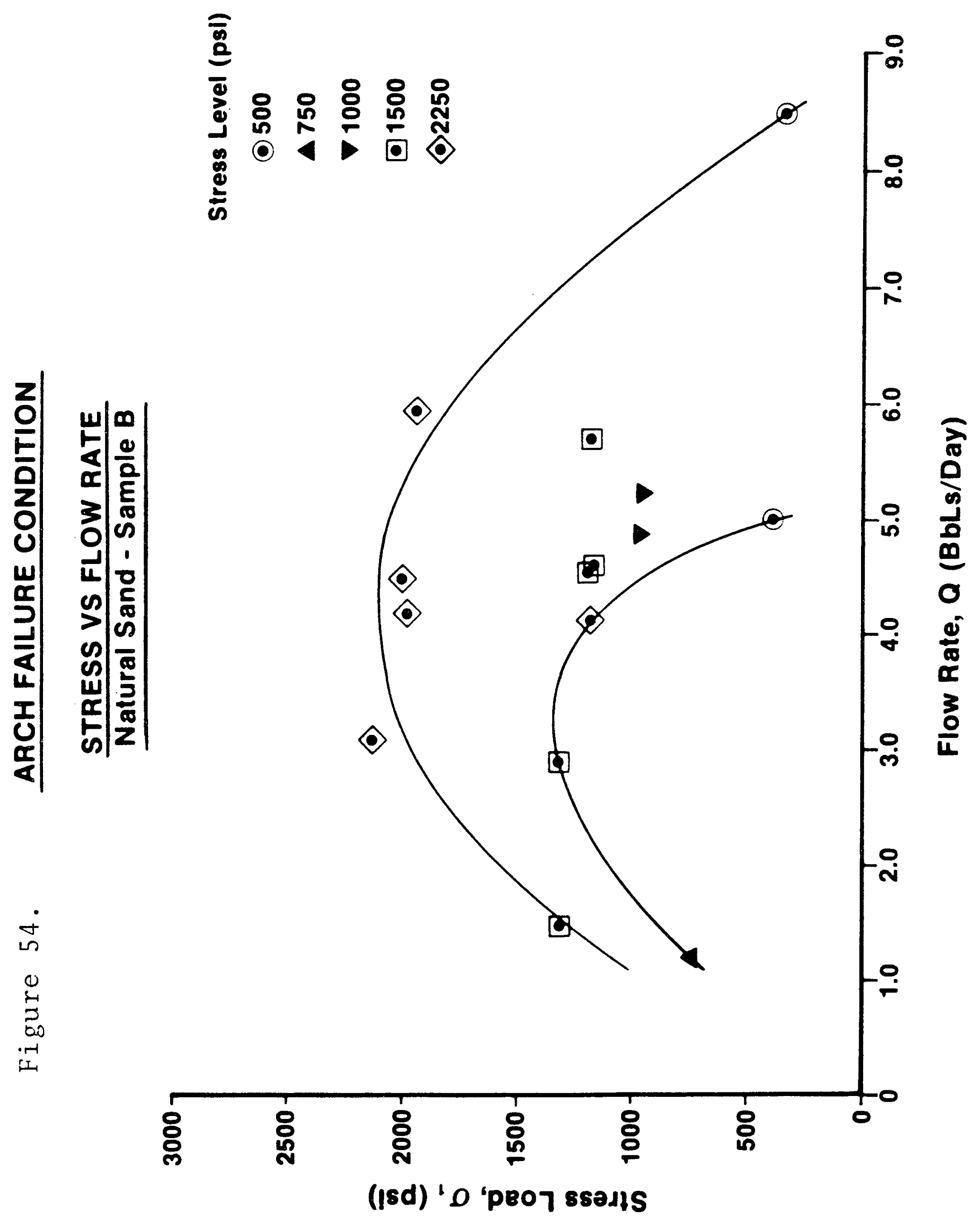
ARCH FAILURE CONDITION
STRESS VS FLOW RATE
Natural Sand - Sample B
Stress Level (psi)
500
750
1000
1500
2250
Stress Load, σ, (psi)
3000
2500
2000
1500
1000
500
0
Flow Rate, Q (BbLs/Day)
1.0
2.0
3.0
4.0
5.0
6.0
7.0
8.0
9.0

Figure 54.

Figure 55. **ARCH FAILURE CONDITION**

STRESS VS FLOW RATE

Natural Sand - Sample C

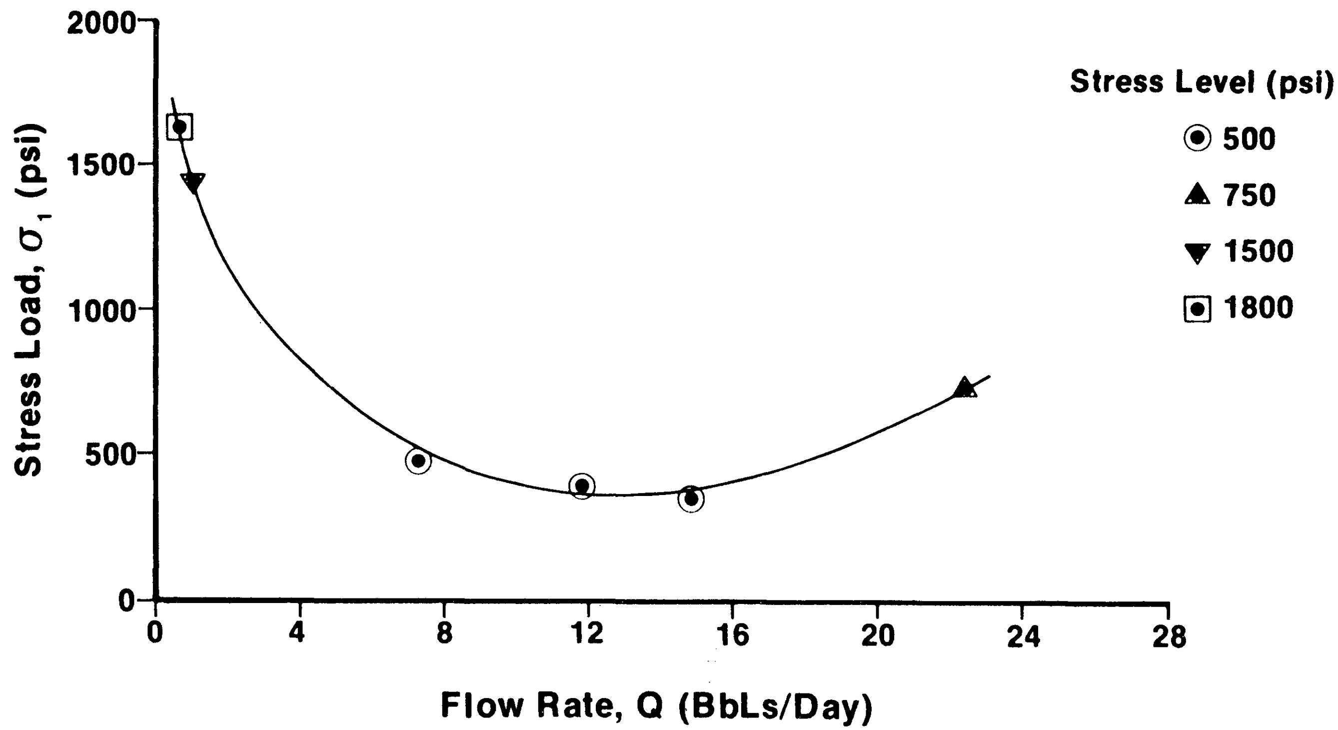

Figure 56. **ARCH FAILURE CONDITION**

STRESS VS PRESSURE DROP

GOPHER STATE FRAC. SAND

(20 - 40 / 80 - 100 US Mesh)

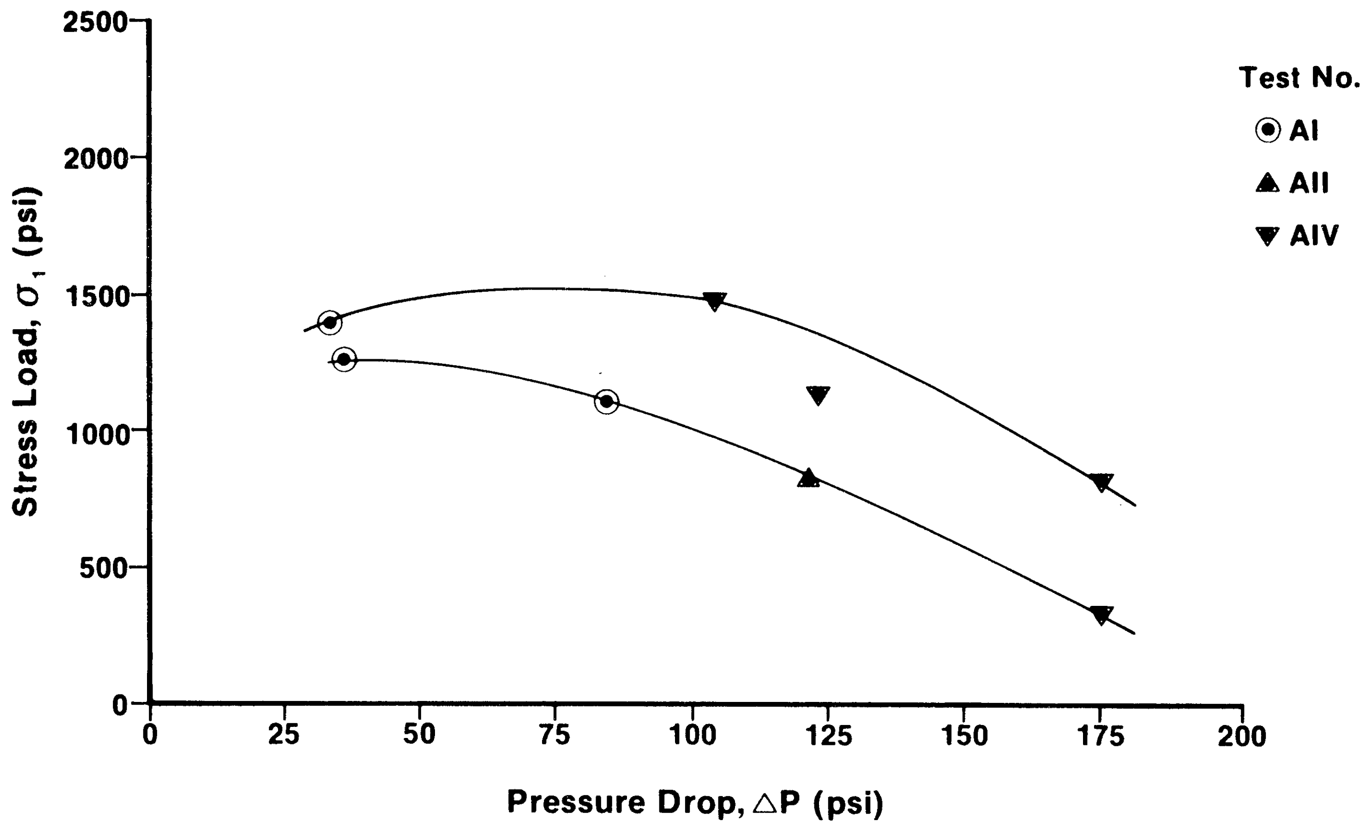

Figure 57. **ARCH FAILURE CONDITION**

STRESS VS PRESSURE DROP

Natural Sand - Sample B

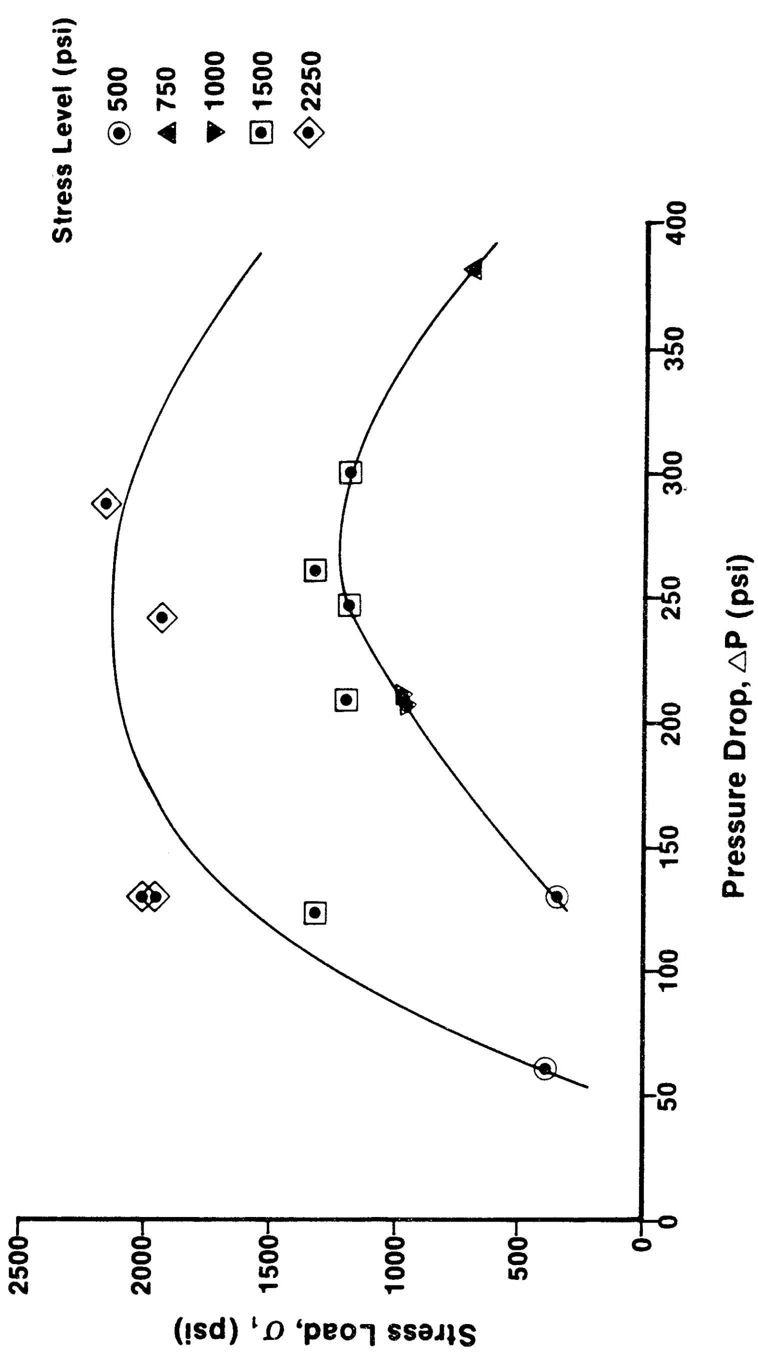

Figure 58. **ARCH FAILURE CONDITION**

STRESS VS PRESSURE DROP

Natural Sand - Sample C

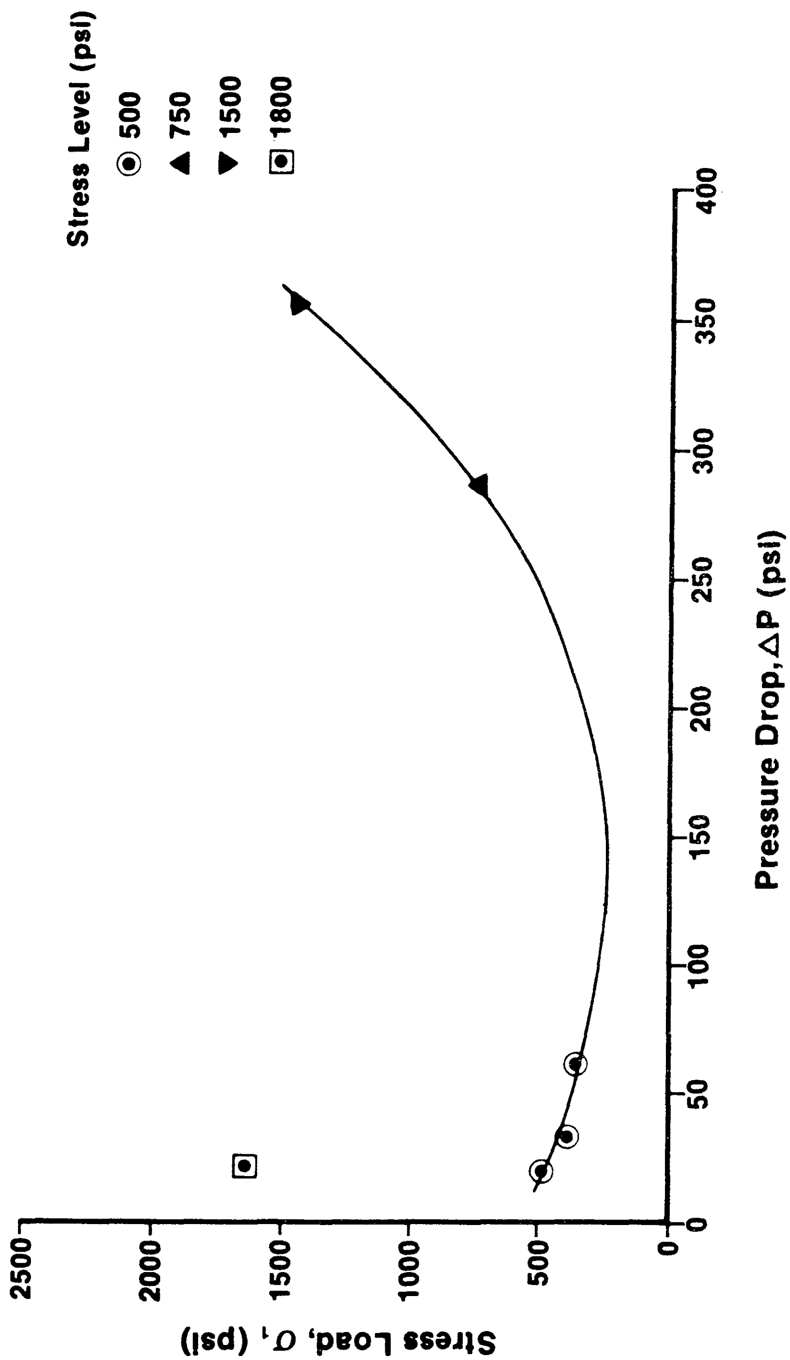

Figure 59. **ARCH FAILURE CONDITION**
STRESS CHANGE VS STRESS LOAD

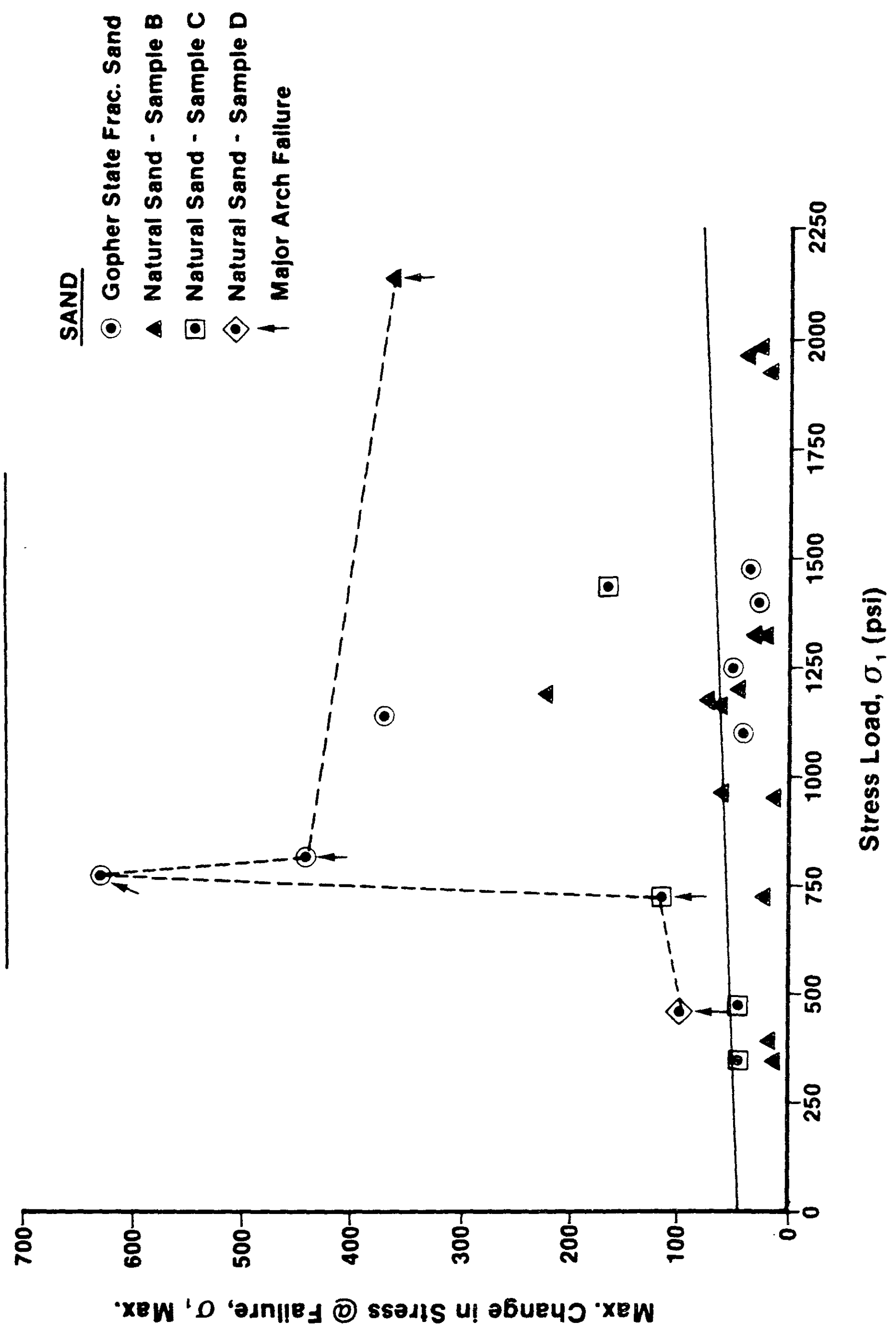

Figure 60. LINEAR FRACTIONAL TRANSFORMATION SHOWING CAVITY EFFECT

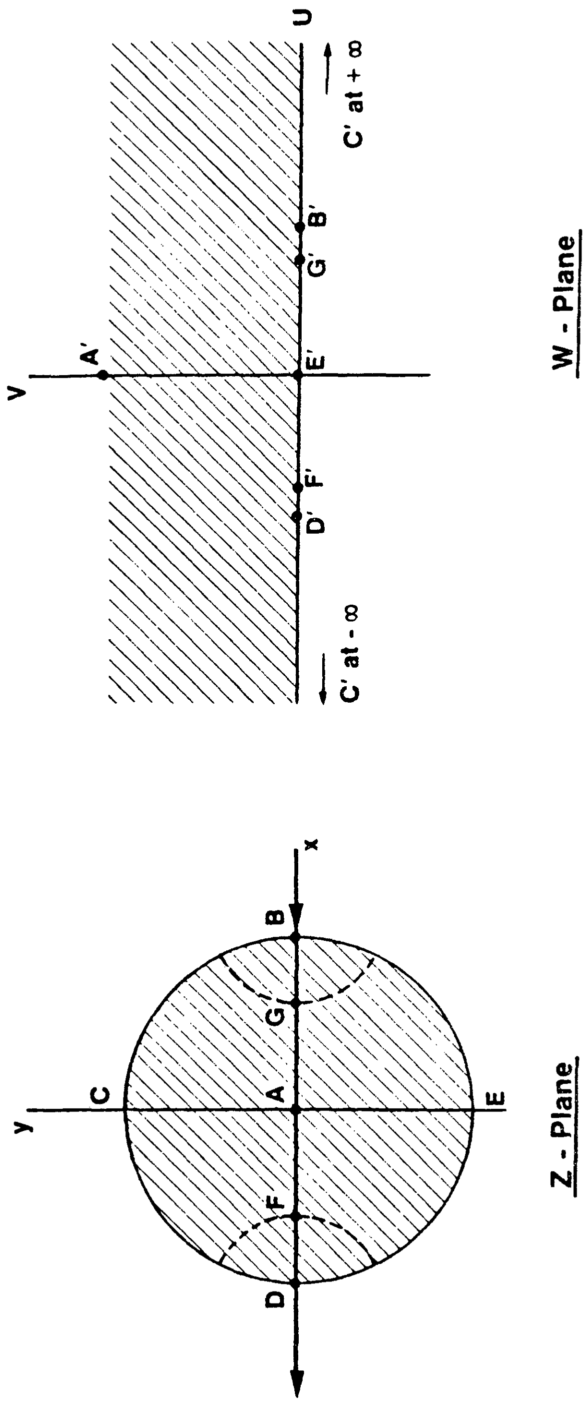

Figure 61.

EFFECT OF ARCH RADIUS ON PRESSURE DROP

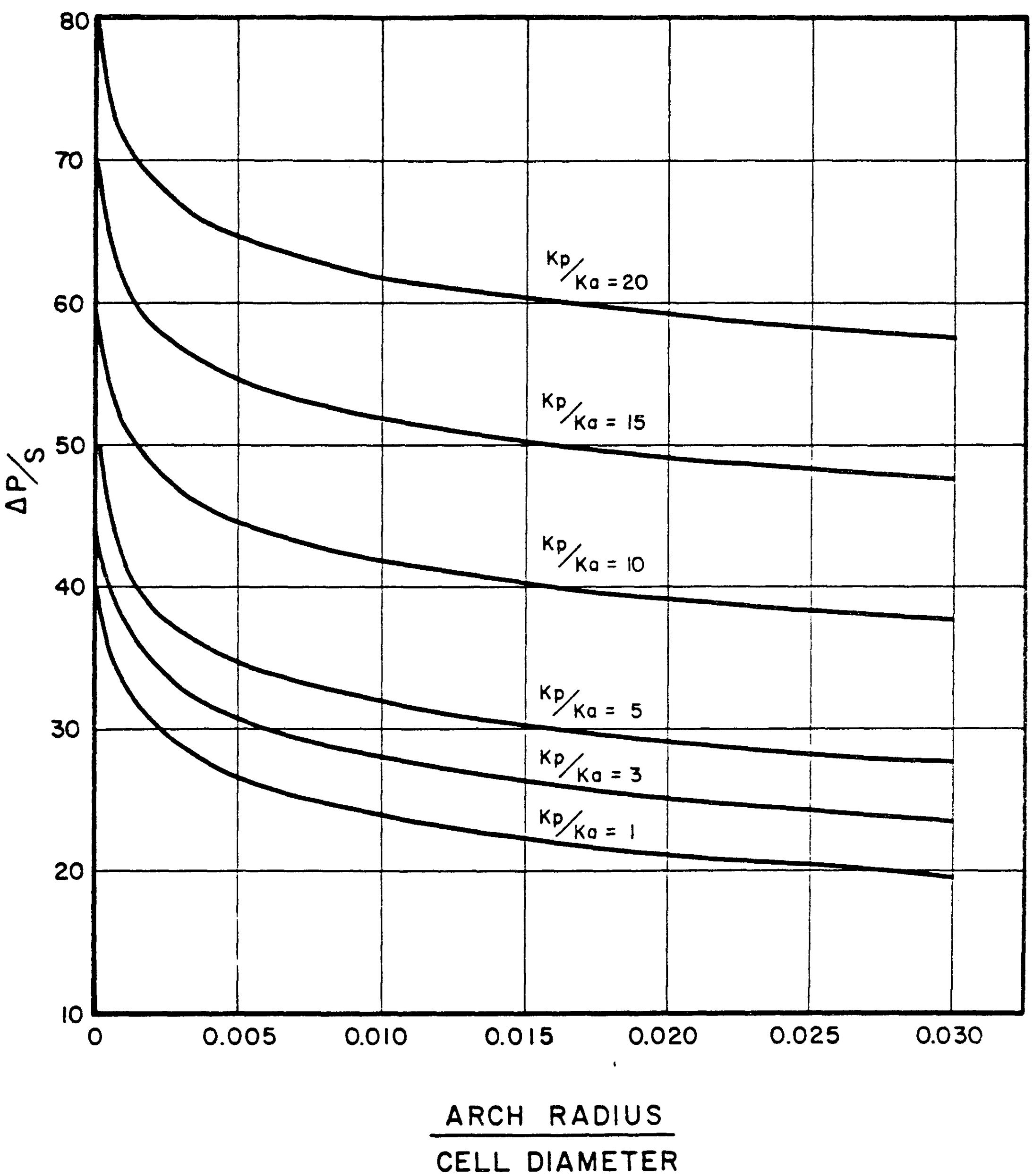

Figure 62. **EFFECT OF ARCH RADIUS ON PRESSURE DROP**

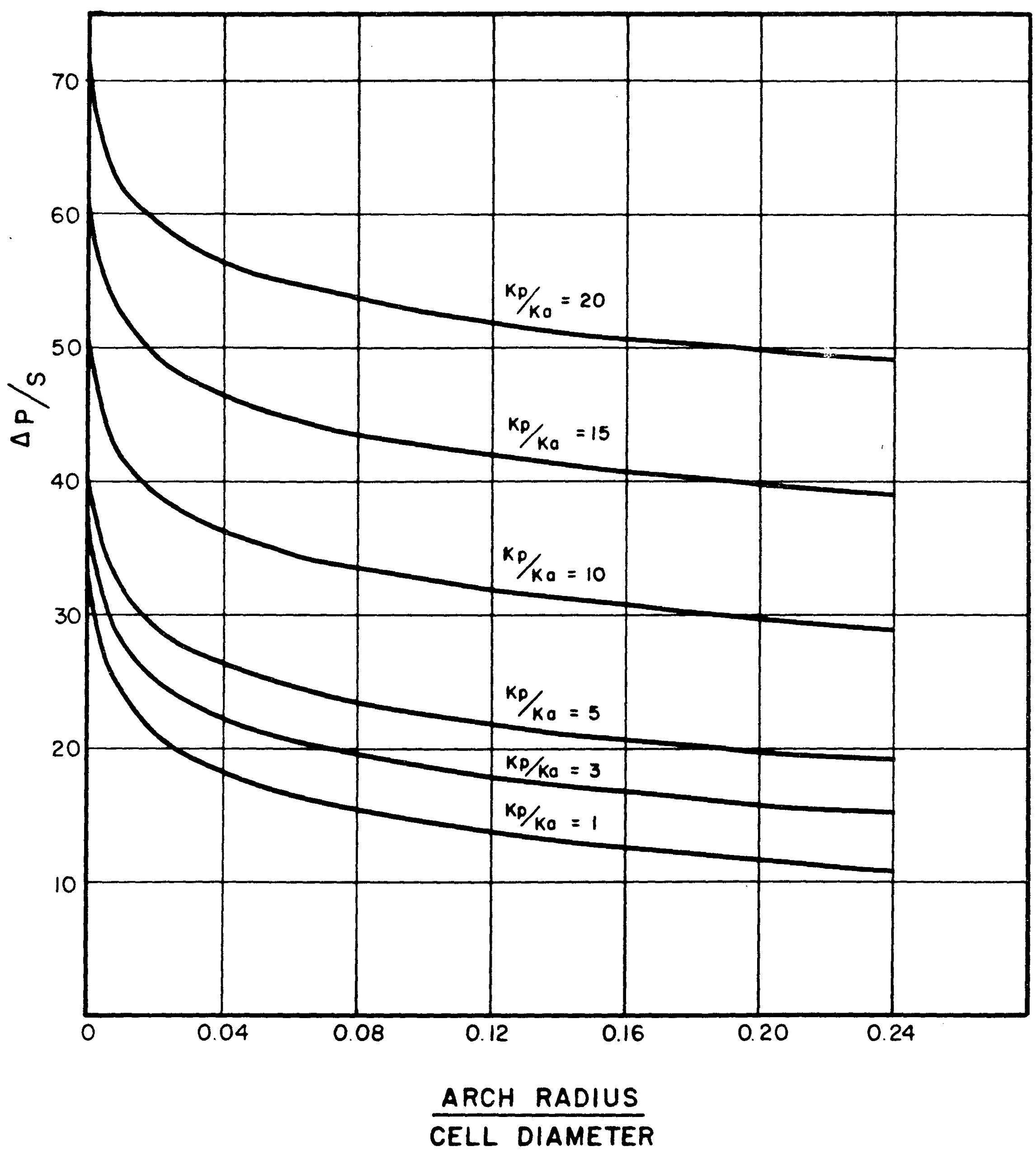

Figure 63.

CHANGE IN PERMEABILITY WITH PSEUDO-EFFECTIVE STRESS

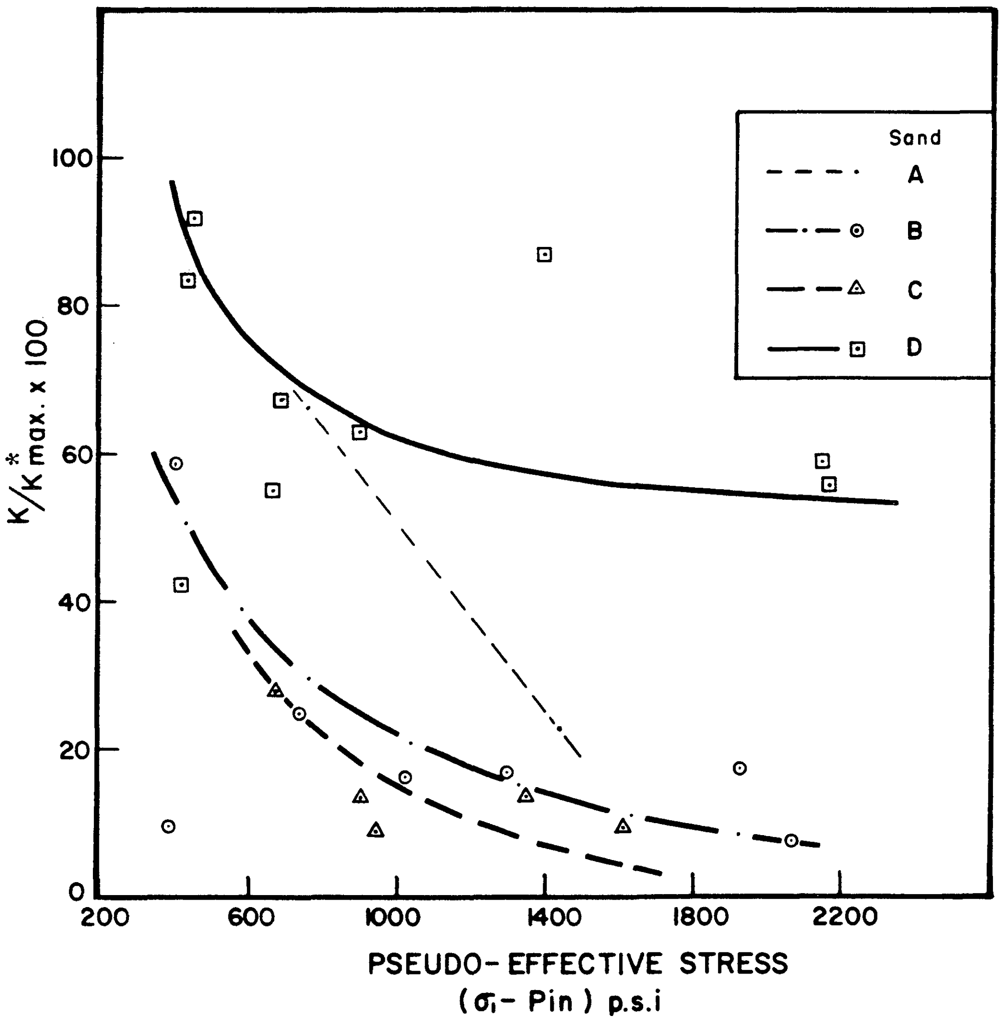

* Values of k_{max}: 4.73md for Sand A, 9.49 for sand B, 21.25 for Sand C, and 2.09 for sand D.

Figure 64.

FLOW POTENTIAL AROUND PERFORATION

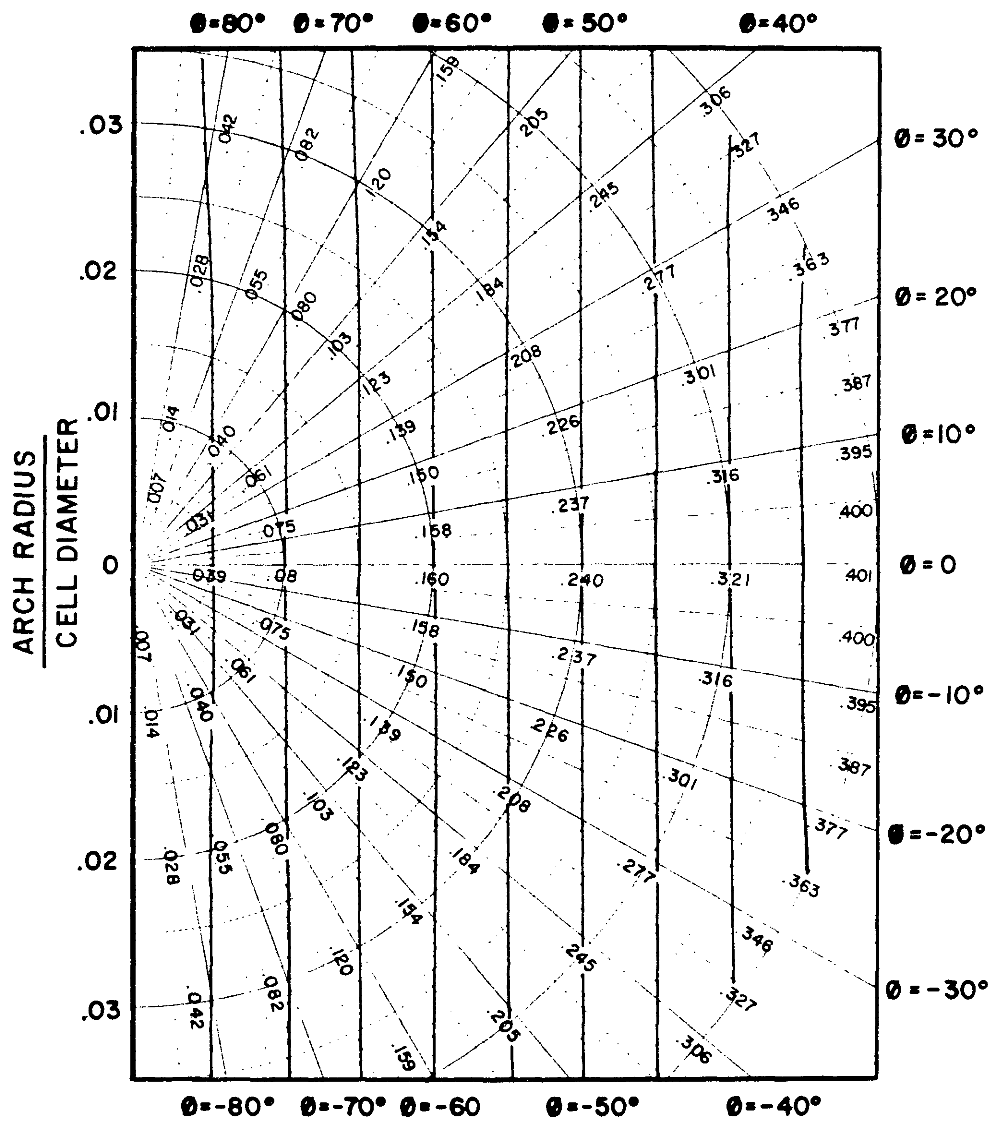

Figure 65. Log ($\Delta P_D'$) Versus σ_{eD} At Failure Conditions

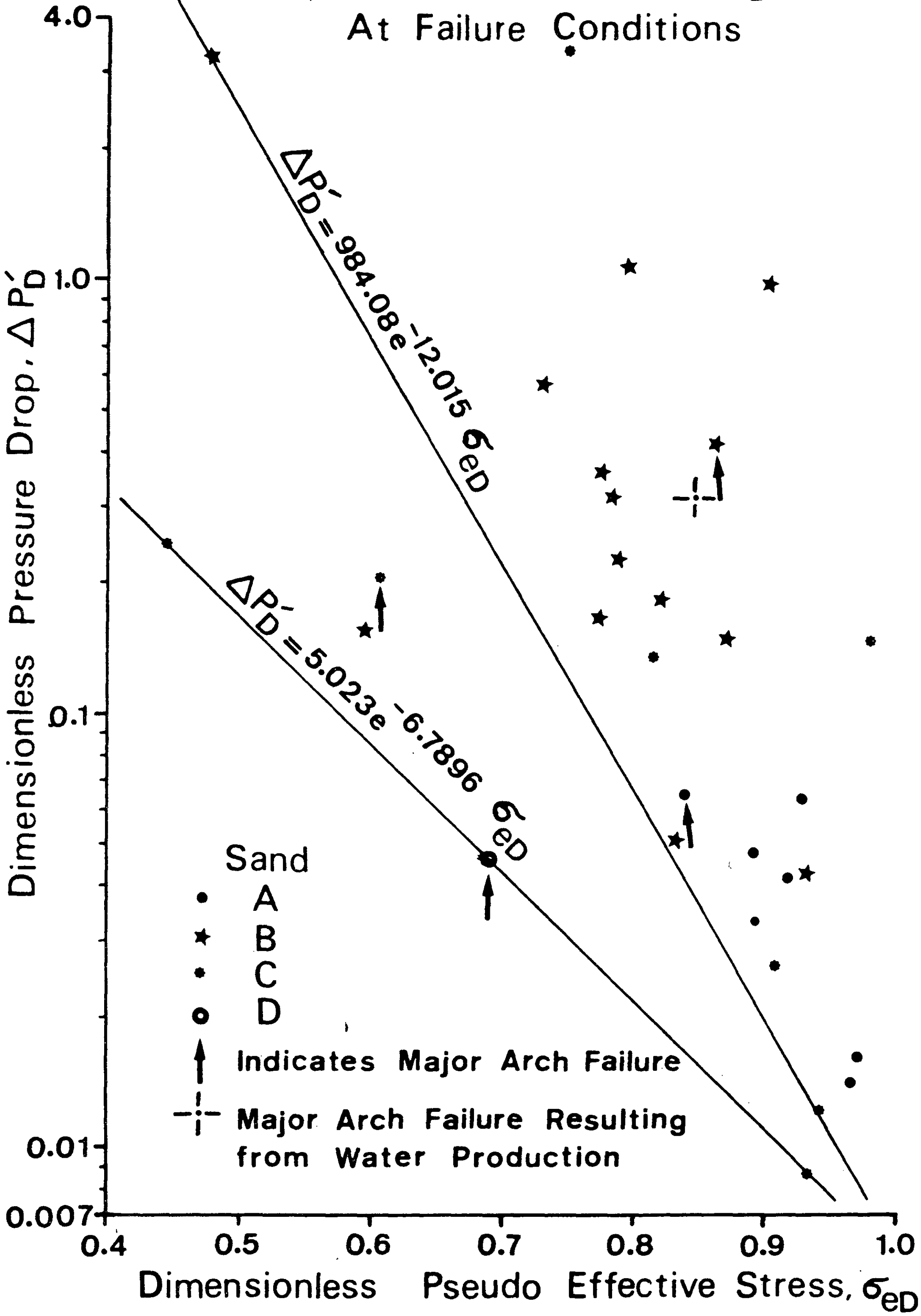

Figure 66. Log (ΔP_D) Versus σ_{eD} At Failure Conditions

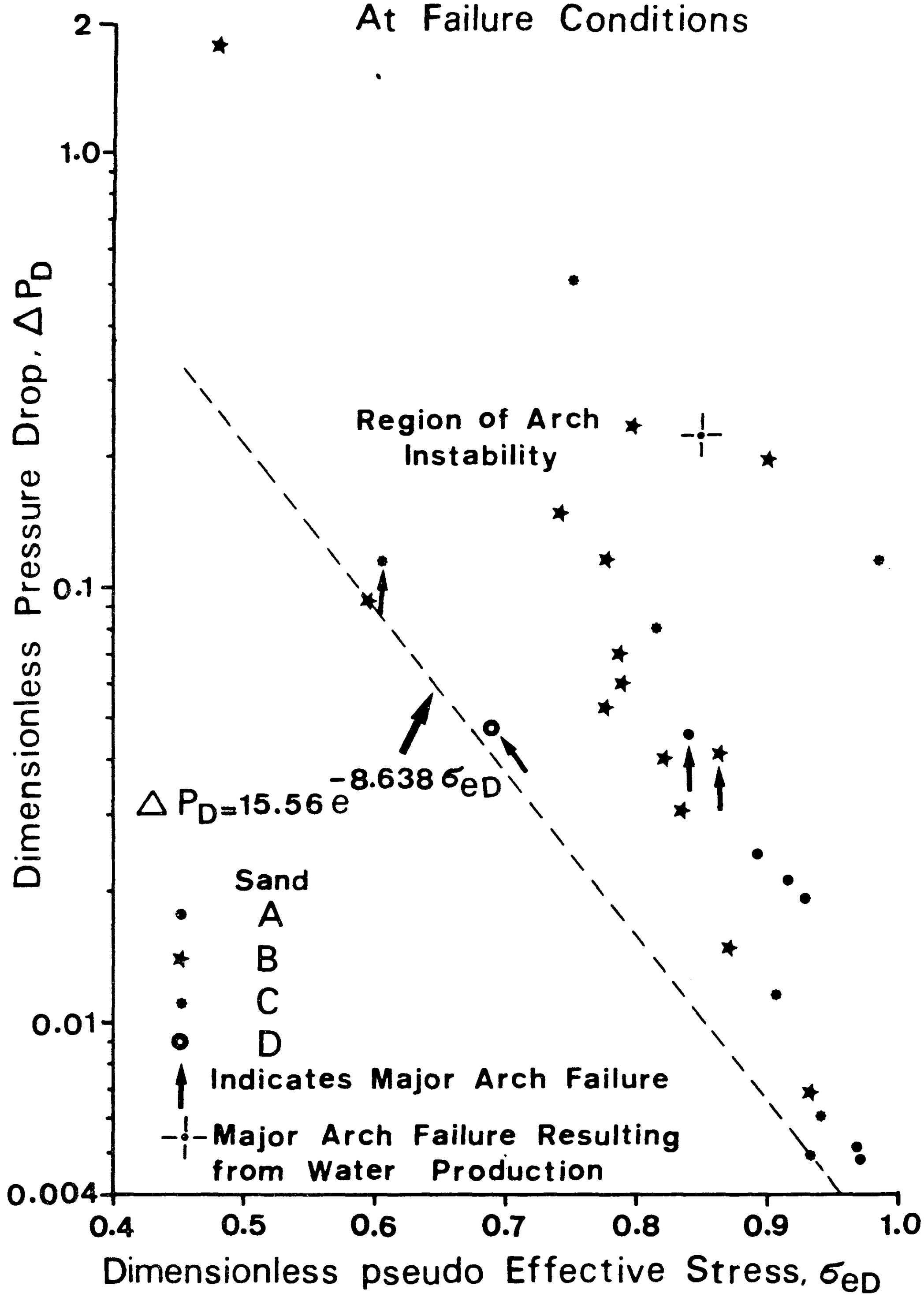

Figure 67.

Log (σ_{eD}) Versus Log (ΔP_D) at Failure Conditions

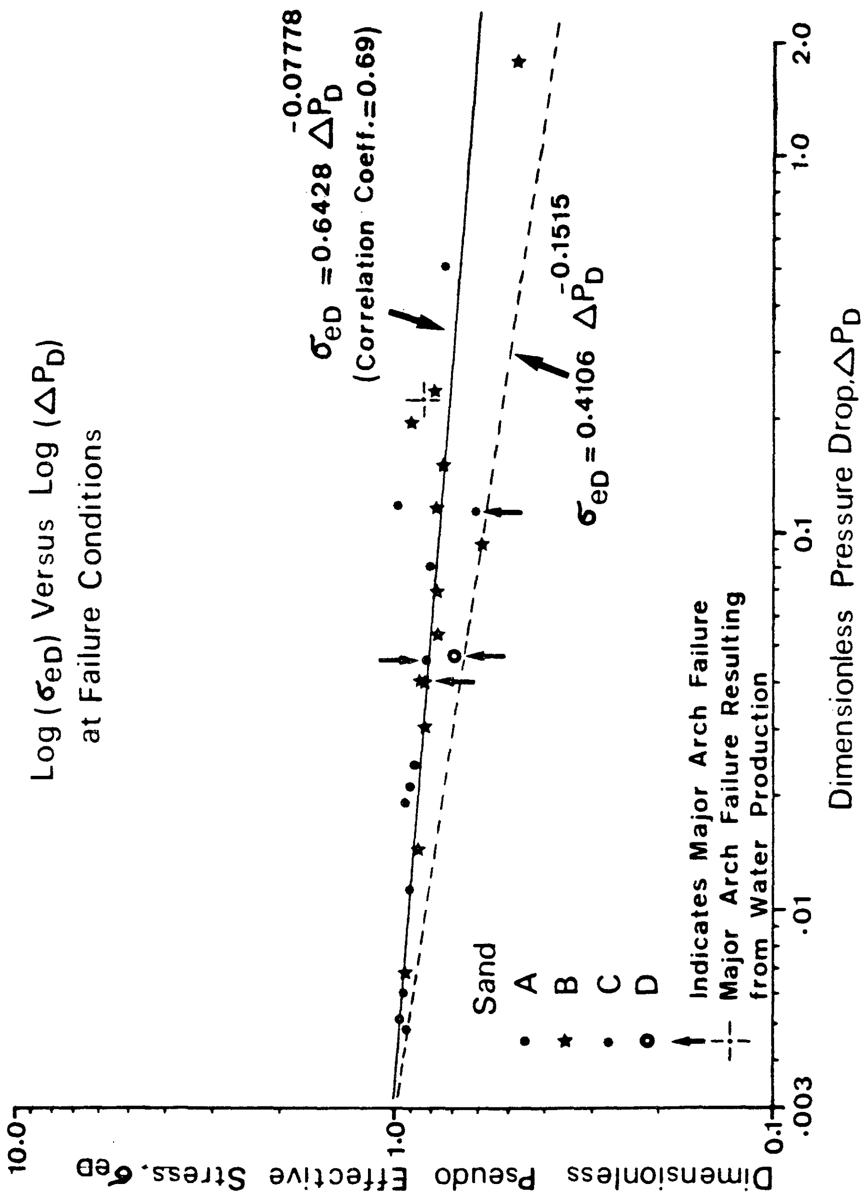

Figure 68.
Log (σ_{fD}) Versus Log (ΔP_D)
at Failure Conditions

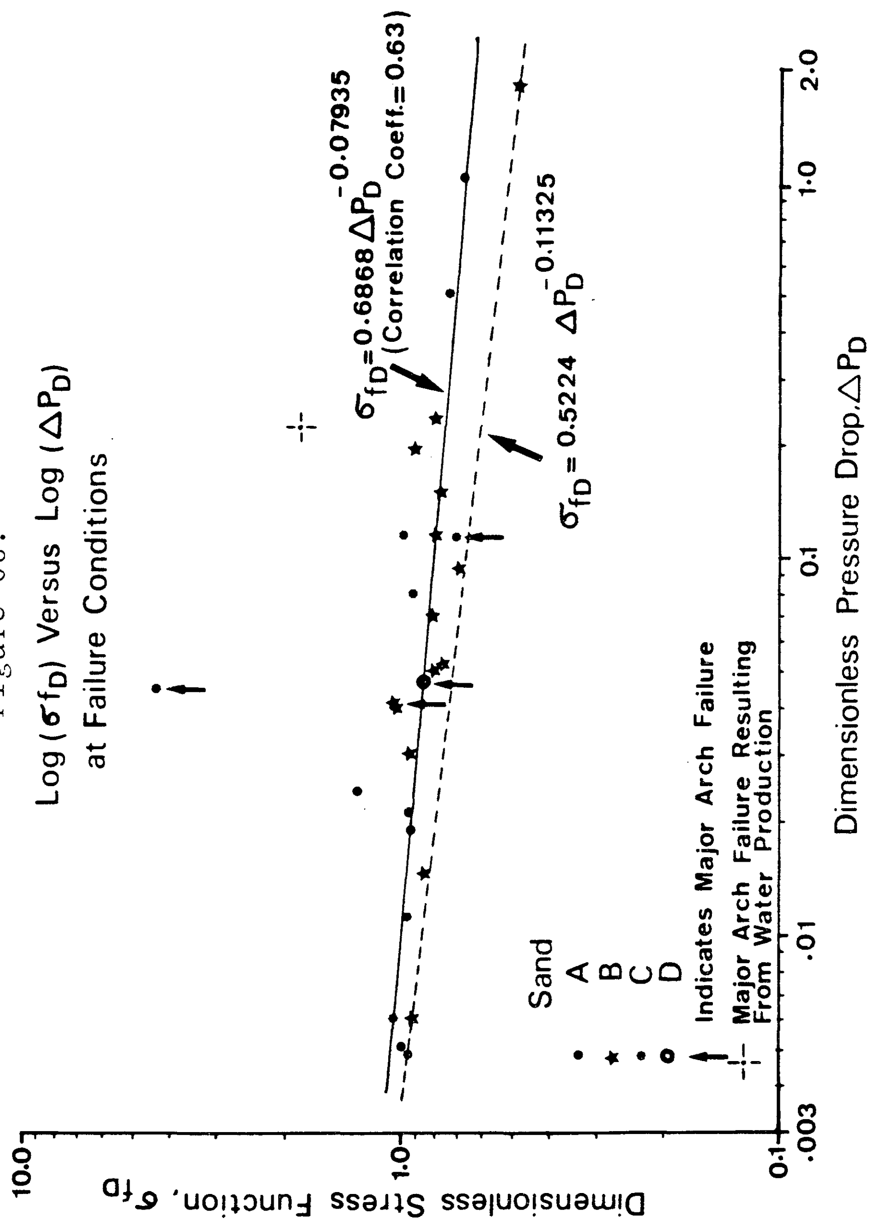

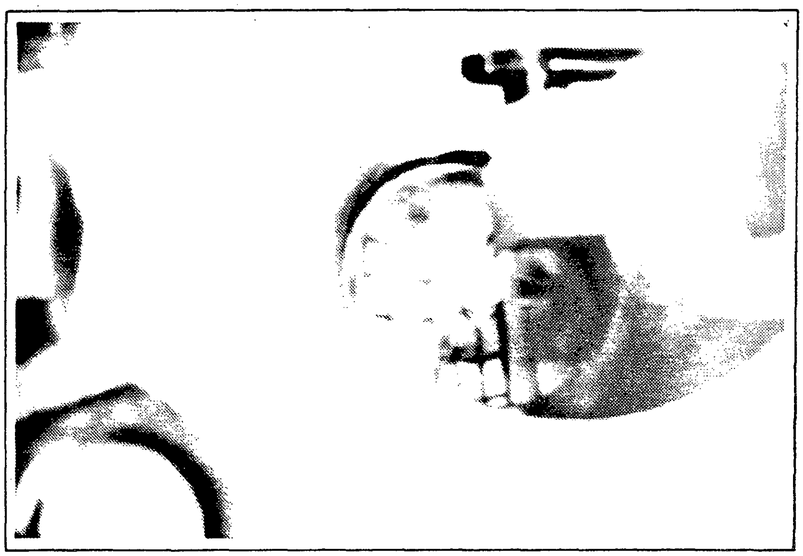

Figure 69a. Perforation View Area Showing a Cavity.

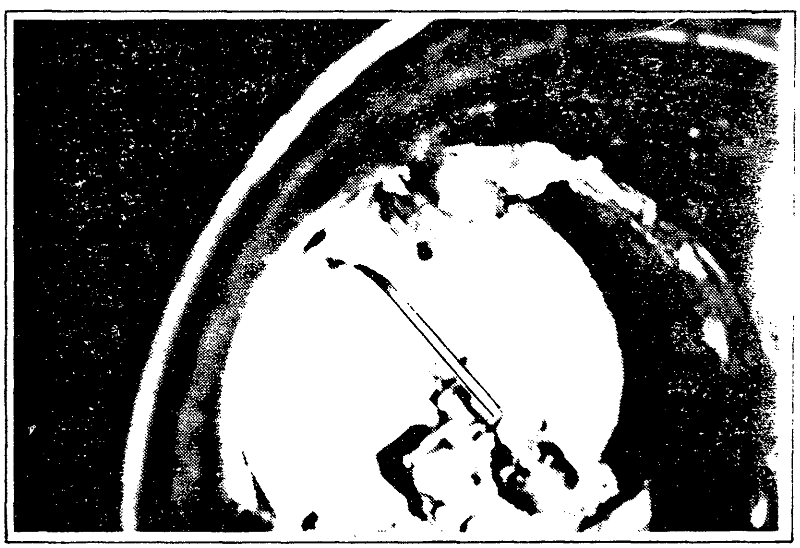

Figure 69b. The inside of the Cell after unloading part of the sand.

Figure 70a. Triaxial Test Printouts.

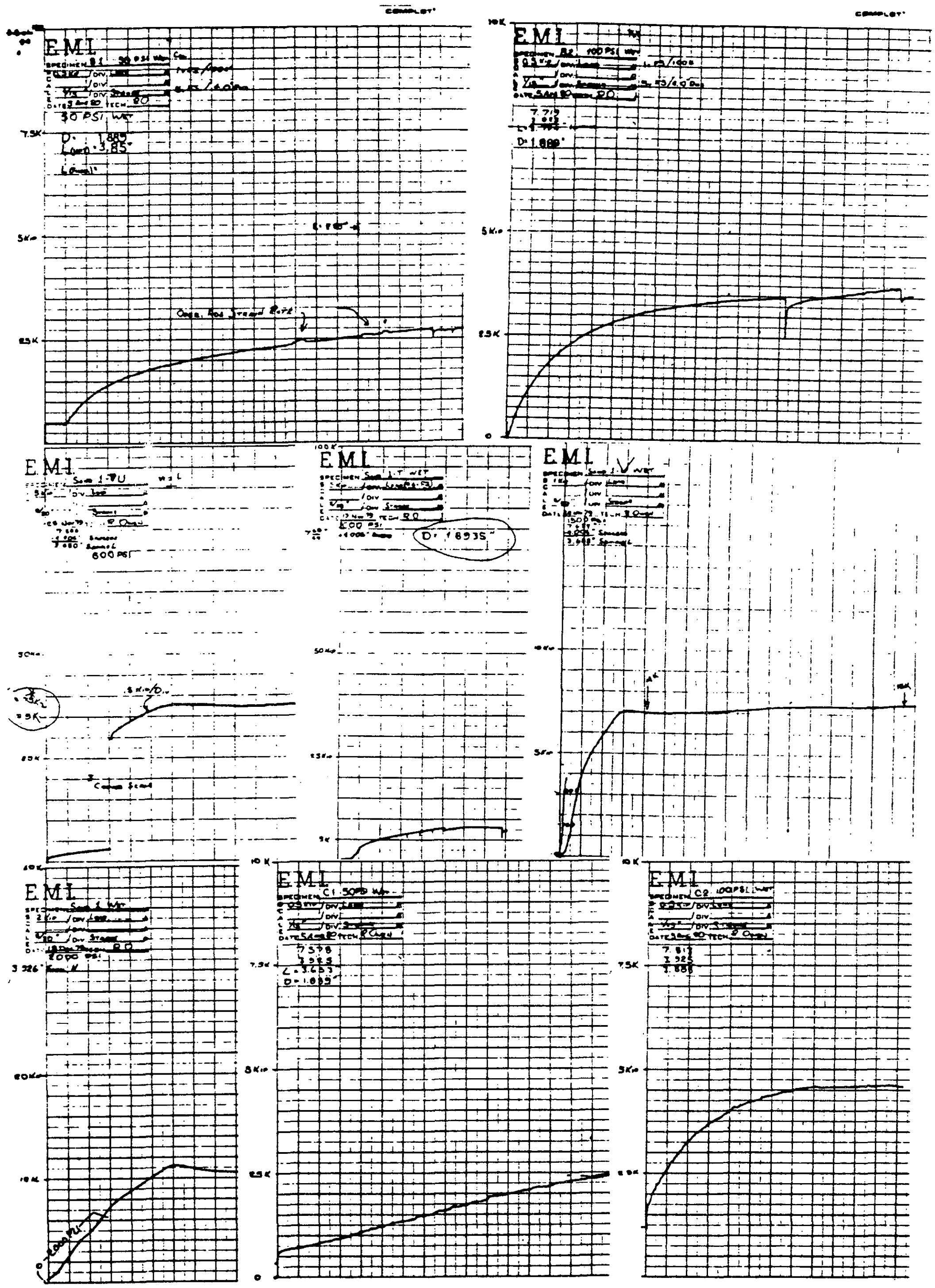

Figure 70b. Triaxial Test Printouts.